Department of Chemistry, Materials and Chemical Engineering “Giulio Natta”

PhD in Industrial Chemistry and Chemical Engineering

Deep Eutectic Solvents: New Tools for Biomass Valorization

Doctoral thesis of Letizia Anna Maria Rossato

Coordinator: prof. Alessio Frassoldati
Supervisor: prof. Paola D’Arrigo
Tutor: prof. Francesco G. Gatti

XXXVI cycle- Academic years 2020-2023

Summary

Preface

The present thesis has been organized as a collection of the five papers published throughout the entire PhD period. Therefore, each of the publications has been adapted into a standalone chapter that can be read independently.
The collection of papers is preceded by a general Aim of the thesis work and an Introductory Chapter which summarizes the "state of the art" and provides general information about the main topics of this thesis, in particular focusing on exploited biomasses, deep eutectic solvents and final products applications.
Moreover, all the experimental sections published within the papers have been included, whereas the additional data published in the supporting information section of each publication are indicated with the corresponding web link and reported at the end of every chapter.
The Executive Summary of the entire three-year research work presented to the Faculty Board of the PhD programme has been attached at the end of the thesis, providing a comprehensive overview of the work conducted.

Abstract

In this PhD thesis, deep eutectic solvents (DESs) were investigated as new tools for biomasses valorization thanks to their versatility and unique properties.
DESs are easily prepared by mixing together a hydrogen bond donor (HBD) and a hydrogen bond acceptor (HBA) at high temperatures (50-100 °C) for few hours.
Frequently HBA and HBD are natural compounds, leading to the classification of these DESs as natural DESs (NADESs). For many years, DESs were considered similar to ionic liquids (ILs) as "new green solvents", but recently DESs have gained more relevance because they offer some advantages over ILs, such as no-toxicity, biocompatibility, biodegradability and cost-effectiveness. Consequently, DESs are largely exploited in many fields, such as biocatalysis, biomass fractionation, CO_2 capture and metallurgy.
However, despite their widespread exploitation, the scientific community is highly debating about what can be considered a DES and what a simple mixture of compounds, which are the main parameters to consider in the definition of a DES and how the presence of water influences the DES formation. In fact, the term "DES" is often abused because of the limited number of publications devoted to understand DESs nature, and the absence of a standardized, cost-effective method for their characterization. For this reason, we set up a new analytical tool based on the NMR technique for the study of trimethylglycine betaine-based DESs. In particular we focused on understanding how the relaxation time (T_1) of this set of DESs changes with the HBD molar fraction, and how this correlation might be modified by progressive additions of water.

The first DESs application here reported involves their utilization in the biocatalytic synthesis of polar head-modified phospholipids. In particular DESs in biocatalysis are known to work as co-solvents with water, as pure solvents or as solvent and substrate of the reaction. In the latter case, these DESs are referred to as reactive DESs (RDESs), and we exploited them for the enzymatic transphosphatidylation of phosphatidylcholine (PC). PC is the most abundant natural phospholipid and is esterified at *sn-1* and *sn-2* positions with saturated and unsaturated long chain fatty acids, which constitute the lipophilic moieties, and in *sn-3* with a phosphate diester as the polar head group. In particular, the enzyme phospholipase D (PLD) catalyzes the transphosphatidylation of the substrate in presence of an alcohol (X-OH) leading to PX formation. So, in this work, we investigated the potentialities of alcohol-based RDESs for the enzymatic transformation of PC into two polar head-modified phospholipids of pharmaceutical interest, phosphatidylglycerol (PG) and phosphatidylethyleneglycol (P-EG).

The second application addressed has been the set-up of a multistep DES-mediated process to fractionate two abundant regional agrifood wastes biomasses: brewers' spent grain (BSG) and rice husks (RHs). The primary objective was the recovery and exploitation of their main fractions, with a particular attention focused on recovered lignins. In detail, the developed process was based on an initial biomass pretreatment in hot water in autoclave that led to the formation of a soluble fraction and of an insoluble one. For BSG, the soluble fraction (accounting for 25% of the initial biomass) consisted in sugars subsequently exploited for the preparation of growth media for microbial fermentation, instead, in RHs cases, we recovered by extraction phenyl-propanoids (2-3%). For all biomasses, after filtration, the insoluble fraction was successively submitted

to a DES-mediated fractionation process, which allowed the recovery of the cellulose-enriched fraction and the lignin. The recovered lignin fractions (almost 15-20% of the initial biomass) have been deeply characterized, and a preliminary evaluation of their potentiality as precursors of cement water reducers gave encouraging results.

The studies on lignin recovery from waste biomasses led more recently to exploit this material for nanoparticles (NPs) preparation in the third part of the PhD work. Initially, the set-up of the NPs synthesis protocol using the technical lignin Protobind has been studied thanks to its quite low cost and large availability in research laboratory. The final aim of this work was the set-up of a sustainable scaffold for enzyme immobilization that could be employed in phospholipids biotransformations. In particular, stable lignin nanoparticles were synthetized starting from hydroxymethylated lignin, and then PLD was immobilized on them by direct adsorption without use of any crosslinkers. The immobilized PLD was employed in the biotransformation of PC in three natural high-value polar head-modified phospholipids: phosphatidylglycerol (PG), phosphatidylserine (PS) and phosphatidylethanolamine (PE).

Aim of the thesis

The current PhD research work has been focused on the preparation and the exploitation of deep eutectic solvents for the treatment and valorization of biomasses that are particularly abundant in our region and typically disposed of as wastes. This work fits into the Green Chemistry and Circular Economy concepts, which comprehend respectively the utilization of less hazardous solvents and renewable feedstocks, and the creation of a market for secondary raw materials, that can be fed back into the economy as new high value-added compounds. Recently, DESs have gained significant attention in the scientific community thanks to their interesting properties, such as low toxicity, biodegradability and the natural origin of their main components, replacing another type of green solvents, the so-called ionic liquids (ILs). In fact, DESs and ILs share similar physical characteristics, but differ in their chemical properties and facility of preparation, making DESs the subject of extensive research. Despite this, there is still a lack of understanding the principles behind DESs formation and preparation. In fact, in literature different stoichiometric ratios of the component for the same DES are reported, and also it is not clear in the application of water-DES solutions which is the maximum quantity of tolerated water before the H-bond disruption of the supramolecule.
Specifically, the present research work has been focused on three main topics:

1. DESs analysis by ^{1}H NMR measurements: Preparation of timethylglycine betaine based-DESs and investigation of their structure through NMR experiments, with the aims of (i) verifying if and how the ^{1}H NMR spin-lattice relaxation time (T_1) of a set of selected DESs changes with the HBD molar fraction (X), and (ii) of ascertaining how such a suggested correlation might be modified by progressive additions of water.
2. DESs in biocatalysis: Preparation and exploitation of different DESs in the biocatalytic conversion of PC into two important polar head-modified phospholipids, using phospholipase D as enzyme. In this work these solvents were considered reactive DESs (RDESs) because they were not only the reaction solvents of the enzymatic transphosphatidylation, but also the donors of the alcoholic moiety reacting with the substrate, allowing the preparation of high value-added compounds recovered easily by filtration, avoiding the use of hazardous organic solvents.
3. DESs in biomass fractionation: Lignocellulosic waste biomass DES-mediated fractionation. Different fractions were recovered (cellulose, hemicellulose and lignin) and in particular lignin was deeply analyzed and tested as water reducers for concrete preparations and as starting material for nanoparticles preparation to be used as bio-based scaffolds for further enzyme immobilization. In particular, our aim was to perform the immobilization of an expensive enzyme, PLD, on a sustainable scaffold derived from an agrifood waste, paving the way for the circularity of the process.

Introduction

1. Circular Economy and Green Chemistry

The Circular Economy concept is defined as a production and consumption model that implies waste reduction and recycle of end-life material creating further value. It comprehends sharing, leasing, reusing, recycling to extend products life cycle. It differs from the traditional linear economic model, and it relies on a large amount of by-products material. The Ellen MacArthur Foundation describes the Circular Economy as a system in which materials never become wastes: products and materials are kept in the market through processes like reuse, composting, refurbishment and many others. The necessity to introduce the Circular Economy concept to the market arose in response to the global challenges we are currently facing, such as climate change, biodiversity loss, pollution and consumerism. The three core principles are (i) the elimination of waste and pollution, (ii) the circulation of products and materials, and (iii) the nature regeneration. These are described by the butterfly diagram, which represents the continuous flow of materials through two main cycles: the technical (right) and the biological (left) ones.

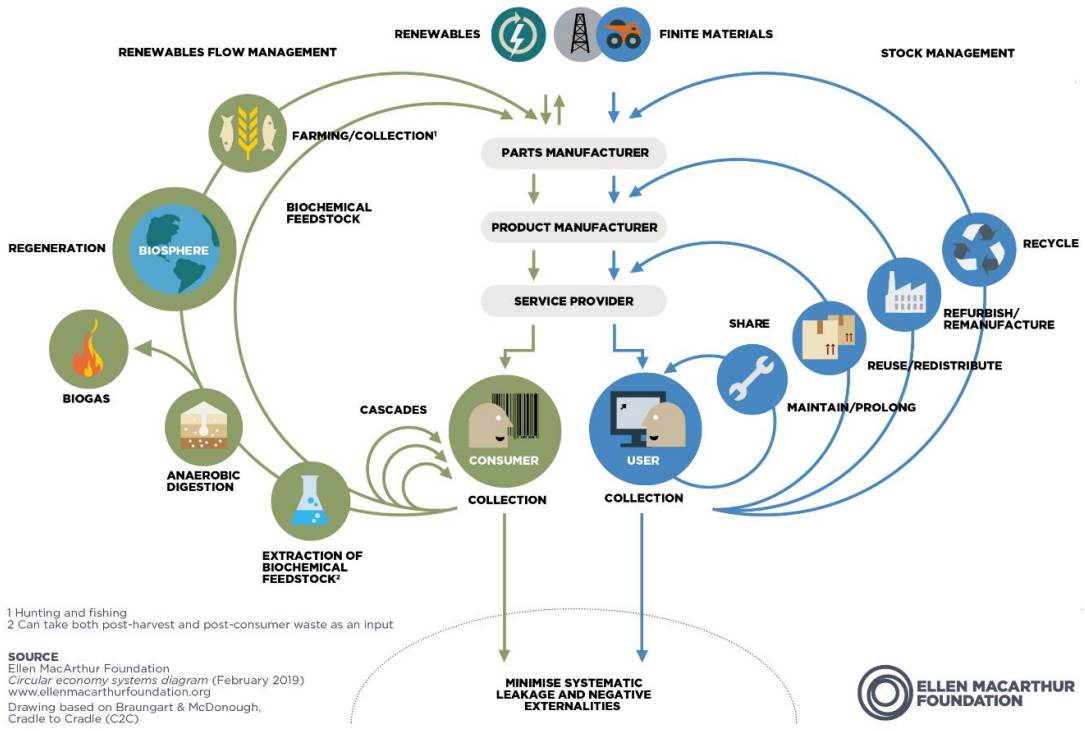

Figure 1: Butterfly diagram for Circular Economy representation.

On one hand the technical cycle describes how the products and materials are kept in circulation thanks to processes like repair, reuse, recycling and remanufacturing. On the other hand, the biological cycle shows how the nutrients from biodegradable materials are returned to the Earth to restore nature.

The European Union is actively promoting the Circular Economy concept. In fact, in March 2020 the European Commission presented a Circular Economy action plan to encourage the design of more sustainable products, the reduction of wastes and the creation of a market for secondary raw materials. In this scenario, low value by–products of traditional production chains, usually disposed of as waste, can be fed back into the economy as new raw materials.

Green Chemistry is the "design of chemical products and processes to reduce or eliminate the use and generation of hazardous substances". This definition was first introduced by P.T. Anastas and J.C. Warner, in Green Chemistry: Theory and Practice, 1998,[1] and this goal is pursued through 12 key principles, which comprehends for example waste prevention, use of safer solvents and auxiliaries and renewable feedstocks. Some variables were also introduced to measure how much a process is sustainable, and these are called Environmental Factor (E-factor), Atom Economy and Reaction Mass efficiency (RME). They are respectively defined as the conversion efficiency of a chemical process, the amount of waste produced and the percentage of reagents that end up in the product:

- E-Factor (g)= mass of waste (g)/mass of product (g)
- Atom Economy= Mw products/Mw reagents
- RME= (mass products/mass reagents)*100

The Green Chemistry can be applied almost to all the chemistry fields, such as organic, inorganic, analytical and so on. Many effort to make chemistry more environmentally friendly focus on the use of cleaner and more benign solvents (water, ionic liquids, deep eutectic solvents), renewable feedstocks (biomasses) and mild reaction conditions (microwave, sonication).
The concept of Green Chemistry can be applied not only to the academic research, but also to industry and many other fields, since the achievement of the sustainability is profitable not only for the research itself, but it is also one of the goals of the modern world.

Figure 2: Representation of Green Chemistry 12 principles.[2]

In this project, we pursued the Circular Economy and Green Chemistry principles by the exploitation of a new class of green solvents, the deep eutectic solvents (DESs), for the valorization of different agrifood wastes. From this perspective, the valorization through DESs of edible residues from vegetable oil industry and lignocellulose aims to decrease waste production, representing a tentative to achieve the goal of sustainability by using renewable feedstocks for the obtainment of high value-added compounds.

2. Biomasses Exploited in the Project

2.1. Residue from Edible Vegetable Oil Industry

One of the aim of the following thesis has been the valorization of acid degumming waste from seed oil for the production of high added value phospholipids (PLs).
Our interest on phospholipids started in our research group in 2017 with the beginning of the "SOAVE" project (Seed and Vegetable Oils Active Valorization through Enzymes), supported by Fondazione Cariplo and Innovhub (grant n. 2017–1015). This project was a collaboration between Politecnico di Milano, SCITEC-CNR and Oleificio Zucchi to develop enzymatic methods for the preparation of high value compounds from the by-products derived from the refining process of vegetable oils. In fact, crude vegetable oils are mainly composed of triacylglycerols, and minor components, such as PLs, diacyl and monoglycerols, fatty acids, tocopherols, sterols and many others, which effect the final quality of the products. These components are removed and recovered by a refining process, which consists in the following steps:

- Degumming: it aims to remove PLs and colloidal substances from vegetable oils, by a first water-based treatment, followed by an acidic one. In fact, the addition of water allows to remove the hydratable PLs, such as phosphatidylcholine and phosphatidylinositol, from the oil, while the treatment with an acid removes the non-hydratable PLs that are still present, such as phosphatidylethanolamine and phosphatidic acid.
- Deacidification: it reduces the free acidity of the fatty acids present in the oil to the neutralization, and it is usually carried out using NaOH.
- Winterization: it is essential to remove the crystallized components (waxes for examples) that are responsible for the turbidity of the oil.
- Deodorization: it removes the oxidized components with undesired taste and odor, to produce oils with better sensorial and organoleptic properties.
- Clarification: it eliminates the substances responsible for the excessive coloring of the oil.

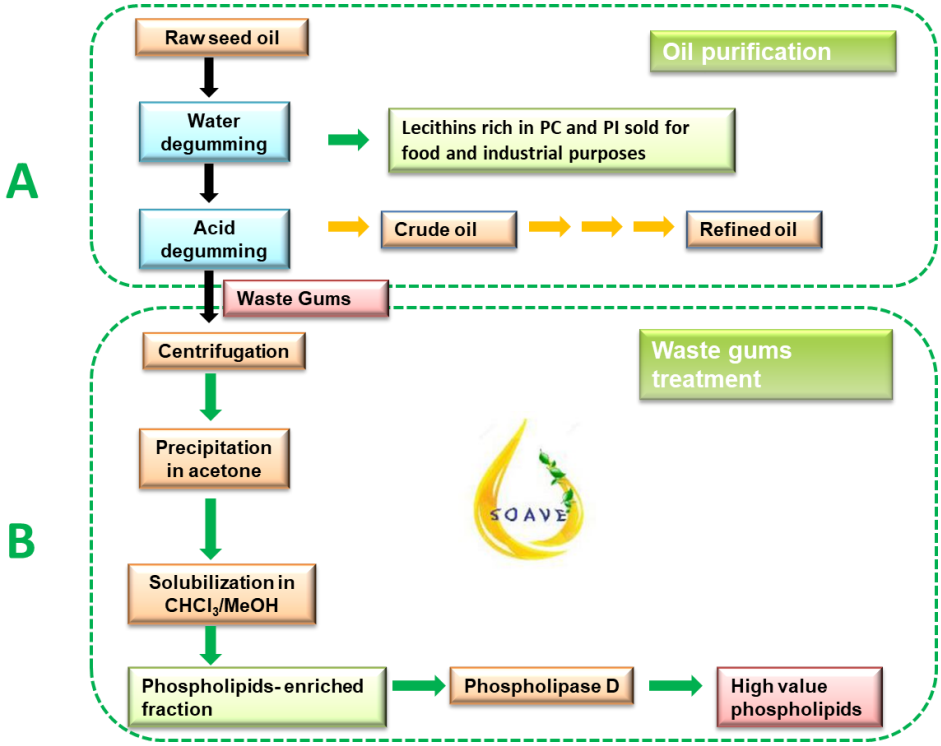

Figure 3: Summary scheme of vegetable seed oil purification and PLs extraction.

We focused on the residue recovered after the acid treatment of the degumming phase, called "waste gums", which is rich in PLs and other compounds in different concentration according to their origin. This residue was submitted to several physical separation steps to isolate the PLs, that were then enzymatically transformed to generate high value compounds.

The necessity to prepare modified PLs depends on the fact that PLs biological activity and commercial value are strictly correlated to the chemical identify of the polar head and the acyl chains. In fact, PLs are amphiphilic molecules that are ubiquitous in nature and play a fundamental structural role in all biological membranes.[3] From a structural point of view, PLs present a glycerol backbone, esterified at *sn-1* and *sn-2* positions with saturated and unsaturated long chain fatty acids, which constitute the lipophilic moieties, and in *sn-3* with a phosphate diester as the polar head group.

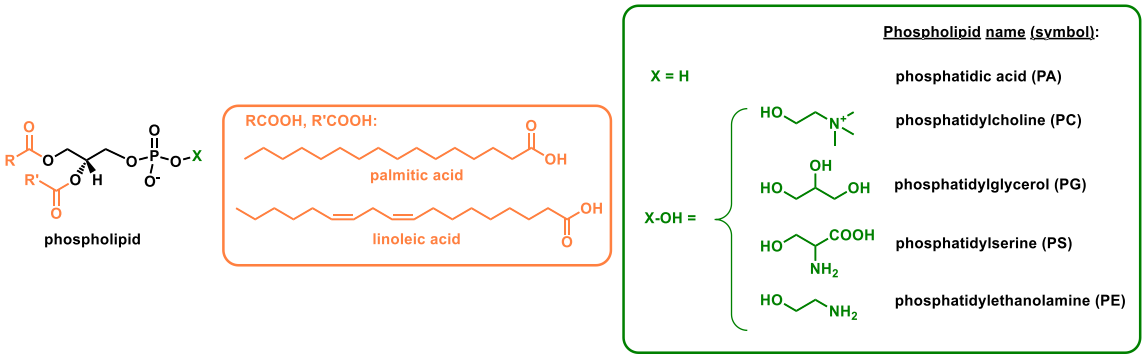

Figure 4: Structure of the main natural phospholipids. The acyl chains in orange are the most abundant in phospholipids extracted from soybeans.

Because of their structure, PLs present excellent biocompatibility and are studied in many different fields. Moreover, PLs are a nutritious source of fatty acid, organic phosphate and choline, and they are recognized to possess beneficial effects to human health, and for these reasons they are investigated for several biomedical applications. In particular, thanks to their amphiphilic nature, PLs are able to self-assemble to form liposome and micelles, and this characteristic has been largely exploited in the drug delivery studies, to design biocompatible carrier systems.[4-6] In addition, the capacity to spontaneously form aggregates made PLs interesting also as diagnostic markers[7] and as cosmetic additives.[8] Furthermore, PLs, in particular lecithin, are used in the food industry as emulsifiers and stabilizers thanks to their antioxidant properties[9] and because of their ability to be at the interface in an oil-water solution stabilizing lipid droplets.[10]

All these applications lead to a strong demand for PLs preparation methodologies, and the possibility to synthetize different PLs derivatives constitutes a central point in the research on this topic. Their chemical synthesis from appropriate homochiral precursors could be exploited, but it requires a multistep process and the use of a complex sequence of protection and deprotection step to introduce the desired functional group. Also, the extraction of PLs from natural sources could be done, but it could be particularly expensive, especially for some PLs derivatives. Therefore, the demand for biocatalytic approaches is increasing, especially when the final products destinations are to the food and the pharmaceutical industries, since they allow to work at milder conditions avoiding the use of hazardous and toxic reagents.
In particular, phosphatidylcholine derivatives are widely demanded, since PC is the most abundant natural PL, and it constitutes the 15% of lecithin composition. Its modification can occur both on the acyl chains and on the polar head leading to high value-added products, and their enzyme-mediated modifications include hydrolysis, transphosphatidylation and transesterification. In particular, phospholipase A_1 and A_2 (PLA_1 and PLA_2) perform hydrolysis respectively of the acyl chain in position *sn-1* and *sn-2*, producing 2-acyl and 1-acyl-lysophospholipids (1-lysoPL and 2-lysoPL); phospholipase C (PLC) eliminates the phosphoric ester on the glycerol side, and phospholipase D (PLD) cleaves the molecule on the polar head.[11-12]

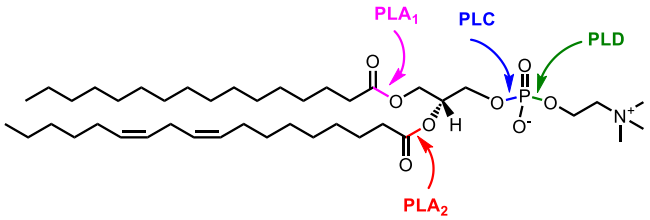

Figure 5: Enzymes acting on phosphatidylcholine (here reported as 1-palmitoyl-2-linoleoyl-phosphatidylcholine) and their specific site of action.

In particular, in the SOAVE project, we focused on the recovery of PLs from soybean, peanuts and corn oil, and their transformation by phospholipase D enzyme, which catalyzes, in addition to the PC hydrolysis into phosphatidic acid (PA), the transphosphatidylation of the substrate in presence of an alcohol (X-OH) leading to PX formation.

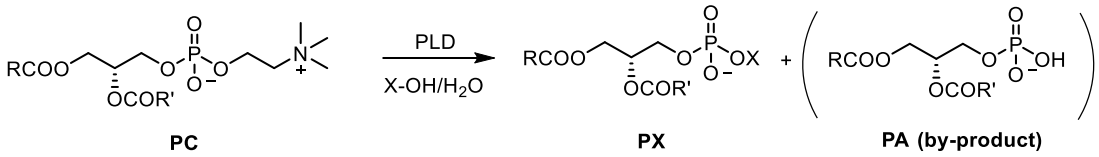

Figure 6: Reaction scheme of a phospholipase D (PLD)-mediated polar head transphosphatidylation of PC.

Thanks to the acquired knowledge, in this work we present the transphosphatidylation reaction of PC derived from commercial soybean lecithin into phospholipids of commercial interest obtained using alternative green reaction media.

2.2. Lignocellulose Based Biomasses

Lignocellulose, also known as plant biomass, is categorized in hardwood, softwood, agrifood waste, and grasses, and its composition is strictly dependent on its origin. However, lignocellulose main components are polysaccharides (cellulose (29-47%), hemicellulose (25-35%)) and lignin (16-31%), linked together in a highly heterogeneous structure (Figure 7).[13]

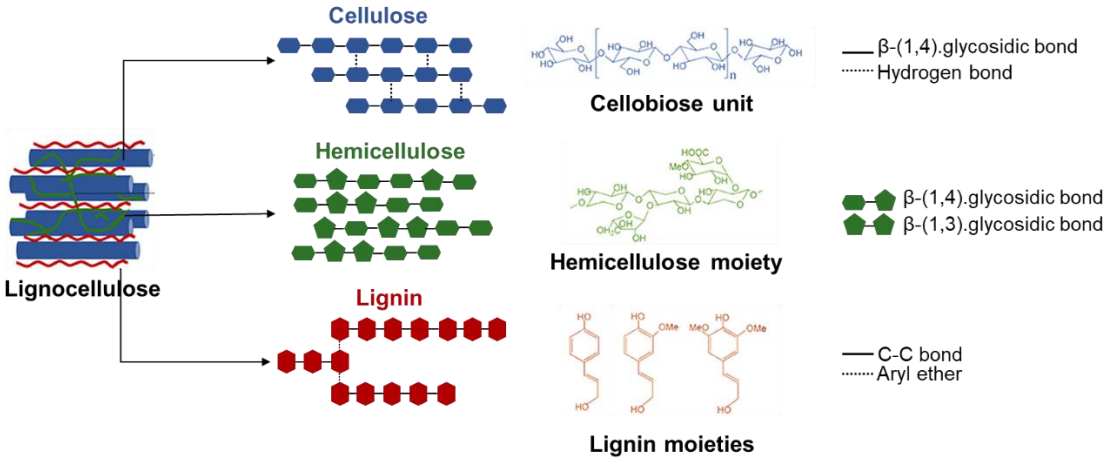

Figure 7: Schematic structure of lignocellulose.[14]

Other factors that could influence lignocellulose composition are the part of the plant, growth conditions, and harvesting time. Moreover, traces of inorganic compounds (such as calcium, sodium, potassium, magnesium, phosphorus, silicon, aluminum, and iron), pigments, alkaloids, and waxes could be detected in lignocellulosic biomass.[15]
Briefly, cellulose is considered the most abundant biopolymer, and it is a linear polymer constituted by the repetition of D-glucose units linked by β-1,4 glycosidic bonds, and has a degree of polymerization between 4000 and 6000 in woody biomass. Cellulose contains both crystalline and amorphous structures, which are linked together to form microfibrils and covered by hemicellulose and lignin.[16-17]
Hemicellulose is a polysaccharide composed of monosaccharides such as pentoses (arabinose, xylose) and hexoses (glucose, galactose and mannose), and also of uronic

acids, rhamnose and fucose in some traces. All these molecules are bonded together by glycosidic and fructose ether linkages and form a branched polymeric structure.[18-19] Hemicellulose has a low degree of polymerization (80-200), is highly amorphous and susceptible to hydrolysis, making it the appropriate subject for valorization studies.
Finally, lignin is an aromatic polymer obtained by the oxidative coupling of phenylpropane units called monolignols: *p*-coumaryl alcohol, coniferyl alcohol and synapyl alcohol, containing zero, one and two methoxy groups respectively. The corresponding units in lignin are known as p-hydroxyphenyl (H), guaiacyl (G) and syringyl (S) units, and they are organized randomly in the totality of the structure.[20]

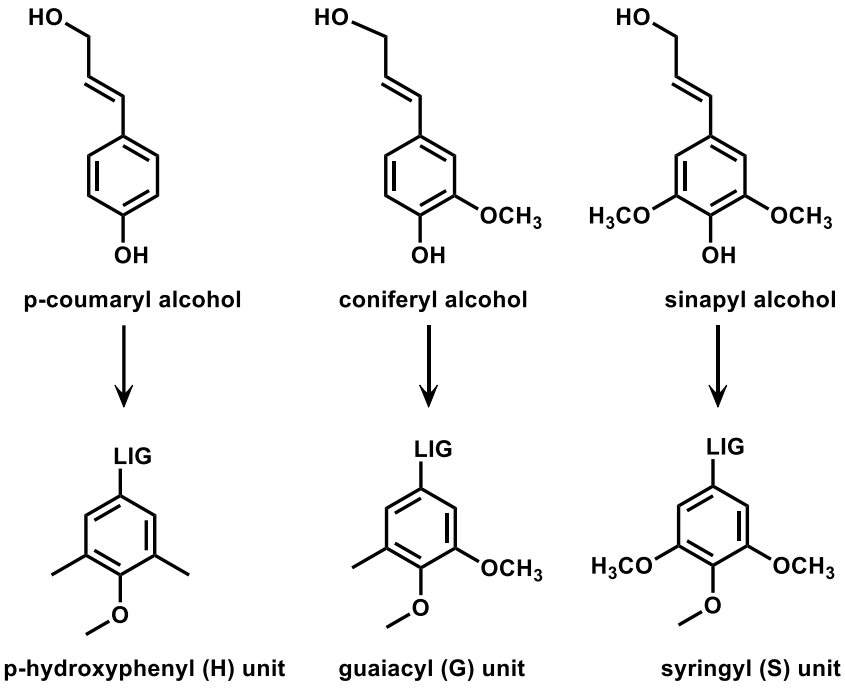

Figure 8: Lignin monolignols.

These monomers are linked by several C-C and C-O-C non-hydrolyzable bonds, and the mojority of them consists in β-O-4 bonds. Lignin also is a hydrophobic polymer, that makes the cell wall impermeable to water, and ensures water and nutrients transport into the cells.[21]
In this work, the focus has been pointed on lignocelllosic biomass pretreatments and on the recovered lignin fractions. In fact, biomass pretreatments are necessary for lignocellulose exploitation, since it allows the separation of the main components and their recovery. It is calculated that about 181.5 billion tons of lignocellulosic biomass are generated each year, and the majority is disposed of as waste or burned, to avoid the storage costs. However, lignocellulose, thanks to its low cost, availability and composition can find applications in many different fields, from biofuels, to polymers, to the synthesis of food or pharmaceutical precursors.[22-23]

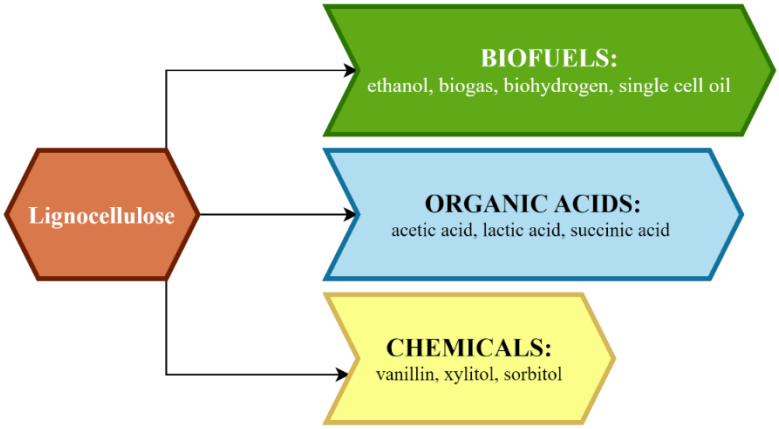

Figure 9: Lignocellulose possible applications.

In the past, the main aim of the biomass pretreatments was the obtainment of biofuels, while lignin and hemicellulose were disposed of. Only recently, the focus has been moved on the recovery and the whole exploitation of each fraction of the biomass. In general, pretreatments can be categorized as physical, chemical, physicochemical and biological approaches, and the ideal pretreatment is economically advantageous, enviromental friendly and simple. The principal focus should be the obtainment of a high value compounds from a waste biomass using a low-cost process.

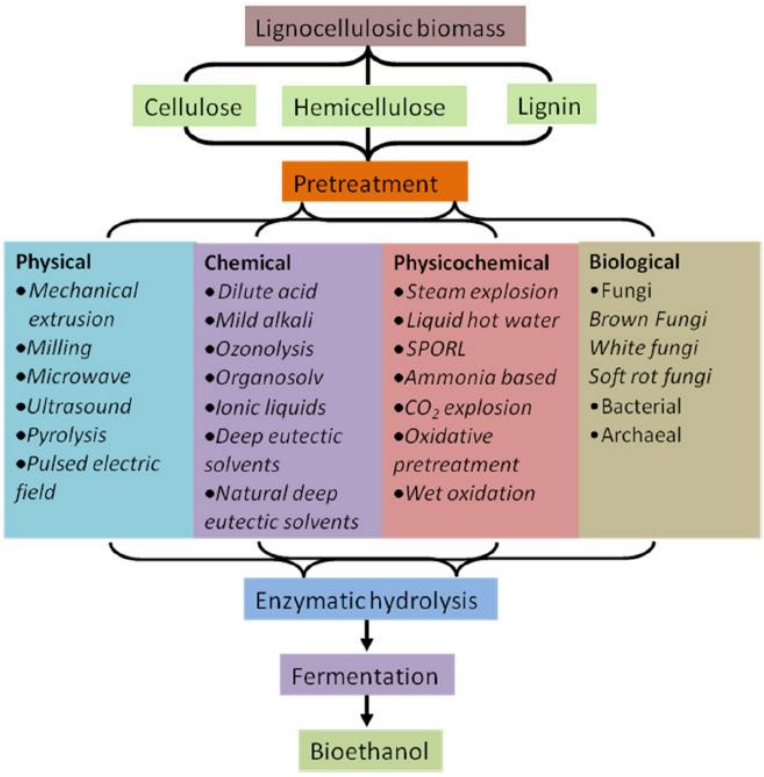

Figure 10: Scheme of the most important lignocellulosic pretreatments.[24]

1) Physical pretreatments: they aim to the reduction of biomass size and of its crystallinity. They include milling, extrusion, freeze pretreatments and pyrolysis. They

are all based on the reduction of the biomass size and of its crystallinity. However, their main drawback is that these methods often require to be combined with others and are too expensive to be used in a full-scale process.

2) Chemical pretreatments: they are the most used, also in industries on large scale since most of them have a significant effect on biomass structure. They are the most promising methods to separate cellulose/hemicellulose/lignin and to reduce crystallinity of cellulose. They are also particularly interesting since they can operate at normal temperatures and pressure, however they are responsible for the production of hazardous and toxic wastes Chemical pretreatments include acid/alkaline processes and organosolv methods. Acid/alkaline methods are the most used to recover cellulose/hemicellulose, and in general to delignify the biomass. On the other hand, the organosolv ones are used in lignocellulose with a high percentage of lignin, because it is able to extract lignin that can be valorized.

3) Physicochemical pretreatments: the most exploited is the steam explosion in which the biomass particles are treated with steam at high temperature for few minutes in order to increase successively the activity of enzyme on cellulose and hemicellulose. Also, CO_2 explosion pretreatment can be used, and one of the major advantage is that CO_2 molecules can penetrate into lignocellulose pores. This process requires lower temperatures and it is less toxic and non-flammable.

4) Biological pretreatments: they don't require chemical solvents or particular physical conditions, such as temperature and pressure. For these reasons, biological pretreatments are environmentally friendly, and they especially use white rot fungi to delignify the substrate and to facilitate the enzymatic hydrolysis of cellulose and hemicellulose. The efficiency of this method can be influenced by the particle size, moisture content, time and temperature. However, they are not largely used in industry since they require long process time, large scale requirement and continuous monitoring of microorganisms.[25-26]

5) New approaches: they are born to solve some problems of the methods already mentioned, like the production of toxic wastes or the requirement of high levels of energy. For these reasons new green solutions are now emerging, especially in the food industry, and they comprehend ionic liquid (ILs), DESs, the utilization of microwaves and ultrasound technologies. These methods have some advantages in environmental terms, however, they also show some drawbacks, like the production costs and minor efficiency that make them less exploited than the traditional ones.

In this thesis work, we decided to exploit DESs for the fractionation of two different biomasses particularly abundant in our regional territory: brewer's spent grain (BSG) and rice husk (RH).

2.2.1. Brewer's Spent Grain

BSG is the main by-product of the brewing industry and it is estimated to be the 85% (w/w) of the total waste. In fact, for every kilogram of beer, about 0.12 kg of dried BSG are produced (equivalent to 0.2 kg of wet BSG), and the estimated global annual production of beer is around 38,600,000 metric tons.[27-28]

BSG is the final residue obtained by the beer making process. Firstly, the malted grains and the other requested materials are crushed, mixed with water and then heated. In this step, called mashing, the sugars are solubilized in water and two enzymes, α and β amylases, are added. Then the lautering step starts: the enzymes are inactivated, the insoluble spent grain (BSG) and the wort are removed and the hops boiled and filtrated away. At the end the yeasts are added, essential for beer fermentation and aroma. [28]

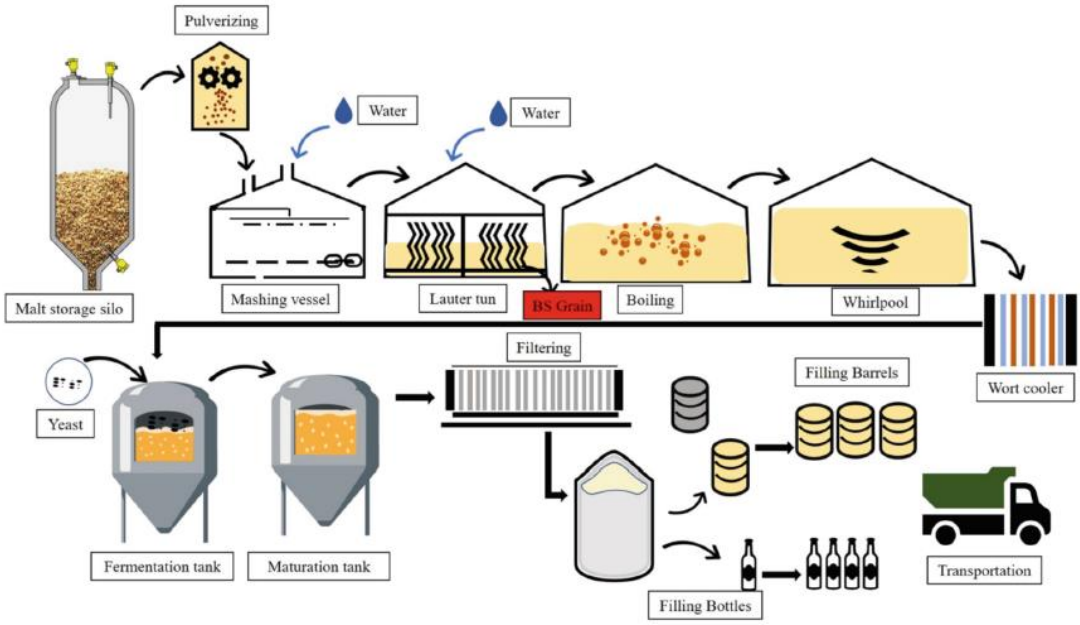

Figure 11: Scheme of beer preparation.[28]

The residual grains are composed of layers of peel, pericarp, and seeds with residual amounts of endosperm and aleurone from barley used as raw material.[29] BSG composition depends on several factor, such as the type of barley grains, the harvesting time, the brewing technology, and the process parameters. However, typically it comprehends 15-25% proteins, 50-70% fibre (hemicellulose, cellulose, and lignin), 5-10% fats, and 2-5% ashes. In particular, glucose, xylose, and arabinose are the most abundant monosaccharides in BSG, while hordeins, glutelins, globulins, and albumins are the majority of the proteins. For what concern the lipids, BSG contains triglycerides at high percentage, followed by free fatty acids.[30] Even if at minor concentration, BSG contains several minerals (calcium, iron, magnesium, phosphorous, manganese ecc), vitamins (biotin, choline, folic acid, pantothenic acid ecc) and amino acids (essential: leucine, valine, threonine and lysine; non-essential: alanine, serine, glycine, glutamic acid, aspartic acid, tyrosine, proline, arginine). In addition, some hydroxycinnamic acids with interesting anti-inflammatory and antioxidant activity, such as ferulic and coumaric acid derivatives, could be extracted from BSG.

However, one of the main drawbacks of BSG production is its moisture content, which is around 80%, that, in addition to its high content in lipids and protein, make this biomass particularly subject to microbial contamination. Thus, BSG has a very short lifespan (7-10 days), and this makes difficult its storage and further exploitation. Also, even if this biomass is disposed of, it is counted that, without drying pretreatments, every ton of BSG

release 513 kg of CO_2.[31-33] The majority of the BSG processes for its further exploitation aims to reduce the moisture from 80 to 10%, by drying (oven or autoclave) or pressing and filtering the biomass.[29]

The whole biomass actually is used in several fields, that comprehends mainly pet/human food production and substrate for fermentations. For what concern the food industry, it is counted that currently 70% of produced BSG is send from the breweries to farms as animals feed, since it provides, together with a nitrogen source, the essential amino acids for ruminants. BSG is also used in food production, for a maximum of 15% on the total mass, for example in pasta, bread and pastry products. In fact, thanks to its high content in fibres and protein, and its low content in ash, it has some beneficial gastrointestinal effect.[34-35] Regarding the utilization of BSG as fermentation substrate, it could be used as source of sugars for different microbial cultivation, for the synthesis of enzymes (such as cellulase, amylase)[36], high value compounds like xylitol[37] and lactic acid,[38] prebiotics[39] and ethanol.
However, thanks to the spreading of Green Chemistry and Circular Economy, BSG fractionation and pretreatments are gaining relevance in the scientific scenario, allowing the complete exploitation of the whole biomass and the extraction of its valuable compounds. In literature different techniques are reported, summarized in Figure 12, and they allow the separation of sugars from lignin, and the extraction of proteins, lipids and phenolic compounds.

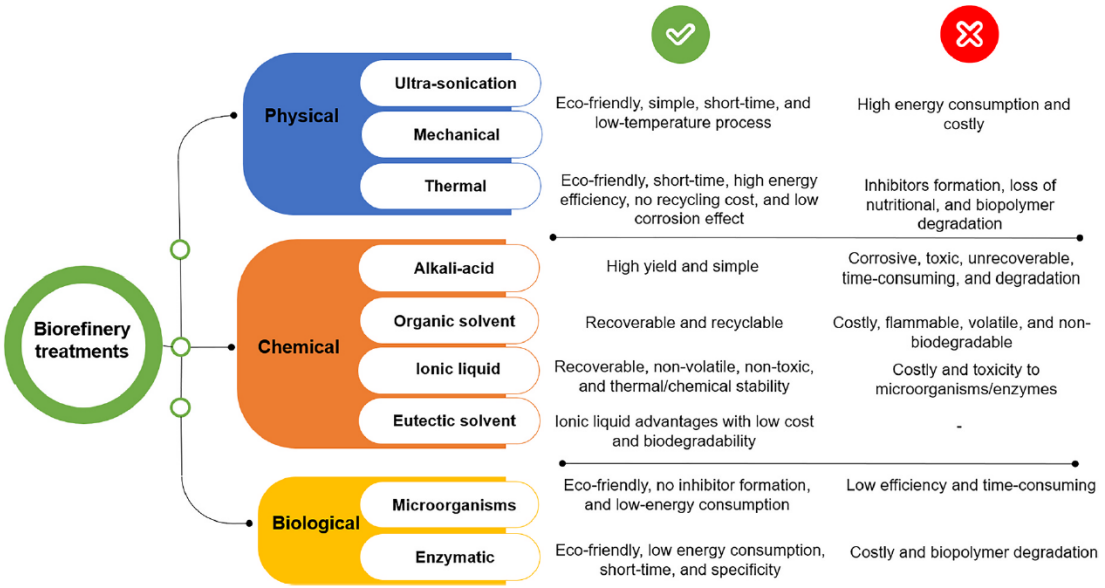

Figure 12: Scheme of possible BSG pretreatments.[33]

2.2.2. Rice Husk

Rice, botanically known as Oryze, is a monocotyledon plant, and consists of two cultivated species and 21 wild species. The cultivated ones, called Oryza sativa and Oryza glaberrism, are native of Asia and Africa respectively. In Asia, over 90% of the total worldwide rice production is satisfied, especially in China and India, where the

production corresponds to 28 and 19% respectively. Rice constitutes the major source of supply for approximately half of the world population, and its request is expected to remain unchanged over the years, thanks to the continuous economic and population growth in Africa and Asia.[40]
It is estimated that 755 million tons of rough rice (also known as paddy rice) were produced worldwide in 2019, and it is counted that for every kg of paddy rice, between 0.41 and 3.96 kg of rice straw are produced. Rice husk (RH) consists in the 20-33% of the total paddy weight, and it is possible to estimate a global annual rice husk production of 150 million ton. Typically, paddy rice is composed of 20% of rice hull, 11% of bran layers and 69% of starchy endosperm (total milled rice). RH is the outer layer of the paddy grain, and it is separated from the grains during the dehusking, process,[41] that consists in two rubber rolls where the paddy rice is put in under a continuous steam. The two rolls rotate in different directions and at different speed allowing the separation of the husk.[42]

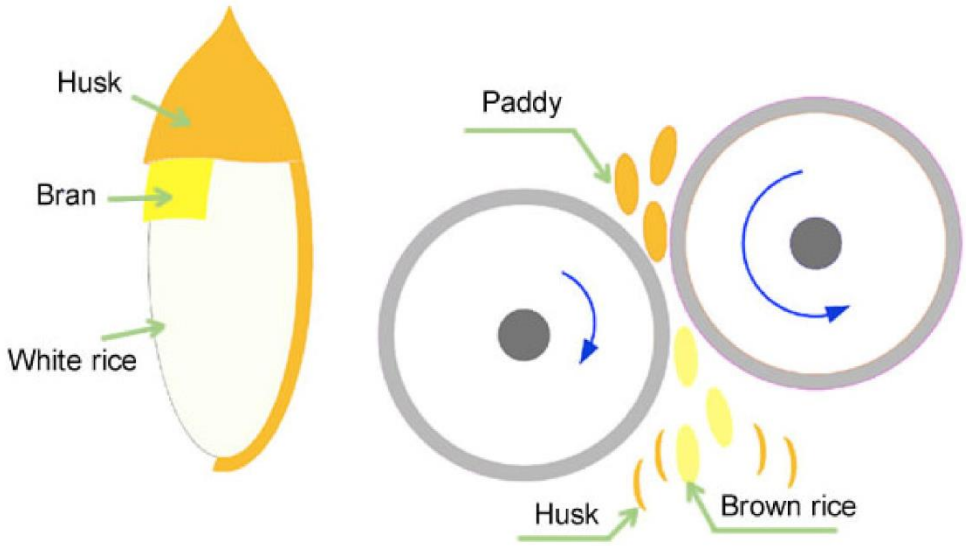

Figure 13: Scheme of dehusking process (Rice Knowledge Bank).

Almost 20% of the worldwide rice is submitted to a parboiled process to obtain the parboiled variety (also called white rice). This process consists into a rice starch hydrothermal treatment which aim to its gelatinization. Parboiled rice has some advantages respect to the non-parboiled one (raw or yellow rice), such as improved yields, enzyme inactivation, sterilization, retention of vitamins and amino acids. For these reasons, the demand for parboiled rice has increased during the last years, thanks especially to its low costs and beneficial effects on the human health.[42-44]
RH composition depends on many factors, like the type of paddy rice, the climate and the geographical location, but it is mainly composed by cellulose (29-42%), hemicellulose (14-29%) and lignin (13-24%), and it differs from other lignocellulosic biomasses by its high content of silica and ashes (10-15%), which makes it suitable for the production of building materials, bio-based adsorbents and for pollutants removal from wastewater. In addition, RH presents low nutritional values, so it is mainly burned to produce the so-called rice husk ashes (RHA). Usually, they are prepared through a two-step process, which involves firstly the biomass carbonization in absence of oxygen and then its

physical or chemical activation. RHA are mainly used as fertilizers, adsorbent, biochar and in concrete preparation.
On the other hand, if RH is submitted to pretreatments processes, it can be used also as raw material for the production of interesting chemicals such as ethanol, furfural, xylitol, acetic acid, and lignosulfonic acids. Therefore, the availability of this huge quantity of wastes and their low cost have pushed the current research towards the investigation and development of new sustainable possible applications for such materials.[45-47]

3. Deep Eutectic Solvents

The term eutectic derives from greek ευτηκτος (eutektos) and means easy to melt, and was first used by the British physicist Frederick Guthrie in 1884 to describe "a lower temperature of liquefaction than that given by any other proportion".[48] Only in 2003 Abbott used the term "deep eutectic solvent" to describe a liquid eutectic mixture with lower melting temperature than its components, property derived from the charge delocalization caused by the hydrogen bonds formation.[49] In fact, DESs are described as a binary or ternary mixtures between a hydrogen bond donor (HBD) and a hydrogen bond acceptor (HBA) which form a HBD—HBA supramolecule.[50-51] The first DES reported by Abbot consisted of urea and choline chloride. DESs can be described by the formula Cat^+X^-zY, where

- Cat^+: any possible ammonium, phosphonium or sulfonium cation
- X^-: Lewis base anion
- Y: Lewis or Bronsted acid
- *z*: number of molecules of Y interacting with X^-.

Commonly DESs are described by a phase diagram, that shows how the HBA and HBD mixture only at a specific molar ratio reach the "deep" eutectic point that corresponds to the lowest melting temperature of the two compounds, while, before and after this point, the solvent is just the simple mixture of the two compounds, and it is not possible to properly talk about DESs.

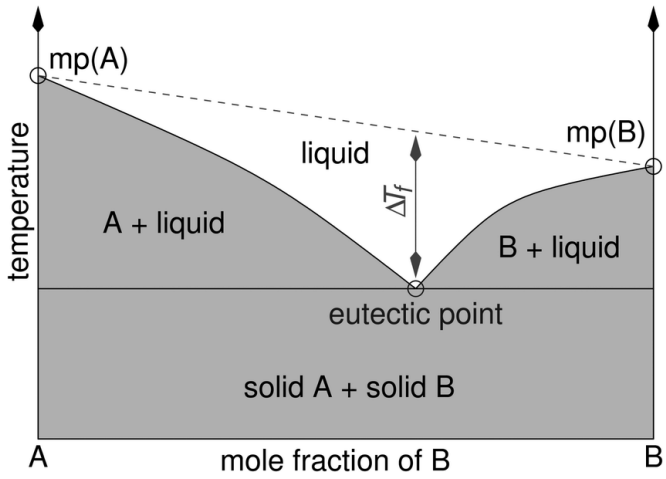

Figure 14: Phase diagram of a solid-liquid mixture.[52]

In general, it is possible to distinguish DESs into five categories according to their

components: (i) Type I: quaternary ammonium salt and metal chloride; (ii) quaternary ammonium salt and a metal chloride hydrate; (iii) quaternary ammonium salt and a HBD (typically an organic molecular component such as an amide, carboxylic acid, or polyol); (iv) metal chloride hydrate and HBD; (v) relatively new class composed of only nonionic HBAs and HBDs.[53] The type III DESs are usually the most studied and reported in literature, especially the mixtures composed by choline chloride as quaternary ammonium salt. In fact, choline chloride is widely used since it is approved as a natural additive for many animals' species, is cheap, biodegradable and non-toxic. In this category of DESs, many different HBD are used, in particular amides, alcohols, and carboxylic acids. More recently, the use of hydrophobic compounds such as tetrabutylammonium bromide, menthol, thymol, and fatty acids as hydrogen bond acceptors together with long alkyl chain alcohols and carboxylic acids as hydrogen bond donors, led to the introduction of a new type of DES: the so-called hydrophobic DES.[54]
Recently, in 2011, Choi *et al.*[55] introduced the concept of "natural DES" (NADES), derived by the combination of quaternary salts with primary metabolites such as organic acids, amino acids and sugars.

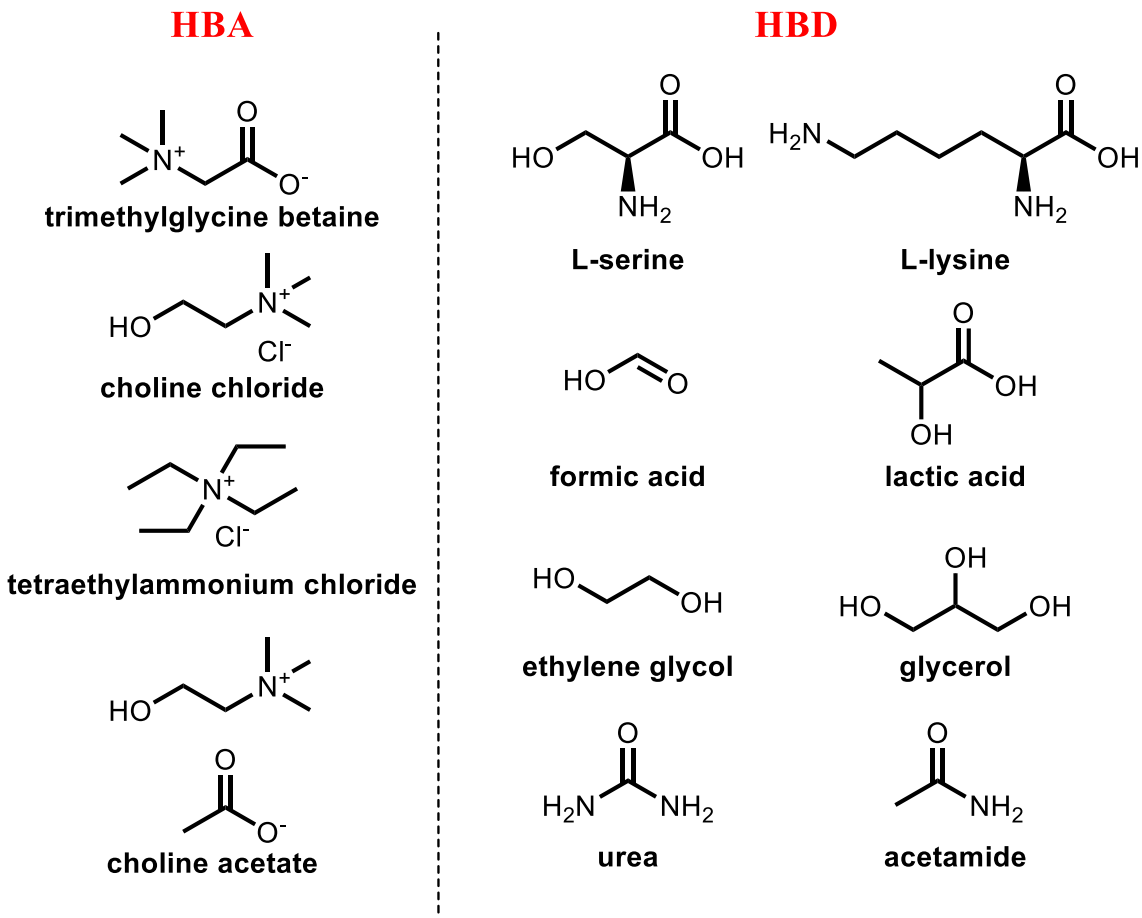

Figure 15: Examples of typical hydrogen bond acceptors (HBAs) and hydrogen bond donors (HBDs) used in DES preparation.

Furthermore, DESs preparation is very easy, and two principal techniques are used: the

heating and the grinding methods. For what concern the first one, it only requires the mixing of the main components (solid and liquid, or solid and solid) at high temperatures (50-100 °C) for few hours, until a clear and homogeneous mixture is obtained.

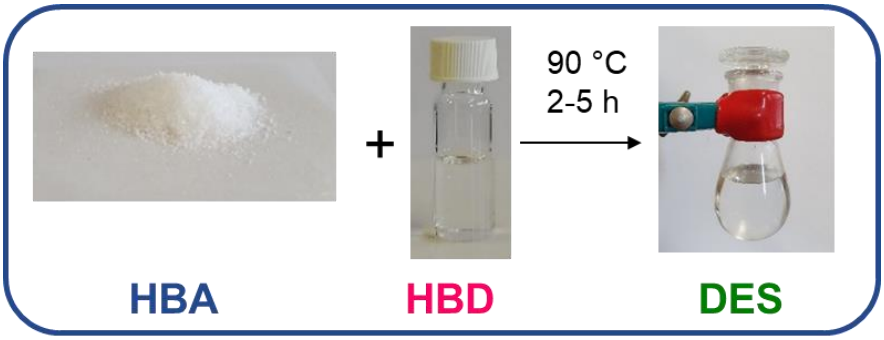

Figure 16: Schematic representation of DES preparation by heating method.

However, one of the main drawbacks of this method is the possibility of esterification reaction between HBA and HBD, especially when carboxylic acids are used as HBD, leading to DES degradation.[56] Instead, the grinding method consists in mixing the DES components at high temperature and then grinding them in a mortar until a homogeneous clear liquid is obtained.[57] Even if less exploited, in literature other DESs preparation procedures are reported, such as the freeze-drying,[58] the evaporation methods and the microwave/ultra-sound-assisted approaches.[59-60]

DESs are particularly attractive not only for the many possible combinations of the components and their easy preparation, but also due to their peculiar physicochemical properties such as low volatility, non-flammability, low vapour pressure, chemical and thermal stability, and low toxicity.[61] Thanks to these characteristics, in the last decade DESs became highly investigated, also replacing ionic liquids (ILs) as a green solvent option, since DESs are cheaper to produce, biodegradable and less toxic. Until few years ago, DESs and ILs tent to be considered equals, and ILs were widely exploited for many different applications. It is only from the beginning of 21st century that DESs became popular and have been proposed as a greener and cheaper alternative to ILs. Prompted by all these above considerations, DESs are studied in many different fields like metallurgy,[62] liquid-liquid extraction,[63] CO_2 capture,[64] biocatalysis and organic chemistry, biomass processing[65-66] and many others. However, despite their large exploitation, the scientific community is highly debating about what can be considered a DES and what a simple mixture of compounds, which are the main parameters to consider in the definition of a DES and how the presence of water influences the DES formation.[67] With this in mind, the term "DES" is often abused because of the limited number of publications devoted to understand DESs nature, and the absence of a standard cheap and replicable method to define theme. In fact, it is common in literature to find different molar ratios of the same HBA-HBD combination all defined as DESs. Concerning the water role in DESs formation, the maximum quantity at which DES supramolecule resist, and how water influence DES properties is also not well clarified. In fact, it is known that a small percentage of water, called embedded water, is necessary for DES preparation,[68] but at high concentration it pervades the DES supramolecular structure forming H-bond both with HBA and HBD, disrupting the system and changing its characteristics, like viscosity, density and electrical conductivity.[69]

In this PhD thesis, the preparation of various DESs has been investigated and analytically studied together with their utilization in biocatalysis and biomass fractionation.

3.1. DESs Analysis by ^{1}H NMR Measurements

Even if DESs are largely applied in many fields, it is still unclear how HBA and HBD interacts, how the supramolecule is formed and the influence of water in it. To answer these questions, scientific community often uses NMR technique, since it is a powerful tool in understanding the structure, the dynamic and the interactions in DESs. In literature many different NMR analysis are reported, such as ^{1}H NMR,[70] ^{13}C NMR, NOESY[71] and relaxation time (T_1 and T_2) measurements,[72] and in this thesis we applied the NMR on DESs in several studies for different purposes.
Firstly, ^{1}H NMR has been used to evaluate the HBA/HBD molar ratio in DESs composition. In particular, the analysis was conducted at room temperature and it took only few minutes allowing to understand the real composition of the solution, only by simply integrating the spectrum signals. An example is reported in Figure 17, where the composition of DES trimethylglycine betaine/ethylene glycol 1:2 has been verified. In particular, the signals at 3.22 and 3.85 ppm correspond respectively to N-$\underline{(CH_3)_3}$ (s, 9H) and N-$\underline{CH_2}$-COOH (s, 2H) of trimethylglycine betaine, and the signal at 3.63 pmm to OH-$\underline{CH_2}$-$\underline{CH_2}$-OH (s, 8H) of ethylene glycol, and the integral of ethylene glycol signal confirms that the HBD is twice the HBA in molar ratio.

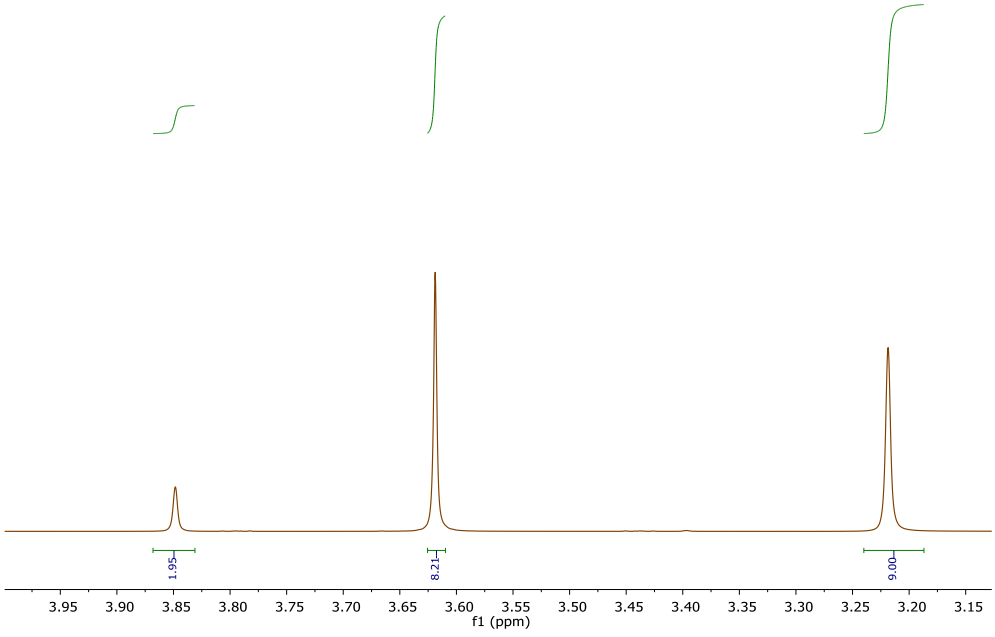

Figure 17: ^{1}H NMR of DES trimethylglycine betaine/ethylene glycol 1:2.

Another application here reported is the validation of DESs recycling in Chapter 2 and 3. In fact, after the lignocellulose fractionation, DES choline chloride/lactic acid has been recycled by water evaporation, and the purity was tested by ^{1}H NMR (Figure 18). As reported in the spectrum, the recycled DES (Figure 18 b) doesn't present peaks attributable to lignocellulosic material.

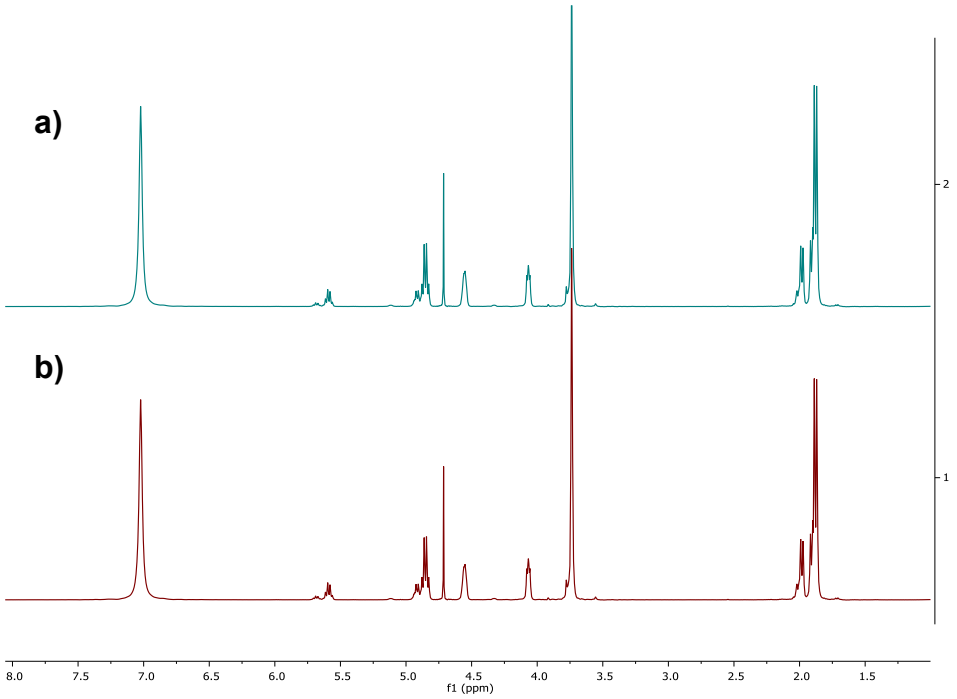

Figure 18: ^{1}H NMR of a) pure DES choline chloride/lactic acid; b) recycled DES choline chloride/lactic acid.

Finally, the T_1 relaxation time parameter has been investigated in order to identify the molar ratio at which the HBA-HBD solution is a DES and not only the simple mixture of the two components. In fact, T_1 measurements quantify the rate of transfer of energy from the spin to the environment and, for this reason, is strictly dependent on molecules weight and size. Prompted by these considerations, we recreated the DESs phase diagram (Figure 14) by ^{1}H NMR relaxation time measurements, identifying the eutectic point as the HBA-HBD mixture with the lowest relaxation time, calculated by inversion recovery (see Figure 3 of Chapter 1). In fact, firstly a 180° pulse was applied to the sample at a specific timing, so the magnetization went from z to -z, then a 90° pulse flipped the magnetization from z axis to xy plane to be detected, and it resulted in the fitting reported in Figure 19.

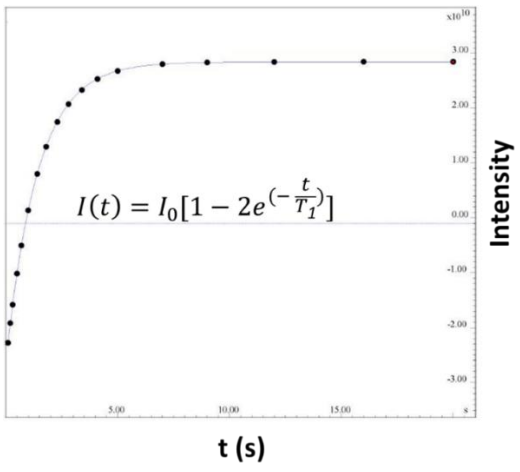

Figure 19: Inversion recovery spectrum of DES trimethylglycine betaine/ethylene glycol (1:3).

3.2. DESs in Biocatalysis

Water is the main solvent used in biocatalysis, but this often represents a problem, since the majority of substrates and reagents possess a hydrophobic nature, which leads to a low solubility in the media. For this reason, nowadays research in biocatalysis is focusing on finding alternative non-aqueous solvents, which show some advantages such as positive effect on the reaction equilibrium and decrease in water side-effects. In this sense, organic solvents (mainly hexane, toluene, dichloromethane) are mostly used, but they don't reflect the need of Green Chemistry on finding green solutions that promote the utilization of biocompatible, biodegradable and non-toxic solvents. Thus, the exploitation of DESs is gaining relevance and many studies are reported with different combinations of HBA and HBD. DESs in biocatalysis can have different application: (i) co-solvent together with water/buffer to solubilize the substrate; (ii) reaction medium without addition of water; (iii) reaction solvent and substrate of the reaction.[73]

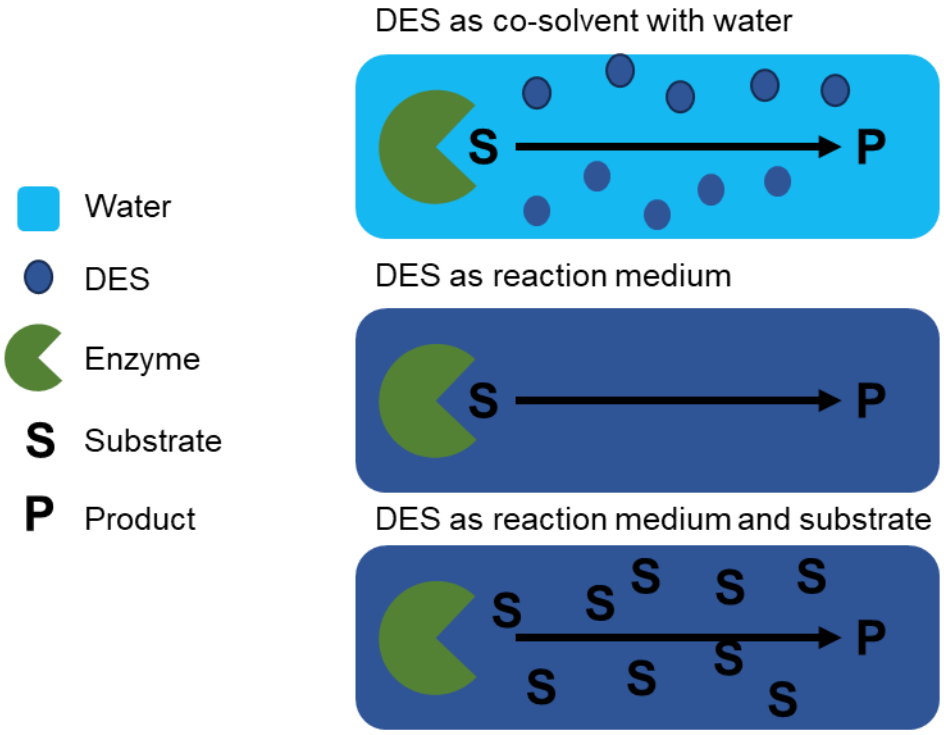

Figure 20: DESs applications in biocatalysis.

Some crucial factors must be considered when DESs are applied to biocatalysis, such as the necessity to add water and the combination of HBA and HBD used. For what regard the water addition, it seems that a small amount of water is necessary to decrease the DESs viscosity making the reaction more manageable, and to enhance the activity of several enzymes. However, in literature it is not clear how much water is tolerated by the eutectic mixtures before its dissolution. Concerning the HBA/HBD choice and ratio, this can influence DESs viscosity, the mass transfer and reaction rate, and interfere with the enzyme. In fact, DESs intramolecular H-bonds could be responsible for increasing enzyme affinity for the substrate, and DESs composition could change the secondary and 3D structure of enzymes, provoking unfolding and refolding processes that influence stability over time and activity. For example, choline chloride-based DESs seem to be

more likely to disrupt the α-helix structures, provoking enzyme instability. Finally, water content and DESs composition are two influencing factors on the total reaction efficiency.[74]
DESs in biocatalysis have been particularly exploited for lipase reactions.[75] For example, Cao *et al*. tested different DESs on the transesterification of benzyl alcohol with vinyl acetate performed by *Candida antartica* lipase B (CALB) and found out that hydrophobic DESs had positive effects on enzyme activity, reaching 57% of yield in 12 hours.[76] Lately DESs have been tested also as solvent/co-solvent for whole-cell catalysis. Yang *et al*. proposed the enzymatic conversion of isoeugenol to vanillin by *Lysinibacillus fusiformis* CGMCC1347 cells, testing more than 40 DESs/NADESs, improving the final yield of 130-140% respect to the DESs-free reactions.[77]

The novelty of this PhD work consists into the use of DESs to perform PLD-catalyzed biotransformation of PC derived from soybean. In fact, usually, PC transformation is performed in a biphasic system organic solvent/buffer in presence of an alcohol, and then the products are recovered by extraction. In this study, DESs, called for that reason reactive-DESs (RDESs), have been used as solvents and as the donors of the alcoholic moiety reacting with the substrate, allowing the preparation of added-value compounds recovered easily only by filtration, avoiding the use of hazardous organic solvents.

3.3. DESs in Biomass Fractionation

One of the main steps for an efficient lignin valorization is the lignocellulose fractionation. In the last 15 years, different methods have been reported, such as acid or basic treatments, but often they generated a modified/condensed lignin. Prompted by these results, researchers have studied the development of new systems to fractionate biomasses and recover native lignin, such as the use of ILs and DESs. DESs were firstly used in biomass fractionation in 2012, and since that type III DESs were the most studied for this purpose, like for example choline chloride mixed with lactic acid/glycerol/ethylene glycol/2-propandiol and amines.[78] The effectiveness of the process depends on several factors such as pretreatment conditions (temperature, time, and solid-to-liquid ratio), type of HBA and HBD, and type of raw material. In general, DES-mediated fractionation starts with the hemicellulose hydrolysis and lignin extraction, while cellulose tendentially remains insoluble in DESs. Lignin extraction is promoted by the cleavage of ether bonds between lignin polymers and ester and carbohydrate complex between hemicellulose and lignin,[79] as reported in Figure 21.

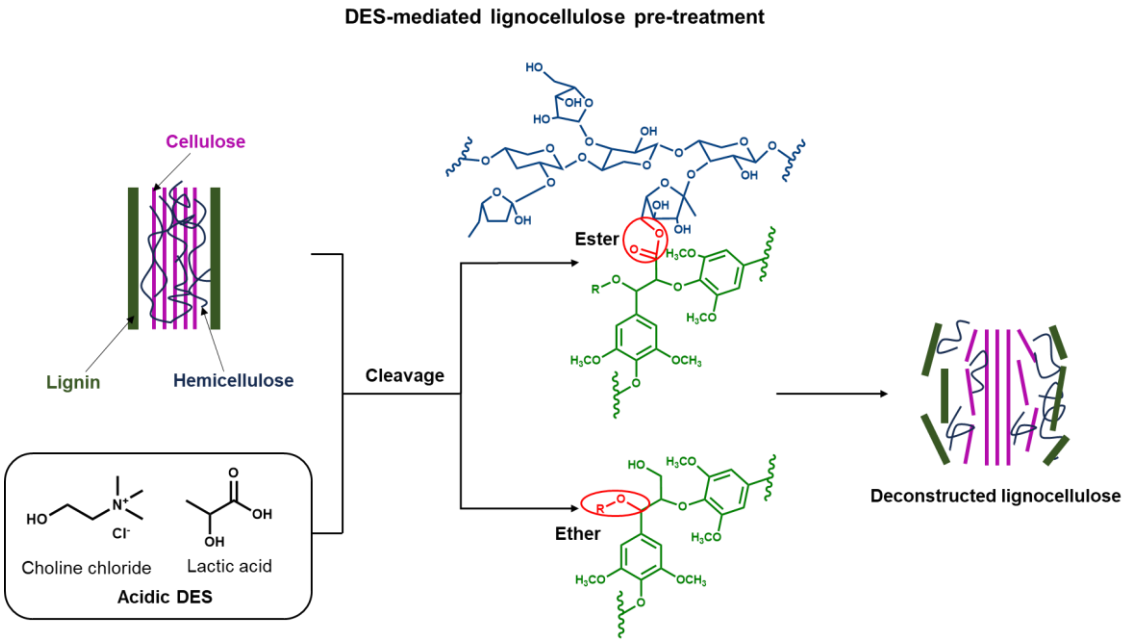

Figure 21: Schematic representation of lignocellulose cleavage by DESs.

Since lignin and hemicellulose are the first two polymers to be affected by DES-treatments, it could be challenging to recover them in high yield in a single pretreatment. For this reason, it could be necessary to perform a two-step mediated fractionation process, in order to first pre-extract hemicellulose, and then lignin. Tian *et al.*[80] for example presented a method in which biomass is firstly submitted to a hot water pretreatment (160-240 °C) that easily depolymerize/solubilize hemicellulose, facilitating the subsequent lignin extraction using various solvent systems. This pretreatment allows to obtain both a high-quality lignin and a high-purity cellulose fraction.
DESs treatments efficiency depends on several factors, such as ratio biomass/DES, temperature and time. Commonly, DESs are used in excess to the biomass, and the most used ratios biomass/DES are 1:5, 1:8 and 1:10. This parameter could influence lignin recovery, cellulose crystallinity and DES recycle. For what regard temperature and time, a wide range of them has been tested (temperature: 60-200 °C; time: 0.5-24 h), but prolonged pretreatments at high temperature could successfully solubilize carbohydrates and increase final lignin yields.[80]
Acidic DESs are the most effective in biomass deconstruction, and tendentially natural hydrogen bond donors are used, such as formic acid, lactic and acetic acid. In general monocarboxylic acid–based DESs are recommended for lignin extraction, since the lignocellulose bonds are easily cleaved by the proton provided by the carboxylic acid. In this respect, in literature the combination choline chloride and lactic acid in different ratios has been reported, since both HBA and HBD are cost–effective and can be produced from renewable raw materials. In general, cellulose is insoluble in this mixture while, by increasing lactic acid content, lignin becomes more soluble, less easy to recover and biomass delignification occurs.[81]

In this thesis, a two-step DESs-mediated fractionation process has been set-up in order to fractionate BSG and RH biomasses, kindly furnished by Orso Verde brewery and Riso

Scotti S.p.A. In this process, the biomasses have been firstly submitted to a hot-water pretreatment, and then to a DES-mediated fractionation in order to separate the cellulosic fraction from lignin, that was further highly characterized and investigated.

4. Applications of the Final Products

4.1. Phospholipids Applications

In this PhD thesis the obtainment of polar head-modified phospholipids has been studied since the commercial value of PLs in the pharmaceutical, cosmetic and food industry depend on the nature of their polar head and lipophilic tails. The development of practical methods for the preparation of structurally variable polar head-modified PLs is an important prerequisite to achieve the establishment of structure-activity relationships of these compounds, and a biocatalytic approach for the synthesis of modified PLs is preferred when compared to the chemical processes, especially due to the very high selectivity and the use of safer reagents and milder conditions.
In this work we proposed the PLD-catalyzed synthesis of three polar head-modified phospholipids of pharmaceutical interest: phosphatidylserine, phosphatidylglycerol and phosphatidylethanolamine.

a) Phosphatidylserine (PS): it has achieved a great commercial interest for a long time as it is a membrane PL ubiquitously present in all cellular membranes, especially in the brain, and is involved in many neurological processes.[82] It is a molecule that presents many nutritional and medical functions as low levels of PS is linked to memory problems, to Alzheimer's and other mental diseases. It is demonstrated that the assumption of PS leads to positive benefits in terms of mind and memory enhancement. It reduces the age-related decline in mental function, it prevents Alzheimer's and dementia, it is considered a mood enhancer to cure depression, it improves athletic performance, it is a stress reducer and it is an important ingredient of liposomes used in drug delivery.[83] The main drawback is linked to its low availability in nature and high costs of extraction from natural sources.[84]

b) Phosphatidylglycerol (PG): it is one of the most abundant PLs found in natural membranes. It possesses an excellent liposome forming ability and has been studied from a long time, since 1985, as an emulsifier for drug delivery systems.[85-87] In fact, PG is known to have unique surfactant/lubricant properties, particularly when mixed with appropriate proteins. It has been found, for example, in relatively large amounts in mammalian lungs compared to other mammalian membranes pushing the research on the development of surfactant preparations for therapeutic practices for the relief of a variety of diseases such as neonatal respiratory distress syndrome.[88]

c) Phosphatidylethanolamine (PE): it is another major PL in the membranes of eukaryotic cells. The importance of PE metabolism in mammalian health has recently emerged following its association with Alzheimer's, Parkinson's and nonalcoholic liver diseases, as well as with the virulence of certain pathogenic organisms.[89-90] Moreover, PE has a significant influence on the heart to prevent cell damage. This product also presents good antioxidant activity against free radicals, which is another characteristic

which could provide beneficial effects to human health.

4.2. Lignin Applications

In this thesis, subsequently to biomass fractionation, we have focused on the exploitation of the recovered lignin fractions, since this polymer could be suitable for many different applications that are here briefly reported. In particular, we have focused on the lignin exploitation in the constructions and nanoparticles fields, and, for this reason, these two sections will be here widely investigated. In general, it is possible to distinguish lignin utilization into different categories:

a) Extraction of monomers/macromolecules and fine chemicals: since the fossil reserves are running out, research is focusing on finding a way to use renewable resources, such as lignin, for the production of environmentally friendly and competitive products, such as vanillin, lipids, muconic acid and polyhidroxyalkanoates.[91-93] In fact, thanks to its structure and monomers composition, these chemicals can be obtained by submitting lignin to different treatments, processes of depolymerization and separation methods. For example, in literature are reported thermochemical (pyrolysis and microwave), biological (fungi and bacteria) and chemical processes (oxidation, acid catalysis, metallic catalysis, homogeneous/heterogeneous catalysis).

b) Polymer synthesis: lignin, thanks to its interesting properties, could be used to replace petroleum derivatives in polymer synthesis (such as polyurethanes and resins) thanks to two different methods. The first method consists into using functional monomers developed from phenolic lignin model compound. In fact, lignin presents aliphatic/hydroxyl groups that could be exploited for their further modification, like alkylation, amination and esterification (see Figure 22). Instead, the second method consists into directly incorporate lignin in polymers thanks to the grafting technique: lignin works as a core unit on which new polymer chains are directly grown.[94-95]

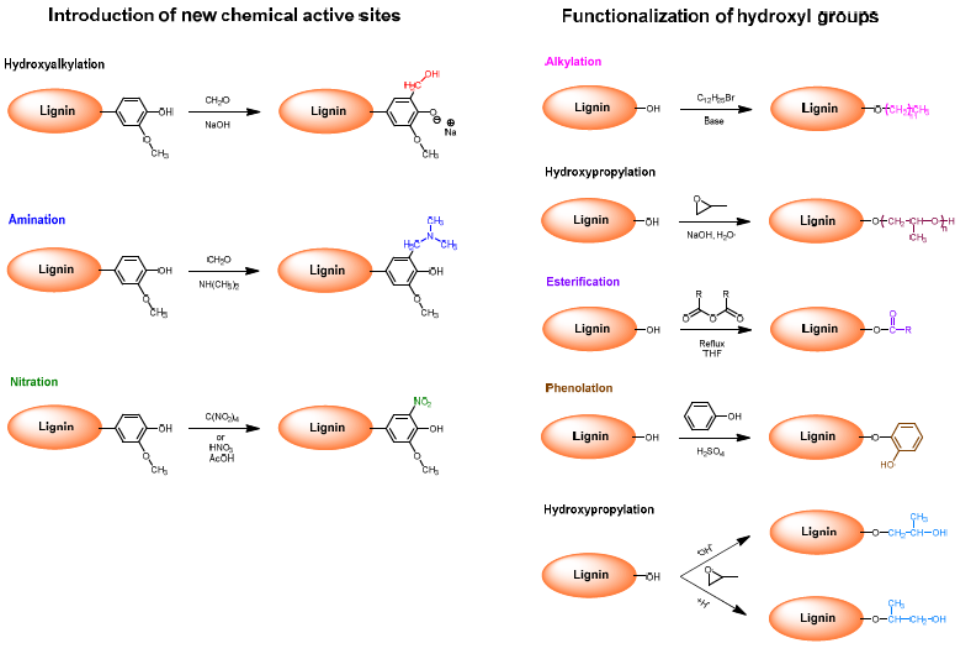

Figure 22: Main lignin possible modifications.

c) Biofuels: the energy demand is constantly increasing, and the biorefineries based on the utilization of lignocellulose are a promising tool to solve this problem. In particular biorefineries tends to use the cellulose and hemicellulose fractions to produce ethanol, while lignin is disposed of as a waste. Recently researchers are also focusing on recovering the maximum possible energy from lignin. In fact, for example, lignin can be depolymerized into aromatic monomers that are then dearomatized and reduced to generate CO_2, H_2 and acetate that lead to the formation of methane.[92, 96] It is important to consider that lignin is environmentally friendly not only because it is renewable and abundant, but also because lignin-derived biofuels generates a lower carbon footprint respect to the fossil ones.

d) Building materials: cement production represents the third largest source of carbon dioxide emissions, since almost 8% of the total carbon dioxide emitted in atmosphere are caused by concrete preparation. Therefore, researchers and industrialists are looking for new materials to be used to prepare eco-friendly concretes and, in this respect, several agro-industrial by-products have been successfully exploited as potential building materials. Concretes main required characteristics are workability, strength and durability, and these are enhanced by the use of lignin in cements as concrete water reducers (or concrete plasticizers), which are necessary to reduce the water amount in concrete preparation. Concrete is prepared by adding between 0.06-0.6% wt of plasticizers on cement. The demand of water reducers is estimated about 1-1.5 million tons per year, and of this 700.000 tons are lignosulfonate and post-sulfonate alkali lignins. Concretes are prepared in an alkaline environment, and so plasticizers work through electrostatic and steric repulsion between the cement grains. In fact, the water reducers, thanks to their negative charges (carboxylic and sulfonic groups), are adsorbed on cement particles, usually made of calcium aluminate, giving them a negative charge that force the particles apart.

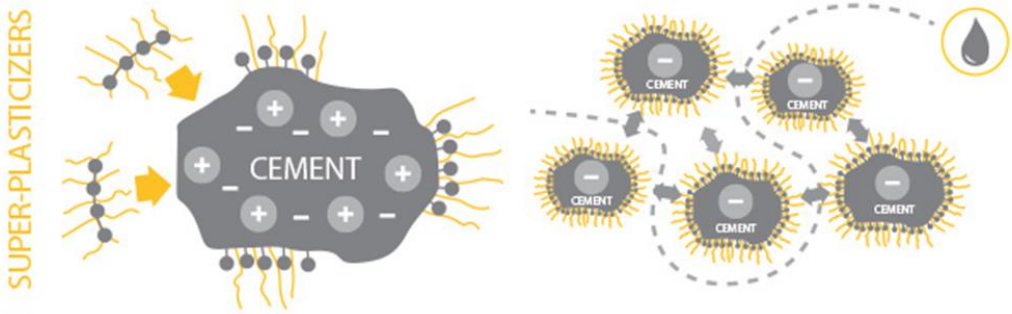

Figure 23: Scheme of superplasticizers mechanism on cement grains.

It is possible to distinguish water reducers in "ordinary" ones, like lignosulfonates, and superplasticizers that are commonly petroleum derivatives (naphthalene and polycarboxylate). Usually good plasticizers are able to reduce water amount by at least 12%, and lignin usually doesn't reach this criteria because of its low amount of hydrophilic groups and typical high polydispersity. For these reasons, lignin can be modified through fractionation and oxidation-sulfomethylation to enhance its efficiency as water reducer. For example, Li *et al.* fractionated lignocellulose biomass by using formic acid, and then submitted lignin firstly to organosolv fractionation to homogenise its molecular weight distribution, and then to sulfonation to increase its hydrophilic content. In this way they increased cement workability by 21%.[97] Another example is reported by Kalliola *et al.*, which performed oxidation on soda lignin in alkaline conditions, introducing acidic groups in the polymer structure. The obtained lignin showed a higher efficiency than the commercial lignosulfonates, and equal performance to synthetic superplasticizers.[98]

At least, in literature the utilization as plasticizers of lignin grafted to other polymers is reported. In fact, Aso *et al*. successfully proposed the grafting of kraft lignin to epoxylathed polyethylene glycol derivatives, showing positive results respect to commercial lignosulfonate.[99]

In this PhD work, we have successfully investigated the utilization of lignins recovered by BSG and RH fractionation and compared them to a technical lignin, Protobind 1000, as water reducers in concrete preparation, with a concentration of 0.2 % wt. These experiments gave positive results, showing a comparable activity between the lignins recovered from the two biomasses and the technical one, paving the way for the generation of lignin-based plasticizers.

e) Nanomaterials: the utilization of lignin without previous modifications is usually limited due to is heterogeneity and complex structure. However, it is possible to overcome this problem by transforming lignin into nanomaterials, such as nanoparticles (LNPs), nanotubes, nanofibers and hydrogels.[100] In particular, in this thesis we have focused on LNPs synthesis and exploitation for further enzyme immobilization, so they will be here reported, and their characteristics investigated.

LNPs were chosen thanks to some advantageous properties, such as sustainability, biodegradability, biocompatibility and low cost. Another important characteristic is that LNPs on the surface are rich in functional groups that could be further modified according to the final application.[101] The nanoparticles characteristics, such as dimension, size, exposed functional groups, depends on the method of lignin extraction

from biomass (physical/chemical/biological), if lignin underwent some chemical modifications, and the technique used for LNPs preparation.[101-102] LNPs could be obtained by different methods, that comprehends anti-solvent precipitation, acid precipitation, dialysis, polymerization, solvent exchange, sonication and many others. Nanoparticles formation is possible thanks to lignin amphiphilic nature, since it possesses hydrophobic groups, such as phenylpropanoid acids, and hydrophilic ones, like hydroxyl and carboxylic groups. For this reason, tendentially LNPs formation starts with lignin solubilization in a polar solvent, which breaks lignin intramolecular H-bonds, and then the solution is added into water and nanoparticles formation takes place. In particular, the lignin hydrophobic groups tend to self-assemble as the core of the nanoparticles, while the hydrophilic groups to remain on the surface, forming non-covalent interactions on the surface. In this mainframe, lignin tendency to self-assemble into spherical particles allows to minimize the surface area in contact with the non-solvent phase, typically water.

Lignin nanoparticles main characteristic is their stability over time in aqueous solution, in which they preserve their spherical shape and small size. In this sense final lignin concentration is a critical factor since an increase in lignin concentration could provoke the nanoparticles agglomeration and an increase in their size.[103]

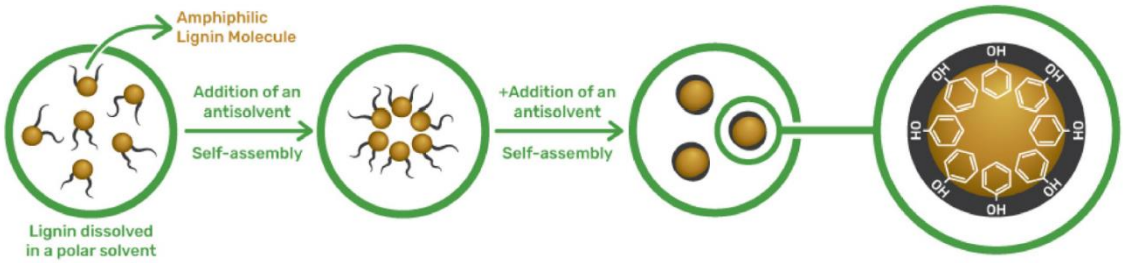

Figure 24: Scheme of lignin nanoparticles preparation.[103]

LNPs are particularly interesting for many different applications because of some relevant properties, such as antioxidant and antibacterial activity, ultraviolet adsorption properties, biocompatibility and biodegradability. For this reason, LNPs are replacing traditional hazardous nanomaterials, in accordance with the Green Chemistry principles in a plethora of different materials chemistry applications, including drug carriers,[104] UV protectants and hosts for enzyme immobilization. For what regard this last point, in this thesis work we focused on PLD immobilization on LNPs for phospholipids transformation inspired by some recent publications with redox enzymes. For example, Capecchi *et al*. described LNPs for the immobilization of tyrosinase for the synthesis of catechol derivatives,[105] and glucose oxidase and peroxidase immobilization to obtain biosensors for the detection of glucose.[106]

References

1. Anastas, P. T.; Warner, J. C., Principles of green chemistry. *Green chemistry: Theory and practice* **1998,** *29*, 14821-42.
2. Harrison, E.; Smith, H.; Dekker, I., Designing & Facilitating a Bioeconomy in the Capital Regional District. **2021**.
3. Nickels, J. D.; Smith, J. C.; Cheng, X., Lateral organization, bilayer asymmetry, and inter-leaflet coupling of biological membranes. *Chem Phys Lipids* **2015,** *192*, 87-99.

4. Santhosh, P. B.; Thomas, N.; Sudhakar, S.; Chadha, A.; Mani, E., Phospholipid stabilized gold nanorods: towards improved colloidal stability and biocompatibility. *Phys Chem Chem Phys* **2017,** *19* (28), 18494-18504.
5. Li, J.; Wang, X.; Zhang, T.; Wang, C.; Huang, Z.; Luo, X.; Deng, Y., A review on phospholipids and their main applications in drug delivery systems. *Asian Journal of Pharmaceutical Sciences* **2015,** *10* (2), 81-98.
6. Singh, R. P.; Gangadharappa, H. V.; Mruthunjaya, K., Phospholipids: Unique carriers for drug delivery systems. *Journal of Drug Delivery Science and Technology* **2017,** *39*, 166-179.
7. Bandu, R.; Mok, H. J.; Kim, K. P., Phospholipids as cancer biomarkers: Mass spectrometry-based analysis. *Mass Spectrom Rev* **2018,** *37* (2), 107-138.
8. Alhajj, M. J.; Montero, N.; Yarce, C. J.; Salamanca, C. H., Lecithins from Vegetable, Land, and Marine Animal Sources and Their Potential Applications for Cosmetic, Food, and Pharmaceutical Sectors. *Cosmetics* **2020,** *7* (4), 87.
9. Cui, L.; Decker, E. A., Phospholipids in foods: prooxidants or antioxidants? *J Sci Food Agric* **2016,** *96* (1), 18-31.
10. McClements, D. J.; Gumus, C. E., Natural emulsifiers - Biosurfactants, phospholipids, biopolymers, and colloidal particles: Molecular and physicochemical basis of functional performance. *Adv Colloid Interface Sci* **2016,** *234*, 3-26.
11. Zhang, Z.; Chen, M.; Xu, W.; Zhang, W.; Zhang, T.; Guang, C.; Mu, W., Microbial phospholipase D: Identification, modification and application. *Trends in Food Science & Technology* **2020,** *96*, 145-156.
12. de Crane d'Heysselaer, S.; Bockstal, L.; Jacquet, N.; Schmetz, Q.; Richel, A., Potential for the valorisation of brewer's spent grains: A case study for the sequential extraction of saccharides and lignin. *Waste Manag Res* **2022,** *40* (7), 1007-1014.
13. Shen, X.; Sun, R., Recent advances in lignocellulose prior-fractionation for biomaterials, biochemicals, and bioenergy. *Carbohydr Polym* **2021,** *261*, 117884.
14. Baruah, J.; Nath, B. K.; Sharma, R.; Kumar, S.; Deka, R. C.; Baruah, D. C.; Kalita, E., Recent Trends in the Pretreatment of Lignocellulosic Biomass for Value-Added Products. *Frontiers in Energy Research* **2018,** *6*.
15. Tursi, A., A review on biomass: importance, chemistry, classification, and conversion. *Biofuel Research Journal* **2019,** *6* (2), 962-979.
16. Liu, W.; Liu, K.; Du, H.; Zheng, T.; Zhang, N.; Xu, T.; Pang, B.; Zhang, X.; Si, C.; Zhang, K., Cellulose Nanopaper: Fabrication, Functionalization, and Applications. *Nanomicro Lett* **2022,** *14* (1), 104.
17. Liu, K.; Du, H.; Zheng, T.; Liu, H.; Zhang, M.; Zhang, R.; Li, H.; Xie, H.; Zhang, X.; Ma, M.; Si, C., Recent advances in cellulose and its derivatives for oilfield applications. *Carbohydr Polym* **2021,** *259*, 117740.
18. Scapini, T.; Dos Santos, M. S. N.; Bonatto, C.; Wancura, J. H. C.; Mulinari, J.; Camargo, A. F.; Klanovicz, N.; Zabot, G. L.; Tres, M. V.; Fongaro, G.; Treichel, H., Hydrothermal pretreatment of lignocellulosic biomass for hemicellulose recovery. *Bioresour Technol* **2021,** *342*, 126033.
19. Qaseem, M. F.; Shaheen, H.; Wu, A.-M., Cell wall hemicellulose for sustainable industrial utilization. *Renewable and Sustainable Energy Reviews* **2021,** *144*.
20. Ralph, J.; Lapierre, C.; Boerjan, W., Lignin structure and its engineering. *Curr Opin Biotechnol* **2019,** *56*, 240-249.
21. Sethupathy, S.; Murillo Morales, G.; Gao, L.; Wang, H.; Yang, B.; Jiang, J.; Sun, J.; Zhu, D., Lignin valorization: Status, challenges and opportunities. *Bioresour Technol* **2022,** *347*, 126696.
22. Dahmen, N.; Lewandowski, I.; Zibek, S.; Weidtmann, A., Integrated lignocellulosic value chains in a growing bioeconomy: Status quo and perspectives. *GCB Bioenergy* **2019,** *11* (1), 107-117.
23. Tripathi, N.; Hills, C. D.; Singh, R. S.; Atkinson, C. J., Biomass waste utilisation in low-carbon products: harnessing a major potential resource. *npj Climate and Atmospheric Science* **2019,** *2* (1).
24. Kumar, A. K.; Sharma, S., Recent updates on different methods of pretreatment of lignocellulosic feedstocks: a review. *Bioresour Bioprocess* **2017,** *4* (1), 7.
25. Wu, Z.; Peng, K.; Zhang, Y.; Wang, M.; Yong, C.; Chen, L.; Qu, P.; Huang, H.; Sun, E.; Pan, M., Lignocellulose dissociation with biological pretreatment towards the biochemical platform: A review. *Mater Today Bio* **2022,** *16*, 100445.
26. Sharma, H. K.; Xu, C.; Qin, W., Biological Pretreatment of Lignocellulosic Biomass for Biofuels and Bioproducts: An Overview. *Waste and Biomass Valorization* **2017,** *10* (2), 235-251.
27. He, Y.; Kuhn, D. D.; Ogejo, J. A.; O'Keefe, S. F.; Fraguas, C. F.; Wiersema, B. D.; Jin, Q.; Yu, D.; Huang, H., Wet fractionation process to produce high protein and high fiber products from brewer's spent grain. *Food and Bioproducts Processing* **2019,** *117*, 266-274.

28. Pabbathi, N. P. P.; Velidandi, A.; Pogula, S.; Gandam, P. K.; Baadhe, R. R.; Sharma, M.; Sirohi, R.; Thakur, V. K.; Gupta, V. K., Brewer's spent grains-based biorefineries: A critical review. *Fuel* **2022,** *317*.
29. Chetrariu, A.; Dabija, A., Brewer's Spent Grains: Possibilities of Valorization, a Review. *Applied Sciences* **2020,** *10* (16), 5619.
30. Mitri, S.; Salameh, S.-J.; Khelfa, A.; Leonard, E.; Maroun, R. G.; Louka, N.; Koubaa, M., Valorization of Brewers’ Spent Grains: Pretreatments and Fermentation, a Review. *Fermentation* **2022,** *8* (2), 50.
31. San Martin, D.; Orive, M.; Iñarra, B.; Castelo, J.; Estévez, A.; Nazzaro, J.; Iloro, I.; Elortza, F.; Zufía, J., Brewers' Spent Yeast and Grain Protein Hydrolysates as Second-Generation Feedstuff for Aquaculture Feed. *Waste and Biomass Valorization* **2020,** *11* (10), 5307-5320.
32. Rojas-Chamorro, J. A.; Cara, C.; Romero, I.; Ruiz, E.; Romero-García, J. M.; Mussatto, S. I.; Castro, E., Ethanol Production from Brewers' Spent Grain Pretreated by Dilute Phosphoric Acid. *Energy & Fuels* **2018,** *32* (4), 5226-5233.
33. Qazanfarzadeh, Z.; Ganesan, A. R.; Mariniello, L.; Conterno, L.; Kumaravel, V., Valorization of brewer's spent grain for sustainable food packaging. *Journal of Cleaner Production* **2023,** *385*.
34. Mussatto, S. I., Brewer's spent grain: a valuable feedstock for industrial applications. *J Sci Food Agric* **2014,** *94* (7), 1264-75.
35. Stojceska, V.; Ainsworth, P., The effect of different enzymes on the quality of high-fibre enriched brewer's spent grain breads. *Food Chem* **2008,** *110* (4), 865-72.
36. Lynch, K. M.; Steffen, E. J.; Arendt, E. K., Brewers' spent grain: a review with an emphasis on food and health. *Journal of the Institute of Brewing* **2016,** *122* (4), 553-568.
37. Mussatto, S. I.; Roberto, I. C., Chemical characterization and liberation of pentose sugars from brewer's spent grain. *Journal of Chemical Technology & Biotechnology* **2006,** *81* (3), 268-274.
38. Guido, L. F.; Moreira, M. M., Techniques for Extraction of Brewer's Spent Grain Polyphenols: a Review. *Food and Bioprocess Technology* **2017,** *10* (7), 1192-1209.
39. Amorim, C.; Silverio, S. C.; Prather, K. L. J.; Rodrigues, L. R., [Not Available]. *Biotechnol Adv* **2019,** *37* (7), 107397.
40. Lim, J. S.; Abdul Manan, Z.; Wan Alwi, S. R.; Hashim, H., A review on utilisation of biomass from rice industry as a source of renewable energy. *Renewable and Sustainable Energy Reviews* **2012,** *16* (5), 3084-3094.
41. Pode, R., Potential applications of rice husk ash waste from rice husk biomass power plant. *Renewable and Sustainable Energy Reviews* **2016,** *53*, 1468-1485.
42. Buggenhout, J.; Brijs, K.; Celus, I.; Delcour, J. A., The breakage susceptibility of raw and parboiled rice: A review. *Journal of Food Engineering* **2013,** *117* (3), 304-315.
43. Balbinoti, T. C. V.; Nicolin, D. J.; de Matos Jorge, L. M.; Jorge, R. M. M., Parboiled Rice and Parboiling Process. *Food Engineering Reviews* **2018,** *10* (3), 165-185.
44. Haist, M.; Link, J.; Nicia, D.; Leinitz, S.; Baumert, C.; von Bronk, T.; Cotardo, D.; Eslami Pirharati, M.; Fataei, S.; Garrecht, H., Interlaboratory study on rheological properties of cement pastes and reference substances: comparability of measurements performed with different rheometers and measurement geometries. *Materials and Structures* **2020,** *53*, 1-26.
45. Arun, V.; Perumal, E. M.; Prakash, K. A.; Rajesh, M.; Tamilarasan, K., Sequential fractionation and characterization of lignin and cellulose fiber from waste rice bran. *Journal of Environmental Chemical Engineering* **2020,** *8* (5).
46. Zhang, Y.; Zhu, L.; Wu, G.; Wang, X.; Jin, Q.; Qi, X.; Zhang, H., Design of amino-functionalized hollow mesoporous silica cube for enzyme immobilization and its application in synthesis of phosphatidylserine. *Colloids and Surfaces B: Biointerfaces* **2021,** *202*, 111668.
47. Nguyen, N. T.; Tran, N. T.; Phan, T. P.; Nguyen, A. T.; Nguyen, M. X. T.; Nguyen, N. N.; Ko, Y. H.; Nguyen, D. H.; Van, T. T. T.; Hoang, D., The extraction of lignocelluloses and silica from rice husk using a single biorefinery process and their characteristics. *Journal of Industrial and Engineering Chemistry* **2022,** *108*, 150-158.
48. Guthrie, F., LII. On eutexia. *The London, Edinburgh, and Dublin Philosophical Magazine and Journal of Science* **1884,** *17* (108), 462-482.
49. Abbott, A. P.; Capper, G.; Davies, D. L.; Rasheed, R. K.; Tambyrajah, V., Novel solvent properties of choline chloride/urea mixtures. *Chemical communications* **2003,** (1), 70-71.
50. Paiva, A.; Craveiro, R.; Aroso, I.; Martins, M.; Reis, R. L.; Duarte, A. R. C., Natural deep eutectic solvents–solvents for the 21st century. *ACS Sustainable Chemistry & Engineering* **2014,** *2* (5), 1063-1071.

51. Cao, J.; Su, E., Hydrophobic deep eutectic solvents: The new generation of green solvents for diversified and colorful applications in green chemistry. *Journal of Cleaner Production* **2021,** *314*, 127965.
52. Smith, E. L.; Abbott, A. P.; Ryder, K. S., Deep eutectic solvents (DESs) and their applications. *Chemical reviews* **2014,** *114* (21), 11060-11082.
53. Hansen, B. B.; Spittle, S.; Chen, B.; Poe, D.; Zhang, Y.; Klein, J. M.; Horton, A.; Adhikari, L.; Zelovich, T.; Doherty, B. W., Deep eutectic solvents: A review of fundamentals and applications. *Chemical reviews* **2020,** *121* (3), 1232-1285.
54. Dai, Y.; van Spronsen, J.; Witkamp, G.-J.; Verpoorte, R.; Choi, Y. H., Natural deep eutectic solvents as new potential media for green technology. *Analytica chimica acta* **2013,** *766*, 61-68.
55. Choi, Y. H.; van Spronsen, J.; Dai, Y.; Verberne, M.; Hollmann, F.; Arends, I. W.; Witkamp, G.-J.; Verpoorte, R., Are natural deep eutectic solvents the missing link in understanding cellular metabolism and physiology? *Plant physiology* **2011,** *156* (4), 1701-1705.
56. Rodriguez Rodriguez, N.; van den Bruinhorst, A.; Kollau, L. J. B. M.; Kroon, M. C.; Binnemans, K., Degradation of Deep-Eutectic Solvents Based on Choline Chloride and Carboxylic Acids. *ACS Sustainable Chemistry & Engineering* **2019,** *7* (13), 11521-11528.
57. Florindo, C.; Oliveira, F. S.; Rebelo, L. P. N.; Fernandes, A. M.; Marrucho, I. M., Insights into the Synthesis and Properties of Deep Eutectic Solvents Based on Cholinium Chloride and Carboxylic Acids. *ACS Sustainable Chemistry & Engineering* **2014,** *2* (10), 2416-2425.
58. Gutierrez, M. C.; Ferrer, M. L.; Mateo, C. R.; del Monte, F., Freeze-drying of aqueous solutions of deep eutectic solvents: a suitable approach to deep eutectic suspensions of self-assembled structures. *Langmuir* **2009,** *25* (10), 5509-15.
59. Gomez, F. J. V.; Espino, M.; Fernández, M. A.; Silva, M. F., A Greener Approach to Prepare Natural Deep Eutectic Solvents. *ChemistrySelect* **2018,** *3* (22), 6122-6125.
60. Santana, A. P. R.; Mora-Vargas, J. A.; Guimarães, T. G. S.; Amaral, C. D. B.; Oliveira, A.; Gonzalez, M. H., Sustainable synthesis of natural deep eutectic solvents (NADES) by different methods. *Journal of Molecular Liquids* **2019,** *293*.
61. El Achkar, T.; Greige-Gerges, H.; Fourmentin, S., Basics and properties of deep eutectic solvents: a review. *Environmental Chemistry Letters* **2021,** *19* (4), 3397-3408.
62. Akretche, H.; Pierre, G.; Moussaoui, R.; Michaud, P.; Delattre, C., Valorization of olive mill wastewater for the development of biobased polymer films with antioxidant properties using eco-friendly processes. *Green Chemistry* **2019,** *21* (11), 3065-3073.
63. Verevkin, S. P.; Sazonova, A. Y.; Frolkova, A. K.; Zaitsau, D. H.; Prikhodko, I. V.; Held, C., Separation Performance of BioRenewable Deep Eutectic Solvents. *Industrial & Engineering Chemistry Research* **2015,** *54* (13), 3498-3504.
64. Sarmad, S.; Xie, Y.; Mikkola, J.-P.; Ji, X., Screening of deep eutectic solvents (DESs) as green CO2 sorbents: from solubility to viscosity. *New Journal of Chemistry* **2017,** *41* (1), 290-301.
65. Allegretti, C.; Bellinetto, E.; D'Arrigo, P.; Griffini, G.; Marzorati, S.; Rossato, L. A. M.; Ruffini, E.; Schiavi, L.; Serra, S.; Strini, A.; Tessaro, D.; Turri, S., Towards a Complete Exploitation of Brewers’ Spent Grain from a Circular Economy Perspective. *Fermentation* **2022,** *8* (4), 151.
66. Allegretti, C.; Bellinetto, E.; D'Arrigo, P.; Ferro, M.; Griffini, G.; Rossato, L. A. M.; Ruffini, E.; Schiavi, L.; Serra, S.; Strini, A.; Turri, S., Fractionation of Raw and Parboiled Rice Husks with Deep Eutectic Solvents and Characterization of the Extracted Lignins towards a Circular Economy Perspective. *Molecules* **2022,** *27* (24), 8879.
67. Kaur, S.; Kumari, M.; Kashyap, H. K., Microstructure of Deep Eutectic Solvents: Current Understanding and Challenges. *J Phys Chem B* **2020,** *124* (47), 10601-10616.
68. Ma, C.; Laaksonen, A.; Liu, C.; Lu, X.; Ji, X., The peculiar effect of water on ionic liquids and deep eutectic solvents. *Chemical Society Reviews* **2018,** *47* (23), 8685-8720.
69. Gabriele, F.; Chiarini, M.; Germani, R.; Tiecco, M.; Spreti, N., Effect of water addition on choline chloride/glycol deep eutectic solvents: Characterization of their structural and physicochemical properties. *Journal of Molecular Liquids* **2019,** *291*.
70. Delso, I.; Lafuente, C.; Muñoz-Embid, J.; Artal, M., NMR study of choline chloride-based deep eutectic solvents. *Journal of Molecular Liquids* **2019,** *290*, 111236.
71. Sil, A.; Bhati, R.; Das, S.; Guchhait, B., Ion clustering, aggregation and diffusion in amide based deep eutectic solvents: A microstructural investigation using various NMR spectroscopic techniques and molecular dynamics simulation. *Journal of Molecular Liquids* **2023,** *388*, 122761.
72. Dugoni, G. C.; Di Pietro, M. E.; Ferro, M.; Castiglione, F.; Ruellan, S.; Moufawad, T.; Moura, L.; Costa Gomes, M. F.; Fourmentin, S.; Mele, A., Effect of water on deep eutectic solvent/β-cyclodextrin systems. *ACS Sustainable Chemistry & Engineering* **2019,** *7* (7), 7277-7285.

73. Pätzold, M.; Siebenhaller, S.; Kara, S.; Liese, A.; Syldatk, C.; Holtmann, D., Deep eutectic solvents as efficient solvents in biocatalysis. *Trends in biotechnology* **2019,** *37* (9), 943-959.
74. Xu, P.; Zheng, G. W.; Zong, M. H.; Li, N.; Lou, W. Y., Recent progress on deep eutectic solvents in biocatalysis. *Bioresour Bioprocess* **2017,** *4* (1), 34.
75. Tan, J.-N.; Dou, Y., Deep eutectic solvents for biocatalytic transformations: Focused lipase-catalyzed organic reactions. *Applied microbiology and biotechnology* **2020,** *104*, 1481-1496.
76. Cao, J.; Wu, R.; Zhu, F.; Dong, Q.; Su, E., How to improve the efficiency of biocatalysis in non-aqueous pure deep eutectic solvents: A case study on the lipase-catalyzed transesterification reaction. *Biochemical Engineering Journal* **2022,** *179*, 108336.
77. Yang, T.-X.; Zhao, L.-Q.; Wang, J.; Song, G.-L.; Liu, H.-M.; Cheng, H.; Yang, Z., Improving whole-cell biocatalysis by addition of deep eutectic solvents and natural deep eutectic solvents. *ACS Sustainable Chemistry & Engineering* **2017,** *5* (7), 5713-5722.
78. Zhou, M.; Fakayode, O. A.; Yagoub, A. E. A.; Ji, Q.; Zhou, C., Lignin fractionation from lignocellulosic biomass using deep eutectic solvents and its valorization. *Renewable and Sustainable Energy Reviews* **2022,** *156*, 111986.
79. Francisco, M.; Van Den Bruinhorst, A.; Kroon, M. C., New natural and renewable low transition temperature mixtures (LTTMs): screening as solvents for lignocellulosic biomass processing. *Green chemistry* **2012,** *14* (8), 2153-2157.
80. Tian, D.; Guo, Y.; Hu, J.; Yang, G.; Zhang, J.; Luo, L.; Xiao, Y.; Deng, S.; Deng, O.; Zhou, W., Acidic deep eutectic solvents pretreatment for selective lignocellulosic biomass fractionation with enhanced cellulose reactivity. *International journal of biological macromolecules* **2020,** *142*, 288-297.
81. Liu, Q.; Yuan, T.; Fu, Q.-j.; Bai, Y.-y.; Peng, F.; Yao, C.-l., Choline chloride-lactic acid deep eutectic solvent for delignification and nanocellulose production of moso bamboo. *Cellulose* **2019,** *26*, 9447-9462.
82. Lindberg, J.; Ekeroth, J.; Konradsson, P., Efficient synthesis of phospholipids from glycidyl phosphates. *The Journal of Organic Chemistry* **2002,** *67* (1), 194-199.
83. Liu, X.; Shiihara, M.; Taniwaki, N.; Shirasaka, N.; Atsumi, Y.; Shiojiri, M., 6 - Phosphatidylserine: Biology, Technologies, and Applications. In *Polar Lipids*, Ahmad, M. U.; Xu, X., Eds. Elsevier: 2015; pp 145-184.
84. Cerminati, S.; Paoletti, L.; Aguirre, A.; Peirú, S.; Menzella, H. G.; Castelli, M. E., Industrial uses of phospholipases: current state and future applications. *Applied microbiology and biotechnology* **2019,** *103*, 2571-2582.
85. Gregoriadis, G., Liposomes for drugs and vaccines. *Trends in Biotechnology* **1985,** *3* (9), 235-241.
86. Sakdiset, P.; Okada, A.; Todo, H.; Sugibayashi, K., Selection of phospholipids to design liposome preparations with high skin penetration-enhancing effects. *Journal of Drug Delivery Science and Technology* **2018,** *44*, 58-64.
87. Hossann, M.; Wiggenhorn, M.; Schwerdt, A.; Wachholz, K.; Teichert, N.; Eibl, H.; Issels, R. D.; Lindner, L. H., In vitro stability and content release properties of phosphatidylglyceroglycerol containing thermosensitive liposomes. *Biochimica et Biophysica Acta (BBA)-Biomembranes* **2007,** *1768* (10), 2491-2499.
88. Mazela, J.; Merritt, T. A.; Gadzinowski, J.; Sinha, S., Evolution of pulmonary surfactants for the treatment of neonatal respiratory distress syndrome and paediatric lung diseases. *Acta paediatrica* **2006,** *95* (9), 1036-1048.
89. Calzada, E.; Onguka, O.; Claypool, S. M., Phosphatidylethanolamine Metabolism in Health and Disease. *International review of cell and molecular biology* **2016,** *321*, 29-88.
90. Patel, D.; Witt, S. N., Ethanolamine and phosphatidylethanolamine: partners in health and disease. *Oxidative medicine and cellular longevity* **2017,** *2017*.
91. Chio, C.; Sain, M.; Qin, W., Lignin utilization: A review of lignin depolymerization from various aspects. *Renewable and Sustainable Energy Reviews* **2019,** *107*, 232-249.
92. Radhika, N. L.; Sachdeva, S.; Kumar, M., Lignin depolymerization and biotransformation to industrially important chemicals/biofuels. *Fuel* **2022,** *312*.
93. Cao, L.; Yu, I. K. M.; Liu, Y.; Ruan, X.; Tsang, D. C. W.; Hunt, A. J.; Ok, Y. S.; Song, H.; Zhang, S., Lignin valorization for the production of renewable chemicals: State-of-the-art review and future prospects. *Bioresour Technol* **2018,** *269*, 465-475.
94. Ganewatta, M. S.; Lokupitiya, H. N.; Tang, C., Lignin Biopolymers in the Age of Controlled Polymerization. *Polymers* **2019,** *11* (7), 1176.
95. Gao, W.; Fatehi, P., Lignin for polymer and nanoparticle production: Current status and challenges. *The Canadian Journal of Chemical Engineering* **2019,** *97* (11), 2827-2842.

96. Kocaturk, E.; Salan, T.; Ozcelik, O.; Alma, M. H.; Candan, Z., Recent Advances in Lignin-Based Biofuel Production. *Energies* **2023,** *16* (8), 3382.
97. Li, S.; Li, Z.; Zhang, Y.; Liu, C.; Yu, G.; Li, B.; Mu, X.; Peng, H., Preparation of Concrete Water Reducer via Fractionation and Modification of Lignin Extracted from Pine Wood by Formic Acid. *ACS Sustainable Chemistry & Engineering* **2017,** *5* (5), 4214-4222.
98. Kalliola, A.; Vehmas, T.; Liitiä, T.; Tamminen, T., Alkali-O2 oxidized lignin – A bio-based concrete plasticizer. *Industrial Crops and Products* **2015,** *74*, 150-157.
99. Aso, T.; Koda, K.; Kubo, S.; Yamada, T.; Nakajima, I.; Uraki, Y., Preparation of Novel Lignin-Based Cement Dispersants from Isolated Lignins. *Journal of Wood Chemistry and Technology* **2013,** *33* (4), 286-298.
100. Figueiredo, P.; Lintinen, K.; Hirvonen, J. T.; Kostiainen, M. A.; Santos, H. A., Properties and chemical modifications of lignin: Towards lignin-based nanomaterials for biomedical applications. *Progress in Materials Science* **2018,** *93*, 233-269.
101. Yang, Y.; Xu, J.; Zhou, J.; Wang, X., Preparation, characterization and formation mechanism of size-controlled lignin nanoparticles. *International Journal of Biological Macromolecules* **2022,** *217*, 312-320.
102. Yadav, V. K.; Gupta, N.; Kumar, P.; Dashti, M. G.; Tirth, V.; Khan, S. H.; Yadav, K. K.; Islam, S.; Choudhary, N.; Algahtani, A., Recent advances in synthesis and degradation of lignin and lignin nanoparticles and their emerging applications in nanotechnology. *Materials* **2022,** *15* (3), 953.
103. Schneider, W. D. H.; Dillon, A. J. P.; Camassola, M., Lignin nanoparticles enter the scene: A promising versatile green tool for multiple applications. *Biotechnology Advances* **2021,** *47*, 107685.
104. Henn, A.; Mattinen, M. L., Chemo-enzymatically prepared lignin nanoparticles for value-added applications. *World J Microbiol Biotechnol* **2019,** *35* (8), 125.
105. Capecchi, E.; Piccinino, D.; Delfino, I.; Bollella, P.; Antiochia, R.; Saladino, R., Functionalized Tyrosinase-Lignin Nanoparticles as Sustainable Catalysts for the Oxidation of Phenols. *Nanomaterials (Basel)* **2018,** *8* (6).
106. Capecchi, E.; Piccinino, D.; Tomaino, E.; Bizzarri, B. M.; Polli, F.; Antiochia, R.; Mazzei, F.; Saladino, R., Lignin nanoparticles are renewable and functional platforms for the concanavalin a oriented immobilization of glucose oxidase–peroxidase in cascade bio-sensing. *RSC Advances* **2020,** *10* (48), 29031-29042.

Chapter 1

Dependence of ^{1}H NMR T_1 relaxation time of trimethylglycine betaine deep eutectic solvents on the molar composition and on the presence of water

Chiara Allegretti,[a] Paola D'Arrigo,*[,a,b] Francesco G. Gatti,*[,a] Letizia A. M. Rossato[a] and Eleonora Ruffini[a]

[a] Department of Chemistry, Materials and Chemical Engineering "Giulio Natta", Politecnico di Milano, P.zza Leonardo da Vinci 32, Milano, 20133, Italy.

[b] Istituto di Scienze e Tecnologie Chimiche "Giulio Natta" - Consiglio Nazionale delle Ricerche (SCITEC-CNR), Via Luigi Mancinelli 7, Milano, 20131, Italy

Published on *RSC Advances* **2023**, 13(5), 3004-3007.

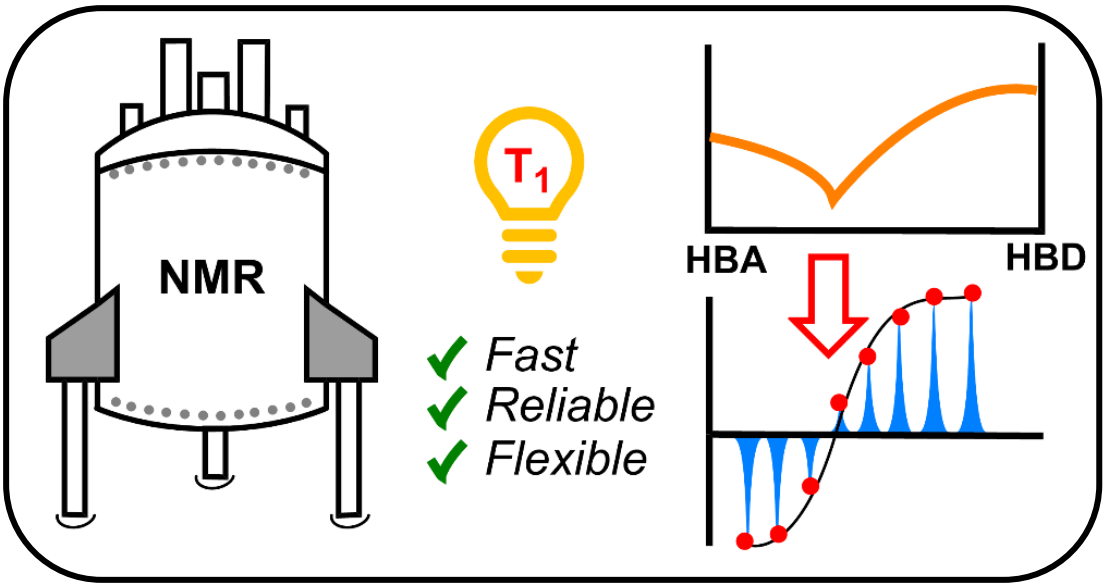

Abstract

^{1}H NMR spin lattice relaxation times (T_1), measured by inversion recovery technique, allowed to establish the stoichiometric coefficient (ratio between the H-bond acceptor and H-bond donor) of a series of trimethylglycine betaine/diol based deep eutectic solvents (DESs); ethylene glycol, triethylene glycol and 1,3-propandiol were selected as H-bond donors. The maximum amount of water tolerated by the DES, before its complete hydration, was determined as well. Finally, the method was validated comparing the eutectic composition of the betaine/glycol system with that determined by means of differential scanning calorimetry analysis, the stoichiometric coefficients resulted identical.

Paper

The term eutectic was coined by Guthrie in 1884 from the old Greek eutecticos, easy meltdown, to describe the melting point depression of a mixture with respect to its pure components.[1] The term deep eutectic solvent (DES) was used for the first time in the seminal work of Abbott in 2003,[2] where the adjective "deep" was meant to describe a much lower melting temperature than the ideal mixture of its components, typically two. Ever since many others DESs were discovered, and nowadays this new class of solvents has become extremely popular, especially in green chemistry. Later in 2011, Choi introduced the term natural DES (NADES), to describe the so called third liquid phase in microbial mammalian and plant cells, besides water phase and membrane lipids phase.[3-4] Even though the scientific community is still debating on a full comprehension of the nature of these solvents,[5] during the last decades, the number of DES-based applications in a wide range of fields has rapidly grown.[6-8]

In addition to their melting/freezing point, these solvents are characterized by many other physicochemical properties such as viscosity, density, ionic conductivity, surface tension, vapor pressure and refractive index.[9] Some of these observables (ionic conductivity, solvent polarity and viscosity) vary significantly with the molar composition of the mixture.[9-10] Noteworthy, very recently, it was found that the presence of small amounts of water (embedded water) might play an important role in promoting the DES formation.[11]

At nanoscopic level, the combination of a hydrogen bond acceptor HBA (usually solid) with a hydrogen bond donor HBD (either liquid or solid) leads to the formation of an HBA···HBD supramolecule, self-assembled by means of a cluster of H-bonds, and accordingly the mixture becomes liquid at eutectic temperature only at a definite HBA/HBD molar ratio (eutectic composition). However, it is not rare to find in literature different stoichiometric coefficients for the same DES. For instance, the formation of trimethylglycine betaine/ethylene glycol DES has been reported with three different stoichiometries: the ratio of 1:2 was used for the biocatalyzed synthesis of phospholipids in water,[12] whereas for the purification of gasoline a ratio of 1:3 was preferred,[13] the same composition was later found by Paiva,[14] instead, for the extraction of palmitic acid from palm oil, a mixture with more glycol (1:4) was applied.[15] Lastly, it is not always clear which is the maximum amount of water tolerated before that the H-bond disruption of the supramolecule occurs, in any case, the water added, typically does not exceed the 30-50% in weight.[16]

Prompted by the above considerations, the following study aims: (i) to verify if and how

the ^{1}H NMR spin-lattice relaxation time (T_1) of a set of selected DESs changes with the HBD molar fraction (X), and (ii) to ascertain how such a suggested correlation might be modified by progressive additions of water.
Our choice of the longitudinal relaxation time constant T_1 as an observable potentially informative of DES-supramolecule formation is based on its well-known dependence on the molecular tumbling motion (random molecular rotations and diffusion movements) in a liquid.[17-18] Thus, it is reasonable to think that larger and more rigid is an organic molecule, slower is its tumbling in solution. Indeed, without going too much in details of the complex spin-lattice relaxation theory, T_1 depends, among many other variables, on the molecular size and therefore on the molecular weight. Now, such relationship hints our tentative conjecture that the DES-supramolecule formed at the eutectic point might be characterized by a lower tumbling rate than its HBD component and conceivably by a specific value of T_1.

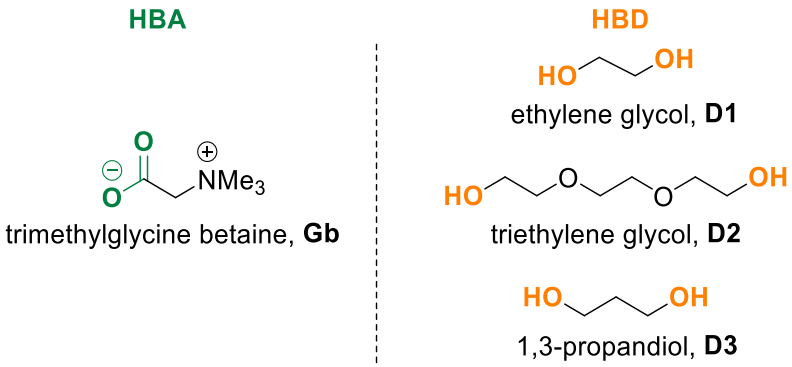

Figure 1: Components of trimethylglycine betaine-based DESs.

In the frame of our ongoing research work[12] we focused our attention on the trimethylglycine betaine/diol based DESs. In Figure 1 the selected HBD diols to be combined with the HBA trimethylglycine betaine (**Gb**) are shown: ethylene glycol (**D1**), triethylene glycol (**D2**) and 1,3-propandiol (**D3**), for more details on sample's preparation see the experimental part. However, the moisture content of diols was checked by Karl Fischer titration (< 1.5% in weight) before mixing with Gb.
The T_1 were measured by inversion recovery method at 75 °C, to avoid detrimental effects of viscosity on the linewidth (i.e., spectral resolution) of the ^{1}H NMR spectra. In addition, at this temperature we could widen the number of observable HBA/HBD mixtures, especially those with molar fraction X (X=[diol]/([diol]+[Gb])) lower than the eutectic mixture (infra eutectic region), which otherwise at room temperature would precipitate.
In Figure 2a we show the ^{1}H NMR spectra of **Gb/D1** DES (molar ratio 1:3, at 75 °C, external lock on D_2O in a coaxial tube). The OH resonance (broad singlet, chemical shift= 5.53 ppm) is clearly well separated from the other signals, moreover, using a long relaxation delay (d= 20 sec), the integrals result fully consistent with the ethylene glycol molar fraction of the mixture ($X_{D1}\approx 0.75$). Then, by adding 3 eq. of water to the freshly prepared DES, the OH signal appears significantly shielded (from 5.53 to 5.19 ppm) indicating a partial disruption of the H-bond self-assembled supramolecule (Figure 2b), whereas the chemical shift of the other signals did not change so much.
Since both OH protons of DES and of water at 75 °C are under rapid chemical exchange, the observed chemical shift is the weighted average of the chemical shifts of the two

species. Indeed, by lowering the temperature at 29 °C it was possible to discriminate the different nature of OHs (5.39 ppm vs 4.72 ppm, Figure 2c).

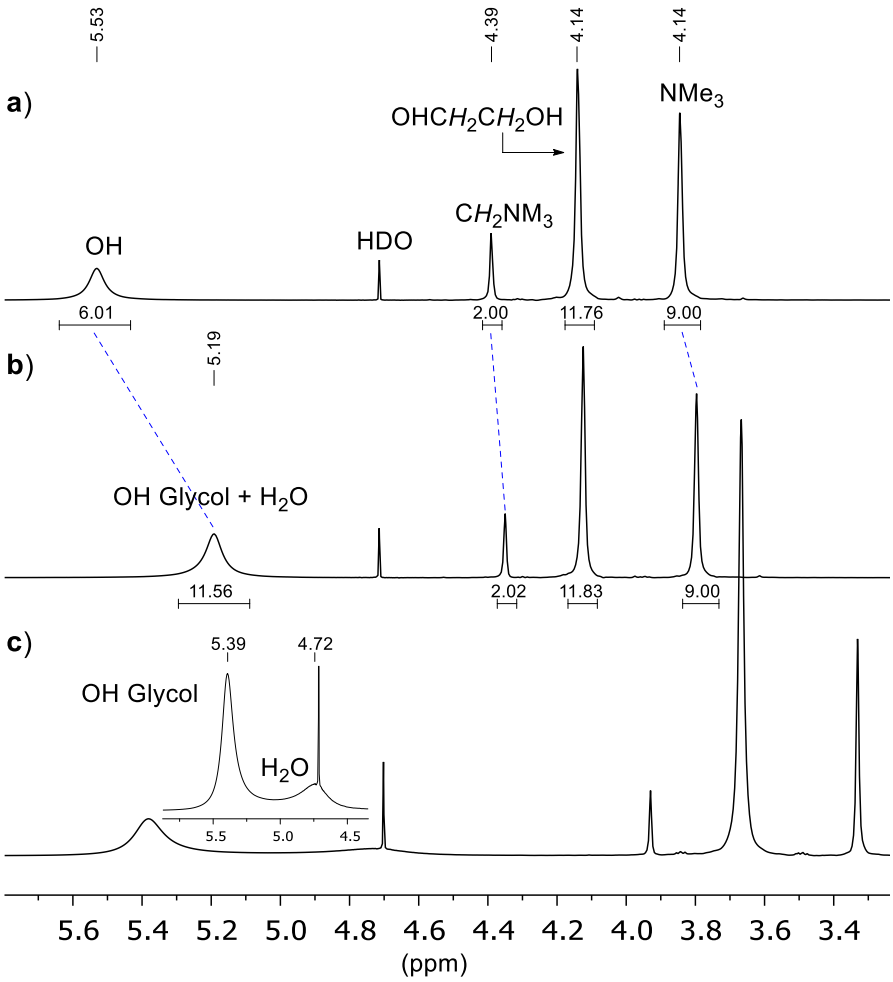

Figure 2: ^{1}H NMR spectra (400 MHz) of trimethylglycine betaine/ethylene glycol DES (1:3, $X_{D1}\approx 0.75$), the sample was externally locked using D_2O in a coaxial insert tube, the chemical shift calibration was done with respect to HDO (=4.71 ppm, residual signal of D_2O), and a recovery delay d= 20 sec was applied: a) DES at 75 °C; b) sample a) plus 3 eq. of H_2O with respect to HBA betaine; c) sample a) plus few drops of water at 29 °C.

Now, to begin with aim (i), the measured T_1 of OH proton in **Gb/D1** mixtures appears to change with the molar fraction (X_{D1}) as shown in Figure 3a. Indeed, the diagram T_1 versus X_{D1} exhibits a minimum (T_1= 1.26 sec) in correspondence of the molar composition **Gb/D1**= 1:3 ($X_{D1}\approx 0.75$), somehow reminding the customary solid-liquid phase diagram of binary eutectic mixtures. However, this point should correspond to the formation of the $Gb(D1)_3$ supramolecule, in which the lowest mobility of OH is most likely due to the formation of stronger H-bonds in the newly self-assembled supramolecule. Besides, in the ultra-eutectic region, the relaxation time increases linearly as the X_{D1} increases (linear regression equation: T_1= -2.46 + 5.0 X_{D1}, R^2=0.98) reaching the upper value of neat D1 (technical glycol T_1= 2.63 sec vs T_1= 2.11 sec of pure and anhydrous glycol,[19] purity

≥99.8%, the two values are different likely for the moisture, lit.[20] H_2O T_1= 9.11 sec at 75 °C).

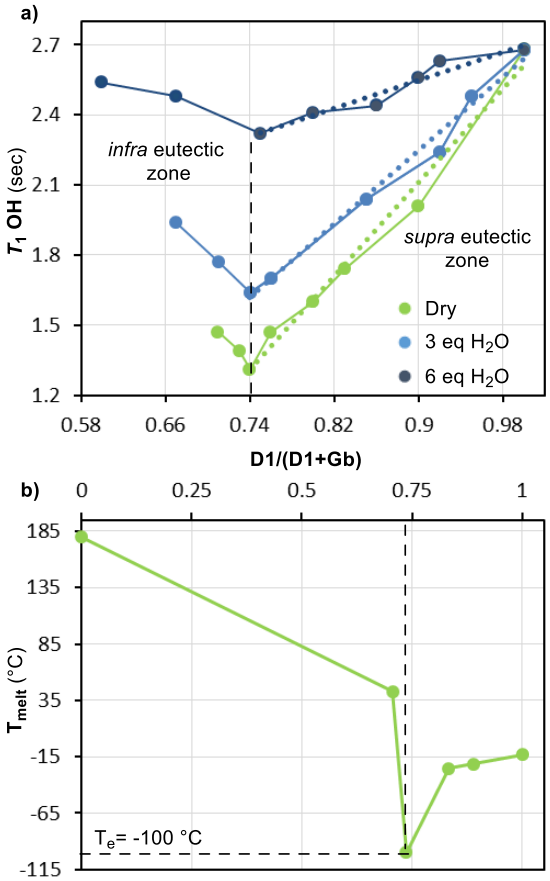

Figure 3: a) Plot of OH T_1 (measured with external lock) vs X_{D1} at 75 °C for the **Gb/D1** system, using commercial ethylene glycol (H_2O< 1.5% w/w). Green solid line: mixtures without addition of water; blue solid line: addition of 3 eq. of H_2O with respect to Gb; blue-navy solid line: addition of 6 eq. of H_2O with respect to Gb. The dashed lines correspond to the linear regression fitting. b) DSC analysis: plot of melting point T (°C) vs X_{D1}, without addition of water.

As initial approximation, we reckon that the T_1 observed in this region of the diagram is the molar average of the eutectic point and neat glycol values. However, quite recently, it was shown by IR and Raman spectroscopy that ethylene glycol is in equilibrium with its H-bond self-assembled dimer,[21] thus it is not unreasonable to think that the measured T_1 might be arise also from other supramolecular species present in solution.
On the other hand, in the infra-eutectic region of the diagram, the relaxation time becomes longer as X_{D1} decreases. However, since the leftmost point of this region was determined from a mixture with $X_{D1}\approx$ 0.71, not much different from that of the eutectic composition ($X_{D1}\approx$ 0.75), the correlation between the small increments of T_1 (from 1.26 sec to 1.42 sec) and the progressive dissociation of DES supramolecule was not reliable.
Finally, the 1:3 eutectic stoichiometry found by OH T_1 measurements (data in agreement with that reported by Paiva)[14] was confirmed by differential scanning calorimetry (DSC) analysis (Figure 3b), and a eutectic temperature (T_e) of -100 °C was determined.
Intrigued by the net influence of DES formation on the OH bonding donor mobility, the relaxation times of the remaining proton signals were analysed as well (see ESI);

however, the variations of T_1 were not anymore significantly traceable to a neat formation of $Gb(D1)_3$, mainly for two reasons: (i) these hydrogens are not involved in strong non-covalent interactions and therefore their mobility is less influenced by the formation of the H-bond self-assembled supramolecule; (ii) the chemical shift of these signals may change with X, and in some mixtures partial overlap of signals occurred, making the T_1 measure less accurate and reliable, and consequentially not anymore diagnostic of DES formation.

Concerning aim (ii), the relaxation time measurements of the **Gb/D1** mixtures were repeated on samples containing three and then six equivalents of water with respect to the HBA Gb (Figure 3a, blue and blue-navy solid lines, respectively). The T_1 diagrams of the wet mixtures have a similar shape to that of the "dry" system (H_2O< 1.5% in weight), but there are two discernible differences. First, by adding H_2O the T_1 value at the eutectic point becomes longer, in agreement with recently published studies,[22] secondly, the slopes of both regions of the diagram decrease remarkably (for instance in the ultra-eutectic region T_1= 1.35 + 3.95 X_{D1} with 3 eq of H_2O and T_1= 1.14 + 1.51 X_{D1} with 6 eq of H_2O, R^2=0.98 and R^2=0.94, respectively).

These observations suggest that the addition of water has the beneficial effect of reducing the viscosity, while the eutecticity of the system is partially conserved; however, it is conceivable that higher concentrations of water promote the complete dissociation of the eutectic supramolecule $Gb(D1)_3$ in the individual hydrated components.

Lastly, we repeated the T_1 measurements for the **Gb/D2** and **Gb/D3** mixtures (Figure 4a-b), and analogously to that seen for the **Gb/D1** system, the OH mobility of each diol decreased linearly to a minimum value in the correspondence of the eutectic point. More precisely, for the **Gb/D2** system the T_1 of triethylene glycol decreased from 2.03 sec to 1.35 sec, (T_1= 1.30 – 3.29 X_{D2}, R^2= 0.98), suggesting that the formation of DES-supramolecule occurs most likely with the $Gb(D2)_4$ stoichiometry (ratio 1:4, $X_{D3}\approx$ 0.80), such eutectic composition fully agreed with the one reported in literature.[23] While for **Gb/D3**, the formation of DES-supramolecule was achieved by mixing Gb with D3 in a ratio of 1:3 ($X_{D3}\approx$ 0.75, $Gb(D3)_3$), indeed at such molar composition the OH relaxation time reached the lowest value (i.e., T_1= 1.11 sec with T_1= 0.25 – 1.78 X_{D3}, R^2= 0.99). Even in this case, the eutectic composition determined by T_1 measurements resulted in full agreement with the literature data.[23]

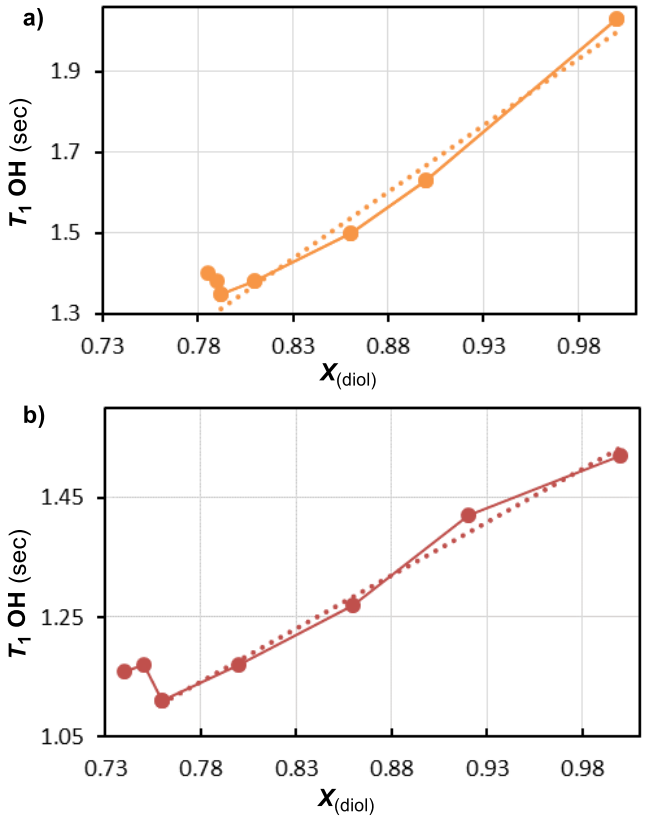

Figure 4: Plot of OH T_1 (measured with external lock) vs X_{diol} at 75 °C for the trimethylglycine betaine/diol system: a) with triethylene glycol **D2**; b) with the 1,3-propandiol **D3**. Dashed lines correspond to the linear regression fitting in the ultra-eutectic region.

In conclusion, we have shown that T_1 measurements allow to establish the appropriate stoichiometry to which the trimethylglycine betaine and the diol form the corresponding DES. The T_1 values were determined by inversion recovery method on a standard NMR instrumentation using an automated system; the eutectic compositions were validated by DSC analysis. All in all, the presented methodology compares well in terms of simplicity and time consuming with other analytical methods, especially if it will be updated with the new rapid T_1 estimation technique, recently reported.[24]
Lastly, our study shows that the trimethylglycine betaine/glycol DES can tolerate a maximum of 15% in weight of water, indeed, using a higher amount of water (26% in weight), the ethylene glycol seems no longer H-bonded to the glycine betaine.

Notes

The trimethylglycine betaine and diols were used as received by the suppliers without any further treatment. Trimethylglycine betaine (1.17 g, 1.0 mmol) were mixed with diol (see the ESI for the molar ratio) and stirred at 75 °C until the reaction mixture appeared completely homogeneous, then, it was left to stir for others 2 hours. The freshly prepared mixtures were submitted to NMR analysis. All NMR experiments were carried out on an Avance 400 Bruker instrument at 75 °C or at 29 °C, using an automation routine (IconNMR software). ^{1}H NMR T_1 relaxation times were measured using the Bruker library inversion recovery pulse program (Topspin software, version 2.5). D_2O was used as external lock in coaxial tube (5 mm), and the chemical shift calibration was done on

the HDO residual signal (= 4.71 ppm). Acquisition and processing parameters: number of scans= 1; relaxation delay d1= 20 sec; dummy scans ds= 2; variable delay list (sec): 0.1,0.2, 0.3, 0.5, 0.7, 1.0, 1.4, 1.8, 2.3, 2.8, 3.4, 4.1, 5.0, 7.0, 9.0, 12.0, 16.0, 20.0; line broadening lb= 2 Hz. T_1 fittings were obtained using Dynamic Center software, version 2.7.4 (see ESI).

Electronic supplementary information (ESI) available: Copies of ^{1}H NMR spectra and T_1 fitting. See DOI: https://doi.org/10.1039/d2ra08082f

References

1. Guthrie, F., LII. On eutexia. *The London, Edinburgh, and Dublin Philosophical Magazine and Journal of Science* **1884,** *17* (108), 462-482.
2. Abbott, A. P.; Capper, G.; Davies, D. L.; Rasheed, R. K.; Tambyrajah, V., Novel solvent properties of choline chloride/urea mixtures. *Chemical communications* **2003,** (1), 70-71.
3. Choi, Y. H.; van Spronsen, J.; Dai, Y.; Verberne, M.; Hollmann, F.; Arends, I. W.; Witkamp, G.-J.; Verpoorte, R., Are natural deep eutectic solvents the missing link in understanding cellular metabolism and physiology? *Plant physiology* **2011,** *156* (4), 1701-1705.
4. Triolo, A.; Celso, F. L.; Brehm, M.; Di Lisio, V.; Russina, O., Liquid structure of a choline chloride-water natural deep eutectic solvent: A molecular dynamics characterization. *Journal of Molecular Liquids* **2021,** *331*, 115750.
5. Martins, M. A.; Pinho, S. P.; Coutinho, J. A., Insights into the nature of eutectic and deep eutectic mixtures. *Journal of Solution Chemistry* **2019,** *48*, 962-982.
6. Smith, E. L.; Abbott, A. P.; Ryder, K. S., Deep eutectic solvents (DESs) and their applications. *Chemical reviews* **2014,** *114* (21), 11060-11082.
7. Perna, F. M.; Vitale, P.; Capriati, V., Deep eutectic solvents and their applications as green solvents. *Current Opinion in Green and Sustainable Chemistry* **2020,** *21*, 27-33.
8. Allegretti, C.; Bellinetto, E.; D'Arrigo, P.; Griffini, G.; Marzorati, S.; Rossato, L. A. M.; Ruffini, E.; Schiavi, L.; Serra, S.; Strini, A.; Tessaro, D.; Turri, S., Towards a Complete Exploitation of Brewers’ Spent Grain from a Circular Economy Perspective. *Fermentation* **2022,** *8* (4), 151.
9. Hansen, B. B.; Spittle, S.; Chen, B.; Poe, D.; Zhang, Y.; Klein, J. M.; Horton, A.; Adhikari, L.; Zelovich, T.; Doherty, B. W., Deep eutectic solvents: A review of fundamentals and applications. *Chemical reviews* **2020,** *121* (3), 1232-1285.
10. Zhang, Q.; Vigier, K. D. O.; Royer, S.; Jérôme, F., Deep eutectic solvents: syntheses, properties and applications. *Chemical Society Reviews* **2012,** *41* (21), 7108-7146.
11. Ma, C.; Laaksonen, A.; Liu, C.; Lu, X.; Ji, X., The peculiar effect of water on ionic liquids and deep eutectic solvents. *Chemical Society Reviews* **2018,** *47* (23), 8685-8720.
12. Allegretti, C.; Gatti, F. G.; Marzorati, S.; Rossato, L. A. M.; Serra, S.; Strini, A.; D'Arrigo, P., Reactive Deep Eutectic Solvents (RDESs): A new tool for phospholipase D-catalyzed preparation of phospholipids. *Catalysts* **2021,** *11* (6), 655.
13. Kučan, K. Z.; Perković, M.; Cmrk, K.; Načinović, D.; Rogošić, M., Betaine+(glycerol or ethylene glycol or propylene glycol) deep eutectic solvents for extractive purification of gasoline. *ChemistrySelect* **2018,** *3* (44), 12582-12590.
14. Rodrigues, L. A.; Cardeira, M.; Leonardo, I. C.; Gaspar, F. B.; Redovniković, I. R.; Duarte, A. R. C.; Paiva, A.; Matias, A. A., Deep eutectic systems from betaine and polyols–Physicochemical and toxicological properties. *Journal of Molecular Liquids* **2021,** *335*, 116201.
15. Mulia, K.; Adam, D.; Zahrina, I.; Krisanti, E. A., Green extraction of palmitic acid from palm oil using betaine-based Natural Deep Eutectic Solvents. *International Journal of Technology* **2018,** *9* (2), 335-344.
16. Dai, Y.; Witkamp, G.-J.; Verpoorte, R.; Choi, Y. H., Tailoring properties of natural deep eutectic solvents with water to facilitate their applications. *Food chemistry* **2015,** *187*, 14-19.
17. Bloembergen, N.; Purcell, E. M.; Pound, R. V., Relaxation effects in nuclear magnetic resonance absorption. *Physical review* **1948,** *73* (7), 679.
18. Levitt, M. H., *Spin dynamics: basics of nuclear magnetic resonance*. John Wiley & Sons: 2013.

19. Spees, W. M.; Song, S. K.; Garbow, J. R.; Neil, J. J.; Ackerman, J. J., Use of ethylene glycol to evaluate gradient performance in gradient-intensive diffusion MR sequences. *Magnetic resonance in medicine* **2012,** *68* (1), 319-324.
20. Krynicki, K., Proton spin-lattice relaxation in pure water between 0 C and 100 C. *Physica* **1966,** *32* (1), 167-178.
21. Kollipost, F.; Otto, K. E.; Suhm, M. A., A Symmetric Recognition Motif between Vicinal Diols: The Fourfold Grip in Ethylene Glycol Dimer. *Angewandte Chemie* **2016,** *128* (14), 4667-4671.
22. Di Pietro, M. E.; Tortora, M.; Bottari, C.; Colombo Dugoni, G.; Pivato, R. V.; Rossi, B.; Paolantoni, M.; Mele, A., In competition for water: hydrated choline chloride: urea vs choline acetate: urea deep eutectic solvents. *ACS Sustainable Chemistry & Engineering* **2021,** *9* (36), 12262-12273.
23. Hsieh, Y.-H.; Li, Y.; Pan, Z.; Chen, Z.; Lu, J.; Yuan, J.; Zhu, Z.; Zhang, J., Ultrasonication-assisted synthesis of alcohol-based deep eutectic solvents for extraction of active compounds from ginger. *Ultrasonics Sonochemistry* **2020,** *63*, 104915.
24. Wei, R.; Dickson, C. L.; Uhrin, D.; Lloyd-Jones, G. C., Rapid Estimation of T 1 for Quantitative NMR. *The Journal of Organic Chemistry* **2021,** *86* (13), 9023-9029.

Chapter 2

Reactive Deep Eutectic Solvents (RDESs): A New Tool for Phospholipase D-Catalyzed Preparation of Phospholipids

Chiara Allegretti,[a] Francesco G. Gatti,[a] Stefano Marzorati,[b] Letizia A. M. Rossato,[a] Stefano Serra,[b] Alberto Strini,[c] and Paola D'Arrigo*[,a,b]

[a] Department of Chemistry, Materials and Chemical Engineering "Giulio Natta", Politecnico di Milano, p.zza L. da Vinci 32, Milano 20133, Italy.

[b] Istituto di Scienze e Tecnologie Chimiche "Giulio Natta", Consiglio Nazionale delle Ricerche (SCITEC-CNR), via Luigi Mancinelli 7, Milano 20131, Italy.

[c] Istituto per le Tecnologie della Costruzione, Consiglio Nazionale delle Ricerche (ITC-CNR), via Lombardia 49, San Giuliano Milanese 20098, Italy.

Published on *Catalysts* **2021**, 11, 655

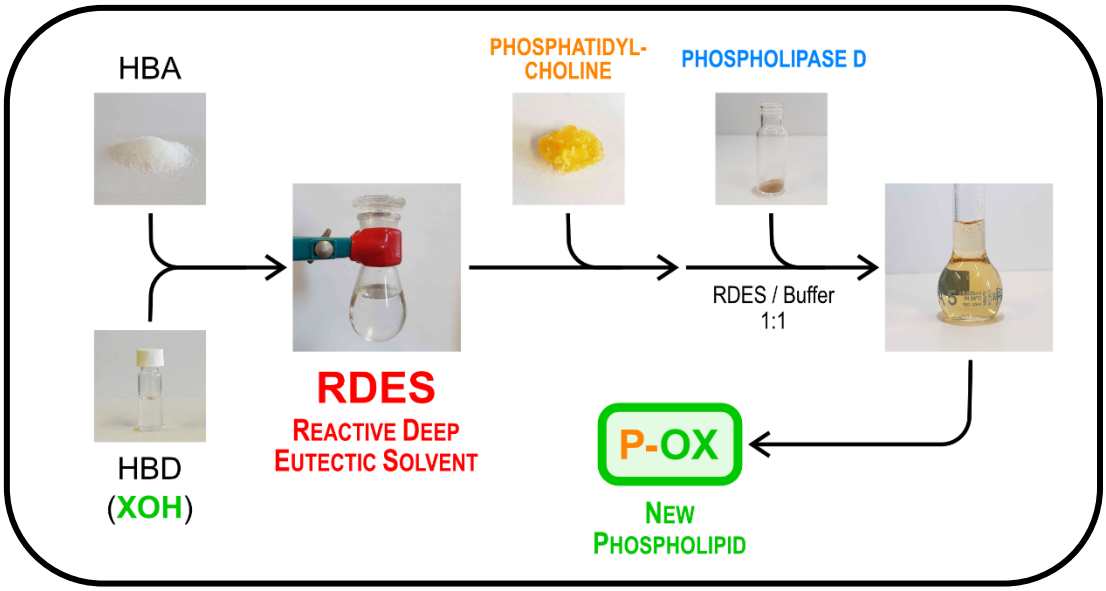

Abstract

The use of Reactive Deep Eutectic Solvents (RDESs) in the preparation of polar head-modified phospholipids (PLs) with phospholipase D (PLD)-catalyzed biotransformations has been investigated. Natural phosphatidylcholine (PC) has been submitted to PLD-catalyzed transphosphatidylations using a new reaction medium composed by a mixture of RDES/buffer. Instead of exploiting deep eutectic solvents conventionally, just as the reaction media, these solvents have been designed here in order to contribute actively to the synthetic processes by participating as reagents. RDESs were prepared using choline chloride or trimethyl glycine as hydrogen-bond acceptors and glycerol or ethylene glycol, as hydrogen-bond donors as well as nucleophiles for choline substitution. Specifically designed RDES/buffer reaction media allowed the obtainment of PLs with optimized yields in the perspective of a sustainable process implementation.

1. Introduction

In recent years, the demand for new synthetic approaches with reduced environmental impact is highly present in the political agenda. In this context, the use of new protocols involving biocatalysis as well as the investigation of greener suitable solvents in the chemical modification of organic materials fits perfectly the research focused on the achievement of the Sustainable Development Goals.[1-4]

Deep Eutectic Solvents (DESs) are a relatively new class of solvents[5-6] prepared for the first time by Abbott *et al.* in 2003[7] and, since then, deeply studied in many fields including, among the others, materials science,[8] analytical and preparative separation,[9-10] biomass processing,[11-12] organic synthesis,[13-14] and biocatalysis.[15-19] DESs are eutectic mixtures composed by a hydrogen bond acceptor (HBA) and a hydrogen bond donor (HBD) that can be easily prepared by mixing and heating the components generating clear liquid phases, which present a significantly lower melting point compared to their individual components. Clearly, these solvents are a promising alternative to ionic liquids (ILs), since they share many important features[20] such as low volatility, conductivity, high thermal stability, negligible flammability, and a broad liquid range. DESs can be prepared from a broad range of components including biomass-derivatives and renewable organic compounds. DESs have there-fore a key advantage in the development of reaction media for environment-friendly and sustainable chemical processes.[21] Moreover, a distinctive feature of DESs is the extensive hydrogen bonding that, besides ensuring very good and modulable solvating properties, can actively participate in the process as catalyst or co-catalyst.[13] Because of the very large combinatorial space of the main components[6] and the possibility to add co-solvents or anti-solvents such as water,[22] DES-based process media benefit from an exceptional versatility, which allows the design of highly optimized mixtures with special characteristics such as specific catalytic activities and adjusted solvation properties. All of these qualities lead the way to the development of tailored biocatalytic processes,[16, 23-24] particularly with the possible addition of a water component in order to ensure the establishment of an enzyme-friendly environment.[24-25] On top of that, a recent and very interesting development is the promotion of the DESs role from solvent/catalyst to actual reactive component. Reactive Deep Eutectic Solvents (RDESs) can exploit the versatility of DESs in such a way to provide a reaction medium mixture containing one or more process reagents, resulting in several advantages that include a substantial mass effect due to the very high concentration. Moreover, the highly adaptable

solvating properties allow for the designing of specifically tuned mixtures for the reactants dissolution as well as for the efficient separation of products by precipitation, enhancing the overall process yield. This can be particularly important in the optimization of enzymatic processes based on equilibrium reactions, a common case in bio-based sustainable Green Chemistry. RDESs are known to have been successfully employed in cellulose derivatization,[26-27] free-radical polymerizations,[28] heterocyclic synthesis,[29-30] and in biocatalytic processes[24] such as the enzymatic synthesis of 1,3-diacylglycerols,[31] glycolipids,[32] and menthol fatty acid esters.[33]

Phospholipids (PLs) represent the main constituents of all biological membranes and they are the topic of many areas of biomedical research due to their natural involvement in many cellular functions such as cellular regeneration processes, differentiation of neurological pathways, and promotion of molecules transportation through cell membranes.[34-35] Furthermore, they are able to promote the biological activity of various membrane linked proteins and receptors, and they have been successfully exploited as therapeutic agents, drug-delivery systems, and diagnostic markers for different diseases.[36-39] Moreover, some neurological pathologies such as stress-related disorders, schizophrenia, dementia, and Parkinson's disease have showed to be associated with a disequilibrium in PLs metabolism, signaling, and transport.[40-41] Dietary PLs are essential for preventing a broad range of human diseases such as inflammation, cancer, and coronary heart issues.[42-43] Other interesting applications involve their use as natural emulsifiers, surfactants, food stabilizers, and detergents.[44-45] From a structural point of view, as reported in Figure 1, PLs molecules present a glycerol backbone, esterified in *sn-1* and *sn-2* positions with saturated or unsaturated long chain fatty acids (lipophilic moieties) and in *sn-3* with a phosphate diester (polar head group).

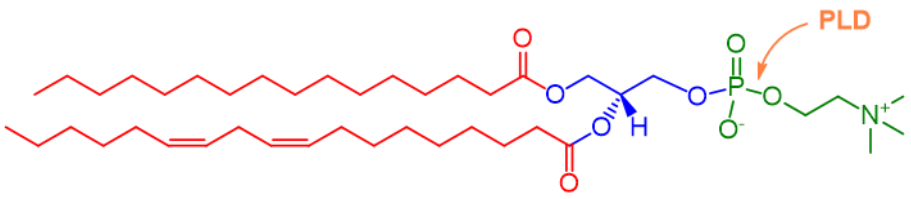

Figure 1: General structure describing the PC (here 1-palmitoyl-2-linoleyl-PC) structure composed by two acyl chains (in red), a glycerol backbone (in blue) and a polar head (in green). The attack position cleaved by PLD is also indicated with the orange arrow.

The amphiphilic nature of these molecules, due their peculiar structure, is the key factor responsible for their spontaneous aggregation (in bilayers and micelles) in aqueous environments, a very appealing property for the applications within the drug delivery and cosmetic sectors.[46] In the last year, after the beginning of the Covid-19 pandemic, the design of new vaccines has been the major studied worldwide topic. In particular, the design considerations about the new formulations have focused on liposome preparations, which are employed in modern vaccine technologies because their design is mandatory to ensure proper immune responses.[47-48] Liposomes serve in fact as adjuvants with the role of potentiating the immune response of the vaccines by improving their efficacy.[49]

The biological activity of PLs is strictly dependent on the chemical identity of the polar head and the acyl chains. The commercial values of these compounds are highly related to the source and the purity of the products.[50] Natural PLs can be obtained from vegetable sources such as soybeans, sunflower, corn, peanut, flaxseed, rape (canola) seed

wheatgerm, and animal sources like egg yolk, meat, milk and krill.[51-54] The challenging chemical preparation of the different PLs can be achieved by semi- or total synthesis starting from appropriate chiral precursors. These procedures usually require, in addition to the introduction of the desired functional groups, a complex sequence of protection and deprotection steps. For these reasons, the set-up of simpler biocatalytic approaches for the preparation of these specific PLs from natural sources is a suitable alternative. Furthermore, these greener protocols based on the use of harmless, natural, and safer reagents are especially preferred when the product's destination is for the food or pharmaceutical sectors.[53, 55-56]

The most abundant PL in nature is phosphatidylcholine (PC, reported in Figure 1 as 1-palmitoyl-2-linoleyl-PC). This compound can be modified in its polar head moiety by means of phospholipase D (PLD, E.C.3.1.4.4), an enzyme able to hydrolyze PC into phosphatidic acid (PA). In particular, different bacterial PLDs from *Streptomyces sp.* were studied in our research group.[57-59] Although they are extracellular hydrolytic enzymes with a broad substrate specificity, they are also able to catalyze a transphosphatidylation reaction in the presence of an alcohol (X-OH) allowing the formation of PX by the polar head modification even in the presence of water as a cosolvent.[60-62] This property is quite unique among hydrolytic enzymes, and it is essential in practical applications for the preparation of non-natural PLs or less natural abundant ones, starting from crude or purified PC (see Figure 2).

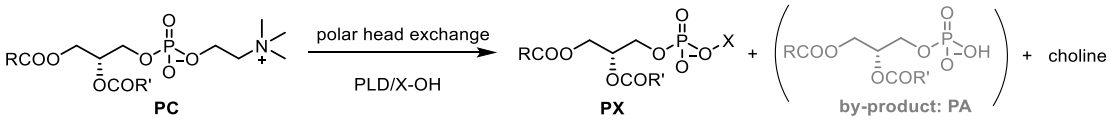

Figure 2: Phospholipase D-catalysed transformations of PC.

These reactions are usually carried out in aqueous/organic solvents biphasic systems because, due to their amphiphilic features, PLs are only soluble in organic solvents with low polarity such as chloroform, diethylether, hexane, and toluene. However, in these reaction media, the formation of PA as a by-product is quite unavoidable, but the extent of the competing hydrolytic reaction depends on the nature of the nucleophile and on the reaction conditions (see Figure 2). Hence, the competitive production of PA lowers the transphosphatidylation yield, and the need of further purification procedures becomes mandatory. The purification of the final products PX is not straightforward, and it requires various chromatographic and selective precipitation steps. For this reason, the modification and the improvement of the reaction conditions in the synthesis of polar head-modified PLs have been the object of many studies exploiting new biocatalytic strategies.[63] In particular, the screening of a great number of novel eco-friendly solvents such as γ-valerolactone, limonene, and p-cymene were used for the synthesis of phosphatidylserine (PS), a PL with a high commercial interest because of its nutritional and medical functions.[64-67] On this topic, the authors investigated the possibility to perform the preparation of PS, exploiting a new solvent composed by the ionic liquid (IL) 1-butyl-3-methylimidazolium hexafluorophosphate [BMIm][PF_6] that allowed the preparation of the desired product with 91.4% yield with a quite complete suppression of unwanted hydrolytic side reaction.[68]

The use of DESs as a solvent for the PLD-catalyzed transformations of PC was only

reported by Yang *et al.*[69] for the preparation of PS using a commercial enzyme from *Streptomyces chromofuscus*. In this work, the authors reported the screening of different DESs and identified ChCl/Glycerol (Gly) and ChCl/ethylene glycol (EG) including 5% of water as the most suitable solvents for PS synthesis.
In the present work, the use of RDES-based protocols for the biocatalytic conversion of PC in two different PLs, the natural phosphatidylglycerol (PG), and the non-natural phosphatidylethyleneglycol (P-EG) has been investigated. All conversions were catalyzed by PLD from *Streptomyces netropsis*. The glycerol and ethylene glycol needed for the transphosphatidylation reactions were supplied as the reactant part of RDESs. Tailored RDES/buffer mixtures have been developed in order to optimize the effects of the medium composition in a perspective of a more sustainable process definition. Reaction yields have been optimized both by the high reactant concentration due to the use of RDES and by tuning the solvation capability of the RDES/buffer medium in order to obtain the product separation by precipitation. Moreover, using RDES/buffer medium, unwanted PC hydrolysis appears nearly completely inhibited leading to a yield enhancement and a higher product purity.

2. Results and Discussion

2.1. Preliminary Method Development

The first tests were carried out to screen the solubility of PC in order to select the potential DES candidates for the biocatalytic transformations aiming to produce PS, using PLD from *Streptomyces netropsis*. In particular, ChCl/Gly 1/2 (mol/mol), ChCl/acetic acid 1/2, choline p-toluensulphonate/acetic acid 1/2, ChCl/urea/acetic acid 1/1/1, and ChCl/levulinic acid 1/2 were tested. The starting PC was soluble in all these solvents, but only the first DES of the list was selected for the first enzymatic trials. The low pH (around 3) associated with all other DESs was in fact unsuitable for the enzymatic activity. However, using ChCl/Gly, besides the desired PS, the presence of PG (derived from the parasitic reaction with DES) was detected as well as a high quantity of unreacted PC. This leads to the decision of developing a specific RDES reaction medium, where the reacting nucleophile was provided as part of the process medium. The nature of the HBA component of RDES and the water content of the reaction medium (needed to preserve the enzymatic activity) were studied in order to increase the solubility of PC and decrease those of the products. The limitation of the product concentration in the reaction medium by precipitation allowed the enhancement of the yields. The RDES design process yielded to the formulations of four RDESs (Section 2.2) and, of the final reaction medium, composed by a RDES/water buffer mixture (1:1, v/v).

2.2. Preparation of RDES Media

In this work, four different RDESs consisting of mixture of HBA/HBD in a 1:2 molar ratio have been prepared. The quaternary ammonium salts choline chloride (ChCl) and trimethylglycine (also called betaine glycine; BetG) have been used as HBAs, whereas glycerol (Gly) and ethylene glycol (EG) constituted HBDs and reactants (see Table 1).

Table 1: Structure, name, and symbols of the HBAs and HBDs used here as components in the preparation of RDESs.

Hydrogen–Bond Acceptors (HBAs)		Hydrogen–Bond Donors (HBDs)	
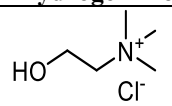	choline chloride (ChCl)	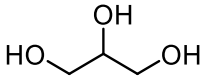	Glycerol (Gly)
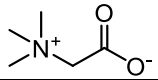	trimethyl glycine (BetG)	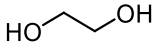	ethylene glycol (EG)

The RDESs have been prepared by using a defined protocol which consisted of mixing the components in a defined molar ratio and heating them at 90 °C for 2–5 h, under constant stirring in a sealed vial until a stable homogeneous colorless one phase liquid was formed (see Supplementary Materials Figure S1). They have been dried at reduced pressure for 24 h, preserved under argon, and then characterized by ^{1}H NMR spectra (see Supplementary Materials Figure S2). The selected HBAs, ChCl, and BetG possess an evident biocompatibility and an availability from natural products which constitute one of their major advantages. In addition, the HBDs Gly and EG are highly available as bulk commodity chemicals. Furthermore, Gly is produced as a by-product of different hydrolysis and transesterification processes of oils and fats most notably in the soap and biodiesel manufacturing industries.

These RDES were suitable for PL modifications because their density was in the range of 1.06 to 1.16 g/cm^3, which allowed a good mass transfer and interaction between the reaction components (see Table 2). For that reason, many other RDESs, showing higher density values, have been excluded from the screening. According to the literature, DES's densities are usually higher than water's value and are dependent on the working temperatures. As reported in Table 2, the densities of Gly-containing RDESs (RDES A1 and B1) were higher than the densities of EG-containing ones (RDES A2 and B2).

Table 2: List, composition, and density of RDESs (measured at 18 °C) and reaction mixtures (RDES/buffer 1/1) which have been prepared and used in this study.

RDES Symbol	HBA	HBD	Molar Ratio (HBA/HBD)	Density of Pure RDES (g/cm^3)	Density of RDES/Buffer Solutions (g/cm^3)
RDES A1	choline chloride	glycerol	1:2	1.16	1.09
RDES A2	choline chloride	ethylene glycol	1:2	1.06	1.03
RDES B1	trimethyl glycine	glycerol	1:2	1.16	1.08
RDES B2	trimethyl glycine	ethylene glycol	1:2	1.11	1.05

2.3. Transphosphatidylation Reactions

The substrate used for all experiments was a commercial PC from soya beans which was preliminarily purified by precipitation in cold acetone. The acyl chains pattern of PC was identified with the method by ESI/MS and GC/MS previously reported.[70] The fatty acid chains composition is reported in Figure 3 and Table 3.

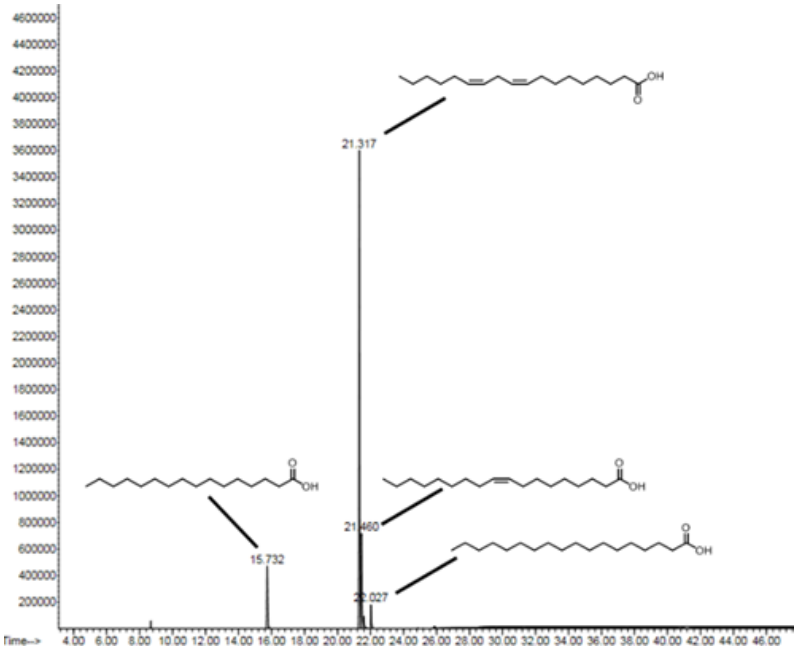

Figure 3: GC/MS analysis of acyl chains in starting PC with the indication of the chemical formula of each acid (Retention time reported in min).

Table 3: Fatty acid composition of PC (results obtained by GC analysis reported in Figure 3).

Acid	Chain	t_R	% in PC
palmitic acid	C16:0	15.7	11.2
linoleic acid	C18:2	21.3	69.3
oleic acid	C18:1	21.4	15.8
stearic acid	C18:0	22.0	3.6

2.3.1. Preparation of Phosphatidylglycerol

Phosphatidylglycerol (PG) constitutes one of the most abundant PLs at the basis of natural membranes. PG possesses an excellent liposome forming ability and unique surfactant/lubricant properties, especially when mixed with appropriate proteins, and, for these reasons, it has been studied for a long time,[71] especially as an emulsifier for drug delivery systems.[72-73] Moreover, in mammalian lungs, PG is highly present compared to other mammalian membranes and therefore the research has been focused on the development of new surfactant preparations based on PG derivatives for therapeutic treatment of diseases such as a neonatal respiratory distress syndrome.[74] Moreover, it has been used for the preparation of plasmid-DNA lipid and polymeric nanovaccines showing that anionic PLs could increase antigen delivery, transport, and stability.[75] Unfortunately, PG could be recovered only in small amounts from natural sources and, even if it has been prepared by different groups,[76-78] the possibility to set-up new strategies of synthesis is mandatory especially for the biomedical investigations.

Up to now, PG, when enzymatically synthesized, was usually prepared from natural PC by a PLD-mediated process in an organic solvent/buffer biphasic system containing glycerol as the nucleophile. In this work, a new protocol was investigated aiming to avoid

the presence of the organic solvent in the reaction medium by using a RDES (see Figure 4). In the first attempts, PLD had been suspended in pure RDES, but the total absence of water completely inactivated the enzyme. As already shown for ILs, a minimal concentration of at least 5% of water was mandatory for the enzyme activity.[29] The process medium composition was optimized by water addition setting the RDES/aqueous phase ratio to the value 1:1 (v/v), resulting also in a modulation of the solvating properties leading to the product precipitation. In particular, the aqueous phase was a 0.1 M NaOAc buffer solution at pH 5.6 containing 0.1 M $CaCl_2$. PC was fully solubilized in RDES and then a buffer solution containing PLD was added. After 40 h at 45 °C, the products that precipitated in the reaction mixture were recovered and analyzed. Remarkably, the extraction of the remaining reaction mixture demonstrated that most of the products were effectively in the precipitate and just a minor amount (≈ 5%) remained dissolved in the RDES/buffer medium. This proved the effectiveness of the RDES/buffer medium design in order to minimize the product concentration in the liquid phase and thus pushing the equilibrium towards the reaction completeness.

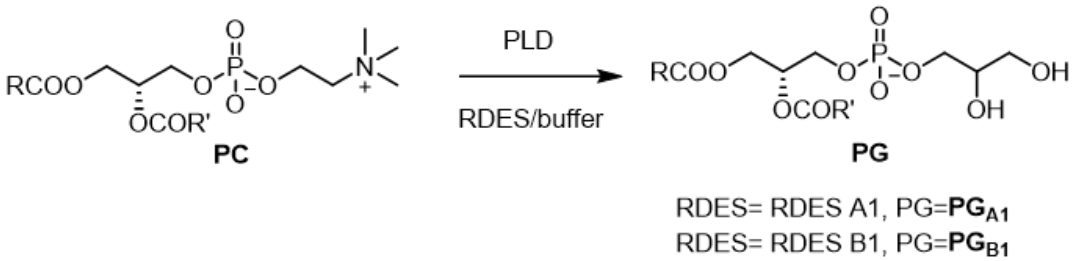

Figure 4: Transphosphatidylation of PC to PG.

When the reaction was performed with RDES A1 (ChCl/Gly 1:2) unreacted PC (≈ 14 %, value obtained by HPLC analysis) was revealed, whereas, in RDES B1 (BetG/Gly 1:2), PC was completely converted in PG. In the first case, the presence of choline as HBA probably prevented the reaction to be completely shifted versus products because of its mass effect opposed to the HBD component (pushing the equilibrium point to-wards the substrate). In fact, as it resulted in the ^{1}H NMR spectrum (see Figure 5, green spectrum), PG_{A1} showed a residual peak around 3.2 ppm, which demonstrated the presence of residual unreacted PC. This peak disappeared completely in PG_{B1}, because of the total conversion of PC to the final desired product.

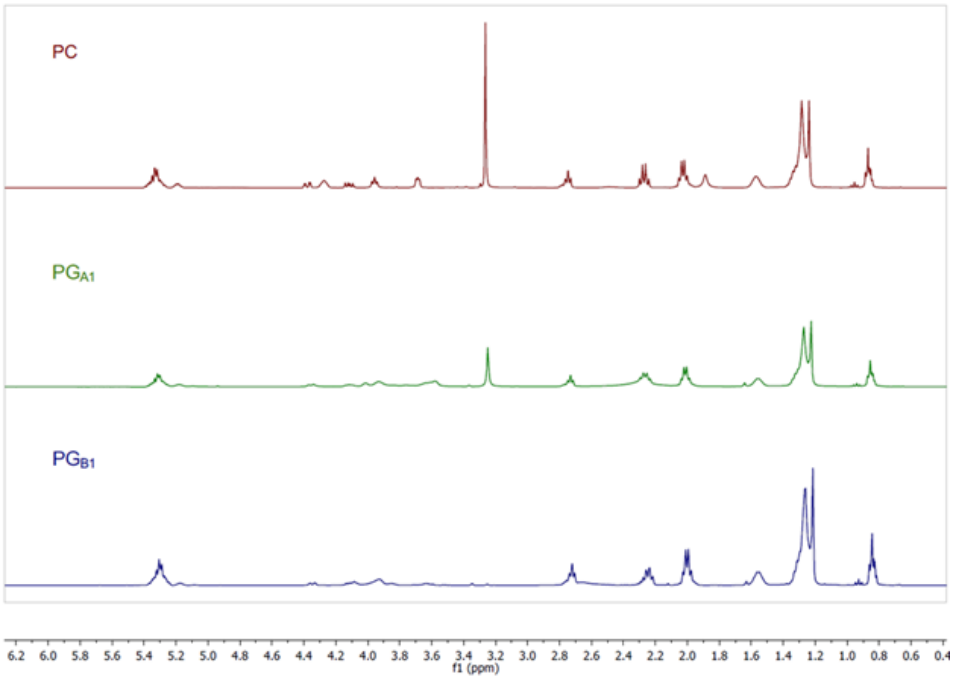

Figure 5: ^{1}H NMR spectra of starting PC (red line), PG_{A1} (green line) and PG_{B1} (blue line) in $CDCl_3/CD_3OD$.

Moreover, the presence of the RDES medium seems to inhibit nearly completely the hydrolysis side-reaction driving the conversion toward transphosphatidylation in comparison to what happened when the reaction was conducted in organic solvent/water as ESI/MS analysis confirmed (see Supplementary Materials).

2.3.2. Preparation of Phosphatidylethyleneglycol (P-EG)

Polyethyleneglycol (PEG)-grafted PLs are widely studied in the medical field, as they are one of the main components of liposomes used as carriers for mRNA, siRNA,[79] and for anticancer active compounds such as paclixatel.[80] The relationship between PEG chain length and concentration in PEG-grafted PLs based vesicles has been deeply investigated,[81] aiming to obtain optimized properties, in terms of water permeability and membrane strength, which resulted in a higher liposome lifetime in the blood circulation, and a better drug delivery. In this context, the authors decided to synthesize a non-natural phosphatidylethyleneglycol (P-EG), which could be an interesting building block for the production of new P-EG containing PLs. The free OH on the polar head could be then available to undergo esterification reactions, allowing the production of novel tailor-made products. In order to obtain a reference P-EG, the product has been firstly prepared with the conventional method in toluene/buffer solution. Subsequently, PC was fully solubilized in RDESs A2 (ChCl/EG 1:2) and B2 (BetG/EG 1:2) containing both ethylene glycol which constituted HBD as well as the nucleophile in the PLD catalyzed transphosphatidylation (see Figure 6). A buffer solution containing PLD was added to the solution to start the reaction. After 40 h at 45 °C, the products, precipitated in the reaction medium, were recovered and analyzed.

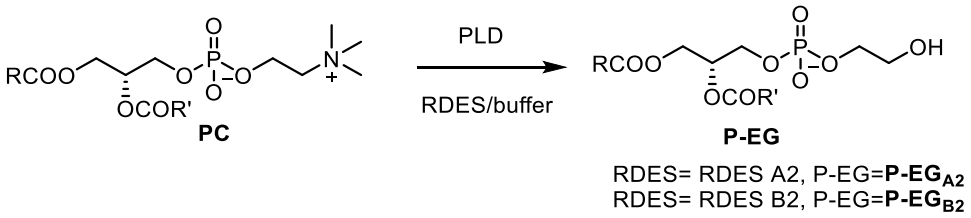

Figure 6: Scheme of transphosphatidylation reaction of PC to P-EG.

Also in this case, as described in Section 2.3.1, most of the products precipitated and just a minor part (≈ 10%) was recovered by solvent extraction from the RDES/buffer medium. This confirmed again the efficacy of the process medium optimization in the modulation of the reagent and products solubility. ^{1}H NMR spectra of the final products are reported in Figure 7 (P-EG$_{A2}$, green line, and P-EG$_{B2}$ blue line). As already observed in the PGs preparation in 2.2.1, when the reaction was performed in RDES containing ChCl, namely RDES A2, a small quantity of PC (≈ 8%, value obtained by HPLC analysis) remained unreacted, whereas, in RDES B2 (BetG/EG 1:2), PC was completely converted to P-EG.

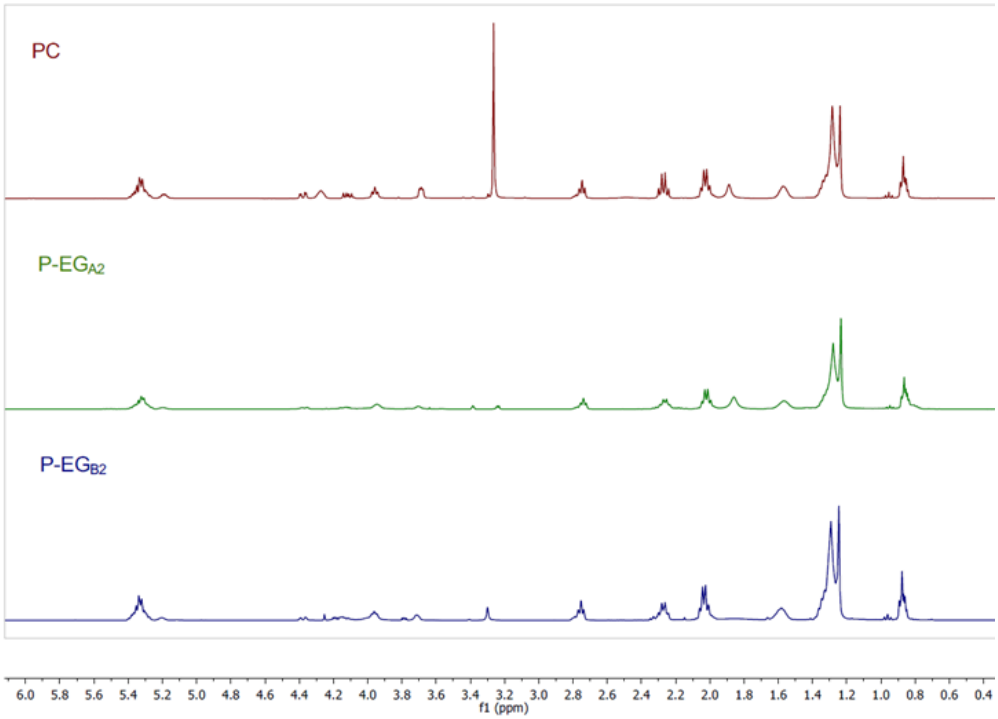

Figure 7: ^{1}H NMR spectra of starting PC (red line), P-EG$_{A2}$ (green line) and P-EG$_{B2}$ (blue line) in D_2O.

3. Materials and Methods

All chemicals were purchased from Merck (Merck Life Science S.r.l., Milan, Italy) and used without further purification. The employed solvents were of analytical or HPLC grade when necessary. Phosphatidylcholine was supplied from Lucas Meyer (Epikuron 200, soya lecithin, Hamburg, Germany) and used after precipitation in cold acetone (10 g Ep200 dissolved in 15 mL of CH_2Cl_2, added to 300 mL of cold acetone). ^{1}H NMR and ^{31}P NMR spectra were recorded on a 400 MHz Bruker Avance spectrometer (Milano,

Italy). Acquisition and data treatment were performed with Bruker TopSpin 3.2 software. Chemical shifts were reported in δ units (ppm), relative to tetramethylsilane (TMS) as the internal standard and all spectra were recorded in D_2O or $CDCl_3/CD_3OD$. Deuterated solvents were purchased from Eurisotop (Saint-Aubin, France).

3.1 ^{31}P NMR Sample Preparation

In addition, 50 mg of the sample was dissolved with 5 mg of triphenyl phosphate in 0.6 mL of a $CDCl_3/CH_3OH$ 2:1 solution mixed with 0.4 mL of a CsEDTA solution (prepared. by titration of 0.2 M EDTA in D_2O with $CsCO_3$ until pH 7.6 and then diluted 1:4 (v/v) with methanol). Low-soluble samples were vigorously stirring to allow the dissolution. After the complete solubilization, 0.2 mL of water was added to the mixture and, after stirring, the solution was transferred into an NMR tube and left to rest in order to achieve the correct separation of the two liquid phases. The ^{31}P uncoupled experiments were performed with the following parameters: D1= 10 s, SW= 40 ppm, O1=: 10 ppm, FID size= 32768, ns= 32, T= 320 K.

3.2. Thin Layer Chromatography (TLC)

TLC plates Silica gel 60 SIL G-25 UV254 glass 250 μm (Macherey Nagel, Düren, Germany) were used for analytical TLC. The employed eluents were constituted by or $CHCl_3/CH_3OH/CH_3COCH_3/CH_3COOH/H_2O$: 50/10/20/10/5 and $CHCl_3/CH_3OH/NH_3$ (33% aq.): 65/30/2.5 (ratios reported in volume). Detection was performed by staining with a cerium molibdate reagent.

3.3. Gas Chromatography

To determine the fatty acid composition in PC from soya, fatty acid methyl esters (FAMEs) were obtained by hydrolysis of PC with methanol/ 2 M NaOH under reflux for 4 h. The reaction mixture was then cooled, evaporated to remove methanol, acidified, and extracted carefully three times with ethylacetate. The organic solutions were collected, anhydrified on sodium sulphate and evaporated at p.r.. The residue has been dissolved in diethyl ether and treated with an ethereal solution of diazomethane 30 min at r.t. After evaporation, the residue was dissolved in CH_2Cl_2 and analyzed using a gas chromatograph system HP-6890 equipped with a HP-5973 mass detector and a HP-5MS column (30 m length x 250 μm internal diameter, 0.25 μm film thickness, Hewlett Packard, Palo Alto, CA, USA). Helium was the carrier gas with a flux of 1 mL min^{-1}; the splitting ratio was 1:30. The injector and detector temperatures were set at 250 °C. The used temperature program is reported here: 120 °C (3 min)-12 °C/min-195 °C (10 min)-12 °C/min-300 °C (10 min). The FAMEs were identified by comparison with known standards and by means of NIST 2008 mass spectral library search.

3.4. High Performance Liquid Chromatography (HPLC)

HPLC analyses were performed on a Merck Hitachi L4000 apparatus (Japan) fit-ted with a Sepachrom Adamas®Silica (Rho, Milano, Italy) 5μ-2 column, length/ internal diameter 250/4.6, and a UV detector set to λ= 206 nm. The column temperature was maintained at r.t. PL mixtures were analyzed using an isocratic mobile phase consisting of $CH_3CN/CH_3OH/H_3PO_4$ 952/36/10.9 at a flow rate of 0.5 mL/min. The samples were dissolved in a mixture of hexane/isopropanol (1:1, v/v) with a final concentration of 1

mg/mL and filtered through a 0.45 μm filter before injection.

3.5. Electrospray Ionization Mass Spectrometry

Mass spectra were recorded on a ESI/MS Bruker Esquire 3000 PLUS (ESI Ion Trap LC/MSn System, Bruker, Milano, Italy), by direct infusion of a dichloromethane solution of compounds with an infusion rate of 4 μL/min. Samples were analyzed using both positive and negative ionization modes to allow the detection of all relevant compounds.

3.6. PLD Preparation

3.6.1. Microorganism Fermentation

PLD was obtained from the fermentation broth of *Streptomyces netropsis* (DSM 40093). The medium for strain growth and maintenance was composed by glucose 4 g/L; yeast extract 5 g/L; malt extract 10 g/L.

Medium for PLD preparation: glucose 5 g/L; yeast extract 5 g/L; malt extract 10 g/L; peptone from soyabean 3 g/L; peptone from casein 1 g/L; $MgSO_4$ 0.2 g/L; NaCl 0.2 g/L. A single colony of active *Streptomyces netropsis* culture was picked up from a Petri dish, was suspended in 1 mL of sterile water, and was then inoculated in a 500 mL conical Pyrex flask containing 150 mL of the growth medium. The flask was shaken for 5 days at 30 °C and 140 rpm. After this period, the cells were centrifuged for 15 min (4 °C, 4000 g) and collected, removing the medium. The cells were suspended in 10 mL of fresh medium and were added to a sterilized fermenter vessel of a 5 L bioreactor (Bio-stat A BB-8822000, Sartorius Stedim, Göttingen, Germany) containing 4 L of medium for PLD preparation. The temperature, the stirring speed, and the pH were set to 30 °C, 250 rpm and 7.0, respectively. The value of pH was controlled by addition of sterilized aqueous solutions (10% w/w in water) of either acetic acid or ammonia. The fermentation was performed aerobically, setting a minimum air flow of 2 L/min (0.5 v/v/min). After 48 h, the fermentation broth was filtered through a celite pad, and the clear liquid was stored at 4 °C in dark bottles.

3.6.2. Precipitation and Dialysis

To 1 L of the filtered broth, 430 g of ammonium sulfate was added over 1 h at 4 °C under stirring. Once the ammonium sulfate was completely dissolved, the broth was left overnight at 4 °C to allow the precipitation. After 24 h, the precipitated pellet was separated from the broth by centrifugation at 8000 rpm for 15 min at 4 °C. The solid was then dissolved in a small amount of supernatant broth and dialyzed with a seam-less cellulose tube (D0655 Sigma-Aldrich, Milano, Italy) against 10 mM sodium acetate buffer at pH 5. The dialyzed broth (80 mL), which had an activity of 0.525 U/mL, was finally lyophilized (240 mg, 0.175 U/mg) and used as solid powder for bioconversions.

3.7. Protein Determination

Protein concentration was determined in the dialyzed broth by the Bradford method using bovine serum albumin (BSA) as standard[82] and was 0.94 mg/mL (analysis performed in triplicate).

3.8. PLD Activity Determination

In addition, 360 mg of phosphatidyl-p-nitrophenol (PpNP), prepared as described in our previous work,[83] was dissolved in diethylether (1 mL) and added with 15 mL of 0.1 M Tris buffer and 15 mL of a solution of 10% Triton X-100 in the same buffer, giving a final concentration of 16 mM. The mixture was heated gently to 60 °C until it became clear, the organic solvent was removed under reduced pressure, and the solution was stored in dark vials at -18 °C. PLD activity was determined spectrophotometrically using a UV-Vis Double Beam spectrophotometer V-730 Jasco (Jasco Europe, Cremella, Italy) in 0.05 M Tris Buffer, pH 8, by monitoring the hydrolysis of PpNP to phosphatidic acid and p-nitrophenol at 405 nm using a molar extinction coefficient of 18.450 $mmol^{-1}$ L cm^{-1}. One unit (U) is defined as the amount of enzyme able to hydrolyze one μmol of PpNP in 1 min.

3.9. RDES Preparation

HBA (choline chloride or glycine betaine) and HBD (glycerol or ethylene glycol) were previously dried for 10 h under vacuum. They were then mixed in a 1:2 molar ratio (see Table 2 for detailed composition) and heated under magnetic stirring for 2-4 h at 70-90 °C until a homogeneous and clear liquid phase was obtained. The synthesized RDESs were left to cool slowly to r.t., and they were stored in a sealed vial under argon until used. They were analyzed by ^{1}H NMR (spectra are reported in Supplementary Materials Figure S2).

3.10. RDES Density Measurement

The density of the RDESs prepared in 3.9 has been measured at atmospheric pressure and at 18 °C with the following procedure. In addition, 2 mL volumetric flasks have been weighed on an analytical balance with a resolution of 0.1 mg. Then, they have been filled with the opportune RDES and thermostated at 18 °C for 1 h. Then, the volume was adjusted to the right value and the flasks were weighted. Each measure had been performed in duplicate. The density has been calculated for each RDES as the ratio between the mass of RDES (mass of filled flask–mass of empty flask) and the volume of the flask. The final value reported in Table 2 is the average of the two measurements.

3.11. RDES Preparation of Phosphatidylglycerols PG_{A1} and PG_{B1} in RDES A1 and B1

Furthermore, 150 mg of PC was dissolved at 45 °C in 10 mL of RDES (A1 or B1). Once full solubilization of the substrate in RDES was achieved, 10 mL of buffer solution containing 0.1 M of sodium acetate, 0.1 M of calcium chloride, and 15 mg (2.6 U) of solid PLD adjusted to pH 5.6 were added to the solution. This mixture was left stirring at 45 °C for 40 h. The product precipitated in the reaction mixture and was isolated by filtration on a Buchner under vacuum. The liquid solution was extracted with toluene, in order to check the presence of residual PLs. The precipitated products for RDES B1 accounted for 60% (w/w, 90 mg) of the reaction yield, while the products recovered from the medium extraction were instead 3% (w/w, 5 mg) of the reaction yield. The product was then purified from residual RDES: it was dissolved in 1 mL of toluene, and the solution was left stirring with 5 mL of water for 30 min at r.t. The organic phase was then separated and evaporated under reduced pressure. The PLs mixture recoveries were 130 mg (86% w/w) for PG_{A1} preparation and 95 mg (63% w/w) for PG_{B1}. The final mixtures

were analyzed by ESI/MS and NMR.
PG_{A1} ESI/MS negative ion spectrum m/z values: 16:0/18:2-PG $[745.6]^-$, 18:2/18:2-PG $[769.5]^-$. Residual PC was seen in the positive ion spectrum with m/z: 16:0/18.2-PC $[780.7 + Na]^+$, 18:2/18:2-PC $[804.6 + Na]^+$. ^{1}H NMR: δH 0.84−0.85 (m, 6H, CH_3), 1.23−1.27 (m, 34 H, CH_2 acyl chains), 1.50−1.60 (m, 4H, $\underline{CH_2}CH_2CO$), 1.99−2.04 (m, 7 H, $\underline{CH_2}$−CHCH), 2.23−2.30 (m, 4H, $\underline{CH_2}CO$), 2.72−2.77 (m, 3H, CHCH−$\underline{CH}$−CHCH), 3.58−3.64 (m, 3H, CHOH-$\underline{CH_2}$-OH), 3.93−4.12 (m, 5H, O−$\underline{CH_2}$−CHOH−$\underline{CH_2}$O and $\underline{CH_2}$−OPO_3), 4.34−4.37 (m, 1H, $\underline{CH_2}$−OPO_3), 5.18 (m, 1H, $\underline{CH}$−OH), 5.29−5.35 (m, 6H, $\underline{CHCH}$). ^{31}P NMR δ: 0.59 ppm.
PG_{B1} ESI/MS negative ion spectrum: the desired product was identified with the following m/z values: 16:0/18:2-PG $[745.5]^-$, 18:2/18:2-PG $[769.5]^-$. No residual PC was observed in the positive ion spectra. ^{1}H NMR: δH 0.82−0.86 (m, 6H, CH_3), 1.21−1.27 (m, 34 H, CH_2 acyl chains), 1.50−1.60 (m, 4H, $\underline{CH_2}CH_2CO$), 1.98−2.03 (m, 7 H, $\underline{CH_2}$−CHCH), 2.22-2.29 (m, 4H, $\underline{CH_2}CO$), 2.71-2.76 (m, 3H, CHCH−$\underline{CH}$−CHCH), 3.59−3.64 (m, 3H, $\underline{CH}$OH-$\underline{CH_2}$-OH), 3.85−4.13 (m, 5H, O−$\underline{CH_2}$−CHOH−$\underline{CH_2}$O and $\underline{CH_2}$−OPO_3), 4.33−4.36 (m, 1H, $\underline{CH_2}$−OPO_3), 5.17 (m, 1H, $\underline{CH}$−OH), 5.27−5.35 (m, 6H, $\underline{CHCH}$). ^{31}P NMR δ: 0.59 ppm.

3.12. RDES Preparation of Phosphatidylethyleneglycols P-EG$_{A2}$ and P-EG$_{B2}$ in RDES A2 and B2

In addition, 150 mg of PC was dissolved at 45 °C in 10 mL of RDES (A2 or B2). Once full solubilization of the substrate in RDES was achieved, 10 mL of buffer solution containing 0.1 M of sodium acetate, 0.1 M of calcium chloride, and 15 mg (2.6 U) of PLD powder adjusted to pH 5.6 were added to the solution. This mixture was left stirring at 45 °C for 40 h. The liquid solution was then separated by filtration from the solid product. The solution was extracted with toluene, whereas the solid was dissolved in toluene. The precipitated products for RDES B2 accounted for 63.3% (w/w, 95 mg) of the reaction yield, while the products recovered from the medium extraction were instead 6.6% (w/w, 10 mg) of the reaction yield. All the organic phases were collected and evaporated under reduced pressure. The product containing RDES residues was dissolved in 1 mL of toluene, and the solution was left stirring with 5 mL of water for 30 min at r.t. The organic phase was separated and evaporated under reduced pressure. The PL mixture recoveries were 140 mg (93% w/w) for P-EG_{A2} and 105 mg (70% w/w) for P-EG_{B2}. The final mixtures were analyzed by ESI/MS and NMR.
P-EG_{A2}: ESI/MS negative ion spectrum: the desired product was identified with the following m/z values: 16:0/18:2-P-EG $[715.6]^-$, 18:2/18:2-P-EG $[739.6]^-$. Some PC was recorded in the positive ion spectrum with m/z: 16:0/18.2-PC $[780+Na]^+$, 18:2/18:2-PC $[804.7+Na]^+$. ^{1}H NMR: δH 0.84−0.88 (m, 6H, CH_3), 1.23−1.27 (m, 34 H, CH_2 acyl chains), 1.56 (m, 4H, $\underline{CH_2}CH_2CO$), 2.00−2.05 (m, 7 H, $\underline{CH_2}$−CHCH), 2.24−2.29 (m, 4H, $\underline{CH_2}CO$), 2.72−2.76 (m, 3H, CHCH−$\underline{CH}$−CHCH), 3.38 (m, 1H, CH_2-$\underline{CH_2}$-OH), 3.64−4.24 (m, 6H, O−$\underline{CH_2}$−CHO−$\underline{CH_2}$O and $\underline{CH_2}$−OPO_3), 4.35−4.38 (m, 1H, $\underline{CH_2}$−OPO_3), 5.19 (m, 1H, $\underline{CH}$−OH), 5.31−5.37 (m, 6H, $\underline{CHCH}$). ^{31}P NMR δ: 0.35 ppm.
P-EG_{B2}: ESI/MS negative ion spectrum: the desired product P-EG was identified with the following m/z values: 16:0/18:2-P-EG $[715.8]^-$, 18:2/18:2-P-EG $[739.6]^-$. No PC was recorded in the positive ion spectrum. ^{1}H NMR: δH 0.86−0.89 (m, 6H, CH_3), 1.25−1.29 (m, 34 H, CH_2 acyl chains), 1.58 (m, 4H, $\underline{CH_2}CH_2CO$), 2.01−2.06 (m, 7 H, $\underline{CH_2}$−CHCH), 2.24−2.30 (m, 4H, $\underline{CH_2}CO$), 2.74−2.77 (m, 3H, CHCH−$\underline{CH}$−CHCH), 3.30 (m, 1H, $CH_2\underline{CH_2}OH$), 3.71−4.25 (m, 6H, O−$\underline{CH_2}$−CHO−$\underline{CH_2}$O and $\underline{CH_2}$−OPO_3), 4.36−4.40 (m,

1H, $\underline{CH_2}$−OPO_3), 5.20 (m, 1H, $\underline{CH}$−OH), 5.30−5.38 (m, 6H, $\underline{CHCH}$). ^{31}P NMR δ: 0.35 ppm.

4. Conclusions

The present work constitutes an innovative approach for the biocatalytic preparation of polar head-modified PLs based on the use of RDESs/buffer mixtures, which allows the conversion of natural PC in high yields. RDESs act both as solvents and reactants because they contain the alcoholic nucleophiles that will substitute the choline moiety in the transphosphatidylation reaction. The best results have been obtained using two RDESs constituted by glycine betaine as HBA and glycerol or ethylene glycol as HBD with a total conversion of starting PC due to the absence of choline in the composition of RDES. The implementation of specifically designed reaction media based on RDESs and buffer resulted in several distinctive advantages, including the yield enhancement by the synergic combination of a substantial mass effect (due to the high concentration of nucleophile reactant in the RDES) and the product precipitation (which maintains at a low value its concentration in the medium). Moreover, the implementation of RDES/buffer reaction medium demonstrates the inhibition of the parasitic competitive hydrolysis of PC to PA, improving the reaction yields and easing the product recovery and purification. Detailed studies about the interaction of RDESs with PLD catalysis are under way. In fact, the effect of RDESs (and DESs) on the phospholipase's active site as well as on PLs aggregates is hardly predictable, and further studies are needed to fully exploit this promising approach to biocatalysis.

Supplementary Materials

The following are available online at https://www.mdpi.com/article/10.3390/catal11060655/s1, Figure S1: RDES preparation example (left image: initial mixture of ChCl (HBD) and ethylene glycol (HBA), right image: RDES A2). Figure S2: ^{1}H NMR spectra of the four RDES A1, A2, B1 and B2 in D_2O. Figure S3: ^{1}H NMR Spectrum of PC. Figure S4: Mass spectra of PG_{A1} obtained in RDES A1. Figure S5: Mass spectra of PG_{B1} obtained in RDES B1. Figure S6: Mass spectra of P-EG_{A2} obtained in RDES A2. Figure S7: Mass spectra of P-EG_{B2} obtained in RDES B2.

References

1. Sheldon, R. A.; Woodley, J. M., Role of biocatalysis in sustainable chemistry. *Chemical reviews* **2018,** *118* (2), 801-838.
2. Tan, B. L.; Norhaizan, M. E., *Rice by-products: Phytochemicals and food products application*. Springer: 2020.
3. Akretche, H.; Pierre, G.; Moussaoui, R.; Michaud, P.; Delattre, C., Valorization of olive mill wastewater for the development of biobased polymer films with antioxidant properties using eco-friendly processes. *Green Chemistry* **2019,** *21* (11), 3065-3073.
4. Cicco, L.; Dilauro, G.; Perna, F. M.; Vitale, P.; Capriati, V., Advances in deep eutectic solvents and water: applications in metal-and biocatalyzed processes, in the synthesis of APIs, and other biologically active compounds. *Organic & Biomolecular Chemistry* **2021,** *19* (12), 2558-2577.
5. Smith, E. L.; Abbott, A. P.; Ryder, K. S., Deep eutectic solvents (DESs) and their applications. *Chemical reviews* **2014,** *114* (21), 11060-11082.
6. Hansen, B. B.; Spittle, S.; Chen, B.; Poe, D.; Zhang, Y.; Klein, J. M.; Horton, A.; Adhikari, L.; Zelovich, T.; Doherty, B. W., Deep eutectic solvents: A review of fundamentals and applications. *Chemical reviews* **2020,** *121* (3), 1232-1285.

7. Abbott, A. P.; Capper, G.; Davies, D. L.; Rasheed, R. K.; Tambyrajah, V., Novel solvent properties of choline chloride/urea mixtures. *Chemical communications* **2003,** (1), 70-71.
8. Nahar, Y.; Thickett, S. C., Greener, faster, stronger: the benefits of deep eutectic solvents in polymer and materials science. *Polymers* **2021,** *13* (3), 447.
9. Santana-Mayor, Á.; Rodríguez-Ramos, R.; Herrera-Herrera, A. V.; Socas-Rodríguez, B.; Rodríguez-Delgado, M. Á., Deep eutectic solvents. The new generation of green solvents in analytical chemistry. *TrAC Trends in Analytical Chemistry* **2021,** *134*, 116108.
10. Şahin, S., Tailor-designed deep eutectic liquids as a sustainable extraction media: An alternative to ionic liquids. *Journal of Pharmaceutical and Biomedical Analysis* **2019,** *174*, 324-329.
11. Grudniewska, A.; de Melo, E. M.; Chan, A.; Gniłka, R.; Boratynski, F.; Matharu, A. S., Enhanced protein extraction from oilseed cakes using glycerol–choline chloride deep eutectic solvents: a biorefinery approach. *ACS Sustainable Chemistry & Engineering* **2018,** *6* (11), 15791-15800.
12. Kalhor, P.; Ghandi, K., Deep eutectic solvents as catalysts for upgrading biomass. *Catalysts* **2021,** *11* (2), 178.
13. Hooshmand, S. E.; Afshari, R.; Ramón, D. J.; Varma, R. S., Deep eutectic solvents: cutting-edge applications in cross-coupling reactions. *Green Chemistry* **2020,** *22* (12), 3668-3692.
14. Di Carmine, G.; Abbott, A. P.; D'Agostino, C., Deep eutectic solvents: alternative reaction media for organic oxidation reactions. *Reaction Chemistry & Engineering* **2021,** *6* (4), 582-598.
15. Durand, E.; Lecomte, J.; Baréa, B.; Piombo, G.; Dubreucq, E.; Villeneuve, P., Evaluation of deep eutectic solvents as new media for Candida antarctica B lipase catalyzed reactions. *Process Biochemistry* **2012,** *47* (12), 2081-2089.
16. Panić, M.; Cvjetko Bubalo, M.; Radojčić Redovniković, I., Designing a biocatalytic process involving deep eutectic solvents. *Journal of Chemical Technology & Biotechnology* **2020,** *96* (1), 14-30.
17. Xu, P.; Zheng, G. W.; Zong, M. H.; Li, N.; Lou, W. Y., Recent progress on deep eutectic solvents in biocatalysis. *Bioresour Bioprocess* **2017,** *4* (1), 34.
18. Cicco, L.; Ríos-Lombardía, N.; Rodríguez-Álvarez, M. J.; Morís, F.; Perna, F. M.; Capriati, V.; García-Álvarez, J.; González-Sabín, J., Programming cascade reactions interfacing biocatalysis with transition-metal catalysis in Deep Eutectic Solvents as biorenewable reaction media. *Green Chemistry* **2018,** *20* (15), 3468-3475.
19. Vitale, P.; Perna, F. M.; Agrimi, G.; Pisano, I.; Mirizzi, F.; Capobianco, R. V.; Capriati, V., Whole-Cell Biocatalyst for Chemoenzymatic Total Synthesis of Rivastigmine. *Catalysts* **2018,** *8* (2), 55.
20. Płotka-Wasylka, J.; de la Guardia, M.; Andruch, V.; Vilková, M., Deep eutectic solvents vs ionic liquids: Similarities and differences. *Microchemical Journal* **2020,** *159*.
21. Perna, F. M.; Vitale, P.; Capriati, V., Deep eutectic solvents and their applications as green solvents. *Current Opinion in Green and Sustainable Chemistry* **2020,** *21*, 27-33.
22. Vilková, M.; Płotka-Wasylka, J.; Andruch, V., The role of water in deep eutectic solvent-base extraction. *Journal of Molecular Liquids* **2020,** *304*.
23. Tan, J.-N.; Dou, Y., Deep eutectic solvents for biocatalytic transformations: Focused lipase-catalyzed organic reactions. *Applied microbiology and biotechnology* **2020,** *104*, 1481-1496.
24. Pätzold, M.; Siebenhaller, S.; Kara, S.; Liese, A.; Syldatk, C.; Holtmann, D., Deep eutectic solvents as efficient solvents in biocatalysis. *Trends in biotechnology* **2019,** *37* (9), 943-959.
25. Guajardo, N.; Domínguez de María, P.; Ahumada, K.; Schrebler, R. A.; Ramírez-Tagle, R.; Crespo, F. A.; Carlesi, C., Water as Cosolvent: Nonviscous Deep Eutectic Solvents for Efficient Lipase-Catalyzed Esterifications. *ChemCatChem* **2017,** *9* (8), 1393-1396.
26. Sirviö, J. A.; Visanko, M., Lignin-rich sulfated wood nanofibers as high-performing adsorbents for the removal of lead and copper from water. *Journal of hazardous materials* **2020,** *383*, 121174.
27. Sirviö, J. A.; Heiskanen, J. P., Synthesis of Alkaline-Soluble Cellulose Methyl Carbamate Using a Reactive Deep Eutectic Solvent. *ChemSusChem* **2017,** *10* (2), 455-460.
28. Mota-Morales, J. D.; Sánchez-Leija, R. J.; Carranza, A.; Pojman, J. A.; del Monte, F.; Luna-Bárcenas, G., Free-radical polymerizations of and in deep eutectic solvents: Green synthesis of functional materials. *Progress in Polymer Science* **2018,** *78*, 139-153.
29. Gore, S.; Baskaran, S.; Koenig, B., Efficient synthesis of 3, 4-dihydropyrimidin-2-ones in low melting tartaric acid–urea mixtures. *Green Chemistry* **2011,** *13* (4), 1009-1013.
30. Singh, B. S.; Lobo, H. R.; Pinjari, D. V.; Jarag, K. J.; Pandit, A. B.; Shankarling, G. S., Comparative material study and synthesis of 4-(4-nitrophenyl) oxazol-2-amine via sonochemical and thermal method. *Ultrasonics sonochemistry* **2013,** *20* (2), 633-639.

31. Zeng, C.-X.; Qi, S.-J.; Xin, R.-P.; Yang, B.; Wang, Y.-H., Enzymatic selective synthesis of 1, 3-DAG based on deep eutectic solvent acting as substrate and solvent. *Bioprocess and biosystems engineering* **2015,** *38*, 2053-2061.
32. Siebenhaller, S.; Muhle-Goll, C.; Luy, B.; Kirschhöfer, F.; Brenner-Weiss, G.; Hiller, E.; Günther, M.; Rupp, S.; Zibek, S.; Syldatk, C., Sustainable enzymatic synthesis of glycolipids in a deep eutectic solvent system. *Journal of Molecular Catalysis B: Enzymatic* **2016,** *133*, S281-S287.
33. Hümmer, M.; Kara, S.; Liese, A.; Huth, I.; Schrader, J.; Holtmann, D., Synthesis of (-)-menthol fatty acid esters in and from (-)-menthol and fatty acids–novel concept for lipase catalyzed esterification based on eutectic solvents. *Molecular Catalysis* **2018,** *458*, 67-72.
34. Lamari, F.; Mochel, F.; Sedel, F.; Saudubray, J., Disorders of phospholipids, sphingolipids and fatty acids biosynthesis: toward a new category of inherited metabolic diseases. *Journal of inherited metabolic disease* **2013,** *36*, 411-425.
35. Calvano, C. D.; Losito, I.; Cataldi, T., Editorial to the Special Issue "Lipidomics and Neurodegenerative Diseases". MDPI: 2021; Vol. 22, p 1270.
36. D'Arrigo, P.; Scotti, M., Lysophospholipids: synthesis and biological aspects. *Current Organic Chemistry* **2013,** *17* (8), 812-830.
37. Li, J.; Wang, X.; Zhang, T.; Wang, C.; Huang, Z.; Luo, X.; Deng, Y., A review on phospholipids and their main applications in drug delivery systems. *Asian Journal of Pharmaceutical Sciences* **2015,** *10* (2), 81-98.
38. Gliszczyńska, A.; Niezgoda, N.; Gładkowski, W.; Czarnecka, M.; Świtalska, M.; Wietrzyk, J., Synthesis and biological evaluation of novel phosphatidylcholine analogues containing monoterpene acids as potent antiproliferative agents. *PLoS One* **2016,** *11* (6), e0157278.
39. Falconi, M.; Ciccone, S.; D'Arrigo, P.; Viani, F.; Sorge, R.; Novelli, G.; Patrizi, P.; Desideri, A.; Biocca, S., Design of a novel LOX-1 receptor antagonist mimicking the natural substrate. *Biochemical and Biophysical Research Communications* **2013,** *438* (2), 340-345.
40. Kosicek, M.; Hecimovic, S., Phospholipids and Alzheimer's disease: alterations, mechanisms and potential biomarkers. *International journal of molecular sciences* **2013,** *14* (1), 1310-1322.
41. Shamim, A.; Mahmood, T.; Ahsan, F.; Kumar, A.; Bagga, P., Lipids: An insight into the neurodegenerative disorders. *Clinical Nutrition Experimental* **2018,** *20*, 1-19.
42. Küllenberg, D.; Taylor, L. A.; Schneider, M.; Massing, U., Health effects of dietary phospholipids. *Lipids in health and disease* **2012,** *11*, 1-16.
43. Schverer, M.; O'Mahony, S. M.; O'Riordan, K. J.; Donoso, F.; Roy, B. L.; Stanton, C.; Dinan, T. G.; Schellekens, H.; Cryan, J. F., Dietary phospholipids: Role in cognitive processes across the lifespan. *Neuroscience & Biobehavioral Reviews* **2020,** *111*, 183-193.
44. Cui, L.; Decker, E. A., Phospholipids in foods: prooxidants or antioxidants? *Journal of the Science of Food and Agriculture* **2016,** *96* (1), 18-31.
45. Sun, N.; Chen, J.; Wang, D.; Lin, S., Advance in food-derived phospholipids: Sources, molecular species and structure as well as their biological activities. *Trends in Food Science & Technology* **2018,** *80*, 199-211.
46. Pucek, A.; Niezgoda, N.; Kulbacka, J.; Wawrzeńczyk, C.; Wilk, K. A., Phosphatidylcholine with conjugated linoleic acid in fabrication of novel lipid nanocarriers. *Colloids and Surfaces A: Physicochemical and Engineering Aspects* **2017,** *532*, 377-388.
47. Aldosari, B. N.; Alfagih, I. M.; Almurshedi, A. S., Lipid nanoparticles as delivery systems for RNA-based vaccines. *Pharmaceutics* **2021,** *13* (2), 206.
48. Samaridou, E.; Heyes, J.; Lutwyche, P., Lipid nanoparticles for nucleic acid delivery: Current perspectives. *Advanced drug delivery reviews* **2020,** *154*, 37-63.
49. De Serrano, L. O.; Burkhart, D. J., Liposomal vaccine formulations as prophylactic agents: design considerations for modern vaccines. *Journal of nanobiotechnology* **2017,** *15* (1), 1-23.
50. D'Arrigo, P.; Giordano, C.; Macchi, P.; Malpezzi, L.; Pedrocchi-Fantoni, G.; Servi, S., Synthesis, platelet adhesion and cytotoxicity studies of new glycerophosphoryl-containing polyurethanes. *The International Journal of Artificial Organs* **2007,** *30* (2), 133-143.
51. Huang, Z.; Zhao, H.; Guan, W.; Liu, J.; Brennan, C.; Kulasiri, D.; Mohan, M. S., Vesicle properties and health benefits of milk phospholipids: a review. *Journal of Food Bioactives* **2019,** *5*, 31–42-31–42.
52. Lordan, R.; Tsoupras, A.; Zabetakis, I., Phospholipids of animal and marine origin: Structure, function, and anti-inflammatory properties. *Molecules* **2017,** *22* (11), 1964.
53. Chojnacka, A.; Gladkowski, W.; Kielbowicz, G.; Wawrzenczyk, C., Isolation of egg-yolk phospholipids and enzymatic modification of their acyl chains. *Lipid Technology* **2012,** *24* (2), 33-35.

54. Niezgoda, N.; Gliszczyńska, A.; Gładkowski, W.; Chojnacka, A.; Kiełbowicz, G.; Wawrzeńczyk, C., Production of concentrates of CLA obtained from sunflower and safflower and their application to the lipase-catalyzed acidolysis of egg yolk phosphatidylcholine. *European Journal of Lipid Science and Technology* **2016,** *118* (10), 1566-1578.
55. D'Arrigo, P.; Servi, S., Using phospholipases for phospholipid modification. *Trends in Biotechnology* **1997,** *15* (3), 90-96.
56. Baldassarre, F.; Allegretti, C.; Tessaro, D.; Carata, E.; Citti, C.; Vergaro, V.; Nobile, C.; Cannazza, G.; D'Arrigo, P.; Mele, A., Biocatalytic synthesis of phospholipids and their application as coating agents for CaCO3 nano–crystals: characterization and intracellular localization analysis. *ChemistrySelect* **2016,** *1* (20), 6507-6514.
57. Leiros, I.; Hough, E.; D'Arrigo, P.; Carrea, G.; Pedrocchi-Fantoni, G.; Secundo, F.; Servi, S., Crystallization and preliminary X-ray diffraction studies of phospholipase D from Streptomyces sp. *Acta Crystallographica Section D: Biological Crystallography* **2000,** *56* (4), 466-468.
58. Carrea, G.; D'Arrigo, P.; Secundo, F.; Servi, S., Purification and applications of a phospholipase D from a new strain of Streptomyces. *Biotechnology letters* **1997,** *19*, 1083-1085.
59. Carrea, G.; D'Arrigo, P.; Piergianni, V.; Roncaglio, S.; Secundo, F.; Servi, S., Purification and properties of two phospholipases D from Streptomyces sp. *Biochimica et Biophysica Acta (BBA)-Lipids and Lipid Metabolism* **1995,** *1255* (3), 273-279.
60. Ferra, L., Preparative transformation of natural phospholipids catalysed by phospholipase D from Streptomyces. *Journal of the Chemical Society, Perkin Transactions 1* **1996,** (21), 2651-2656.
61. Ferra, L., Phospholipase D from Streptomyces catalyses the transfer of secondary alcohols. *Journal of the Chemical Society, Chemical Communications* **1994,** (14), 1709-1710.
62. Bossi, L.; D'Arrigo, P.; Pedrocchi-Fantoni, G.; Mele, A.; Servi, S.; Leiros, I., The substrate requirements of phospholipase D. *Journal of Molecular Catalysis B: Enzymatic* **2001,** *11* (4-6), 433-438.
63. Allegretti, C.; Denuccio, F.; Rossato, L.; D'Arrigo, P., Polar head modified phospholipids by phospholipase D-catalyzed transformations of natural phosphatidylcholine for targeted applications: an overview. *Catalysts* **2020,** *10* (9), 997.
64. Kim, H.-Y.; Huang, B. X.; Spector, A. A., Phosphatidylserine in the brain: metabolism and function. *Progress in lipid research* **2014,** *56*, 1-18.
65. Mozzi, R.; Buratta, S.; Goracci, G., Metabolism and functions of phosphatidylserine in mammalian brain. *Neurochemical research* **2003,** *28*, 195-214.
66. Duan, Z.-Q.; Hu, F., Efficient synthesis of phosphatidylserine in 2-methyltetrahydrofuran. *Journal of biotechnology* **2013,** *163* (1), 45-49.
67. Duan, Z.-Q.; Hu, F., Highly efficient synthesis of phosphatidylserine in the eco-friendly solvent γ-valerolactone. *Green Chemistry* **2012,** *14* (6), 1581-1583.
68. D'Arrigo, P.; Cerioli, L.; Chiappe, C.; Panzeri, W.; Tessaro, D.; Mele, A., Improvements in the enzymatic synthesis of phosphatidylserine employing ionic liquids. *Journal of Molecular Catalysis B: Enzymatic* **2012,** *84*, 132-135.
69. Yang, S.-L.; Duan, Z.-Q., Insight into enzymatic synthesis of phosphatidylserine in deep eutectic solvents. *Catalysis Communications* **2016,** *82*, 16-19.
70. Allegretti, C.; Bono, A.; D'Arrigo, P.; Denuccio, F.; De Simeis, D.; Di Lecce, G.; Serra, S.; Tessaro, D.; Viola, M., Valorization of Corn Seed Oil Acid Degumming Waste for Phospholipids Preparation by Phospholipase D-Mediated Processes. *Catalysts* **2020,** *10* (7), 809.
71. Gregoriadis, G., Liposomes for drugs and vaccines. *Trends in Biotechnology* **1985,** *3* (9), 235-241.
72. Sakdiset, P.; Okada, A.; Todo, H.; Sugibayashi, K., Selection of phospholipids to design liposome preparations with high skin penetration-enhancing effects. *Journal of Drug Delivery Science and Technology* **2018,** *44*, 58-64.
73. Hossann, M.; Wiggenhorn, M.; Schwerdt, A.; Wachholz, K.; Teichert, N.; Eibl, H.; Issels, R. D.; Lindner, L. H., In vitro stability and content release properties of phosphatidylglyceroglycerol containing thermosensitive liposomes. *Biochimica et Biophysica Acta (BBA)-Biomembranes* **2007,** *1768* (10), 2491-2499.
74. Mazela, J.; Merritt, T. A.; Gadzinowski, J.; Sinha, S., Evolution of pulmonary surfactants for the treatment of neonatal respiratory distress syndrome and paediatric lung diseases. *Acta paediatrica* **2006,** *95* (9), 1036-1048.
75. Tejeda-Mansir, A.; García-Rendón, A.; Guerrero-Germán, P., Plasmid-DNA lipid and polymeric nanovaccines: a new strategic in vaccines development. *Biotechnology and Genetic Engineering Reviews* **2019,** *35* (1), 46-68.

76. Juneja, L. R.; Hibi, N.; Inagaki, N.; Yamane, T.; Shimizu, S., Comparative study on conversion of phosphatidylcholine to phosphatidylglycerol by cabbage phospholipase D in micelle and emulsion systems. *Enzyme and Microbial Technology* **1987,** *9* (6), 350-354.
77. Chen, L.; Beppu, F.; Miyashita, K.; Hosokawa, M., Preparation of n-3 Polyunsaturated Phosphatidylglycerol from Salmon Roe Lipids by Phospholipase D and In Vitro Digestion. *European Journal of Lipid Science and Technology* **2020,** *122* (2), 1900201.
78. D'Arrigo, P.; de Ferra, L.; Pedrocchi-Fantoni, G.; Scarcelli, D.; Servi, S.; Strini, A., Enzyme-mediated synthesis of two diastereoisomeric forms of phosphatidylglycerol and of diphosphatidylglycerol (cardiolipin). *Journal of the Chemical Society, Perkin Transactions 1* **1996,** (21), 2657-2660.
79. He, X.; Li, L.; Su, H.; Zhou, D.; Song, H.; Wang, L.; Jiang, X., Poly (ethylene glycol)-block-poly (ε-caprolactone)–and phospholipid-based stealth nanoparticles with enhanced therapeutic efficacy on murine breast cancer by improved intracellular drug delivery. *International journal of nanomedicine* **2015**, 1791-1804.
80. Yamamoto, T.; Teramura, Y.; Itagaki, T.; Arima, Y.; Iwata, H., Interaction of poly (ethylene glycol)-conjugated phospholipids with supported lipid membranes and their influence on protein adsorption. *Science and Technology of advanced MaTerialS* **2016,** *17* (1), 677-684.
81. Mahendra, A.; James, H. P.; Jadhav, S., PEG-grafted phospholipids in vesicles: Effect of PEG chain length and concentration on mechanical properties. *Chemistry and physics of lipids* **2019,** *218*, 47-56.
82. Bradford, M. M., A rapid and sensitive method for the quantitation of microgram quantities of protein utilizing the principle of protein-dye binding. *Analytical biochemistry* **1976,** *72* (1-2), 248-254.
83. Cardillo, R.; D'Arrigo, P.; De Ferra, L.; Piergianni, V.; Scarcelli, D.; Servi, S., A simple assay for the quantitative evaluation of Phospholipase D activity. *Biotechnology techniques* **1993,** *7*, 795-798.

Chapter 3

Towards a Complete Exploitation of Brewers' Spent Grain from a Circular Economy Perspective

Chiara Allegretti,[a] Emanuela Bellinetto,[a] Paola D'Arrigo,[*,a,b] Gianmarco Griffini,[a] Stefano Marzorati,[b] Letizia A. M. Rossato,[a] Eleonora Ruffini,[a] Luca Schiavi,[c] Stefano Serra,[*,b] Alberto Strini,[c] Davide Tessaro [a] and Stefano Turri [a]

[a] Department of Chemistry, Materials and Chemical Engineering "Giulio Natta", Politecnico di Milano, p.zza L. da Vinci 32, 20133 Milano, Italy.

[b] Istituto di Scienze e Tecnologie Chimiche "Giulio Natta", Consiglio Nazionale delle Ricerche (SCITEC-CNR), via Luigi Mancinelli 7, 20131 Milano, Italy.

[c] Istituto per le Tecnologie della Costruzione, Consiglio Nazionale delle Ricerche (ITC-CNR), via Lombardia 49, 20098 San Giuliano Milanese, Italy.

The authors are listed in alphabetical order.

Published on *Fermentation* **2022**, 8, 151.

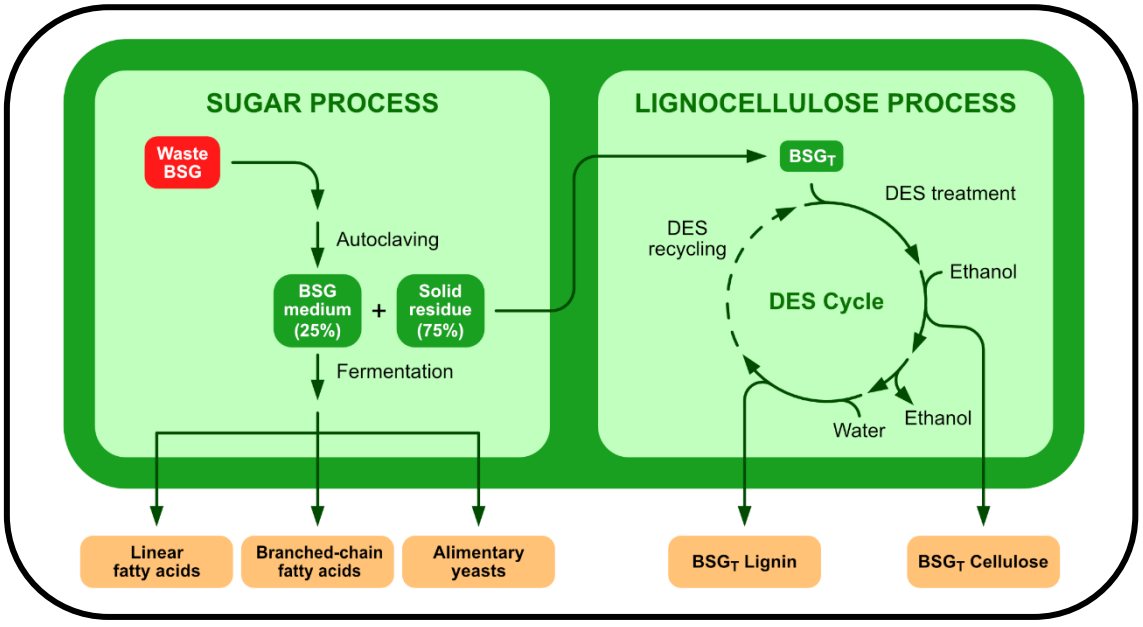

Abstract

In the present work, brewers' spent grain (BSG), which represents the major by-product of the brewing industry, was recovered from a regional brewery and fractionated in order to obtain a complete valorization. In particular, the whole process was divided in two main parts. A first pretreatment with hot water in an autoclave allowed the separation of a solution containing the soluble proteins and sugars, which accounted for 25% of the total starting biomass. This first step allowed the preparation of a medium that was successfully employed as a valuable growing medium for different microbial fermentations, leading to valuable fungal biomass as well as triglycerides with a high content of linear or branched fatty acids, depending on the microorganism used. The solid water-insoluble residue was then submitted to a lignocellulose deep eutectic solvent-mediated fractionation, which allowed the recovery of two important main fractions: BSG cellulose and BSG lignin. The latter product was tested as potential precursor for the development of cement water reducers with encouraging results. This combination of treatments of the waste biomass appeared to be a promising sustainable strategy for the development of the full exploitation of BSG from a circular economy perspective.

1. Introduction

The European Commission has recently presented, under the Green Deal strategy and from the view of a change of paradigm of the industrial production, the so-called Circular Economy Action Plan.[1] This pivotal document includes proposals for sustainable product design, consumer and public purchaser empowerment, and circularity in production processes. The latter concept includes the creation of a well-functioning market for secondary raw materials: low-value by-products of traditional production chains, usually disposed of as waste, that can be fed back into the economy as new raw materials. This serves the dual purpose of decreasing waste production, with its many environmental problems, and finding alternatives for supplying production chains.
From this perspective, increasing attention has been paid to brewers' spent grain (BSG), as documented by the explosion of references in the recent literature (see Figure 1).

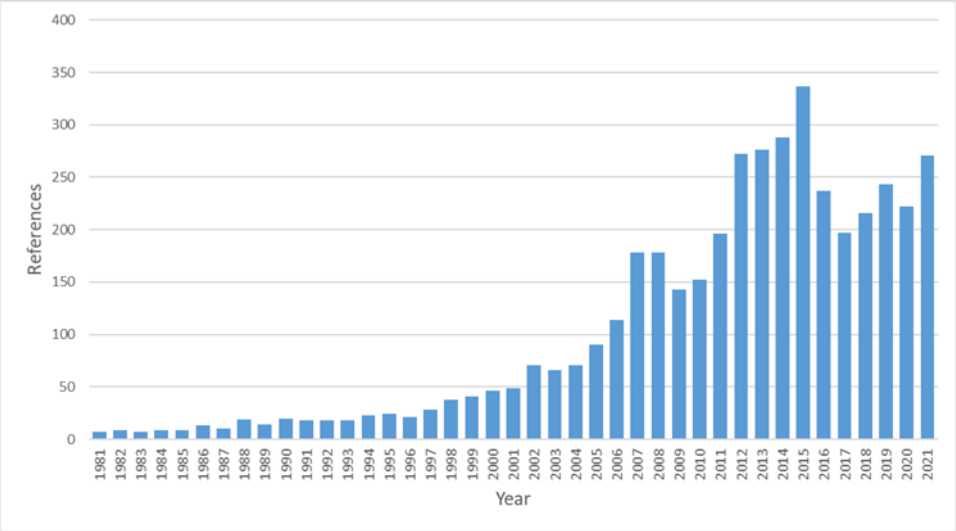

Figure 1: Number of references relative to brewers' spent grain as retrieved by Sci-Findern (CAS, American Chemical Society) on 8 March 2022.

Spent grain constitutes by far the major by-product of the brewing industry, constituting about 85% of the total by-products generated in the process. It was calculated that the production of 100 L of beer results in the generation of around 20 kg of BSG, or 14 kg if we consider the dry weight.[2] According to Eurostat, 30-40 billion liters of beer are produced in Europe every year, translating into the production of 6-8 million tons of BSG. This huge amount of by-products, however, has to be quickly disposed of, since the high amount of humidity, around 75%, promotes the growth of spoilage microorganisms and its simple presence attracts rodents in the brewery. Most frequently, BSG is immediately delivered to neighboring farms, where it is employed for feeding cattle or as a fertilizer in agriculture.[3-4] Of course, problems arise when breweries are located in heavily urbanized areas or in remote non-agricultural areas (for example, in the mountains): in these cases BSG cannot be rapidly delivered and has to be disposed of, constituting a waste of resource and a significant cost for the brewery. The valorization of BSG from a circular economy perspective would thus contribute not only to saving resources, reducing land use, and decreasing the carbon footprint of the brewing process, but would also help the establishment of novel waste processing streams, thus introducing little but significant societal changes. A necessary condition to promote recovery and treatment of BSG is the obtainment of high added-value products which would justify a general interest that would cover the processing costs.

Since BSG is a complex matrix composed of approximately 15-25% proteins, 50-70% fiber (hemicellulose, cellulose, and lignin), 5-10% fats, and 2-5% ashes,[2, 5-8] a careful fractionation is necessary to obtain homogeneous precursors of the target compounds, ensuring the maximum exploitation of the whole material. In this context, a number of studies have described the use of BSG as a source of specific precursors to be employed for the preparation of products of commercial relevance such as alimentary proteins and fiber,[9] enzymes, biopolymers,[10] saccharides, and lignin.[11]

Despite the growing industrial and scientific interest in BSG disposal, very few researchers have investigated the complete valorization of this waste material.[12-13] According to the concept of the circular economy, an industrial process exploiting BSG

should rely on the exploitation of all its chemical components with the production of different products of commercial interest. The aim of such a conceived process is the complete recycling of the starting waste material with the concomitant production of added-value compounds, so as to warrant the economic sustainability of the whole cycle. Following this approach, an innovative process for complete BSG exploitation has been here investigated. Accordingly, a scalable procedure for the separation of the abovementioned material in three different fractions is summarized in Figure 2.

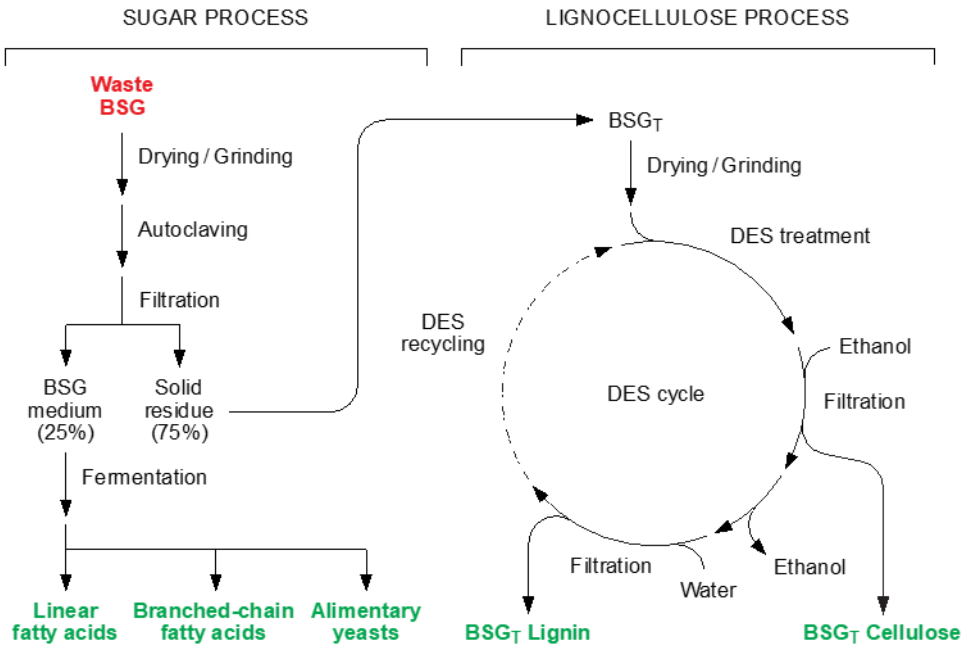

Figure 2: Integrated process for complete BSG waste valorization, subdivided into a sugar process and a lignocellulose process. In the first one, BSG waste is autoclaved and then separated into a sugar-rich medium and a solid residue. Different bioderivatives can be obtained from the former by fermentation. The solid lignocellulosic residue (BSG_T) is instead fractionated with DES to obtain purified lignin and cellulose. The DES is then recovered and recycled in a closed-loop process.

Starting from wet BSG waste recovered from a local brewery, the process has been divided into two main parts consisting of the sequential application of different chemical-physical treatments. A first BSG extraction using water at high temperature allowed the separation of the soluble proteins and polysaccharides (about 25% of the starting BSG) that constitute the basis for a fermentation substrate (BSG medium) and are subsequently transformed into bioderivatives (the sugar process). The solid residue of the first extraction undergoes instead a fractionation by means of a deep eutectic solvent-mediated process leading to the biomass separation in two defined components, namely BSG_T Lignin and BSG_T Cellulose (the lignocellulose process). Therefore, the integrated process leads to the separation of the three main components of BSG (fermentable soluble fraction, cellulose, and lignin). Of the latter, the soluble fraction and lignin were specifically analyzed in this work.
In particular the first fraction was used as a specific medium for microbial fermentation and BSG_T Lignin was investigated as a potential renewable source for the development of enhanced water reducer for concrete production. The BSG extract turned out to be very

rich in soluble starch and contained only a minor amount of other nutrients such as proteins and oligosaccharides. Therefore, in order to ensure a nitrogen content suitable for microbial growth, ammonium sulphate was added to the aqueous extract. The obtained BSG medium can furnish the proper nutrients for different microbial strains; more specifically, fungal and bacterial strains that are able to grow on polysaccharides or have been already employed in the transformation of polysaccharide-containing waste materials were here selected.[14-15] Among the plethora of described microorganisms, the basidiomycetous yeast *Phaffia rhodozyma*, the oleaginous yeast *Yarrowia lipolytica* and selected bacterial strains from the genus *Rhodococcus* and *Streptomyces* were singled out. The results of the present study pointed to the potential employment of the obtained microbial biomass in aquaculture, human alimentation, and biodiesel production.
In the second part of the process (the so-called lignocellulose process, as indicated in Figure 2), the treated BSG (BSG_T) underwent a deep eutectic solvent (DES)-based treatment aiming to deconstruct the lignocellulosic skeleton in order to obtain the separation of the two mains components of the biomass, cellulose and lignin. Lignin is the most abundant aromatic biopolymer in nature, and despite its chemical recalcitrance, its possible exploitation is widely studied for several application fields,[16-18] including materials science,[19-22] materials engineering,[23-24] agriculture,[25] and energy.[26-28] An industrially attractive lignin application is the formulation of cement water reducers, an important component for the production of concrete.[29] In recent years, a renewed interest for lignin in this specific field was spurred by several research efforts aimed at the development of renewable, high-performance lignin-based concrete water reducers capable of competing with modern synthetic products.[30-32] This was carried out by using non-sulfonated lignins as a starting point, such as those deriving either from the soda process[33] or from formic acid extraction.[34] Any sustainable process delivering lignin as a by-product is thus a potential resource for the development of renewable cement water reducers in a circular economy approach. In the present study, a first evaluation of the suitability of the BSG_T Lignin for this specific application was carried out implementing a laboratory rheological test on cement pastes that demonstrated a water reduction performance equivalent to those of Protobind 1000, a well-known commercial soda lignin.

2. Materials and Methods

2.1. Materials

All air- and moisture-sensitive reactions were carried out using dry solvents and under a static atmosphere of nitrogen. Choline chloride (C0329), betaine glycine (B0455) and L-lactic acid (L0165) were provided by TCI (Milano, Italy). BSG was provided by the Brewery "L'Orso Verde" (Busto Arsizio, Italy). Protobind 1000, a mixed wheat straw/sarkanda grass lignin from soda pulping of non-woody biomass) was provided by Tanovis (Alpnach, Switzerland). Riboflavin was purchased from Health Leads UK Ltd., (Horeb, UK). The other reagents and the employed solvents were purchased from Merck (Merck Life Science S.R.L., Milan, Italy) and used without further purification.
Reference standard samples of C_{12}-C_{19} branched-chain fatty acids (BCFAs) were prepared as described in a work in preparation.

2.2. Microorganisms and Growth Media

Yarrowia lipolytica (DSM 8218), *Yarrowia lipolytica* (DSM 70562), *Phaffia rhodozyma* = *Xanthophyllomyces dendrorhous* (DMS 5626), and *Rhodococcus opacus* (DSM 43205) were purchased from DSMZ GmbH collection (Braunschweig, Germany).

Streptomyces cavourensis subsp. *cavourensis* (DSM 112466) and *Streptomyces albidoflavus* (DSM 112467) were isolated as axenic cultures in our laboratory, then identified through the 16S *r*RNA gene sequencing and finally deposited in the DSMZ GmbH collection (Braunschweig, Germany) under the collection number given in brackets.

The growth media used in this work were YUM (Yeasts Universal Medium) implemented with 20 mg/L of riboflavin, TSB (tryptic soy broth), GYM medium, and BSG medium.

YUM medium composition: yeast extract (3 g/L), malt extract (3 g/L), peptone from soybeans (5 g/L), glucose (10 g/L).

TSB medium composition: casein peptone (17 g/L), glucose (2.5 g/L), soya peptone (3 g/L), NaCl (5 g/L), K_2HPO_4 (2.5 g/L).

GYM medium composition: glucose (4 g/L), yeast extract (4 g/L), malt extract (10 g/L).

BSG medium: BSG aqueous extract, $(NH_4)_2SO_4$ (3 g/L), yeast extract (1 g/L), and trace elements solution (10 mL/L). For bacteria fermentation, a further 1 g/L of NaCl was added. The preparation of the BSG aqueous extract is described in the context of the BSG treatment procedure (Section 2.3).

YUM was used for the pre-growth of *Yarrowia lipolytica* and *Xanthophyllomyces dendrorhous*, TSB was used for the pre-growth of *Rhodococcus opacus*, and GYM was used for the pre-growth of *Streptomyces cavourensis* subsp. *cavourensis* and *Streptomyces albidoflavus*.

Trace elements solution: $FeCl_3$ (50 mM), $CaCl_2$ (20 mM), $MnCl_2$ (10 mM), $ZnSO_4$ (10 mM), $CoCl_2$ (2 mM), $CuCl_2$ (2 mM), $NiCl_2$ (2 mM), Na_2MoO_4 (2 mM), Na_2SeO_3 (2 mM), H_3BO_3 (2 mM).

2.3. BSG Aqueous Extraction

BSG waste was obtained as wet residue directly from the brewery within 12 h after a batch of beer production. This material was brought to dryness in a ventilated oven (60 °C, 24 h) and was finely ground with the help of an electric mixer. The obtained BSG, designated as BSG_U (untreated BSG) contained 4.3% residual humidity and was stored sealed and refrigerated (4 °C).

BSG_U (40 g) was suspended in deionized water (700 mL) and was heated in an autoclave (121 °C, 15 min). The solid was filtrated, washed three times with deionized water (3 × 250 mL) and was dried in a ventilated oven (60 °C, 24 h) leading to 29.8 g of treated BSG, named BSG_T, (4.1% of residual humidity). BSG_T was then processed further to separate cellulose and lignin (see Section 2.5) whereas the combined liquid phases were used for the preparation of the BSG microbial growth medium. Accordingly, ammonium sulfate (4.5 g), yeast extract (1.5 g), and trace elements solution (15 mL) were added to the extract. Hence, the final volume of the liquid was adjusted to 1.5 L by addition of further deionized water and the obtained medium was sterilized by autoclaving (121 °C, 15 min).

2.4. Evaluation of Fermentation with BSG Microbial Growth Medium

The BSG medium prepared as described above was used for the growth of five different

strains, namely *Yarrowia lipolytica* (DSM 8218), *Yarrowia lipolytica* (DSM 70562), *Xanthophyllomyces dendrorhous* (DMS 5626), *Rhodococcus opacus* (DSM 43205), *Streptomyces cavourensis* subsp. *cavourensis* (DSM 112466), and *Streptomyces albidoflavus* (DSM 112467). The experiments were carried out in triplicate and the presented results are the media of three experimental data.
Each fermentation trial was performed using a 5 L bioreactor (Biostat A BB-8822000, Sartorius-Stedim (Göttingen, Germany) loaded with 1.5 L of BSG medium. Stirring and aeration were set at 200 rpm and 0.6 L/L/min, respectively whereas the temperature, the pH, and the fermentation duration were set depending on the strain used (Table 1). As soon as the fermentation was stopped, the biomass was collected by centrifugation and was freeze-dried in high vacuum (0.05 mmHg) until the sample reached constant weight. The obtained dry biomass was treated, under a static atmosphere of nitrogen, with aqueous NaOH (10% w/v, 16 mL per gram of biomass) and methanol (4 mL per gram of biomass). The mixture was vigorously stirred and was heated at reflux for 6 h. Hence, the reaction was cooled (0 °C), was acidified by dropwise addition of concentrated HCl aqueous (37% w/v) and was extracted twice with ethyl acetate. The combined organic phases were washed in turn with water and with brine, then were dried ($NaSO_4$), and were concentrated under reduced pressure. The residue consisted of a mixture of free fatty acids. The presence of other metabolites was negligible, as indicated by the chromatographic purification affording the fatty acids mixture with a weight loss of only 10%. A sample of this mixture was treated at 0 °C with an excess of an ethereal solution of freshly-prepared diazomethane. The obtained methyl esters mixture was submitted to GC/MS analysis.

2.5. Preparation of DESs

The DESs were prepared by mixing anhydrous hydrogen bond acceptor (HBA) with hydrogen bond donor (HBD) in the determined molar ratio (see Section 3.2.1) and stirred in a closed flask, at 120 °C for 4 h until the liquid phase appeared completely homogeneous and clear. The product was then dried under vacuum and stored at room temperature in a desiccator in the presence of anhydrous calcium chloride until further use. The ^{1}H NMR spectrum of the selected DES (choline chloride/L-lactic acid 1/5) for the full fractionation is reported in Supplementary Materials Figure S1. The recycling of this DES has been performed for three cycles without any modifications as confirmed by ^{1}H NMR spectrum reported in Supplementary Materials Figure S2.

2.6. BSG Treatment with DES

BSG_U (25 g) was suspended in DES choline chloride/L-lactic acid 1/5 (250 mL) at 130 °C in a round-bottom flask under magnetic stirring for 24 h. After cooling, ethanol (500 mL) was then added gradually over 2 h in order to precipitate the cellulose fraction. The pellet was separated by centrifugation and filtration, washed many times with ethanol and dried to give a final solid BSG_U Cellulose (4–6 g) with a yield of 17–25% (w/w initial biomass). The filtrate was then concentrated by rotary evaporation under vacuum to eliminate ethanol. Water (500 mL) was then added and the suspension was stirred for 24 h at 4 °C. The obtained precipitate was then centrifuged, filtered, and washed three times for 1 h with a solution of water/ethanol 9/1. After centrifugation, filtration, and solvent evaporation, the final fraction (BSG_U Lignin, 2.4 g) was recovered with a final yield of 10% (w/w initial biomass).

Thirty grams of BSG_T, obtained as the effluent of the sugar process performed on 40 g of starting BSG was then treated with 150 mL of DES in the same conditions and procedure as described just above. The final products were: the BSG_T Cellulose fraction (12 g, 40% yield, global yield 30% (w/w initial biomass)), and the lignin fraction BSG_T Lignin (4 g, 13.3% yield, global yield 10% (w/w initial biomass)).

2.7. Lignin Solubility in Organic Solvents

Lignin solubility in the different solvents was determined by treating 1 g of the analyzed lignin with 10 mL of the solvent under stirring at 400 rpm. Each test was carried out overnight at room temperature. The suspension was then filtered and the solvent was evaporated at reduced pressure, and the final residue was dried until a constant weight was achieved prior to quantification.

2.8. Instruments and Analytic Condition

2.8.1. Thin Layer Chromatography

Thin layer chromatography (TLC) Merck silica gel 60 F254 plates (Merck Millipore, Milan, Italy) were used for analytical TLC. Preparative column chromatography was performed with silica gel.

2.8.2. ^1H NMR

^1H NMR spectra were obtained using a Bruker-AC-400 spectrometer (Billerica, MA, USA) at 400 MHz and 348 K; the samples were externally locked using D_2O in a coaxial insert tube and the chemical shifts were recorded in ppm.

2.8.3. Gas Chromatography/Mass Spectrometry

The gas chromatography/mass spectrometry (GC/MS) apparatus was a HP-6890 gas chromatograph equipped with a 5973 mass detector and a HP-5MS column (30 m × 0.25 mm, 0.25 μm film thickness; Hewlett Packard, Palo Alto, CA, USA). The separation of the fatty acid methyl esters was performed with the following temperature program: 120 °C (3 min)-12 °C/min-195 °C (10 min)-12 °C/min-300 °C (10 min); carrier gas: He; constant flow 1 mL/min; split ratio: 1/30.

2.8.4. Gel Permeation Chromatography

A Waters 510 HPLC system equipped with a refractive index detector was used for gel permeation chromatography (GPC) analyses. Tetrahydrofuran (THF) was used as eluent. The analyzed lignin sample (volume 200 μL, concentration 1 mg/mL in THF) was injected into a system of three columns connected in series (Ultrastyragel models HR2, HR3 and HR4, dimensions 7.8 mm (inner diameter) × 300 mm (length), provided by Waters) packed with 5 μm spherical particles and covering a broad range of molecular weights (102-105 g/mol). The analysis was performed at 30 °C at a flow rate of 0.5 mL/min. The GPC system was calibrated against polystyrene standards in the 102–104 g/mol molecular weight range. To allow complete solubility in the THF eluent, before the analysis, the parent lignin and the fractions were acetylated following a standard literature procedure.[35] Briefly the estimation of the number-average and weight-average molecular weights (Mn and Mw respectively) of the obtained lignin fractions was performed

excluding the signals related to the solvent (THF) and the solvent stabilizer (butylated hydroxytoluene), visible at long elution times (>29.5 min).

2.8.5. Total Sugars Quantification

Two stock solutions were prepared fresh every time with a protocol previously described with some modifications.[36] Solution A was prepared by dissolution of 19 mg of disodium 2,2-bicinchoninate, 0.543 g of Na_2CO_3 and 0.242 g of $NaHCO_3$ in 10 mL of distilled water. Solution B was obtained by dissolution of 12.4 mg of $CuSO_4 \cdot 5H_2O$ and 12.6 mg of L-serine in 10 mL of distilled water. BCA working solution was freshly prepared just before use by mixing equal volumes of solution A and solution B.

Method 1: This method was performed for aqueous soluble samples. In detail: 1 mL of BCA working solution was added to 1 mL of sample in a vial and incubated at 70 °C for 30 min. The vials were cooled at room temperature, 1 mL of mixture was transferred to a cuvette, and the absorbance was determined at 560 nm. The total reducing sugar value in the samples was then read from the glucose calibration curve a (see Supplementary Materials Figure S3). The calibration curve was established by using a glucose solution as standard in the 0-72 μM concentration range.

Method 2: This method was performed for aqueous-insoluble samples that showed dimethylsulfoxide (DMSO) solubility. The samples were prepared by dissolving lignin in DMSO with a final concentration of 2 mg/mL. For each determination, 5 μL of the solution were then mixed with 995 μL of water and 1 mL of BCA working solution in a vial and incubated at 70 °C for 30 min. The vials were cooled at room temperature, 1 mL of mixture was transferred to a cuvette, and the absorbance was determined at 560 nm. In all cases, the contribution of DMSO to color development was measured and subtracted from the final value. The calibration curve b (see Supplementary Materials Figure S4) was established by using a glucose solution as standard in the 0-280 μM concentration range.

Method 3: In order to determine the abundance of polysaccharides in lignin samples, acid hydrolysis of the samples was performed by incubation of 100 mg of sample with 100 mL water/HCl 37% 6/4 for 2.5 h at 80 °C. The mixture was then set to neutral pH and then filtered. The total reducing sugar concentration in the filtrate was then measured with method 2.

2.8.6. Phenolic Hydroxyl Group Determination

The total phenolic content of lignins was determined by a modified Folin–Ciocalteu (FC) protocol with some modifications to the sample preparation step previously described.[37] The samples were dissolved in DMSO with a final concentration of 2 mg/mL. DMSO was chosen because, being completely miscible in water, it allowed complete lignin solubilization and did not interfere with the FC assay. For each determination, 5 μL of the working solution (or the standard solution) were then mixed with 120 μL of deionized water, 125 μL of FC reagent (Sigma 47641), and kept for 6 min at room temperature after 30 s of vortex stirring. Then, after the addition of 1.25 mL of 5% sodium carbonate and mixing, the vial was incubated in a thermoshaker at 40 °C for 30 min. The reaction mixture absorbance was measured using a UV–Vis spectrophotometer (Jasco V-560) equipped with a temperature-controlled cuvette holder and a thermostatic water bath

(Haake K10, Karlsruhe, Germany). All spectrophotometric measurements were carried out at 760 nm, 25 °C, using a 1 cm optical path cuvette and deionized water as blank sample. Vanillin was chosen as the reference standard. The calibration curve was constructed with nine different vanillin solutions in DMSO with concentration in the range 0–500 μg/mL (see Supplementary Materials Figure S5). Each FC assay determination was carried out in triplicate.

2.8.7. ^{31}P NMR Analysis

^{31}P NMR spectroscopic analyses were recorded on a Bruker Instrument AVANCE400 spectrometer (Milano, Italy). Acquisition and data treatment were performed with Bruker TopSpin 3.2 software (Milano, Italy). The spectra were collected at 29 °C with a 4 s acquisition time, 5 s relaxation delay, and 256 scans. Prior to analysis, samples were dried for 24 h under vacuum and then derivatized according to the following procedure.
The sample (40 mg) was completely dissolved in 300 μL of N,N-dimethylformamide. To this solution, the following components were added: 200 μL of dry pyridine, 100 μL of solution of internal standard (10 mg of Endo-N-hydroxy-5-norbornene-2,3-dicarboximide (Sigma 226378) dissolved in 0.5 mL of a mixture of pyridine and CDCl3 1.6:1 v/v), 50 μL of a relaxation agent solution (5.7 mg of chromium (III) acetylacetonate (Sigma 574082) dissolved in 0.5 mL of a mixture of pyridine and $CDCl_3$ 1.6:1 v/v), 100 μL of 2-chloro-4,4,5,5-tetramethyl-1,3,2-dioxaphospholane (Sigma 447536), and at the end 200 μL $CDCl_3$. The solution was centrifuged and/or filtered if necessary. All chemical shifts reported were related to the reaction product of the phosphorylating agent with water, which gave a signal at 132.2 ppm.

2.8.8. Fourier transform Infrared Spectroscopy

Fourier-transform infrared spectroscopy (FTIR) was performed by a Nicolet Netxus 760 FTIR spectrophotometer. The samples were prepared by pressing the biomass powders with KBr powder to obtain thin discs. Spectra were obtained in transmission mode, at room temperature, in air, by recording 64 accumulated scans at a resolution of 4 cm^{-1} in the 4000-500 cm^{-1} wavenumber range.

2.8.9. Differential Scanning Calorimetry

Differential scanning calorimetry (DSC) was employed to investigate the thermal transitions of lignin samples. Measurements were carried out on 10–15 mg samples by means of a Mettler-Toledo DSC 823e instrument. Three runs (heating/cooling/heating) were performed: from 25 °C to 150 °C to remove water from samples, from 150 °C to 25 °C, and from 25 °C to 200 °C, at a scan rate of 20 °C/min under nitrogen flux. The glass transition temperature (Tg) of the samples was evaluated as the inflection point in the second heating run.

2.9. Water Reduction in Cement Pastes

A preliminary estimation of the water reduction capability of recovered lignins was carried out evaluating the relative Bingham dynamic yield torque of cement pastes containing 0.2% of lignin (w/w relative to dry cement) at different water/cement (w/c) ratio.[38] This allowed us to compare the water reduction attainable from each lignin in order to obtain a cement paste with the same yield torque of a pure cement paste with

0.45 w/c ratio, taken as reference. The water reduction was evaluated for BSG_U Lignin, for BSG_T Lignin and for the commercial soda lignin Protobind 1000. For each rheological measurement an alkaline (NaOH) lignin solution (10% w/w lignin/water) was prepared taking care to obtain a final content of 0.4 g of lignin and 3.6 g of water. A cement paste was prepared mixing 200 g of ordinary Portland cement (CEM I 42.5 R according to EN 197-1 standard) with water in the required amount minus 3.6 g that was added later to the lignin solution. The cement/water paste was then stirred manually for 2 minutes, after which the lignin solution was added. The paste was further stirred for 2 min and finally transferred into the rheometer cup.
A rotational rheometer (RheolabQC, Anton Paar GmbH, Austria) provided with a 30 mm diameter four blade stirrer and a 42 mm diameter sandblasted stainless steel cup (ST30-4V-40/133 and CC39/S respectively, Anton Paar) was used for all the tests, measuring the torque obtained in a series of decreasing rotational speed steps (from 80 to 1 rpm, 10 s each) after a pre-shear interval (340 s) at 100 rpm. The resulting torque for each measuring step was calculated as mean of the last 5 s of sampled data.
A linear regression for every torque/rotational speed dataset was calculated considering only the data points in the 80-20 rpm rotational speed interval (i.e., in the 14.2–16.3 min interval from the first water–cement contact). The linear regression represents the Bingham model for the given cement paste. This latter was extrapolated to zero rotational speed (i.e., to the ordinate intersect, Figure 3) in order to obtain the Bingham dynamic yield torque T0.[38]

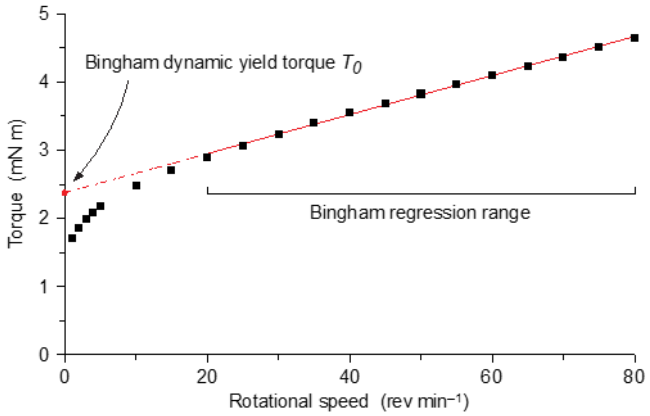

Figure 3: Bingham fitting of torque vs. rotational speed data. The Bingham dynamic yield torque T_0 was obtained by extrapolating the Bingham model to zero rotational speed.

lignin-containing cement paste with the following relation

$$T_R = \frac{T_0}{T_{0,ref}}$$

where T_0 is the obtained Bingham dynamic yield torque and $T_{0,ref}$ is the yield torque measured with the reference paste (0.45 w/c ratio cement paste without lignin). The water/cement ratio W_L at the unit value of T_R (i.e., at the reference Bingham dynamic yield torque) was calculated for each cement paste with the inverse linear regression of the yield torque/water cement ratio dataset (Figure 4).

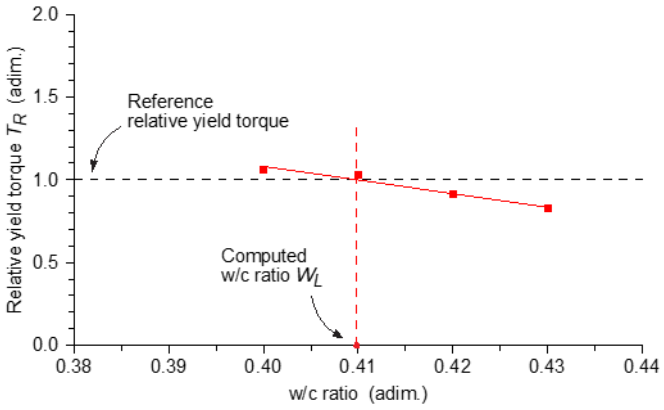

Figure 4: Relative dynamic Bingham yield torque vs. water/cement ratio data set for the BSG_T Lignin cement paste sample and determination of computed w/c ratio W_L. The Bingham yield torque measured at each w/c ratio (red squares) was relative to the yield torque of the reference cement paste (without lignin) at 0.45 w/c ratio. The W_L value obtained with the lignin containing cement paste was calculated intersecting the reference yield torque value (black dotted line) with the sample points data fitting line (red solid line).

The actual water reduction for a given lignin is given by the following relation

$$W_R = 100 \cdot \left(1 - \frac{W_L}{W_{ref}}\right)$$

where W_R is the obtained water reduction (%), W_L is the computed w/c ratio at the reference yield torque for the given lignin, and W_{ref} is the reference w/c ratio (0.45).
This procedure measured the effective water reduction capability of each lignin in the preparation of a cement paste in the given conditions.

3. Results and Discussion

3.1. BSG Waste Pretreatment and Sugar Process

As mentioned before, BSG waste contains a number of components, of which polysaccharides, proteins, fibers (hemicellulose, cellulose, and lignin), fats and inorganic salts are the most representative ones.
Using water as a solvent, preliminary experiments were performed in order to establish how much starch/polysaccharides could be extracted from untreated BSG (BSG_U). The results were encouraging because repeated extractions with hot water allowed a considerable reduction of the initial BSG weight (up to 20%). Therefore, a new protocol based on a strong thermic treatment followed by three aqueous extractions was set up, allowing the separation of a relevant amount of soluble materials. Accordingly, dried BSG was ground, suspended in water, and heated in an autoclave (121 °C, 15 min). The solid was filtrated, washed with water, and dried again. Overall, more than 25% of the initial BSG weight was dissolved in water. The obtained solution, enriched in soluble starch, proteins, and other minor nutrients, could be regarded as a valuable growing medium for microbial fermentation. Therefore, a new medium made up of BSG extract (6.8 g/L), yeast extract (1 g/L), and ammonium sulfate (3 g/L) was defined (reported as BSG medium in Figure 1). The addition of yeast extract, even in low amount, is crucial because it provides vitamins and microelements essential to microbial fermentation. In addition, although BSG contains proteins, the nitrogen content of the aqueous extract is not

sufficient to ensure good biomass production. Consequently, ammonium sulfate as a suitable nitrogen source was selected. The latter compound is a very cheap chemical, largely employed in industry and in microbiology where it is used to replace peptone or other protein sources. Hence, the new medium was tested for the fermentation of some selected microorganisms. Attention was focused on the evaluation of the strains only belonging to the BL-1, with high preference of those generally recognized as safe for human health (GRAS). In addition, they must be able to metabolize starch/ polysaccharides and to produce compounds of commercial interest. More specifically, a preliminary screening allowed us to single out six different microorganisms (Table 1), three fungal and three bacterial strains.
The growth of the strains was tested taking into account the possible scalability to industrial production. Hence, fermentation experiments were performed in a 5 L bioreactor, using at least 1.5 L of BSG medium, with accurate control of the temperature, stirring, and aeration parameters.

Table 1: Production of biomass and fatty acids using the BSG medium and some selected microbial strains.

Entry	Microbial Strain	Growth Conditions [1]	Biomass Productivity [2]	Fatty Acid Productivity [3]
1	*Phaffia rhodozyma* (DMS 5626)	6 days at 22 °C, pH 6.5	3.6 g/L (135 g/Kg BSG)	-
2	*Yarrowia lipolytica* (DSM 8218)	4 days at 25 °C, pH 6.5	1.5 g/L (55 g/Kg BSG)	200 mg/L (7.5 g/Kg BSG)
3	*Yarrowia lipolytica* (DSM 70562)	4 days at 25 °C, pH 6.5	1.6 g/L (61 g/Kg BSG)	220 mg/L (8.2 g/Kg BSG)
4	*Rhodococcus opacus* (DSM 43205)	4 days at 28 °C, pH 7.0	2.4 g/L (89 g/Kg BSG)	547 mg/L (20.5 g/Kg BSG)
5	*Streptomyces cavourensis* (DSM 112466)	4 days at 28 °C, pH 7.0	2.1 g/L (80 g/Kg BSG)	220 mg/L (8.2 g/Kg BSG)
6	*Streptomyces albidoflavus* (DSM 112467)	4 days at 28 °C, pH 7.0	1.7 g/L (64 g/Kg BSG)	180 mg/L (6.7 g/Kg BSG)

[1] Each microbial growth was performed in a 5 L bioreactor, using 1.5 L of BSG medium. Stirring and aeration were set at 200 rpm and 0.6 L/L/min, respectively. [2] The biomass was collected by centrifugation as soon as the fermentation was stopped and then was freeze-dried. The biomass productivity is indicated as both grams of dried biomass produced starting from one liter of BSG medium and grams of dried biomass produced starting from one kilogram of dried BSG_U (value in brackets). [3] The fatty acid productivity is indicated as both milligrams of the fatty acid mixture produced starting from one liter of BSG medium and grams of the fatty acid mixture produced starting from one kilogram of dried BSG_U (value in brackets).

The first investigated strain, *Phaffia rhodozyma*,[39] is a basidiomycetous yeast that was found in slime fluxes of certain broad-leafed trees. This microorganism takes advantage of its fermentative abilities to use the carbohydrates there present for its growth, thus indicating potential employment in the transformation of other polysaccharide-rich substrates. The most remarkable features of *P. rhodozyma* is its pink-orange color due the production of carotenoid pigments and especially of astaxanthin. This compound has great economical relevance because it is a widely used feed ingredient, utilized for the pigmentation of fish and crustaceans, and is one of the most expensive feed ingredients in the aquaculture industry.[40-41] In addition, the European Commission has authorized the direct use of the whole yeast biomass in foodstuffs for salmon and trout,[16] including the

use of astaxanthin overproducing strains.[42] Therefore, we tested the biomass productivity of a wild-type strain of *Phaffia rhodozyma* (DSM 5626) using our BSG medium (Table 1, entry 1). As soon as the microorganism reached the stationary phase of growth, the biomass was separated by centrifugation and then was freeze-dried, until complete removal of the water content. Three-point-six grams of dry biomass per liter of BSG medium were obtained, corresponding to a productivity of 135 g of dry yeast per kilogram of dry BSG. These very good results clearly indicated the potential of BSG medium in biomass production and its specific use for the above-described industrial application.
The other five strains reported in Table 1 were selected taking into account their capacity of lipids accumulation. Indeed, the yeast *Yarrowia lipolytica* and the bacterium *Rhodococcus opacus* are well known oleaginous microorganisms, able to produce triglycerides starting from a number of different waste materials as substrates.[43-44] In particular, *Yarrowia lipolytica* is a GRAS microorganism and the European Commission has authorized the commercialization of the dried and heat-killed biomass of all *Y. lipolytica* strains as a novel food ingredient.[45] Moreover, in specific culture condition, this microorganism can produce lipids having a composition resembling that of cocoa butter[46] and has been selected to integrate by fermentation the limited production of this natural fat. In contrast, *Rhodococcus opacus* has not been used for food applications yet. Since this microorganism has the capacity to grow on different kind of substrates, accumulating high level of triglycerides, *R. opacus* has been used for the production of biodiesel from organic wastes.[47] Similarly, strains belonging to the genus Streptomyces have been studied for their ability in the degradation of lignocellulose wastes leading to the production of branched chain fatty acid (BCFA) derivatives.[48] These compounds possess a number of physical, chemical, and biological properties. Due to their low melting points, BCFAs esters have been selected as preferred biofuels for use in cold environments, whereas BCFAs show protective activity against neonatal necrotizing enterocolitis (NEC), a potentially lethal disease representing the major cause of morbidity in premature infants.[49] For the latter reason, these compounds have been proposed for inclusion in infant food formulas as human milk fat substitutes.[50]
In the context of bacteria degrading lignocellulose wastes, two Streptomyces strains were isolated from a soil sample, polluted with cereal and fodder residues. The strains were identified as *Streptomyces cavourensis* and *Streptomyces albidoflavus* and were deposed in DMSZ collection under the numbers DSM 112466 and DSM 112467, respectively. Both the biomass productivity and the fatty acids productivity of all the above-described fungal and bacterial species, grown on BSG medium, were investigated (Table 1, entry 2–6). As described for *P. rhodozyma*, the biomass was separated by centrifugation as soon as the microorganism reached the stationary phase of growth, freeze-dried, completely hydrolyzed, and analyzed by GC/MS after acidification and extraction as reported in Section 2.4 (Table 2).
The two *Yarrowia lipolytica* strains, DSM 8218 and DSM 70562, were isolated from very different environments, namely from a diesel fuel tank and from marzipan, respectively. Despite this fact, they showed similar characteristics both in term of biomass and fatty acid productivity (Table 1, entry 2 and 3). The dry yeast was obtained in yield of about 1.5 g and 1.6 g per liter of BSG medium respectively, whereas the oil production ranged from 200 mg to 220 mg of isolated fatty acid per liter of BSG, respectively. Otherwise, *Rhodococcus opacus* DSM 43205 showed better performances. The fermentation afforded 2.4 g of dry biomass per liter of BSG medium, yielding 547 g/L of isolated fatty acids (Table 1, entry 3). Finally, the two *Streptomyces* strains showed results

comparable to those obtained with *Y. lipolytica* strains, with *S. cavourensis* showing slightly higher productivity (2.1 g/L biomass and 220 mg/L of FAs) than *S. albidoflavus* (1.7 g/L biomass and 180 mg/L of FAs).
The most relevant differences among the investigated fungal and bacterial species were highlighted by the GC/MS analysis of the fatty acids mixtures isolated from the corresponding biomasses (Table 2). In more detail, *Y. lipolytic*a contained only linear FAs, of which 72% corresponded to polyunsaturated fatty acids (PUFAs), mainly made up of linoleic acid. In contrast, the bacterium *R. opacus* produced predominantly saturated fatty acids (SFAs), although monounsaturated fatty acids (MUFAs), PUFAs, and some specific BCFAs, such as cyclopropane containing FAs and 10-methyl-octadecanoic acid, were present.
The two *Streptomyces* species showed very similar fatty acid composition. Both microorganisms accumulated prevalently BCFAs and the majority of the fatty acid mixture was made up of iso- and anteiso-fatty acids.
Overall, the present study outlines four possible applications of the BSG_T medium. Fermentation of *P. rhodozyma* and *Y. lipolytica* could afford biomass materials to be employed in aquaculture and human alimentation, respectively. Moreover, *R. opacus* and *S. cavourensis* could provide the FA derivatives useful for the preparation of different kinds of biodiesel and for the formulations of the BCFA-containing human milk fat substitutes, respectively.

Table 2: Fatty acid composition of the glycerides produced by the selected microbial strains grown in BSG medium.

Microbial Strain	Branched chain FAs (%) [1]			Linear FAs (%) [1]			Undetermined FAs (%) [1,2]
	iso	*anteiso*	Others	SFAs [3]	MUFAs [4]	PUFAs [5]	
Yarrowia lipolytica (DSM 70562)	-	-	-	16.5	9.0	72.0	2.5
Rhodococcus opacus (DSM 43205)	-	-	4.0 [6]; 15.1 [7]	44.6	21.7	9.1	5.5
Streptomyces cavourensis (DSM 112466)	28.4	37.7	6.8 [6]	15.0	3.7	7.5	0.9
Streptomyces albidoflavus (DSM 112467)	18.6	39.1	8.1 [6]	15.2	7.0	5.8	6.2

[1] The percentages are determined by GC/MS analysis of the crude fatty acids mixture derivatized as methyl ester derivatives. [2] The percentage indicates the sum of the fatty acids whose chemical structure was not determined. [3] Saturated fatty acids. [4] Monounsaturated fatty acids. [5] Polyunsaturated fatty acids. [6] The percentage indicates the sum of the fatty acids possessing a cyclopropyl ring in their chemical framework. [7] Percentage of 10-methyl-octadecanoic acid (tubercolostearic acid).

3.2. Lignocellulose Process

3.2.1. DES-Mediated Fractionation

Recently, some innovative biomass DES-based treatments have been reported in the literature in the context of exploiting agricultural waste in biorefineries.[51-53] However, the described treatments were mainly focused on the obtainment of a high quantity of fermentable sugars as in the majority of the research concerning biomass exploitation.[54]
In this work, a new protocol of biomass DES-based treatment coupled with the previous sugar process step (described in Section 3.1) has been set up with the special aim of lignin

recovery and exploitation.
Different DESs were prepared by heating and stirring the two components, a hydrogen bond acceptor (HBA) and a hydrogen bond donor (HBD), in a defined molar ratio. The quaternary ammonium salts choline chloride (ChCl) and betaine glycine (BetG) were used as HBAs whereas formic acid, acetic acid, and L-lactic acid constituted HBDs, as reported in Table 3.

Table 3: List, composition, density (measured at 18 °C) of prepared DESs and data of mass recovery of BSG_U Cellulose and BSG_U Lignin (ns represents no separation).

Composition DES HBA/HBD	Molar Ratio (HBA/HBD)	Density of Pure DES (g/cm^3)	BSG_U Cellulose Recovery (% w/w Biomass)	BSG_U Lignin Recovery (% w/w Biomass)
Choline chloride/Formic acid	1/2	1.147	ns	ns
Choline chloride/Acetic acid	1/2	1.103	39	7
Choline chloride/L-Lactic acid	1/5	1.184	25	10
Betaine Glycine/Formic acid	1/2	1.161	55	9
Betaine Glycine/Acetic acid	1/2	1.107	32	8
Betaine Glycine/L-Lactic acid	1/5	1.203	53	7

DESs were prepared using a defined protocol, which consisted of mixing the components in a defined ratio (reported in Table 3) and heating them, under constant stirring, at 90 °C for 2-5 h until a stable, homogeneous, colorless single-phase liquid was formed. The obtained mixtures were dried at reduced pressure for 24 h, preserved under argon, and characterized by ^1H NMR spectra. The final mixtures were then conserved in a desiccator in presence of calcium chloride until a constant weight was observed. The densities of DESs were also measured because these data provided important information about the intermolecular forces that occur during DES formation. Typically, DESs show higher density than water and the value depends strongly on the type of the HBD and its molar ratio on HBA.
When the BSG was received from the brewery, it was promptly dried for 24 h, finely milled and labeled as BSG_U (untreated BSG). BSG_U was suspended in DES at 130 °C under magnetic stirring for 24 h. Then ethanol was gradually added in order to precipitate the BSG_U Cellulose fraction, which was separated with yields reported in Table 3 (as w/w initial biomass). The filtrate was then concentrated and treated with water as anti-solvent to induce lignin precipitation. After centrifugation, filtration, and solvent evaporation the final solid fraction (BSG_U Lignin) was recovered with a final yield reported in Table 3. The choline chloride/L-lactic acid 1/5 appeared to be the best DES for the treatment of BSG biomass in terms of solubilization of the starting biomass as well as for the handling of the solutions during the DES treatment, and due to the yields of BSG_U Cellulose and BSG_U Lignin. For that reason, the present study has focused only on the use of the DES choline chloride/L-lactic acid 1/5 for the lignocellulose fractionation.
From the lignocellulose process point of view, the sugar process (Section 3.1) can be considered as a pretreatment of the waste BSG biomass. The sugar process had the effect of improving the successive lignocellulosic fractionation, enhancing the yields of the two fractions, probably because of better interaction between the solvent and the biomass. Moreover, the reduction of the biomass weight derived from the sugar process allowed, if compared to BSG_U fractionation, a substantial saving accounting for around 25%, in terms of DES quantity and solvent volumes. This enables a great improvement of the overall process both in economic and environmental terms. In that case, the yield of BSG_T

Cellulose recovery accounted for 40% (instead of 25%) and up to 15% for BSG_T Lignin instead of 9%.
The ability to recycle DES in a cyclic process would add value to the previous considerations, allowing further potential optimization of the entire process. In this study, a preliminary assessment of the recyclability of DES was conducted by performing a series of three successive treatments recycling the DES after precipitation of the BSG_T Lignin without further purification apart from water evaporation. This study demonstrated a quite good preservation of the DES (by NMR analysis, Supplementary Materials Figure S2) and a substantial conservation of yields indicating a great potential to configure the lignocellulosic process as a closed loop with respect to DES.

3.2.2. BSG_T Lignin Characterization

A deep characterization was carried out on the recovered BSG_T Lignin using as reference a well known commercial soda lignin (Protobind 1000, indicated from now on as Protobind).

Solvent Solubilization Determination

Solubilization studies are a key step in lignin characterization and valorization. In fact, one of the main drawbacks currently hampering effective lignin exploitation is generally its poor solubility in aqueous systems and in the most commonly used organic solvents. In order to determine the solubility characteristics of the present recovered BSG_T and BSG_U Lignins, a solubilization study was performed with water and six organic solvents: n-butyl acetate (BuOAc), ethyl acetate (EtOAc), 2-butanone (MEK), methanol (MeOH), tert-butyl methyl ether (MTBE), and tetrahydrofuran (THF). The resulting extraction yields (as w/w percentage of solubilized fraction vs. total fraction) are reported in Figure 5 (with water solubility as the comparison). For a better evaluation, the data for the commercial lignin Protobind have been also recorded and inserted in Figure 5.

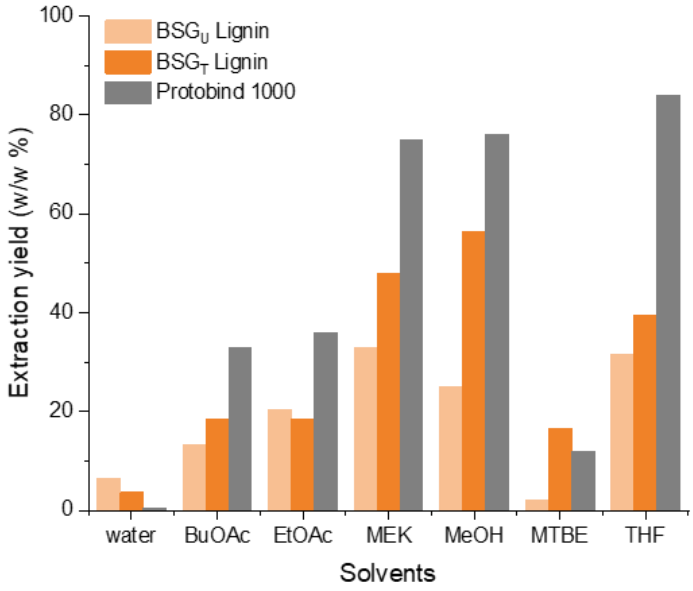

Figure 5: Extraction yield of a commercial technical lignin (Protobind) and the two lignins extracted from BSG (BSG_U and BSG_T Lignins). The data are reported as the percentage (w/w) of solubilized fraction vs. total fraction in 6 different organic solvents and water.

Like Protobind, the two BSG lignins (BSG_U and BSG_T Lignins) were quite insoluble in water, but on the other hand were soluble in the selected organic solvents; showing, however, a general lower solubility when compared to Protobind in all tested organic solvents. MEK, methanol, and THF appeared to be the best choices for the solubilization of these lignins with a range of solubility from 32-35% for BSG_U Lignin and 40-56% for BSG_T Lignin. Moreover, it is clear from the Figure 5 that BSG_T Lignin always presented a higher solubility than BSG_U Lignin in the examined solvents: in THF the solubility was 25% higher, in MEK 45%, and in MeOH 61%. This characteristic constitutes a great advantage in further potential lignin exploitation.

GPC Results

The molecular weight and the molecular weight distribution of the lignin samples were determined by means of GPC. In Table 4, the number average molecular weight (Mn), the weight average molecular weight (Mw), and the polydispersity index (Đ) of BSG lignins and Protobind, used as benchmark, are reported. As can be seen, the lignocellulose process led to BSG lignin fractions characterized by a lower molecular weight and lower Đ compared to Protobind. In particular, a slightly lower Mn was observed in BSG_T Lignin, likely resulting from the isolation method (aqueous extraction), which may lead to an enrichment of low-molecular-weight fractions. This also leads to a slightly higher Đ. In contrast, no significant differences between BSG_T and BSG_U Lignins were observed in terms of Mw.

Table 4: Number average molecular weight (Mn), weight average molecular weight (Mw), and polydispersity index (Đ) of all examined lignins (samples were eluted after acetylation; reported values are relative to polystyrene standards).

Sample	M_n (g/mol)	M_w (g/mol)	*Đ*
BSG_U Lignin	820	1580	1.93
BSG_T Lignin	670	1630	2.43
Protobind 1000	830	2800	3.37

Sugars Quantification

The total reducing sugar quantification in the final BSG_U and BSG_T Lignins was performed using the bincinconic assay method with some modifications (see Section 2.8). It was necessary to set two different calibration curves, a and b (respectively reported in Supplementary Materials Figures S3 and S4), established by using glucose solutions in the 0-80 μM concentration range as standards. In particular, the calibration curve a was used to evaluate the sugar content of samples soluble in water, and the calibration curve b for samples insoluble in water, but soluble in dimethylsulfoxide (DMSO). Curve a was used to analyze aqueous sugar solutions after step 2 (BSG_T medium filtrate) whereas curve b, recorded for DMSO soluble samples, was used to analyze lignins and lignin samples subjected to acid hydrolysis. This procedure was conducted to evaluate the presence of complex saccharides in lignins. The results for BSG_U and BSG_T Lignins are reported in Table 5, as well as the data for Protobind. The reducing sugars in the BSG lignins appeared to be around 0.20% (w/w), lower than the value in Protobind (≈ 0.34%), with a reduction for BSG_T Lignin that demonstrated that the sugar process is quite effective for the recovery of a higher-quality lignin. Furthermore, after hydrolysis,

Protobind showed also the presence of a higher quantity (13%) of complex sugars, whereas in these conditions, for the two BSG lignins this amount was much lower. This result is fundamental in view of the applications of these lignins in the development of cement water reducers.

Table 5: Results of the total reducing sugar quantification.

Sample	Reducing Sugars/Biomass (w/w)	Reducing Sugars/Biomass after Hydrolysis (w/w)
BSG_U Lignin	0.25%	2.9%
BSG_T Lignin	0.18%	3.3%
Protobind 1000	0.34%	13%

Phenolic Hydroxyl Group Determination

The total phenolic content in the recovered BSG_U and BSG_T Lignins was determined using the Folin–Ciocalteu (FC) assay. The test is based on the reaction of phenolic hydroxyl groups with a specific redox reagent (FC reagent), which leads to the formation of a blue chromophore, which is, however, sensitive and unstable in strong bases. Therefore, based on an analytical protocol previously demonstrated by our group,[55] DMSO was used as solvent for the samples in order to obtain their complete solubilization in neutral conditions. The phenolic content results are reported in Table 6 as vanillin equivalents (mmol/g of dry lignin) with the data for Protobind as a reference.

Table 6: Results of the determination of phenolic hydroxyl groups expressed as vanillin equivalents/g of lignin sample. Estimated standard errors ±0.2 mmol/g vanillin equivalent (1 σ, from calibration data).

Sample	Vanillin Equivalent Content (mmol/g)
BSG_U Lignin	1.1
BSG_T Lignin	1.2
Protobind 1000	3.1

BSG_U and BSG_T Lignins show a quite similar content of vanillin equivalents (around 1.15 ± 0.05), which is nearly half the amount value if compared to Protobind. The trend seemed to be confirmed by ^{31}P NMR analysis as will be illustrated later in the text. The quite similar values of the two BSG lignins demonstrated that the pretreatment carried out in the sugar process has no influence on phenolic functionalities.

Total Hydroxyl Groups Quantification by ^{31}P NMR

The different hydroxyl groups present in the recovered BSG lignins were deeply investigated by ^{31}P NMR. The spectra are shown in Figure 6, where Protobind has been also recorded for a comparison.

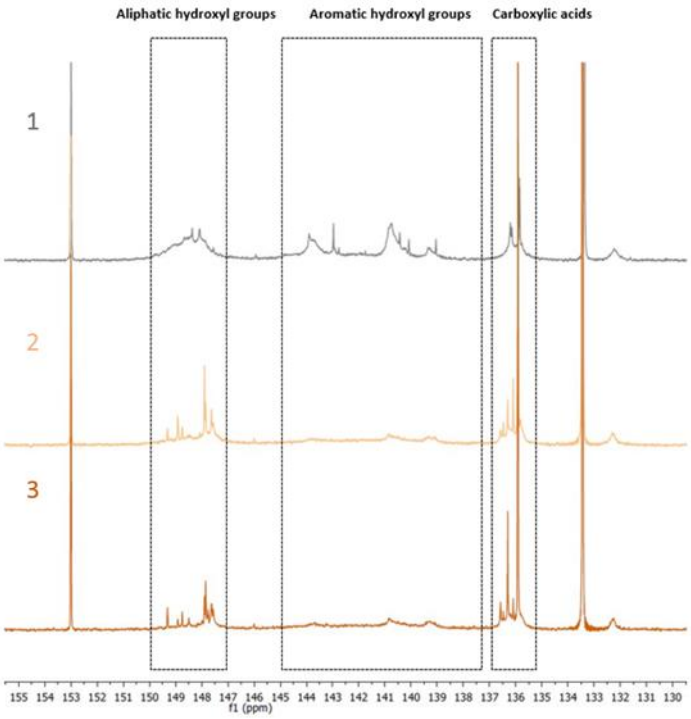

Figure 6: ^{31}P NMR spectra of Protobind 1000 (spectrum 1 in gray), BSG_U Lignin (spectrum 2 pale orange), BSG_T Lignin (spectrum 3 dark orange).

In detail, three sections of the spectra were analyzed and integrated to perform the attribution of the different hydroxyl groups: the signals from 150-147 ppm are associated to the aliphatic hydroxyl groups, the signals from 145-138 ppm represent the signals associated with aromatic hydroxyl groups, whereas the signals centered on 136 ppm account for the carboxylic acid residues. The peak integration in these three parts of the spectra led to the quantification of the total hydroxyl groups expressed in mmol of functional group per g of dry lignin, as reported in Table 7 below.

Table 7: Detailed hydroxyl/carboxyl quantification by ^{31}P NMR (as mmol of functional group per g of dry lignin).

Sample	-OH Aliphatic (mmol/g)	-OH Aromatic (mmol/g)	-COOH (mmol/g)
BSG_U Lignin	2.27	2.77	2.30
BSG_T Lignin	1.78	3.21	3.99
Protobind 1000	3	4.67	1.42

Lignins from BSG seemed to show a higher concentration of carboxylic residues but a lower quantity of aliphatic and aromatic hydroxyl functionalities if compared with Protobind. In particular, it appears very interesting that BSG_T Lignin presented a higher quantity of aromatic OH and carboxylic functionalities when compared to the other samples, which could be a very important tool for the investigation of its use in the preparation of lignin-based macromolecular materials where the presence of such functionalities are mandatory. More specifically, target applications for this lignin fraction may include the field of phenolic resins and adhesives and the field of epoxy-

based systems for fiber-reinforced composite materials.

Fourier Transform Infrared Spectroscopy

FTIR spectroscopy was carried out with the aim of studying the chemical composition of the extracted BSG lignins. The spectrum of Protobind is also presented for comparison purposes. The results obtained are reported in Figure 7, where a zoom of the fingerprint region is also presented. All three lignins showed a broad absorption band in the region 3400-3200 cm^{-1}, attributed to the stretching vibrations of the aliphatic and phenolic O-H groups, and three distinct signals in the region 3050-2800 cm^{-1} related to C-H bond stretching in methyl and methylene groups. The region from 1740 to 1710 cm^{-1} is attributable to the stretching vibration of C=O in unconjugated ketones, carbonyl, and ester groups.[38, 55] Within this region, the signal located at 1710 cm^{-1} is visible in all lignin spectra, whereas the signal located at 1740 cm^{-1} is found only in the cases of BSG lignins (blue arrows). This additional signal can be associated with the higher concentration of C=O moieties from carbohydrate origin contained in the two extracted lignins, which is an indication of the slightly lower purity of the BSG lignins compared to Protobind. In the case of BSG_U Lignin, a signal is clearly detectable at 1660 cm^{-1}, likely attributable to conjugated carbonyl/carboxyl stretching. This signal confirms the presence of the highest concentration of C=O moieties (viz., of carbohydrates species) in the lignin recovered from the untreated biomass.[56] The bands ascribable to the aromatic skeletal vibrations in lignin are located at 1600 cm^{-1}, 1515 cm^{-1}, 1463 cm^{-1}, and 1430 cm^{-1} (the last one barely visible in BSG lignins) in all the three lignin samples. Among these, the two signals at 1463 cm^{-1} and 1430 cm^{-1} derive from the combination of aromatic ring vibration and C-H deformation.[56-57] Below 1430 cm^{-1}, the interpretation of bands becomes more difficult, since the signals are given by complex contributions from different vibrational modes. In more detail, aliphatic O-H group vibrations combined with stretching vibrations of aliphatic C-H in methyl groups were found at around 1370 cm^{-1} in all lignins. Only in the case of Protobind was a further signal at 1330 cm^{-1} attributable to the syringyl ring breathing found. At 1270 cm^{-1} and 1217 cm^{-1}, two peaks associated with C-O vibration in aromatic rings of G-units combined with C=O stretching and C-C, C-O and C=O stretching, respectively, were detected. It is noteworthy that the broadening of these two peaks in both BSG lignins together with the absence of the syringyl ring breathing signal is consistent with the predominant content of guaiacyl units expected in BSG lignins, as reported in the literature.[56, 58] At 1120 cm^{-1} a band associated with CH in-plane deformation in S-units was observable in all cases (more evidently in Protobind), while only in Protobind was the absorption signal at 1153 cm^{-1} related to C=O deformations in conjugated ester groups of G/S/H units visible. In addition to these, signals associated with aromatic C-H in-plane deformation (typical for S-units), secondary alcohols, and C=O stretching were observed in all spectra collected in the region from 1130 cm^{-1} to 1120 cm^{-1}. The shoulder at around 1090 cm^{-1} appearing in all three lignins can be associated with C-O deformations in secondary alcohols and aliphatic ethers.[56]

In general, FTIR results indicated a good match between the chemical structure of the BSG lignins and that of Protobind. The minor differences found between the recovered lignins and the reference system are likely attributable to the lower level of purity of the BSG_U Lignin (higher carbohydrates content) and the large number of G-units in both BSG lignins.

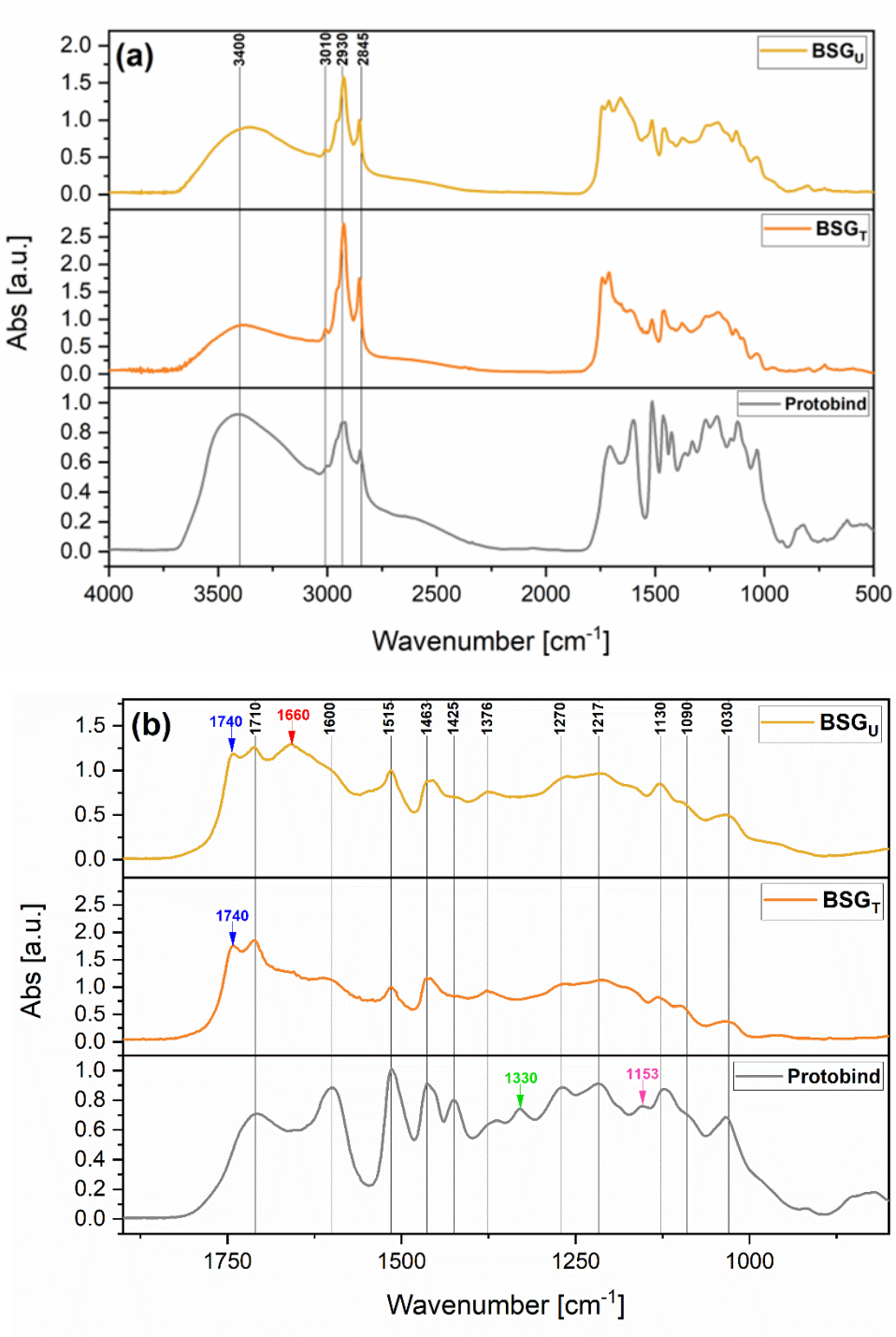

Figure 7: (a) FTIR spectra of BSG_U Lignin, BSG_T Lignin, and Protobind; (b) zoomed view of the fingerprint region.

Differential Scanning Calorimetry

The thermal transitions of the recovered lignins were assessed by DSC analysis. As shown in the DSC scans reported in Figure 8, the glass transition temperature (Tg) for both BSG lignins was found to be higher compared to the Tg of the reference Protobind. In line with the outcomes of ^{31}P NMR analysis, this trend may be associated with the higher content of carboxylic groups found in BSG lignins vs. Protobind, which are likely to yield

increased hydrogen bonding interactions between the macromolecular chains, ultimately leading to reduced macromolecular mobility and thus increased Tg. In more detail, Tg of BSG_T Lignin is found at a slightly higher temperature than that of BSG_U Lignin. In this case, this evidence also appears in line with the higher content of -OH aromatic functionalities and carboxyl groups in this treated lignin fraction vs. the untreated counterpart. The value of Tg is of fundamental importance in lignin valorization, especially in the field of material science and engineering, where high temperature processing is often encountered. In this context, a higher Tg value can be an advantage in those applications that require a good thermal stability of the material, such as in the case of thermosets and composites.

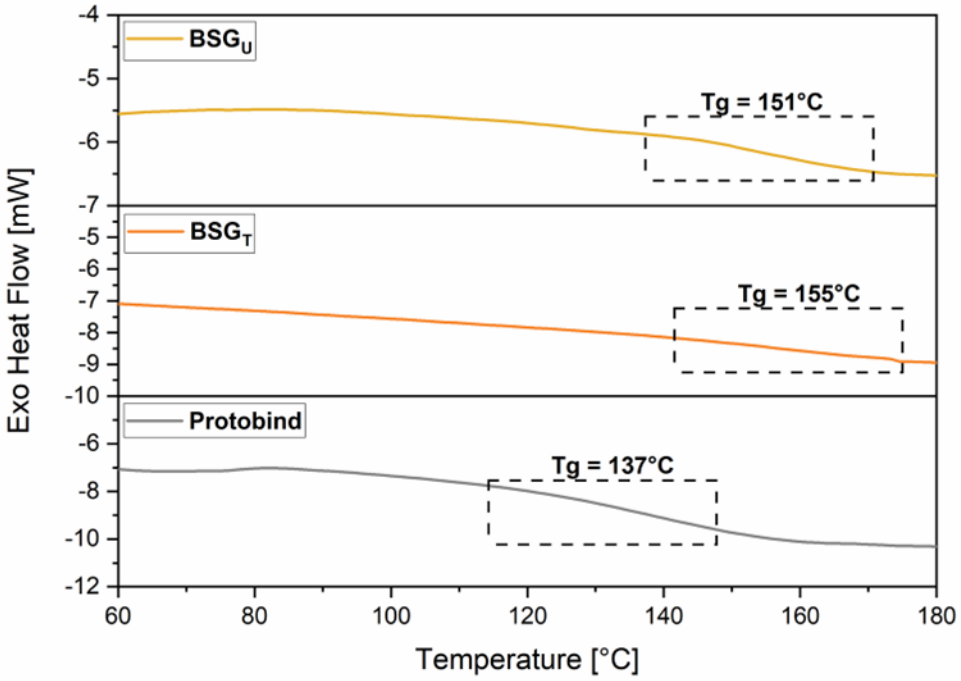

Figure 8: DSC curves of BSG_U Lignin, BSG_T Lignin, and Protobind 1000.

3.2.3. Water Reduction in Cement Pastes

Albeit several lignosulfonates are used directly as low-performance cement plasticizers, natural lignins are very interesting as a basis for the development of sustainable superplasticizers through different types of derivatization. These include, among others, oxidation,[33] sulfomethylation,[42] and grafting with various polymers such as PEG,[59] acrylates,[60] and sulphanilic acid-phenol-formaldehyde condensates.[61] Although lignosulfonates typically demonstrate better water reduction properties than natural lignins, the latter have been successfully adopted in several studies as a starting point in the development of experimental high-performance plasticizers for cement, both with a specific sulfonation step[34] and without sulfonation at all.[33] The use of DES fractionation methods results in the production of an underivatized lignin that is comparable to lignins obtained with mild lignocellulosic fractionation methods such as the organosolv or soda processes. The obtained water reduction capabilities of BSG_T Lignin, BSG_U Lignin, and Protobind (Section 2.9) are reported in Figure 9.

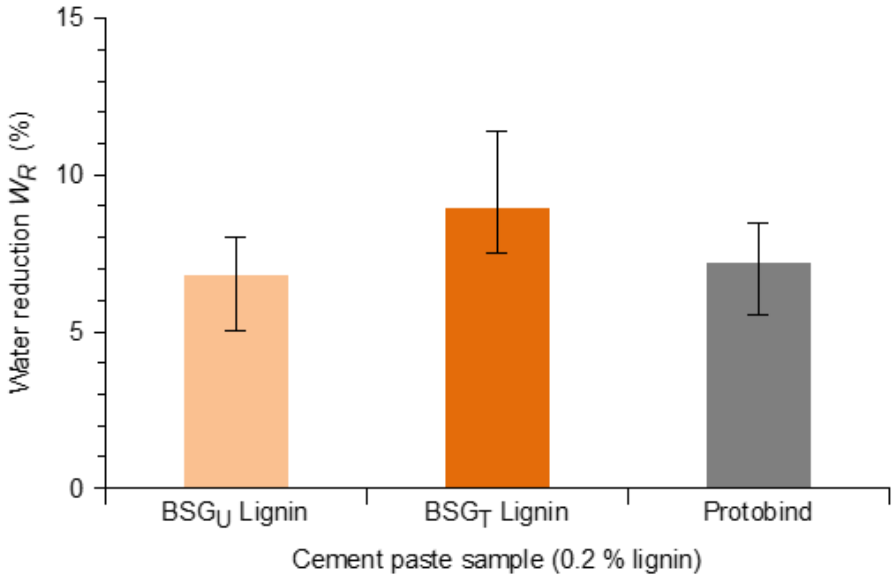

Figure 9: Measured water reduction capability for cement pastes containing 0.2% BSG$_U$ Lignin, BSG$_T$ Lignin, and Protobind. Error bars show confidence interval (95%) of the inverse linear regression.

The measurements were carried out using cement pastes (blends of water and cement powder) that are a quite simpler system in comparison with concrete (blends of water, cement powder, sand, and aggregates) or even mortars (blends of water, cement powder, and sand). This allowed performing the required tests with very low sample volume (about 100 mL) and thus with very little quantity of lignin. The applied procedure allows direct measurement of the water reduction capability of each lignin, keeping constant a specific rheological parameter (the Bingham dynamic yield torque, which estimates the minimum torque needed to maintain an established flow in the given experimental conditions), and it was thus considered a good indication of the potential performance of the lignins in the final system (concrete). The measurements demonstrate a fairly comparable water reduction capability for the BSG$_T$ and the BSG$_U$ Lignins. Moreover, both lignins demonstrate a water reduction capability substantially equivalent to the commercial soda lignin Protobind. This is a good indication that the proposed process, and more generally the DES based fractionation process, is capable of producing a lignin with water reduction capability comparable to a typical industrial soda lignin. Moreover, BSG$_T$ Lignin demonstrated a quite high content of carboxylic and aromatic hydroxylic residues that are exploitable in several derivatization methods. These results suggest that the lignin obtained in the described process is suitable to constitute the basis for the development of a high-performance, sustainable lignin-based water reducer for the production of concrete.

4. Conclusions

In this work, we described in detail a process (reported in Figure 2), which started from wet BSG recovered from a regional brewery and ended with the production of different compounds of industrial interest. Overall, the presented research reports on the almost complete transformation and exploitation of the starting BSG waste. A comprehensive approach combining biomass hot water treatment with successive deep eutectic solvent-

mediated fractionation was developed in order to maximize the process versatility. The upstream phase, which provided an aqueous solution called BSG medium, allowed us to exploit the soluble moiety (which accounted ≈ 35%, w/w) composed of proteins and soluble sugars, as a fermentation medium with high yields of different microorganisms leading to the production of linear and branched chains fatty acids. The solid outcome of the upstream phase underwent fractionation mediated by deep eutectic solvents. A subsequent precipitation firstly with ethanol and then with water provided two main products, BSG_T Cellulose and a BSG_T Lignin, with a final yield of 30% and 10%, respectively. This lignin has been fully characterized in terms of its chemical, physical, thermal, and structural properties. Moreover, BSG_T Lignin has then been tested as water reducer in cement paste with comparable results to technical commercial soda lignin, indicating that it can constitute a good basis for the development of sustainable water reducers for concrete. Overall, our study proposed an integrated multistep fractionation process that could enhance the perspectives of recyclability of BSG. Accordingly, around 75-80% of the mass of the latter important agrifood waste is transformed into high-value-added products of industrial relevance. These results, even in their preliminary form, fulfill the principles of circular economy and give new insights in the field of the biotransformation of agrifood wastes.

Supplementary Materials

The following supporting information can be downloaded at: https://www.mdpi.com/article/10.3390/fermentation8040151/s1, Figure S1. ^{1}H NMR spectrum of DES choline chloride/L-lactic acid (1:5 mol/mol); Figure S2. ^{1}H NMR spectrum of DES choline chloride/L-lactic acid (1:5 mol/mol) after recycling; Figure S3. Calibration curve a for glucose quantification registered in H_2O; Figure S4. Calibration curve b for glucose quantification registered in DMSO; Figure S5. Calibration curve of Folin–Ciocalteu phenol titration with vanillin.

References

1. Zhang, Y.; Zhu, L.; Wu, G.; Wang, X.; Jin, Q.; Qi, X.; Zhang, H., Design of amino-functionalized hollow mesoporous silica cube for enzyme immobilization and its application in synthesis of phosphatidylserine. *Colloids and Surfaces B: Biointerfaces* **2021,** *202*, 111668.
2. Mussatto, S. I.; Dragone, G.; Roberto, I. C., Brewers' spent grain: generation, characteristics and potential applications. *Journal of cereal science* **2006,** *43* (1), 1-14.
3. Kerby, C.; Vriesekoop, F., An overview of the utilisation of brewery by-products as generated by british craft breweries. *Beverages* **2017,** *3* (2), 24.
4. Thomas, K.; Rahman, P., Brewery wastes. Strategies for sustainability. A review. *Aspects of Applied Biology* **2006,** *80*.
5. Buffington, J., The economic potential of brewer's spent grain (BSG) as a biomass feedstock. *Advances in Chemical Engineering and Science* **2014,** *2014*.
6. Aliyu, S.; Bala, M., Brewer's spent grain: A review of its potentials and applications. *African Journal of Biotechnology* **2011,** *10* (3), 324-331.
7. Robertson, J. A.; I'Anson, K. J.; Treimo, J.; Faulds, C. B.; Brocklehurst, T. F.; Eijsink, V. G.; Waldron, K. W., Profiling brewers' spent grain for composition and microbial ecology at the site of production. *LWT-Food Science and Technology* **2010,** *43* (6), 890-896.
8. Wen, C.; Zhang, J.; Duan, Y.; Zhang, H.; Ma, H., A mini-review on brewer's spent grain protein: isolation, physicochemical properties, application of protein, and functional properties of hydrolysates. *Journal of food science* **2019,** *84* (12), 3330-3340.

9. He, Y.; Kuhn, D. D.; Ogejo, J. A.; O'Keefe, S. F.; Fraguas, C. F.; Wiersema, B. D.; Jin, Q.; Yu, D.; Huang, H., Wet fractionation process to produce high protein and high fiber products from brewer's spent grain. *Food and Bioproducts Processing* **2019,** *117*, 266-274.
10. Martínez-Avila, O.; Llenas, L.; Ponsá, S., Sustainable polyhydroxyalkanoates production via solid-state fermentation: Influence of the operational parameters and scaling up of the process. *Food and Bioproducts Processing* **2022,** *132*, 13-22.
11. de Crane d'Heysselaer, S.; Bockstal, L.; Jacquet, N.; Schmetz, Q.; Richel, A., Potential for the valorisation of brewer's spent grains: A case study for the sequential extraction of saccharides and lignin. *Waste Manag Res* **2022,** *40* (7), 1007-1014.
12. Outeirino, D.; Costa-Trigo, I.; de Souza Oliveira, R. P.; Guerra, N. P.; Domínguez, J. M., A novel approach to the biorefinery of brewery spent grain. *Process Biochemistry* **2019,** *85*, 135-142.
13. Parchami, M.; Ferreira, J.; Taherzadeh, M., Brewing process development by integration of edible filamentous fungi to upgrade the quality of Brewer's spent grain (BSG). *BioResources* **2021,** *16* (1), 1686.
14. Dursun, D.; Koulouris, A.; Dalgıç, A. C., Process simulation and techno economic analysis of astaxanthin production from agro-industrial wastes. *Waste and Biomass Valorization* **2020,** *11*, 943-954.
15. Caporusso, A.; Capece, A.; De Bari, I., Oleaginous yeasts as cell factories for the sustainable production of microbial lipids by the valorization of agri-food wastes. *Fermentation* **2021,** *7* (2), 50.
16. Gillet, S.; Aguedo, M.; Petitjean, L.; Morais, A.; da Costa Lopes, A.; Łukasik, R.; Anastas, P., Lignin transformations for high value applications: towards targeted modifications using green chemistry. *Green Chemistry* **2017,** *19* (18), 4200-4233.
17. Collins, M. N.; Nechifor, M.; Tanasă, F.; Zănoagă, M.; McLoughlin, A.; Stróżyk, M. A.; Culebras, M.; Teacă, C.-A., Valorization of lignin in polymer and composite systems for advanced engineering applications–a review. *International journal of biological macromolecules* **2019,** *131*, 828-849.
18. Tribot, A.; Amer, G.; Alio, M. A.; de Baynast, H.; Delattre, C.; Pons, A.; Mathias, J.-D.; Callois, J.-M.; Vial, C.; Michaud, P., Wood-lignin: Supply, extraction processes and use as bio-based material. *European Polymer Journal* **2019,** *112*, 228-240.
19. Iravani, S.; Varma, R. S., Greener synthesis of lignin nanoparticles and their applications. *Green Chemistry* **2020,** *22* (3), 612-636.
20. De Baynast, H.; Tribot, A.; Niez, B.; Audonnet, F.; Badel, E.; Cesar, G.; Dussap, C.-G.; Gastaldi, E.; Massacrier, L.; Michaud, P., Effects of Kraft lignin and corn cob agro-residue on the properties of injected-moulded biocomposites. *Industrial Crops and Products* **2022,** *177*, 114421.
21. Moreno, A.; Sipponen, M. H., Lignin-based smart materials: a roadmap to processing and synthesis for current and future applications. *Materials Horizons* **2020,** *7* (9), 2237-2257.
22. de Haro, J. C.; Allegretti, C.; Smit, A. T.; Turri, S.; D'Arrigo, P.; Griffini, G., Biobased polyurethane coatings with high biomass content: tailored properties by lignin selection. *ACS Sustainable Chemistry & Engineering* **2019,** *7* (13), 11700-11711.
23. Garcia Gonzalez, M. N.; Levi, M.; Turri, S.; Griffini, G., Lignin nanoparticles by ultrasonication and their incorporation in waterborne polymer nanocomposites. *Journal of Applied Polymer Science* **2017,** *134* (38), 45318.
24. Carlos de Haro, J.; Magagnin, L.; Turri, S.; Griffini, G., Lignin-based anticorrosion coatings for the protection of aluminum surfaces. *ACS Sustainable Chemistry & Engineering* **2019,** *7* (6), 6213-6222.
25. Trano, S.; Corsini, F.; Pascuzzi, G.; Giove, E.; Fagiolari, L.; Amici, J.; Francia, C.; Turri, S.; Bodoardo, S.; Griffini, G., Lignin as polymer electrolyte precursor for stable and sustainable potassium batteries. *ChemSusChem* **2022,** *15* (12), e202200294.
26. Chen, W.-J.; Zhao, C.-X.; Li, B.-Q.; Yuan, T.-Q.; Zhang, Q., Lignin-derived materials and their applications in rechargeable batteries. *Green Chemistry* **2022,** *24* (2), 565-584.
27. Budnyak, T. M.; Slabon, A.; Sipponen, M. H., Lignin–inorganic interfaces: Chemistry and applications from adsorbents to catalysts and energy storage materials. *ChemSusChem* **2020,** *13* (17), 4344-4355.
28. de Haro, J. C.; Tatsi, E.; Fagiolari, L.; Bonomo, M.; Barolo, C.; Turri, S.; Bella, F.; Griffini, G., Lignin-based polymer electrolyte membranes for sustainable aqueous dye-sensitized solar cells. *ACS Sustainable Chemistry & Engineering* **2021,** *9* (25), 8550-8560.
29. Edmeades, R. M.; Hewlett, P. C., Cement admixtures. In *Lea's chemistry of cement and concrete*, Elsevier: 1998; pp 841-905.
30. Lou, H.; Lai, H.; Wang, M.; Pang, Y.; Yang, D.; Qiu, X.; Wang, B.; Zhang, H., Preparation of lignin-based superplasticizer by graft sulfonation and investigation of the dispersive performance and mechanism in a cementitious system. *Industrial & Engineering Chemistry Research* **2013,** *52* (46), 16101-16109.

31. Zheng, T.; Zheng, D.; Qiu, X.; Yang, D.; Fan, L.; Zheng, J., A novel branched claw-shape lignin-based polycarboxylate superplasticizer: Preparation, performance and mechanism. *Cement and Concrete Research* **2019,** *119*, 89-101.
32. Gupta, C.; Nadelman, E.; Washburn, N. R.; Kurtis, K. E., Lignopolymer superplasticizers for low-CO2 cements. *ACS Sustainable Chemistry & Engineering* **2017,** *5* (5), 4041-4049.
33. Kalliola, A.; Vehmas, T.; Liitiä, T.; Tamminen, T., Alkali-O2 oxidized lignin–A bio-based concrete plasticizer. *Industrial Crops and Products* **2015,** *74*, 150-157.
34. Li, S.; Li, Z.; Zhang, Y.; Liu, C.; Yu, G.; Li, B.; Mu, X.; Peng, H., Preparation of Concrete Water Reducer via Fractionation and Modification of Lignin Extracted from Pine Wood by Formic Acid. *ACS Sustainable Chemistry & Engineering* **2017,** *5* (5), 4214-4222.
35. Allegretti, C.; Boumezgane, O.; Rossato, L.; Strini, A.; Troquet, J.; Turri, S.; Griffini, G.; D'Arrigo, P., Tuning lignin characteristics by fractionation: A versatile approach based on solvent extraction and membrane-assisted ultrafiltration. *Molecules* **2020,** *25* (12), 2893.
36. D'Arrigo, P.; Allegretti, C.; Tamborini, S.; Formantici, C.; Galante, Y.; Pollegioni, L.; Mele, A., Single-batch, homogeneous phase depolymerization of cellulose catalyzed by a monocomponent endocellulase in ionic liquid [BMIM][Cl]. *Journal of Molecular Catalysis B: Enzymatic* **2014,** *106*, 76-80.
37. Allegretti, C.; Fontanay, S.; Rischka, K.; Strini, A.; Troquet, J.; Turri, S.; Griffini, G.; D'Arrigo, P., Two-step fractionation of a model technical lignin by combined organic solvent extraction and membrane ultrafiltration. *ACS omega* **2019,** *4* (3), 4615-4626.
38. Haist, M.; Link, J.; Nicia, D.; Leinitz, S.; Baumert, C.; von Bronk, T.; Cotardo, D.; Eslami Pirharati, M.; Fataei, S.; Garrecht, H., Interlaboratory study on rheological properties of cement pastes and reference substances: comparability of measurements performed with different rheometers and measurement geometries. *Materials and Structures* **2020,** *53*, 1-26.
39. Johnson, E. A., Phaffia rhodozyma: colorful odyssey. *International Microbiology* **2003,** *6*, 169-174.
40. Zhang, C.; Chen, X.; Too, H.-P., Microbial astaxanthin biosynthesis: recent achievements, challenges, and commercialization outlook. *Applied microbiology and biotechnology* **2020,** *104* (13), 5725-5737.
41. Stachowiak, B.; Szulc, P., Astaxanthin for the food industry. *Molecules* **2021,** *26* (9), 2666.
42. He, W.; Fatehi, P., Preparation of sulfomethylated softwood kraft lignin as a dispersant for cement admixture. *Rsc Advances* **2015,** *5* (58), 47031-47039.
43. Huang, C.; Chen, X.-f.; Xiong, L.; Ma, L.-l.; Chen, Y., Single cell oil production from low-cost substrates: the possibility and potential of its industrialization. *Biotechnology advances* **2013,** *31* (2), 129-139.
44. Qadeer, S.; Khalid, A.; Mahmood, S.; Anjum, M.; Ahmad, Z., Utilizing oleaginous bacteria and fungi for cleaner energy production. *Journal of Cleaner Production* **2017,** *168*, 917-928.
45. EFSA Panel on Nutrition, N. F.; Allergens, F.; Turck, D.; Castenmiller, J.; de Henauw, S.; Hirsch-Ernst, K. I.; Kearney, J.; Maciuk, A.; Mangelsdorf, I.; McArdle, H. J.; Naska, A., Safety of Yarrowia lipolytica yeast biomass as a novel food pursuant to Regulation (EU) 2015/2283. *EFSA journal* **2019,** *17* (2), e05594.
46. Wei, Y.; Siewers, V.; Nielsen, J., Cocoa butter-like lipid production ability of non-oleaginous and oleaginous yeasts under nitrogen-limited culture conditions. *Applied microbiology and biotechnology* **2017,** *101*, 3577-3585.
47. Cho, H. U.; Park, J. M., Biodiesel production by various oleaginous microorganisms from organic wastes. *Bioresource technology* **2018,** *256*, 502-508.
48. Yi, J. S.; Yoo, H.-W.; Kim, E.-J.; Yang, Y.-H.; Kim, B.-G., Engineering Streptomyces coelicolor for production of monomethyl branched chain fatty acids. *Journal of biotechnology* **2020,** *307*, 69-76.
49. Ran-Ressler, R. R.; Khailova, L.; Arganbright, K. M.; Adkins-Rieck, C. K.; Jouni, Z. E.; Koren, O.; Ley, R. E.; Brenna, J. T.; Dvorak, B., Branched chain fatty acids reduce the incidence of necrotizing enterocolitis and alter gastrointestinal microbial ecology in a neonatal rat model. *PloS one* **2011,** *6* (12), e29032.
50. Wang, X.; Xiaohan, W.; Chen, Y.; Jin, W.; Jin, Q.; Wang, X., Enrichment of branched chain fatty acids from lanolin via urea complexation for infant formula use. *Lwt* **2020,** *117*, 108627.
51. Wang, W.; Lee, D.-J., Lignocellulosic biomass pretreatment by deep eutectic solvents on lignin extraction and saccharification enhancement: A review. *Bioresource technology* **2021,** *339*, 125587.
52. Procentese, A.; Raganati, F.; Olivieri, G.; Russo, M. E.; Rehmann, L.; Marzocchella, A., Deep eutectic solvents pretreatment of agro-industrial food waste. *Biotechnology for biofuels* **2018,** *11*, 1-12.

53. Taherzadeh, M. J.; Karimi, K., Pretreatment of lignocellulosic wastes to improve ethanol and biogas production: a review. *International journal of molecular sciences* **2008,** *9* (9), 1621-1651.
54. Sar, T.; Arifa, V. H.; Hilmy, M. R.; Ferreira, J. A.; Wikandari, R.; Millati, R.; Taherzadeh, M. J., Organosolv pretreatment of oat husk using oxalic acid as an alternative organic acid and its potential applications in biorefinery. *Biomass Conversion and Biorefinery* **2022**, 1-10.
55. Allegretti, C.; Fontanay, S.; Krauke, Y.; Luebbert, M.; Strini, A.; Troquet, J.; Turri, S.; Griffini, G.; D'Arrigo, P., Fractionation of soda pulp lignin in aqueous solvent through membrane-assisted ultrafiltration. *ACS Sustainable Chemistry & Engineering* **2018,** *6* (7), 9056-9064.
56. Faix, O., Fourier transform infrared spectroscopy. In *Methods in lignin chemistry*, Springer: 1992; pp 83-109.
57. Boeriu, C. G.; Bravo, D.; Gosselink, R. J.; van Dam, J. E., Characterisation of structure-dependent functional properties of lignin with infrared spectroscopy. *Industrial crops and products* **2004,** *20* (2), 205-218.
58. Rencoret, J.; Marques, G.; Gutiérrez, A.; Nieto, L.; Jiménez-Barbero, J.; Martínez, Á. T.; del Río, J. C., Isolation and structural characterization of the milled-wood lignin from Paulownia fortunei wood. *Industrial Crops and Products* **2009,** *30* (1), 137-143.
59. Takahashi, S.; Hosoya, S.; Hattori, M.; Morimoto, M.; Uraki, Y.; Yamada, T., Performance of softwood soda-anthraquinone lignin–polyethylene glycol derivatives as water-reducing admixture for concrete. *Journal of Wood Chemistry and Technology* **2015,** *35* (5), 348-354.
60. Childs, C. M.; Perkins, K. M.; Menon, A.; Washburn, N. R., Interplay of anionic functionality in polymer-grafted lignin superplasticizers for portland cement. *Industrial & Engineering Chemistry Research* **2019,** *58* (43), 19760-19766.
61. Ji, D.; Luo, Z.; He, M.; Shi, Y.; Gu, X., Effect of both grafting and blending modifications on the performance of lignosulphonate-modified sulphanilic acid–phenol–formaldehyde condensates. *Cement and Concrete Research* **2012,** *42* (9), 1199-1206.

Chapter 4

Fractionation of Raw and Parboiled Rice Husks with Deep Eutectic Solvents and Characterization of the Extracted Lignins towards a Circular Economy Perspective

Chiara Allegretti,[a] Emanuela Bellinetto, [a] Paola D'Arrigo,[*,a,b] Monica Ferro, [a] Gianmarco Griffini, [a] Letizia A. M. Rossato, [a] Eleonora Ruffini, [a] Luca Schiavi, [c] Stefano Serra,[*,b] Alberto Strini [c] and Stefano Turri [a]

[a] Department of Chemistry, Materials and Chemical Engineering "Giulio Natta", Politecnico di Milano, p.zza L. da Vinci 32, 20133 Milano, Italy.

[b] Istituto di Scienze e Tecnologie Chimiche "Giulio Natta", Consiglio Nazionale delle Ricerche (SCITEC-CNR), Via Luigi Mancinelli 7, 20131 Milano, Italy.

[c] Istituto per le Tecnologie della Costruzione, Consiglio Nazionale delle Ricerche (ITC-CNR), Via Lombardia 49, 20098 San Giuliano Milanese, Italy.

The authors are listed in alphabetical order.

Published on *Molecules* **2022**, 27(24), 8879

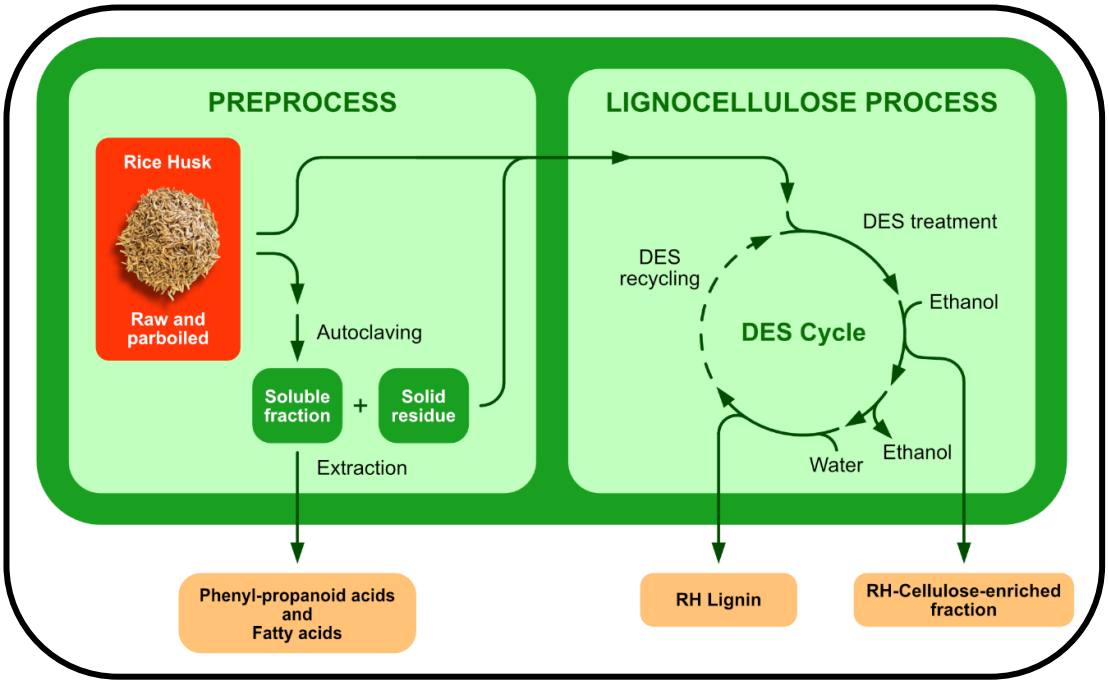

Abstract

In the present work, rice husks (RHs), which, worldwide, represent one of the most abundant agricultural wastes in terms of their quantity, have been treated and fractionated in order to allow for their complete valorization. RHs coming from the raw and parboiled rice production have been submitted at first to a hydrothermal pretreatment followed by a deep eutectic solvent fractionation, allowing for the separation of the different components by means of an environmentally friendly process. The lignins obtained from raw and parboiled RHs have been thoroughly characterized and showed similar physico-chemical characteristics, indicating that the parboiling process does not introduce obvious lignin alterations. In addition, a preliminary evaluation of the potentiality of such lignin fractions as precursors of cement water reducers has provided encouraging results. A fermentation-based optional preprocess has also been investigated. However, both raw and parboiled RHs demonstrated a poor performance as a microbiological growth substrate, even in submerged fermentation using cellulose-degrading fungi. The described methodology ap-pears to be a promising strategy for the valorization of these important waste biomasses coming from the rice industry towards a circular economy perspective.

1. Introduction

Rice (*Oriza sativa*) is one of the most important food crops, with about 755 million tons of rough rice (also known as paddy rice) produced worldwide in 2019[1] and a >25% production increase in the 2000-2020 timeframe.[2] Its importance is undoubtedly established when it is taken into account that it feeds around three billion people all over the world.

Raw rice is composed by an external hull and the brown rice grain, which are separated during the dehusking process. Rice husks (or hull, RH), deriving from paddy rice dehusking, represent a very important source of waste biomass and are one of the most abundant by-products in the rice production line. Considering that ca. 20-25% of paddy rice mass is constituted by the outer husk,[3] it is possible to estimate a global annual rice husk production of >150 million tons, currently used mainly for power generation.[4]

Parboiled (partially boiled) rice is obtained from rough rice by a hydrothermal process constituted by a hydration stage followed by gelatinization and drying. Because of its several nutritional and physical benefits, parboiled rice possesses between two and three times the economic value of white rice and its importance on the global market is currently increasing (about 20% of the produced rice is treated by the parboiling process at the present time).[5] The parboiling process is carried out mainly on rough rice that then must undergo the hulling process, thus leading to the parboiled rice husk as a by-product. As a consequence, this latter constitutes a significant part of the global rice husk production with solid forecasts of a high growth in the coming years.[6]

For these reasons, the exploitation of both a raw rice husk (rRH) and parboiled rice husk (pRH) as lignocellulosic renewable feedstock constitutes a very important objective in a circular economy perspective, where the valorization of bio-agricultural wastes as a secondary raw material is largely preferable to their incineration for heat generation. Globally, this is particularly important in Asian countries where a rice cultivation is the primary food source and, regionally, in local realities where rice is a traditional source (e.g., in Lombardy in Italy). Up to now, RHs are instead mainly exploited as an energy

source in rice processing plants and as bedding for farm animals. Therefore, the availability of this huge quantity of wastes and their low cost have pushed the current research towards the investigation and development of new sustainable possible applications for such materials.

Deep eutectic solvents (DESs) are a promising class of new solvents in the context of sustainable process development that can be prepared from a broad range of components, which are often from biobased sources.[7] DESs are characterized by a low toxicity and the typically high renewability and recyclability of the constituents.[8] Their wide solvating power modulation capabilities make them a first-choice medium for setting up separation processes, with particular reference to the fractionation of agro-industrial lignocellulosic wastes.[9-11] Moreover, it is even more interesting that the potential use of reactive DESs (RDESs)[12-13] could allow for the exploitation of the same DES formulation as a separation medium (for lignocellulosic fractionation) and reaction medium (for lignin derivatization), even possibly in one-pot processes, enhancing the sustainability of the process.[14]

Thus, we have focused on the set-up of a cascade multistep process, reported in Figure 1, composed of a preprocess in hot water and in an autoclave, followed by a DES-mediated treatment of the rRH and pRH biomasses, in order to deconstruct the natural lignocellulosic skeleton that usually hampers the further exploitation of the different components of RHs. The fractionation of these waste materials in two main fractions, i.e., a cellulose-enriched fraction and lignin constitutes the key-point for the successive development of valuable applications. The methodology based on the DES treatment was previously successfully applied by the authors to another common agri-food biomass, i.e., Brewer's Spent Grain (BSG).[15] The main aim of the present work is to study the DES-mediated fractionation process focusing on RHs, and to compare and characterize in detail both the composition and properties of the lignin fractions recovered from rRH and pRH. The latter is particularly interesting because of its aforementioned increase in commercial interest. Indeed, such a detailed characterization should represent a strategic milestone for the successful incorporation of lignin, as a macromolecular precursor, into bio-based polymers of a high added value,[16-18] which have found an application in a variety of industrial[19-22] and technological[23-28] fields.

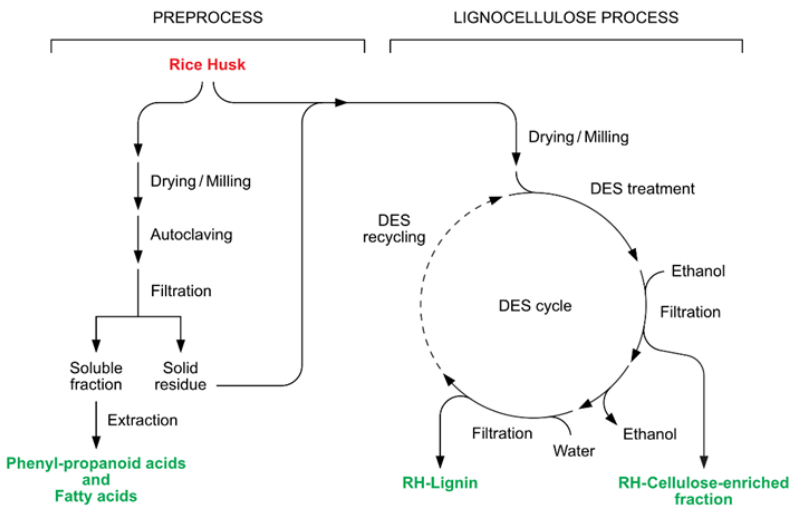

Figure 1: Complete fractionation process of raw and parboiled rice husks constituted by a hydro-thermal preprocess and a DES-mediated lignocellulose process.

Moreover, in this work, the potentialities of these materials were also demonstrated in the field of cement water reducers, the latter being an important component of all modern concrete formulations. Lignin is a well-known component of traditional water reducers and has been widely used for this purpose for a long time.[29] In recent years, several research efforts aimed at the study of renewable high-performance water reducers inspired a renewed interest in advanced formulations based on lignin derivatives.[30-32] Any process resulting in lignin as a by-product is thus a potential resource for the development of sustainable concrete water reducers. For such reasons, the obtained lignins were here assessed for this specific application by rheological measurements on cement pastes. The results clearly indicate a water reducing performance equivalent to that of a commercial soda lignin (Protobind 1000), thus demonstrating the potential of the approach proposed herein.
A fermentation-based pretreatment was also studied, aiming to pretreat the biomass before the fractionation steps. The rationale behind this approach was to verify whether the soluble saccharides components of RHs could be exploitable as substrates in industrial fermentation processes. The expected effect of the pretreatment was the partial deconstruction of the lignocellulose matrix with the reduction in the saccharides' content. However, the limited results obtained indicated that both raw and parboiled RHs are poor performers as a microbiological growth media, possibly due to their relatively low oligosaccharide and high silica contents.

2. Results and Discussion

In this work, two rice husk waste biomasses were selected from raw and parboiled rice production, respectively (see Section 3.1 for details). The present work aims to fractionate and compare them in terms of the composition and properties with the special aim of providing fundamental information for the exploitation of the different fractions, focusing in particular on the isolated lignins. Moreover, a deep comparison between rRH and pRH has not been presented until now.
The two samples of the starting biomasses employed in the present work are illustrated in Figure 2. As it is evident from the picture, pRH (on the right) appeared to be slightly darker than rRH (on the left). As soon as they were received, these biomasses, even if they have been provided in a quite dried form, were put in a ventilated oven (60 °C for 24 h) and finely ground with an electric mixer.

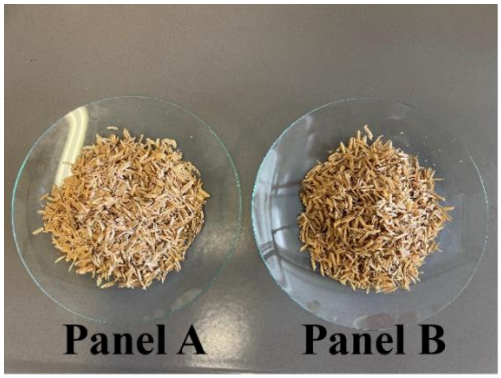

Figure 2: Picture of raw rice husk (Panel A) and parboiled rice husk (Panel B).

2.1. Rice Husks Composition

As most lignocellulosic biomasses, RHs are an intricate material where all the components are closely related to each other. For that reason, in order to separate and quantify the four main constituents of rRH and pRH of this study (hemicellulose, cellulose, silica, and lignin), a multistep process based on a classical method of fractionation by successive water and acid treatments was performed (see Section 3.3 for details).[33] The composition of the presently studied biomasses is reported in Table 1 and appears to be in agreement with those reported in the literature.[34-35]

Table 1: Composition of the studied RHs biomasses.

Sample	Hemicellulose (% *w*/*w*)	Cellulose (% *w*/*w*)	Silica (% *w*/*w*)	Lignin (% *w*/*w*)	Soluble Fraction (% *w*/*w*)
rRH	19.5	43.2	12.9	19.2	5.20
pRH	27.3	36.7	12.4	18.5	5.10

Moreover, the detailed composition, as monosaccharides components, of the isolated hemicellulose fraction (reported in Table 2) has been determined by GC/MS analysis after the total hydrolysis, reduction, and acetylation of the samples following a well-known procedure (see Section 3.3.1 for experimental details).[36] The two main components of RHs hemicellulose were arabinose and xylose, with a low amount of galactose and traces of rhamnose and fucose. The detected glucose residues were probably due to a contamination of the cellulose fraction that appeared to be nearly completely eliminated after the pretreatment of the biomass performed in the fractionation process (the resulting residual glucose was 0.2-0.4%).

Table 2: Relative abundance of the monosaccharides deriving from RHs hemicellulose hydrolysis.

RH	Rhamnose	Fucose	Arabinose	Xylose	Mannose	Glucose	Galactose
rRH	0.4	0.5	49.0	44.9	-	1.2	4.0
pRH	0.2	0.5	22.6	69.2	-	4.9	2.6

2.2. Rice Husks Preprocess

In our previous work, we described an efficient procedure for the water-mediated extraction of Brewer's Spent Grain (BSG).[15] Accordingly, the treatment of BSG with water at a high temperature allowed for the removal of a considerable (25-30% w/w) fraction of this waste material. Hence, we checked the effectiveness of the same procedure when applied to RHs.

2.2.1. Hydro-Thermal Preprocess

We performed a hydro-thermal treatment of rRH and pRH by autoclaving the aqueous suspensions of the latter materials at 121 °C for 20 min. The two suspensions were then filtered, leading to solid residues which were indicated as rRH_T (raw rice husk-treated) and pRH_T (parboiled rice husk-treated), whereas the obtained aqueous extracts were concentrated at a reduced pressure and the weights of the resulting residues were compared to those of the parent RHs samples. We observed that the de-scribed procedure allowed for the extraction of only 2 and 2.8% (w/w) of rRH and of pRH, respectively. This water-mediated extraction gave results comparable with those described in Table 1, proving that rRH and pRH contained a very low amount of soluble sugars. In order to further characterize these soluble fractions, the extracts were further treated with ethyl acetate. The organic solvent soluble fractions were made up of a mixture of fatty acids (≈ 0.05% w/w total biomass) and phenylpropanoid metabolites such as cinnamic acid (≈ 0.74% w/w total biomass) and ferulic acid (0.13% w/w total biomass).

2.2.2. Microbiological Preprocess

As discussed above, the results of the hydro-thermal preprocess have confirmed that both rRH and pRH are waste materials of a very difficult valorization, as they are devoid of water-soluble components such as sugars, starch, or proteins. In addition, the biomass of the RHs was almost unaffected by our thermal treatment. As a consequence, we evaluated whether a biological pretreatment could break up the lignocellulosic structure of the RHs. To this end, we evaluated the potential of some selected fungal strains in the submerged fermentation of the RHs samples. More specifically, we singled out the filamentous fungi *Myceliophthora thermophila*, *Rhizomucor pusillus*, and *Trichoderma viride*. The latter microorganisms have been widely employed in the industry for the production of hydrolytic enzymes such as cellulases, amylases, pectinases, and chitinases.[37-40] In addition, the first two species are thermophiles with two different optimal growth temperatures. Therefore, the fermentation of the three identical samples of pRH with *M. thermophila*, *R. pusillus*, and *T. viride* were performed at 45, 35, and 24 °C, respectively. The pRH biomasses recovered after the fermentation indicated a weight loss of the 18, 19, and 14%, respectively. These results clearly demonstrate that all the tested strains utilized pRH as a carbon source for their growth, regardless of the temperature fermentation. Despite this fact, none of the experiments displayed a weight loss superior to 19%, thus confirming the difficult degradability of RHs, even when using cellulose-degrading fungi. Interestingly, for all the trials, we observed an initial luxuriant growth followed by the transformation of the formed filamentous biomass into a slurry. The microscopic view of the biomasses showed the presence of a very short hypha, most likely deriving by the grinding of the fungal filaments. We supposed that RH, with its high silica content, was not a suitable substrate for a submerged fermentation. The shaking, necessary for oxygenation, damaged the fungal hypha, thus reducing their activity. As a

consequence of the described results, the microbiological preprocessing of this specific waste was considered to be unsuitable and thus excluded from the complete fractionation process depicted in Figure 1.

2.3. DES-Mediated Lignocellulose Process

The subsequent step of the biomass treatment after the previously described pre-process was constituted of a DES-mediated fractionation process. Different DESs have been prepared and tested in this work. They have been obtained by mixing and heating a mixture of the two components: a hydrogen bond acceptor (HBA) such as choline chloride (ChCl) and betaine glycine (BetG), and a hydrogen bond donor (HBD) composed by acetic acid and L-lactic acid. These two HBDs have been selected since it is known that the presence of the carboxylic group in an HBD enhances the lignin yields during the lignocellulosic destructuration.[41-42] The composition and density of the DESs are reported in Table 3. Typically, DESs had a higher density than water and those containing L-lactic acid (DESs 2 and 4) resulted in being denser than those with acetic acid (DESs 1 and 3), likely because of the presence of the hydroxyl group in the HBD molecules, which should allow for the formation of stronger hydrogen bonds.

Table 3: List, composition, and density (measured at 18 °C) of prepared DESs.

DES Number	Composition DES HBA/HBD	Molar Ratio (HBA/HBD)	Density of Pure DES (g/cm^3)
1	Choline chloride/Acetic acid	1/2	1.10
2	Choline chloride/L-Lactic acid	1/5	1.18
3	Betaine Glycine/Acetic acid	1/2	1.11
4	Betaine Glycine/L-Lactic acid	1/5	1.20

Following the scheme of the process reported in Figure 1, dried and finely milled treated biomasses (rRH_T and pRH_T) were submitted to a fractionation. For comparison, the native biomasses (rRH and pRH) were also treated in the same way. The biomasses were then suspended in the different DESs at 120 °C under magnetic stirring for 24 h. After cooling, ethanol was gradually added, leading to the precipitation of the first fractions, the cellulose-enriched fractions, which were then further separated in order to quantify the silica content. To this end, we slightly modified the Yoshida procedure,[43] consisting in the oxidative degradation of all the organic fractions (see Section 3.5.3 for details). The cellulose-enriched fractions were heated at a reflux with a mixture of concentrated nitric acid, sulfuric acid, and perchloric acid, and the resulting silica suspensions allowed for the isolation of the silica samples. Their weights were employed to calculate the silica content of the cellulose-enriched fractions (given as a w/w biomass percentage and reported in Figure 3). The silica content was quantified at around 13%, almost identical in all the samples, confirming that the treatments performed on the RHs did not affect their SiO_2 content.

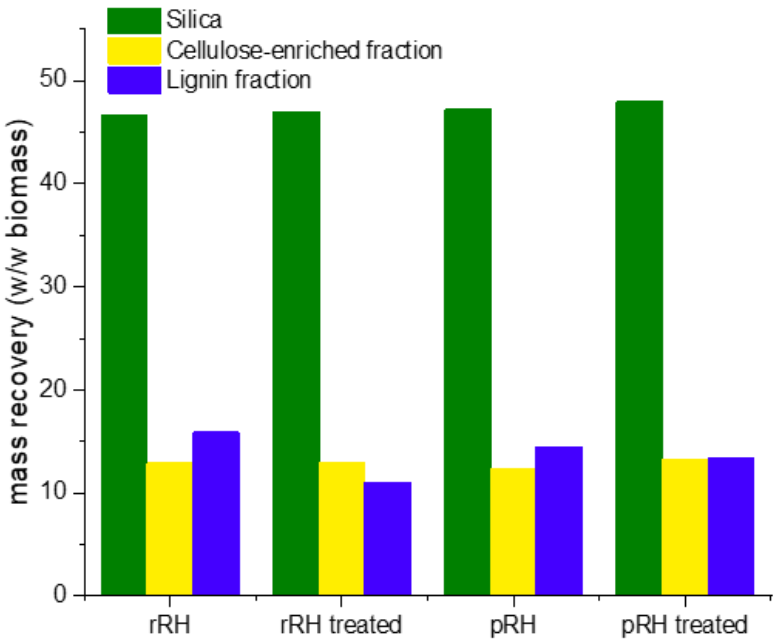

Figure 3: Data of mass recovery of cellulose-enriched fraction (in green), lignin (in yellow), and silica (in blue) during the DES 2-mediated fractionation process of raw rice husk (rRH), raw treated rice husk, parboiled rice husk (pRH), and parboiled treated rice husk.

The filtrates were then concentrated to eliminate ethanol and were treated with water acting as an anti-solvent, to induce the precipitation of the lignins. After the centrifugation, filtration, and solvent evaporation, the final solid fractions (rRH-Lignin, rRH_T-Lignin, pRH-Lignin, and pRH_T-Lignin) were recovered and quantified.
After the examination of the results obtained with the four DESs in terms of the handling of the reaction mixtures and the final mass recovery, DES 2 (choline chloride/L-lactic acid, 1/5) was selected for this work, since it gave the higher yields in terms of the fractions recovery and lignin recovery. The data of the quantitative recovery of the different fractions are reported in the Supplementary Materials (Table S1) for all the tested DESs, whereas the mass recovery results obtained on the DES 2-mediated fractions for the four RHs biomasses have been illustrated more precisely in Figure 3.
As it appears clearly from Figure 3, the weight percentages of the three fractions were almost identical for the four fractionated RHs. The cellulose-enriched fraction accounted for 47% of the total biomass in the three cases, lignin for 15.8 to 11% (for rRH and rRH_T) and to 14.5 to 15.5% (for pRH and pRH_T), and silica at around 13% in all cases. The results clearly prove that both the parboiling process and the autoclave treatment do not influence so much the percentages of the three main fractions and do not induce substantial differences in the natural biomass fractionation.

2.4. Lignin Characterization

Lignins derived from the complete fractionation process (using DES 2) of both raw and parboiled rice husks (rRH-Lignin and pRH-Lignin, respectively) were subjected to an extensive characterization to evaluate their properties and potential differences. A well-known commercial soda lignin (Protobind 1000, indicated from now on as Protobind) was used as the reference.[44]

2.4.1. Solvent Solubilization

One of the key features in the lignin's characterization and valorization is represented by the solubilization studies, which can afford the starting point in the set-up of the best conditions for lignin processing. In fact, it should be stressed that one of the main issues concerning lignin exploitation is its low solubility in the most frequently used organic solvents. In this work, the solubilization screening has been performed in six organic solvents and in water. The selected solvents have been: tert-butyl methyl ether (MTBE), n-butyl acetate (BuOAc), ethyl acetate (EtOAc), 2-butanone (MEK), methanol (MeOH), and tetrahydrofuran (THF). Figure 4 shows the obtained extraction yields for rRH- (in pale yellow), rRH_T- (in dark yellow), pRH- (in orange), pRH_T-Lignins (in brown), and Protobind (in grey) for comparison, as a w/w percentage of the solubilized lignin vs. total lignin.

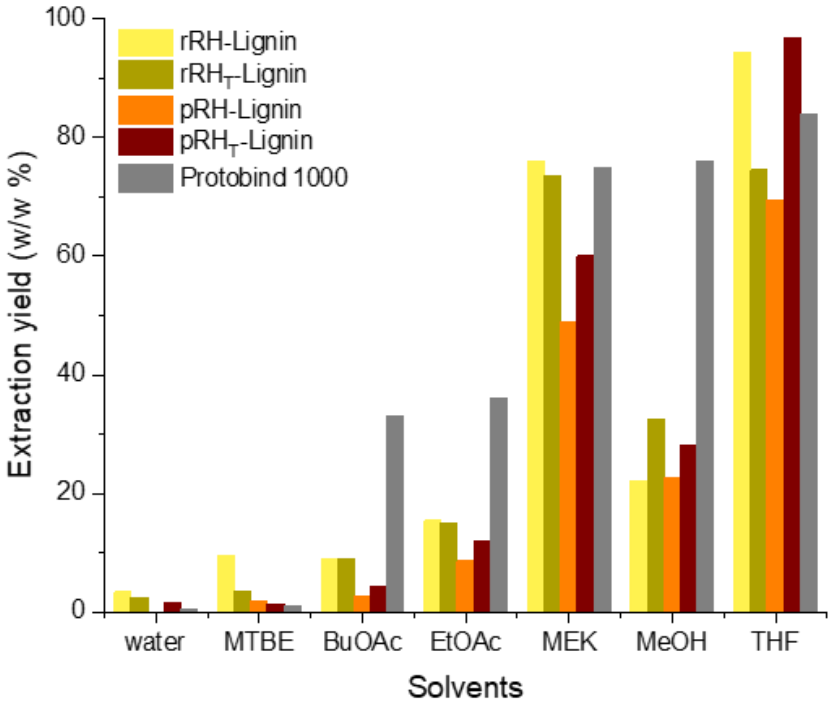

Figure 4: Extraction yield of the commercial technical lignin Protobind (in grey), and the lignins extracted from raw (in pale yellow), raw treated (dark yellow), parboiled (in orange), and parboiled treated (in brown) rice husks. The data are reported as the percentage (w/w) of solubilized fraction vs. total fraction in 6 different organic solvents and water.

As expected, the four RH-lignins are quite insoluble in water, similar to what was observed in the reference material (Protobind). When considering the solubility response to organic solvents, RH-lignins show a substantial similarity in their solubility: a very poor solubility (less than 10% w/w) in MTBE and BuOAc, and a slightly higher solubility in EtOAc and MeOH in a range between 10 and 30% w/w. The best solvents appear to be MEK and THF, as for the reference material (Protobind), where the value of the solubility ranges from 50 up to 99% w/w. It should be noted that the lignins from rRHs seemed to be slightly more soluble in all the solvents, except THF, if compared with the pRHs. Moreover, the solubility of the RH_T-lignins appeared to be higher than the RH-lignins in all the organic solvents (except THF), indicating that the biomass pretreatment could generally positively affect the solubility characteristic of the recovered lignins. This

aspect appears as an interesting outcome and suggests a potential straightforward exploitation of such RH-recovered lignins in line with the similar exploitation routes typical of commercial lignin materials.

2.4.2. Molar Mass Distribution

The evaluation of the molar mass distribution in the lignin recovered fractions is a fundamental tool in order to successfully exploit these biomasses. To that end, GPC analyses were performed to determine the molecular weight and the molecular weight distribution of the extracted lignins. In Table 4, the number average molecular weight (Mn), the weight average molecular weight (Mw), and the polydispersity index (Đ) of all the RH-lignin samples and of the reference lignin Protobind 1000 are reported.

Table 4: Number average molecular weight (Mn), weight average molecular weight (Mw), and polydispersity index (Đ) of all examined lignins (samples were eluted after acetylation; reported values are relative to polystyrene standards).

Sample	M_n (g/mol)	M_w (g/mol)	*Đ*
rRH-Lignin	1380	5330	3.86
rRH_T-Lignin	1360	5195	3.82
pRH-Lignin	1320	3930	2.98
pRH_T-Lignin	1310	3860	2.95
Protobind 1000	830	2800	3.37

The RH-Lignins showed a higher Mn and Mw and a similar Đ, with respect to the Protobind lignin. Especially, in all RH-Lignins, a comparable Mn was observed. In contrast to this, the Mw of both rRH-Lignins was found to be higher compared to both pRH-Lignins, resulting in a higher Đ. No differences were observed between the treated and untreated lignins, indicating that the pretreatment did not affect the molecular weight and the molecular weight distribution of these lignins.
These results are in accordance with what was previously discussed in terms of solubility. Indeed, on average, due to their higher Mn and Mw, RHs-lignins resulted in being slightly less soluble in organic solvents compared to the Protobind lignin.

2.4.3. Sugar Content

The precipitated lignin fractions were washed three times after the water-mediated precipitation from the DES solutions in order to eliminate potential DES residues, which could contaminate the lignins and provide a sticky response of the final products. The sugar quantification, reported in Table 5, was performed with an already established procedure using the bicinchoninic assay method with some modifications.[45-46] Although they were not further purified after the precipitation, all the lignins possessed a very low carbohydrate content similar to the Protobind value; it accounted for less than 0.4% (w/w) of the free reducing sugars. Furthermore, after the hydrolysis, the rRH- and pRH-Lignins showed the presence of a certain quantity of complex sugars (from 5.7 to 9.1%), which was also in this case substantially lower than the Protobind value (13%). However, pRH_T-Lignin exhibited quite the same value as Protobind. This aspect has to be considered in

view of the further applications of these RH-Lignins in the preparation of cement water reducers.

Table 5: Results of the total reducing sugar quantification.

Sample	Reducing Sugars/Biomass (*w*/*w*%)	Reducing Sugars/Biomass after Hydrolysis (*w*/*w*%)
rRH-Lignin	0.19	5.7
rRH_T-Lignin	0.51	9.2
pRH-Lignin	0.31	9.1
pRH_T-Lignin	0.38	14
Protobind 1000	0.34	13

2.4.4. ^{13}C CP-MAS NMR

The solid-state ^{13}C cross-polarization magic angle spinning (CP-MAS) NMR spectroscopy was used to define the fingerprint of each lignin and to highlight the structural differences among the examined samples. Figure 5 shows the superposition of the ^{13}C CP-MAS NMR spectra of the commercial Protobind lignin with the extracted lignin samples. At first, the RHs samples had an almost overlapping profile but clearly differed from the Protobind reference sample (see Figure 5 Panel A). The region between 210 and 190 ppm corresponded to the non-conjugated carbonyl groups C=O of aldehydes. In this range of chemical shifts, there were no substantial differences among the spectra, whereas in the aromatic region (160-100 ppm), Protobind showed a lower signal intensity at 175.7 ppm compared to the other spectra. This indicated a lower presence of both $–CO_2H$ carboxylic and $–CO_2R$ ester groups. In addition, the Protobind spectrum showed another signal which was less intense than the other samples around 115 ppm, which very likely could be attributed to a lower content of the guaiacyl units.

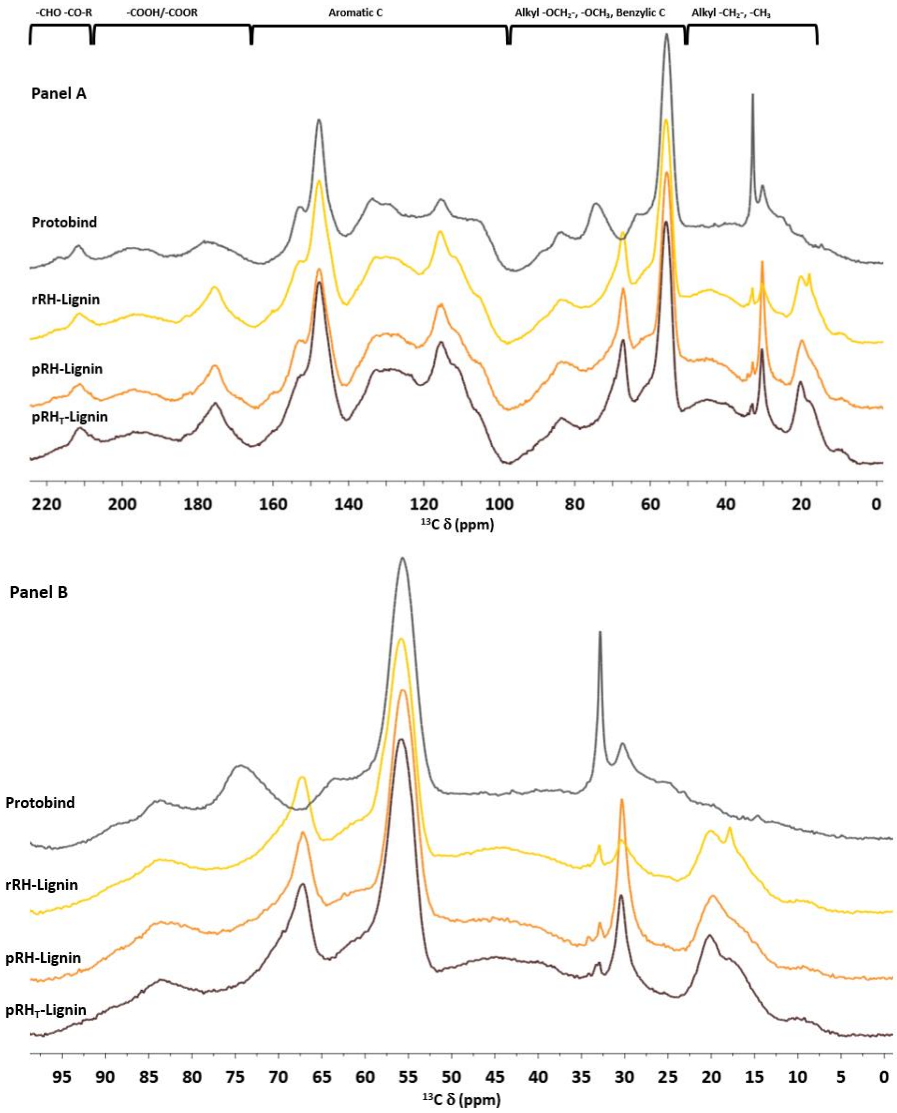

Figure 5: Solid state ^{13}C CP-MAS NMR spectra of Protobind lignin (in grey), rRH-Lignin (in yellow), pRH-Lignin (in orange), pRH_T-Lignin (in brown). (Panel A) the whole spectrum; (Panel B) zoom of 0–100 ppm region.

However, the main spectral differences were between 100 and 0 ppm (Figure 5 in Panel B). Between 65 and 75, Protobind presented two more peaks at 74.5 and 63.7 ppm: peaks in such a region are typical of the β-O-4 structural moiety with the –OH group at the α-position. On the other hand, the extracted lignin samples showed at 67.4 ppm a signal which was not present in the Protobind lignin. This region (62-75 ppm) is diagnostic of β-O-4 structures. In the alkyl part of the spectra, the intensity of the O-CH_3 peak at 55.9 ppm was comparable in all the samples. Lastly, the most significant differences were at around 30 ppm (corresponding to the alkyl CH_2) and around 20 ppm (typical of the methyl groups). This analysis could be a very important tool in order to compare the lignins extracted from different biomasses.

2.4.5. Total Phenolic Content

The total phenolic content was determined in the recovered lignins from RHs using a modified Folin–Ciocalteu (FC) assay (see Section 3.6.5 for details). In this protocol, the samples were initially fully solubilized in DMSO before being incubated with the specific redox reagent (FC reagent). The phenolic content results are summarized in Table 6 as the vanillin equivalents (mmol/g of dry lignin), using the data from Protobind as the reference.

Table 6: Results of the determination of phenolic hydroxyl groups expressed as vanillin equivalents/g of lignin sample. Estimated standard errors ± 0.1 mmol/g vanillin equivalent (1σ, from calibration data).

Sample	Vanillin Equivalent Content (mmol/g)
rRH-Lignin	1.6
rRH_T-Lignin	1.3
pRH-Lignin	1.6
pRH_T-Lignin	1.7
Protobind 1000	3.1

All four lignins from RHs show quite the same content of vanillin equivalents (around 1.3-1.6 mmol/g), which is half the value found in Protobind. In addition, also in this case it appears that the parboiled treatment does not affect the majority of the functionalities of the phenolic lignin.

2.4.6. Hydroxyl Groups Quantification by ^{31}P NMR

The different hydroxyl groups present in the recovered lignins were assessed and identified through high resolution ^{31}P NMR spectroscopy. This technique allows for the quantification of the different hydroxyl groups present in the lignin backbone after derivatization with 2-chloro-4,4,5,5-tetramethyl-1,3,2-dioxaphospholane. The high natural abundance of the ^{31}P nucleus allows us to obtain well-resolved NMR signals.[47-48] Their attribution to the different OH groups in the sample could be performed because the chemical shifts are largely dependent on the surrounding chemical environment of the derivatized hydroxyls. The spectra are reported in Figure 6.

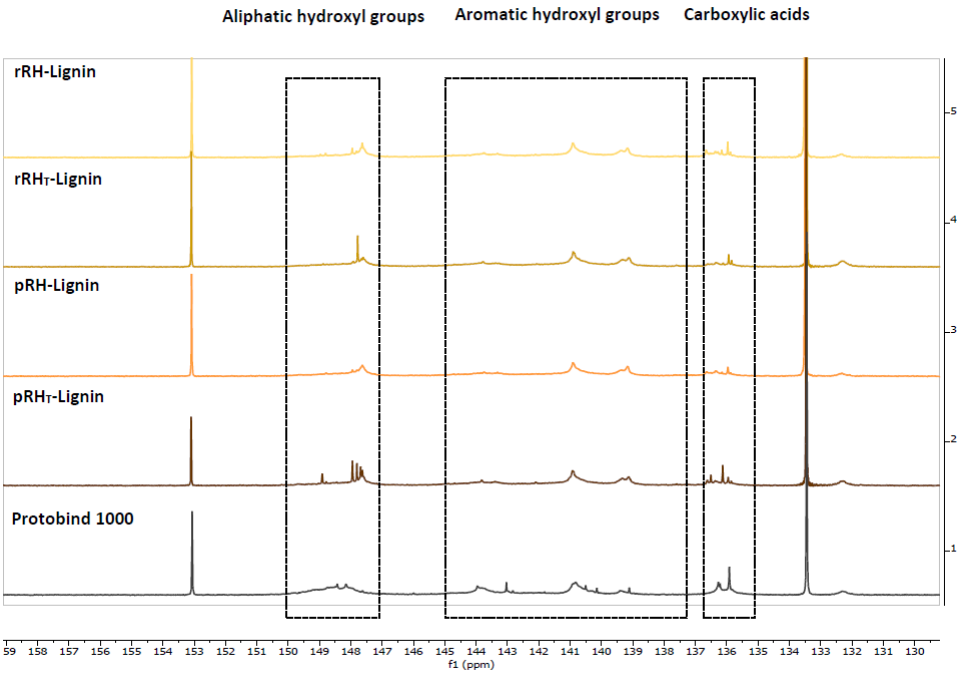

Figure 6: ^{31}P NMR Spectra of isolated Lignins and Protobind as reference.

The signals of the RH-Lignins and Protobind spectra were integrated to differentiate the hydroxyl groups: the signals from 150 to 147 ppm were associated with the aliphatic hydroxyl groups, the signals from 145 to 138 ppm were related to the aromatic hydroxyl groups, and, lastly, the signals centered at 136 ppm were attributed to the carboxylic acid residues. The peak integration of these three chemical shift regions led to the quantification of the total hydroxyl groups expressed in mmol of the functional group per g of dry lignin, as reported in Table 7 below.

Table 7: Detailed hydroxyl/carboxyl quantification by ^{31}P NMR (as mmol of functional group per g of dry lignin).

Sample	–OH Aliphatic (mmol/g)	–OH Aromatic (mmol/g)	–COOH (mmol/g)
rRH-Lignin	2.42	7.12	1.43
rRH$_T$-Lignin	2.48	7.10	1.02
pRH-Lignin	3.01	7.77	1.42
pRH$_T$-Lignin	3.08	7.49	1.36
Protobind 1000	3.00	4.67	1.42

Additionally, in this case, the ^{31}P NMR results showed that the three RH-Lignins had quite the same amount of hydroxyl and carboxyl groups in their composition. In particular, when compared with Protobind, the lignins extracted from RHs appeared to have quite the same quantity of aliphatic OH and carboxylic groups, whereas the main differences were showed in the aromatic hydroxyl groups, which appeared to be one and

a half times higher than in Protobind.

2.4.7. Fourier Transform Infrared Spectroscopy

Fourier transform infrared (FTIR) spectroscopy was carried out to further study the chemical composition of the RH-Lignins. The absorption spectra obtained are shown in Figure 7, where the FTIR spectrum of Protobind is also presented for comparison purposes. In general, no noticeable differences among the recovered lignins could be observed. All the lignin fractions showed a broad absorption band in the region of 3400-3200 cm^{-1}, related to the stretching vibrations of the aliphatic and phenolic OH groups, and the signals in the region of 3050-2800 cm^{-1} were associated with the CH bond stretching in the methyl and methylene groups. The major differences between the RH-Lignins and Protobind lignin were found in the fingerprint region. In particular, while Protobind showed a single signal located at 1710 cm^{-1} attributable to the stretching vibration of C=O in unconjugated ketones, carbonyl, and ester groups, all four RH-Lignins were characterized by an additional peak at 1740 cm^{-1}. This signal was associated with C=O stretching vibrations likely resulting from the presence of different carbohydrate species entrapped in the recovered RH-Lignin fractions, as also evident from Table 5. This result was also confirmed by the signal detectable at 1650 cm^{-1} for such materials, related to conjugated carbonyl/carboxyl stretching in C=O moieties.[49]

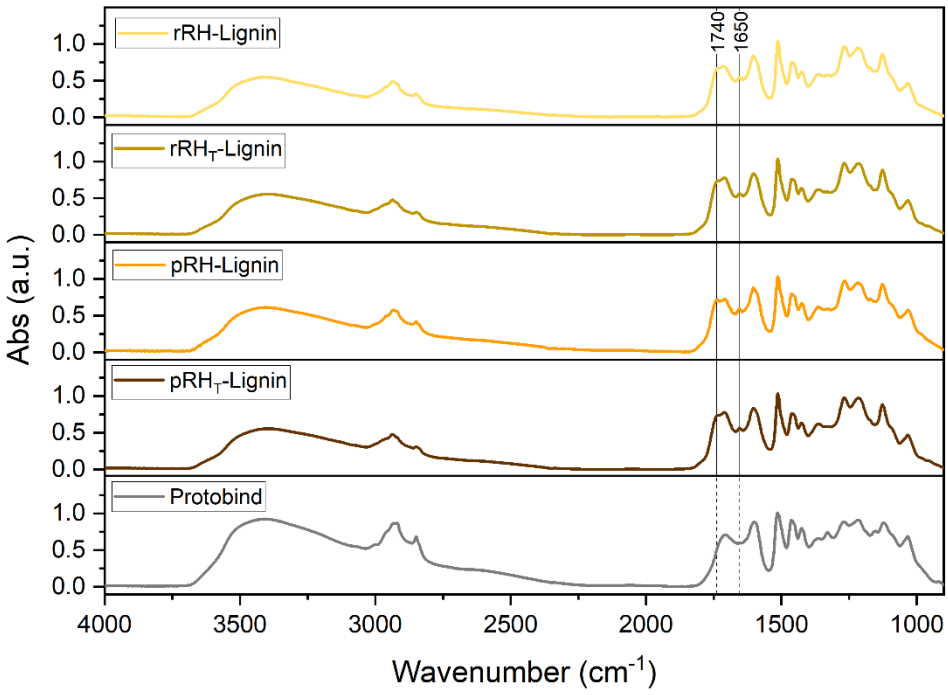

Figure 7: FTIR spectra of rRH-Lignin (in pale yellow), rRH$_T$-Lignin (in dark yellow), pRH-Lignin (in orange), pRH$_T$-Lignin (in brown), and Protobind (in grey).

2.4.8. Thermal Behavior

The glass transition temperatures (Tg) of all the lignin samples were assessed by means of differential scanning calorimetry (DSC). The thermograms reported in Figure 8 showed that the Tg of the recovered RH-Lignins were slightly higher compared to that of the reference lignin material (Protobind). In particular, rRH- and pRH-Lignins were characterized by the same Tg, close to 160 °C. This value was higher compared to the Tg

of the rRH$_T$- and pRH$_T$-Lignin, which instead were detected at around 157 and 149 °C, respectively, meaning that the treatment has slightly affected the molecular structure and thus the macromolecular mobility of such a lignin fraction. The behaviour is perfectly in accordance with the results of both GPC analyses and ^{31}P NMR. Especially, the GPC analyses showed a higher Mw and Mn of the RH-Lignins. Along the same lines, ^{31}P NMR allowed us to detect a higher abundance of OH aromatic functionalities, which can induce the higher intra/intermolecular hydrogen bonding capability, ultimately resulting in a reduced molecular motion (viz., reduced free volume and higher Tg).

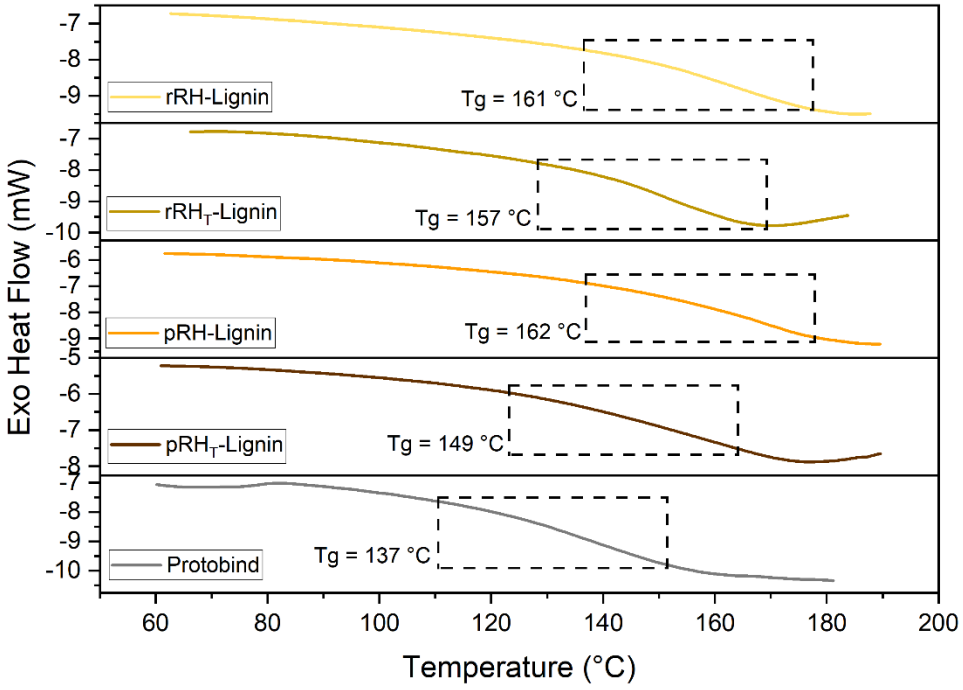

Figure 8: DSC scans (second heating ramp) of rRH-Lignin (in pale yellow), rRH$_T$-Lignin (in dark yellow), pRH-Lignin (in orange), pRH$_T$-Lignin (in brown), and Protobind (in grey).

To study the thermal stability behaviour of the lignin samples, thermogravimetric analysis (TGA) was performed as well. The mass loss traces as a function of the temperature of the RH-Lignins and of Protobind are reported in Figure 9, where the mass derivative (DTG) is also shown.

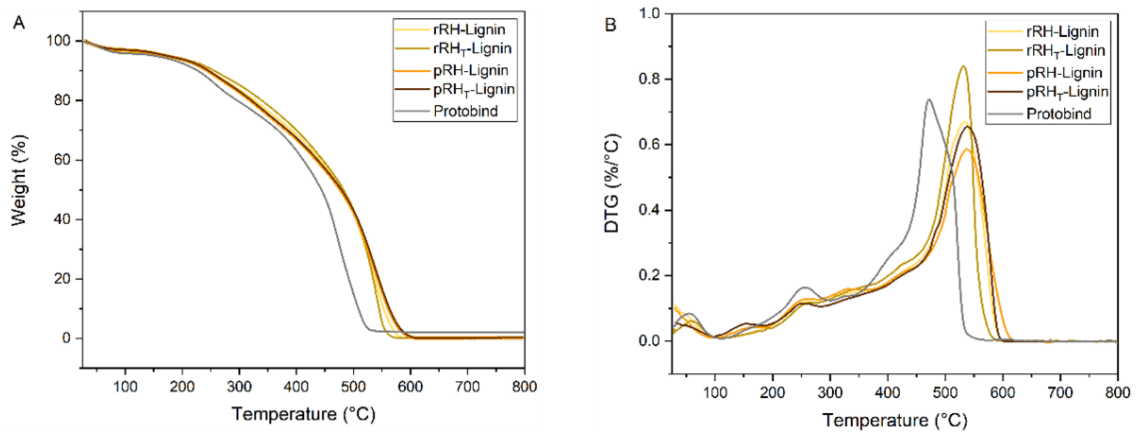

Figure 9: (A) TGA and (B) DTG traces of rRH-Lignin (in pale yellow), rRH$_T$-Lignin (in dark yellow), pRH-Lignin (in orange), pRH$_T$-Lignin (in brown), and Protobind (in grey). Analyses were conducted in air.

As it can be observed, all RH-Lignin fractions exhibited a slightly improved thermal response as compared with the reference material (Protobind) over the entire temperature range which was investigated. This can be associated with the slightly higher molecular weights (and characteristic thermal transitions) found in RH-Lignins, which result in a higher stability towards thermo-oxidative degradation. In particular, a relatively monotonic mass loss response is observed, where a single broad degradation event can be detected. This behaviour is reflected in the temperatures at which 10% and 50% mass losses are registered, which appear in line with Protobind (Table 8).

Table 8: Characteristic mass loss temperatures (10% mass loss, 50% mass loss, and maximum degradation rate) for the analyzed lignins. The reference Protobind system is also reported.

Sample	$T_{10\%}$ (°C)	$T_{50\%}$ (°C)	T_{DTGmax} (°C)
rRH-Lignin	247	480	532
rRH$_T$-Lignin	256	482	531
pRH-Lignin	245	477	538
pRH$_T$-Lignin	243	486	538
Protobind 1000	227	444	472

2.5. Water Reduction in Cement Pastes

Natural lignins are a very interesting resource for the development of sustainable traditional cement water reducers. Moreover, high-performance lignin-based cement water reducers can also be developed through different types of lignin derivatization.[50-53] Typically, lignosulfonates show better water-reducing capabilities than natural lignins, but even the latter have been successfully adopted as a starting point in the development of high-performance experimental cement plasticizers. This was obtained both in the presence[54] and in the absence of sulfonation steps.[55] The DES-mediated fractionation of the lignocellulosic biomass is a mild process that results in the production of non-

derivatized lignins comparable to those obtained by organosolv or soda processes. The lignins (rRH- and pRH-Lignins) obtained in the present study were thus evaluated using a commercial soda lignin (Protobind) as a reference. The measured water reduction capabilities, made by cement pastes (a blend of water and cement powder), are reported in Figure 10.

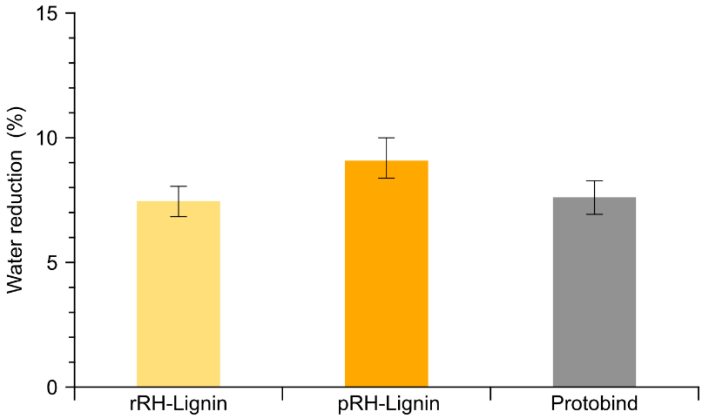

Figure 10: Measured water reduction capability for cement pastes containing 0.2% wt. of lignin. Error bars are the confidence interval (1σ) of the inverse linear regression.

The results indicated a comparable water reduction activity for the lignins derived from the rRH and pRH samples. Both lignins demonstrated an equivalent performance in comparison to the commercial soda lignin Protobind. The reported data are in a good agreement with a previous study based on BSG as a lignocellulosic starting material.[56] Indeed, the obtained results indicate that the lignin derived from the proposed process is comparable to a typical industrial soda lignin and that it constitutes a suitable basis for the development of sustainable, high performance concrete water reducers. Moreover, these results indicate that the lignin derived from the pRH is comparable to that of rRH.

3. Materials and Methods

3.1. Materials

The rice husk samples (from *Oriza sativa*) were kindly provided by Riso Scotti S.p.A. (Pavia, Italy) as raw rice husk derived from the processing of *japonica* (90%) and *indica* (10%) rice varieties and parboiled rice husk derived from *indica* (75%) and *japonica* (25%) varieties. Protobind 1000 (a mixed wheat straw/sarkanda grass lignin from the soda pulping of non-woody biomass) was provided by Tanovis (Alpnach, Switzerland).

All air- and moisture-sensitive reactions were carried out using dry solvents and under a static atmosphere of nitrogen. Choline chloride (C0329), betaine glycine (B0455) and L-lactic acid (L0165), D-(+)-Galactose, and L-(-)-fucose were purchased from TCI (Milano, Italy), whereas (L)-(+)-rhamnose, L-(+)-arabinose, D-(+)-xylose, D-(+)-mannose, D-(+)-glucose, and the other reagents and the employed solvents, used without a further purification, were obtained from Merck (Merck Life Science S.R.L., Milan, Italy).

Thin layer chromatography (TLC) Merck silica gel 60 F254 plates (Merck Millipore, Milan, Italy) were used for analytical TLC.

The identification and the quantification of the low molecular weight aromatic compounds obtained in the pretreatment step were carried out using gas chromatography

coupled with mass spectrometry (GC/MS). The GC/MS apparatus used is an Agilent GC System 7890A, with an inert MSD with a Triple-Axis Detector 7975C. The gas carrier was helium at a flux of 1.18 mL/min. The separation was performed on a DB-5MS column (30 m × 250 μm × 0.25 μm, Phenomenex, Bologna, Italy) with a temperature program of 50 °C (1 min) to 280 °C at 10 °C/min, 280 °C at 15 min (total run time 39 min). A solvent delay of 4 min was selected. The samples were dissolved in methanol or acetone in a concentration of around 0.5-1 mg/mL.

3.2. Microorganisms and Growth Media

Myceliophthora thermophila (CBS 866.85) and *Rhizomucor pusillus* (CBS 354.68) were purchased from the CBS-KNAW collection (Utrecht, The Netherlands). *Trichoderma viride* (DSM 63065) was purchased from the DSMZ GmbH collection (Braun-schweig, Germany).

The microbial inoculum for the RH pretreatment consisted of the suspension of the suitable fungal spores in distilled water. The latter suspensions were prepared adding sterile water to the suitable fungal culture, grown on an agar slant, followed by the scrubbing of the sporulated surface.

Trace elements solution: $FeCl_3$ (50 mM), $CaCl_2$ (20 mM), $MnCl_2$ (10 mM), $ZnSO_4$ (10 mM), $CoCl_2$ (2 mM), $CuCl_2$ (2 mM), $NiCl_2$ (2 mM), Na_2MoO_4 (2 mM), Na_2SeO_3 (2 mM), and H_3BO_3 (2 mM). All inorganic salts were purchased from Carlo Erba (Milano, Italy).

3.3. Determination of Rice Husks Composition

The rRH and pRH compositions have been determined with a known multistep procedure with minor modifications.[33] The RH (1 g, value a) was suspended and stirred in deionized water (150 mL) at 100 °C for 1 h. Then, after filtration, the solid was washed by deionized water (300 mL), dried in an oven at 80 °C, and weighted (value b). The solid was treated with 1 N of H_2SO_4 (150 mL) at 100 °C for 1 h. Then, the suspension was filtered again, washed with water, and the solid was dried and weighted (value c). The solid was mixed with 72% H_2SO_4 (10 mL) for 4 h at r.t. and treated with 1 N of H_2SO_4 (150 mL) under a reflux for 1 h. After cooling, the solid was isolated by filtration, dried, and weighted (value d). The final residue was then calcinated in an oven at 600 °C for 6 h and the residue has been quantified (value e). The fractions of the different components were quantified with the following equations:

$$\text{hemicellulose (\%)} = 100 \times [(b - c)/a];$$

$$\text{cellulose (\%)} = 100 \times [(c - d)/a];$$

$$\text{lignin (\%)} = 100 \times [(d - e)/a].$$

3.3.1. Determination and Quantification of Hemicellulose Components

The procedure was performed according to Foster *et al*., with minor modifications.[36] The monosaccharides fraction obtained from the hemicellulose hydrolysis (obtained in 3.3.) was dissolved in deionized water (30 mL) and was treated with $NaBH_4$ (1 g, 26.4 mmol) stirring at r.t. for 2 h. Then, the reaction was quenched by the careful addition of glacial acetic acid (10 mL), keeping the temperature under 30 °C by external cooling. The solvent

(water) and the excess of acetic acid were removed by evaporation under a reduced pressure and the obtained powder was treated with pyridine (30 mL) and acetic anhydride (30 mL) stirring at a reflux for 1 h. Hence, the reaction was concentrated to the dryness under a reduced pressure and the residue was partitioned between ethyl acetate (70 mL) and water (100 mL). The aqueous phase was extracted again with ethyl acetate (50 mL) and the combined organic phases were washed in turn with saturated $NaHCO_3$ aq. (100 mL) and with brine (100 mL). The resulting solution was dried (Na_2SO_4) and concentrated in vacuo. The residue contained the alditol acetates of the hemicellulose monosaccharides, whose relative composition was determined by GC/MS analysis. GC/MS analyses for the determination of sugar composition in hemicellulose were performed on an HP-6890 gas chromatograph equipped with a 5973 mass detector and using an HP-5MS column (30 m × 0.25 mm, 0.25 μm film thickness; Hewlett Packard, Palo Alto, CA, USA). The temperature program was the following: 120 °C (3 min)-12 °C/min-195 °C (10 min)-12 °C/min-300 °C (10 min); carrier gas: He; constant flow 1 mL/min; and split ratio: 1/30. The reference standards of the alditole acetates were prepared starting from the corresponding monosaccharides, following the reduction/acetylation protocol described above. The retention times of the alditole acetates are given below for each monosaccharide derivative: rhamnose 14.03 min; fucose 14.30 min; arabinose 14.46 min; xylose 14.88 min; mannose 21.55 min; glucose 21.65 min; and galactose 21.96 min.

3.4. Rice Husks Preprocess

3.4.1. Hydro-Thermal Preprocess

A sample of rice husk (30 g) was suspended in distilled water (1 L) and was heated in an autoclave at 121 °C for 20 min. After cooling, the solid residue was removed by filtration and the aqueous phase was concentrated under a reduced pressure until it reached complete dryness. The crude extracts of rRH and pRH were 2.1% and 2.8% w/w of the starting biomass, respectively. They were further fractionated by extraction with ethyl acetate and filtrated on a short silica gel column. The so-obtained solvent soluble fractions were derivatized as previously described and then analyzed by GC/MS.[54] Briefly, a mixture of 25 μL of pyridine, 250 μL of dioxane, and 75 μL of silylation mixture composed of N,O-bis(trimethylsilyl)trifluoroacetamide (BSTFA, Sigma T6381) with trimethylchlorosilane (TMC, Sigma T6381) was incubated with 1 mg of the sample heated in a thermomixer (1.5 mL vial Eppendorf Thermomixer Comfort) at 70 °C and 600 rpm for 30 min. At the end, 100 μL of the mixture were withdrawn, added to 100 μL of dioxane, and analysed by GC/MS with the same apparatus and analytical method reported in Section 3.1. The identification of the compounds was performed by means of an NIST 2008 mass spectral library search and then the selected peaks were confirmed with the known standards (comparing both the mass spectrum and chromatographic coordinate).

3.4.2. Microbiological Preprocess

A sample of ground pRH (25 g) was added to a 1 L flask which contained distilled water (250 mL), yeast extract (0.3 g), NH_4Cl (0.8 g), and the microelement solution (4 mL). The flask was sealed with a cellulose plug and was sterilized at 121 °C for 15 min. Then,

the obtained mixture was inoculated with the selected strain and the microbial growth was performed according to the experimental conditions indicated below.

Myceliophthora thermophila (CBS 866.85): 45 °C, 6 days, 130 rpm

Rhizomucor pusillus (CBS 354.68): 35 °C, 8 days, 130 rpm

Trichoderma viride (DSM 63065): 24 °C, 8 days, 130 rpm

Hence, the microbial transformation was interrupted by filtration on a narrow mesh metallic filter. The recovered RH was washed with deionized water and was dried (ventilated oven, 60 °C, 24 h).
According to this procedure, the difference between the weight of the recovered pRH and the weight of the untreated sample takes into account of the sum of the husk soluble fractions and of the husk organic fraction depleted by the fungal strain during its growth process. Overall, the fraction between this weight difference over the corresponding RH initial weight (given as w/w percentages) indicates the degradative capability of the strain. The obtained results are listed below:

Myceliophthora thermophila: 18%; *Rhizomucor pusillus*: 19%; and *Trichoderma viride*: 14%.

3.5. Rice Husks Lignocellulose Process

3.5.1. Preparation of DESs

The DESs were prepared in a closed flask by mixing the anhydrous hydrogen bond acceptor (HBA) with the hydrogen bond donor (HBD) in the determined molar ratio (see Section 2.3) and was stirred at 120 °C for 4 h until the liquid phase appeared to be completely homogeneous and clear. The products were then dried under a vacuum and stored at room temperature in a desiccator in the presence of anhydrous calcium chloride until further use. The ^{1}H NMR spectrum of the selected DES 2 (choline chloride/L-lactic acid 1/5) for the full fractionation is reported in the Supplementary Materials (Figure S1).

3.5.2. DES-Mediated Lignocellulose Process

The rice husk (25 g) was suspended in a DES of choline chloride/L-lactic acid 1/5 (250 mL) at 130 °C in a round-bottom flask under magnetic stirring for 24 h. After cooling, ethanol (500 mL) was then added gradually over 2 h in order to precipitate the cellulose-enriched fraction. The solid particulate was separated by centrifugation and filtration, washed many times with ethanol, and dried to give a final solid RH-Cellulose-enriched fraction (≈ 15 g) with a yield of 59-61% (w/w initial biomass). This fraction was further fractionated in order to quantify the silica content (see Section 3.5.3). The silica content accounted for 12.8% (w/w biomass).
The filtrate after the ethanol treatment was then concentrated by the rotary evaporation under the vacuum to eliminate the solvent. Water (500 mL) was added, and the suspension was stirred for 24 h at 4 °C. The obtained precipitate was then centrifuged, filtered, and washed three times for 1 h with a solution of water/ethanol 9/1. After the centrifugation, filtration, and solvent evaporation, the final fraction (RH-Lignin, ≈3 g) was recovered with a final yield of 10% (w/w initial biomass).

3.5.3. Determination of Silica Content in Cellulose-Enriched Fractions

The cellulose-enriched fractions, derived from DES-mediated fractionation, were analyzed in order to determine their silica contents, using the Yoshida procedure based on the complete oxidation of the organic materials by heating with a mixture of strong acids with some modifications. We employed an acid mixture with the following composition: HNO_3 aq. (65% w/v) 75 mL, H_2SO_4 aq. (96% w/v) 15 mL, and $HClO_4$ aq. (70% w/v) 30 mL.

Each sample of the cellulose-enriched fractions (about 2 g, dry weight) was placed in a round bottomed flask containing a stirring bar and equipped with a condenser. The fractions were treated with 20 mL of the acid mixture and were allowed to predigest under a fume hood for 3 h. Then, the obtained brown slurries were heated at reflux under stirring for six h. The resulting colourless silica suspensions were ice-cooled, diluted with 60 mL of distilled water, and centrifuged (9000 rpm, 4 °C). The collected silica samples were washed with distilled water (2 × 25 mL), with acetone (25 mL), and were then dried at a reduced pressure. The weights of the obtained silica samples were employed to calculate the silica content of the cellulose-enriched fractions and thus of the starting rice husk samples (both given as a w/w percentage).

3.6. Lignin Characterization

3.6.1. Solvent Solubilization Determination

The lignin solvent's solubility was determined by treating 1 g of the analyzed lignin with 10 mL of the different solvents under stirring at 400 rpm. Each test was carried out overnight at room temperature. The suspension was then filtered and the solvent was evaporated at a reduced pressure, and the final residue was dried until a constant weight was achieved prior to the quantification.

3.6.2. Molar Mass Determination

A Waters 510 HPLC system equipped with a refractive index detector was used for the GPC analyses. Tetrahydrofuran (THF) was used as the eluent. The analyzed lignin sample (volume 200 µL, concentration 1 mg/mL in THF) was injected into a system of the three columns connected in series (Ultrastyragel HR, Waters − dimensions 7.8 mm × 300 mm) and the analysis was performed at 30 °C at a flow rate of 0.5 mL/min. The calibration was performed against polystyrene standards in the 102-104 g/mol molecular weight range. The samples have been acetylated to allow for a complete solubility in the THF eluent. The estimation of the number-average and weight-average molecular weights of the obtained lignin fractions was performed excluding the signals related to the solvent (THF) and the solvent stabilizer (butylated hydroxytoluene), visible at long elution times (> 29.5 min).

3.6.3. Sugar Content Determination

The total sugars quantification was performed with a previously described method based on a bicinchoninic assay.[15, 44]

3.6.4. ^{13}C CP-MAS NMR Analysis

Solid state NMR experiments were carried out on a Bruker NEO 500 MHz spectrometer

(Bruker, Billerica, MA, U.S) equipped with an i-probe solid state probe. The samples (150 mg) were packed into 4 mm zirconia rotors and sealed with Kel-F caps. All the NMR spectra were recorded at 298 K. The ^{13}C CP-MAS NMR spectra were performed at 125 MHz. The spin-rate was kept at 8 KHz. The 90-pulse width was 3.2 μs, the relaxation delay was 4 s, the acquisition number was 17,000, and the contact time was 1.5 ms. The spectra were obtained using 1024 data points in the time domain, zero filled, and Fourier transformed. All the data were processed using the MestreNova 6.0.2 software (Mestrelab Research, Santiago de Compostela, Spain). An adamantane standard was used as the external referencing standard to calibrate the ^{13}C chemical shifts.

3.6.5. Folin–Ciocalteu Analysis

The total phenolic content of the lignins was determined by a modified Folin–Ciocalteu (FC) protocol with some modifications to the sample preparation step, as previously described. [54-55] Briefly, the samples were dissolved in DMSO with a final concentration of 2 mg/mL. For each determination, 5 μL of the working solution (or the standard solution) were then mixed with 120 μL of deionized water, 125 μL of FC reagent (Sigma 47641), and kept for 6 min at room temperature after 30 s of vortex stirring. Then, after the addition of 1.25 mL of 5% sodium carbonate and mixing, the vial was incubated in a thermoshaker at 40 °C for 30 min. The reaction mixture absorbance was measured using a UV–Vis spectrophotometer (Jasco V-560) equipped with a temperature-controlled cuvette holder and a thermostatic water bath (Haake K10, Karlsruhe, Germany). All the spectrophotometric measurements were carried out at 760 nm, 25 °C, using a 1 cm optical path cuvette and deionized water as the blank sample. Vanillin was chosen as the reference standard. The calibration curve was constructed with nine different vanillin solutions in DMSO with a concentration in the range 0-500 μg/mL (see Supplementary Materials Figure S2). Each FC assay determination was carried out in triplicate.

3.6.6. ^{31}P NMR Analysis

^{31}P NMR spectroscopic analyses were recorded on a Bruker Instrument AVANCE400 spectrometer (Milano, Italy). The acquisition and data treatment were performed with Bruker TopSpin 3.2 software (Milano, Italy). The spectra were collected at 29 °C with a 4 s acquisition time, 5 s relaxation delay, and 256 scans. Prior to the analysis, the samples were dried for 24 h under a vacuum and then derivatized according to the following procedure.

The sample (40 mg) was completely dissolved in 300 μL of N,N-dimethylformamide. To this solution, the following components were added: 200 μL of dry pyridine, 100 μL of solution of an internal standard (10 mg of Endo-N-hydroxy-5-norbornene-2,3-dicarboximide (Sigma 226378) dissolved in 0.5 mL of a mixture of pyridine and $CDCl_3$ 1.6:1 v/v), 50 μL of a relaxation agent solution (5.7 mg of chromium (III) acetylacetonate (Sigma 574082) dissolved in 0.5 mL of a mixture of pyridine and $CDCl_3$ 1.6:1 v/v), 100 μL of 2-chloro-4,4,5,5-tetramethyl-1,3,2-dioxaphospholane (Sigma 447536), and, at the end, 200 μL of $CDCl_3$. The solution was centrifuged and/or filtered if necessary. All the chemical shifts reported were related to the reaction product of the phosphorylating agent with water, which gave a signal at 132.2 ppm.

3.6.7. Fourier Transform Infrared Spectroscopy Analysis

The FTIR spectra were collected with a Nicolet Nexus 760 FTIR spectrophotometer. The samples were prepared by pressing the lignin powders with KBr powder to obtain thin discs. The spectra were recorded at room temperature, in air, in transmission mode (64 accumulated scans at a resolution of 4 cm^{-1}) in the 4000-1000 cm^{-1} wavenumber range.

3.6.8. Differential Scanning Calorimetry Analysis

DSC analysis was employed to investigate the thermal transitions in the lignin samples. Measurements were carried out on 10-15 mg samples by means of a Mettler-Toledo DSC 823e instrument. Three runs (heating/cooling/heating) were performed: from 25 °C to 150 °C to remove the water from the samples, from 150 °C to 25 °C, and from 25 °C to 200 °C, at a scan rate of 20 °C/min under a nitrogen flux. The glass transition temperature (Tg) of the samples was evaluated as the inflection point in the second heating run.

3.6.9. Thermogravimetric Analysis

TGA was performed on all the lignin samples (≈15 mg) by means of a Q500 TGA system (TA Instruments, Italy) from an ambient temperature to 800 °C, at a scan rate of 10 °C/min in air.

3.7. Determination of Water Reduction in Cement Pastes

The complete description of the laboratory method for the preliminary estimation of the water reduction capabilities of the fractionated lignins was reported in detail in a previous work.[15]

Briefly, the analysis is based on the evaluation of the relative Bingham dynamic yield torque of cement pastes containing 0.2% of lignin (w/w relative to dry cement) at a different water/cement (w/c) ratio.[56]

By measuring the dynamic yield torque of the cement pastes at various w/c ratios, it is possible to calculate by inverse regression the w/c ratio needed to obtain a predetermined reference torque value and thus to determine the water reduction capacity for each lignin under study. In this study, the reference Bingham dynamic yield torque was obtained with a pure cement paste with a 0.45 w/c ratio. The actual water reduction obtained for each lignin is given by the following equation

$$W_R = 100 \cdot (1 - \frac{W_L}{W_{ref}})$$

where W_R is the water reduction (%), $_{WL}$ is the measured w/c ratio at the reference yield torque for the given lignin, and W_{ref} is the reference w/c ratio (0.45). This procedure allows us to measure the effective water reduction capability of each lignin in the preparation of cement pastes in the given conditions. In the present work, the water reduction capability was measured for rRH-Lignin, for pRH-Lignin and, as a reference, for a well-known commercial soda lignin (Protobind).

4. Conclusions

Among the agri-food cultivations, rice has a huge social and economic importance. For this reason, the exploitation of waste residues coming from its production possesses an

important interest for the scientific community and for the society.
In this work, we demonstrated a multistep lignocellulosic fractionation process of raw and parboiled rice husks by means of DESs based on non-toxic, renewable components. The fractionation allowed us to recover a cellulose/silica fraction, precipitated by the addition of ethanol, and a lignin-based fraction, precipitated by the addition of water.
The lignin fractions obtained from both raw and parboiled rice husks were fully characterized and compared for the first time. The results show similar physico-chemical properties between the two recovered lignins, indicating that the parboiling process does not alter significantly the lignin characteristics. Moreover, because of the mild separation conditions allowed by the DES-mediated process, the resulting lignins were underivatized and demonstrated a limited degradation.
Both lignins were studied as a potential base for the production of cement water reducers, the latter being an important application field for lignin derivatives. The obtained results confirmed the substantial equivalence of the two lignins for the target application and indicated that both are comparable to a commercial soda lignin taken as a reference benchmark.
A preprocess step based on fermentation was also studied. However, the obtained results demonstrated the limited degradability of both raw and parboiled RHs, even using cellulose-degrading fungi. A possible cause for such behaviour was found in the relatively high silica content in both RHs (about 13%).
These preliminary data show, at a 25 g lab-scale, the potentialities of DES-mediated fractionation processes in the lignocellulosic fractionation of RHs. This protocol is a promising base for a future implementation on a larger scale. Considering the very large volume of the worldwide rice production and the environmental friendliness of DES-based processes, the reported results constitute an encouraging step towards the exploitation of RH wastes in line with the strategic objectives of the circular economy.

Supplementary Materials

The following supporting information can be downloaded at: https://www.mdpi.com/article/10.3390/molecules27248879/s1, Figure S1: ^{1}H NMR spectrum of DES 2 choline chloride/L-lactic acid (1:5 mol/mol); Figure S2: Calibration curve of Folin–Ciocalteu phenol titration with vanillin.; Table S1: Yields of mass recovery in the different tested DESs.

References

1. Zhang, Y.; Zhu, L.; Wu, G.; Wang, X.; Jin, Q.; Qi, X.; Zhang, H., Design of amino-functionalized hollow mesoporous silica cube for enzyme immobilization and its application in synthesis of phosphatidylserine. *Colloids and Surfaces B: Biointerfaces* **2021,** *202*, 111668.
2. Database, F. F. www.fao.org/faostat
3. Buggenhout, J.; Brijs, K.; Celus, I.; Delcour, J., The breakage susceptibility of raw and parboiled rice: A review. *Journal of Food Engineering* **2013,** *117* (3), 304-315.
4. Tan, B. L.; Norhaizan, M. E., *Rice by-products: Phytochemicals and food products application*. Springer: 2020.
5. Balbinoti, T. C. V.; Nicolin, D. J.; de Matos Jorge, L. M.; Jorge, R. M. M., Parboiled rice and parboiling process. *Food Engineering Reviews* **2018,** *10*, 165-185.
6. Islam, M. R.; Shimizu, N.; Kimura, T., Quality evaluation of parboiled rice with physical properties. *Food Science and Technology Research* **2001,** *7* (1), 57-63.
7. Liu, J.; Li, X.; Row, K. H., Development of deep eutectic solvents for sustainable chemistry. *Journal of Molecular Liquids* **2022,** *362*, 119654.

8. Isci, A.; Kaltschmitt, M., Recovery and recycling of deep eutectic solvents in biomass conversions: A review. *Biomass Conversion and Biorefinery* **2021**, 1-30.
9. Gong, L.; Zha, J.; Pan, L.; Ma, C.; He, Y.-C., Highly efficient conversion of sunflower stalk-hydrolysate to furfural by sunflower stalk residue-derived carbonaceous solid acid in deep eutectic solvent/organic solvent system. *Bioresource Technology* **2022,** *351*, 126945.
10. Wu, M.; Gong, L.; Ma, C.; He, Y.-C., Enhanced enzymatic saccharification of sorghum straw by effective delignification via combined pretreatment with alkali extraction and deep eutectic solvent soaking. *Bioresource Technology* **2021,** *340*, 125695.
11. Lin, G.; Tang, Q.; Huang, H.; Yu, J.; Li, Z.; Ding, B., Process optimization and comprehensive utilization of recyclable deep eutectic solvent for the production of ramie cellulose fibers. *Cellulose* **2022,** *29* (7), 3689-3701.
12. Zhu, Y.; Yu, Z.; Zhu, J.; Zhang, Y.; Ren, X.; Jiang, F., Developing flame-retardant lignocellulosic nanofibrils through reactive deep eutectic solvent treatment for thermal insulation. *Chemical Engineering Journal* **2022,** *445*, 136748.
13. Allegretti, C.; Gatti, F. G.; Marzorati, S.; Rossato, L. A. M.; Serra, S.; Strini, A.; D'Arrigo, P., Reactive Deep Eutectic Solvents (RDESs): A new tool for phospholipase D-catalyzed preparation of phospholipids. *Catalysts* **2021,** *11* (6), 655.
14. Zhou, M.; Fakayode, O. A.; Yagoub, A. E. A.; Ji, Q.; Zhou, C., Lignin fractionation from lignocellulosic biomass using deep eutectic solvents and its valorization. *Renewable and Sustainable Energy Reviews* **2022,** *156*, 111986.
15. Allegretti, C.; Bellinetto, E.; D'Arrigo, P.; Griffini, G.; Marzorati, S.; Rossato, L. A. M.; Ruffini, E.; Schiavi, L.; Serra, S.; Strini, A.; Tessaro, D.; Turri, S., Towards a Complete Exploitation of Brewers’ Spent Grain from a Circular Economy Perspective. *Fermentation* **2022,** *8* (4), 151.
16. De Baynast, H.; Tribot, A.; Niez, B.; Audonnet, F.; Badel, E.; Cesar, G.; Dussap, C.-G.; Gastaldi, E.; Massacrier, L.; Michaud, P., Effects of Kraft lignin and corn cob agro-residue on the properties of injected-moulded biocomposites. *Industrial Crops and Products* **2022,** *177*, 114421.
17. Fiorani, G.; Crestini, C.; Selva, M.; Perosa, A., Advancements and complexities in the conversion of lignocellulose into chemicals and materials. *Frontiers in Chemistry* **2020,** *8*, 797.
18. Tanase-Opedal, M.; Espinosa, E.; Rodríguez, A.; Chinga-Carrasco, G., Lignin: A biopolymer from forestry biomass for biocomposites and 3D printing. *Materials* **2019,** *12* (18), 3006.
19. Carlos de Haro, J.; Magagnin, L.; Turri, S.; Griffini, G., Lignin-based anticorrosion coatings for the protection of aluminum surfaces. *ACS Sustainable Chemistry & Engineering* **2019,** *7* (6), 6213-6222.
20. de Haro, J. C.; Allegretti, C.; Smit, A. T.; Turri, S.; D'Arrigo, P.; Griffini, G., Biobased polyurethane coatings with high biomass content: tailored properties by lignin selection. *ACS Sustainable Chemistry & Engineering* **2019,** *7* (13), 11700-11711.
21. Tribot, A.; Amer, G.; Alio, M. A.; de Baynast, H.; Delattre, C.; Pons, A.; Mathias, J.-D.; Callois, J.-M.; Vial, C.; Michaud, P., Wood-lignin: Supply, extraction processes and use as bio-based material. *European Polymer Journal* **2019,** *112*, 228-240.
22. Wang, H.; Pu, Y.; Ragauskas, A.; Yang, B., From lignin to valuable products–strategies, challenges, and prospects. *Bioresource technology* **2019,** *271*, 449-461.
23. de Haro, J. C.; Tatsi, E.; Fagiolari, L.; Bonomo, M.; Barolo, C.; Turri, S.; Bella, F.; Griffini, G., Lignin-based polymer electrolyte membranes for sustainable aqueous dye-sensitized solar cells. *ACS Sustainable Chemistry & Engineering* **2021,** *9* (25), 8550-8560.
24. Trano, S.; Corsini, F.; Pascuzzi, G.; Giove, E.; Fagiolari, L.; Amici, J.; Francia, C.; Turri, S.; Bodoardo, S.; Griffini, G., Lignin as polymer electrolyte precursor for stable and sustainable potassium batteries. *ChemSusChem* **2022,** *15* (12), e202200294.
25. Zhao, B.; Borghei, M.; Zou, T.; Wang, L.; Johansson, L.-S.; Majoinen, J.; Sipponen, M. H.; Österberg, M.; Mattos, B. D.; Rojas, O. J., Lignin-based porous supraparticles for carbon capture. *ACS nano* **2021,** *15* (4), 6774-6786.
26. Österberg, M.; Sipponen, M. H.; Mattos, B. D.; Rojas, O. J., Spherical lignin particles: A review on their sustainability and applications. *Green Chemistry* **2020,** *22* (9), 2712-2733.
27. Momayez, F.; Hedenström, M.; Stagge, S.; Jönsson, L. J.; Martín, C., Valorization of hydrolysis lignin from a spruce-based biorefinery by applying γ-valerolactone treatment. *Bioresource Technology* **2022,** *359*, 127466.
28. Giannì, P.; Lange, H.; Crestini, C., Functionalized organosolv lignins suitable for modifications of hard surfaces. *ACS sustainable chemistry & engineering* **2020,** *8* (20), 7628-7638.
29. Edmeades, R. M.; Hewlett, P. C., Cement admixtures. In *Lea's chemistry of cement and concrete*, Elsevier: 1998; pp 841-905.

30. Lou, H.; Lai, H.; Wang, M.; Pang, Y.; Yang, D.; Qiu, X.; Wang, B.; Zhang, H., Preparation of lignin-based superplasticizer by graft sulfonation and investigation of the dispersive performance and mechanism in a cementitious system. *Industrial & Engineering Chemistry Research* **2013,** *52* (46), 16101-16109.
31. Zheng, T.; Zheng, D.; Qiu, X.; Yang, D.; Fan, L.; Zheng, J., A novel branched claw-shape lignin-based polycarboxylate superplasticizer: Preparation, performance and mechanism. *Cement and Concrete Research* **2019,** *119*, 89-101.
32. Gupta, C.; Nadelman, E.; Washburn, N. R.; Kurtis, K. E., Lignopolymer superplasticizers for low-CO2 cements. *ACS Sustainable Chemistry & Engineering* **2017,** *5* (5), 4041-4049.
33. Okur, M.; Koyuncu, D. D. E., Investigation of pretreatment parameters in the delignification of paddy husks with deep eutectic solvents. *Biomass and Bioenergy* **2020,** *142*, 105811.
34. Jackson, M., The alkali treatment of straws. *Animal Feed Science and Technology* **1977,** *2* (2), 105-130.
35. Xiao, B.; Sun, X.; Sun, R., Chemical, structural, and thermal characterizations of alkali-soluble lignins and hemicelluloses, and cellulose from maize stems, rye straw, and rice straw. *Polymer degradation and stability* **2001,** *74* (2), 307-319.
36. Foster, C. E.; Martin, T. M.; Pauly, M., Comprehensive compositional analysis of plant cell walls (lignocellulosic biomass) part I: lignin. *JoVE (Journal of Visualized Experiments)* **2010,** (37), e1745.
37. Zhao, W.; Simmons, B.; Singh, S.; Ragauskas, A.; Cheng, G., From lignin association to nano-/micro-particle preparation: extracting higher value of lignin. *Green Chemistry* **2016,** *18* (21), 5693-5700.
38. Hu, K.; Zhang, Z.; Wang, F.; Fan, Y.; Li, J.; Liu, L.; Wang, J., Optimization of the hydrolysis condition of pretreated corn stover using trichoderma viride broth based on orthogonal design and principal component analysis. *Bioresources* **2018,** *13* (1), 383-398.
39. Adams, P., Extracellular amylase activities of Rhizomucor pusillus and Humicola lanuginosa at initial stages of growth. *Mycopathologia* **1994,** *128* (3), 139-141.
40. Henriksson, G.; Akin, D. E.; Slomczynski, D.; Eriksson, K.-E. L., Production of highly efficient enzymes for flax retting by Rhizomucor pusillus. *Journal of Biotechnology* **1999,** *68* (2-3), 115-123.
41. Hong, S.; Shen, X.-J.; Xue, Z.; Sun, Z.; Yuan, T.-Q., Structure–function relationships of deep eutectic solvents for lignin extraction and chemical transformation. *Green Chemistry* **2020,** *22* (21), 7219-7232.
42. Tan, Y. T.; Ngoh, G. C.; Chua, A. S. M., Effect of functional groups in acid constituent of deep eutectic solvent for extraction of reactive lignin. *Bioresource technology* **2019,** *281*, 359-366.
43. Yoshida, S., Laboratory manual for physiological studies of rice. *Int Rice Res Ins, Philippines* **1976,** *23*, 61-66.
44. Allegretti, C.; Boumezgane, O.; Rossato, L.; Strini, A.; Troquet, J.; Turri, S.; Griffini, G.; D'Arrigo, P., Tuning lignin characteristics by fractionation: A versatile approach based on solvent extraction and membrane-assisted ultrafiltration. *Molecules* **2020,** *25* (12), 2893.
45. D'Arrigo, P.; Allegretti, C.; Tamborini, S.; Formantici, C.; Galante, Y.; Pollegioni, L.; Mele, A., Single-batch, homogeneous phase depolymerization of cellulose catalyzed by a monocomponent endocellulase in ionic liquid [BMIM][Cl]. *Journal of Molecular Catalysis B: Enzymatic* **2014,** *106*, 76-80.
46. Meng, X.; Crestini, C.; Ben, H.; Hao, N.; Pu, Y.; Ragauskas, A. J.; Argyropoulos, D. S., Determination of hydroxyl groups in biorefinery resources via quantitative 31P NMR spectroscopy. *Nature Protocols* **2019,** *14* (9), 2627-2647.
47. Archipov, Y.; Argyropoulos, D.; Bolker, H.; Heitner, C., 31P NMR spectroscopy in wood chemistry. I. Model compounds. *Journal of wood chemistry and technology* **1991,** *11* (2), 137-157.
48. Faix, O., Fourier transform infrared spectroscopy. In *Methods in lignin chemistry*, Springer: 1992; pp 83-109.
49. Kalliola, A.; Vehmas, T.; Liitiä, T.; Tamminen, T., Alkali-O2 oxidized lignin–A bio-based concrete plasticizer. *Industrial Crops and Products* **2015,** *74*, 150-157.
50. He, W.; Fatehi, P., Preparation of sulfomethylated softwood kraft lignin as a dispersant for cement admixture. *Rsc Advances* **2015,** *5* (58), 47031-47039.
51. Takahashi, S.; Hosoya, S.; Hattori, M.; Morimoto, M.; Uraki, Y.; Yamada, T., Performance of softwood soda-anthraquinone lignin–polyethylene glycol derivatives as water-reducing admixture for concrete. *Journal of Wood Chemistry and Technology* **2015,** *35* (5), 348-354.
52. Ji, D.; Luo, Z.; He, M.; Shi, Y.; Gu, X., Effect of both grafting and blending modifications on the performance of lignosulphonate-modified sulphanilic acid–phenol–formaldehyde condensates. *Cement and Concrete Research* **2012,** *42* (9), 1199-1206.

53. Li, S.; Li, Z.; Zhang, Y.; Liu, C.; Yu, G.; Li, B.; Mu, X.; Peng, H., Preparation of Concrete Water Reducer via Fractionation and Modification of Lignin Extracted from Pine Wood by Formic Acid. *ACS Sustainable Chemistry & Engineering* **2017,** *5* (5), 4214-4222.
54. Allegretti, C.; Fontanay, S.; Rischka, K.; Strini, A.; Troquet, J.; Turri, S.; Griffini, G.; D'Arrigo, P., Two-step fractionation of a model technical lignin by combined organic solvent extraction and membrane ultrafiltration. *ACS omega* **2019,** *4* (3), 4615-4626.
55. Allegretti, C.; Fontanay, S.; Krauke, Y.; Luebbert, M.; Strini, A.; Troquet, J.; Turri, S.; Griffini, G.; D'Arrigo, P., Fractionation of soda pulp lignin in aqueous solvent through membrane-assisted ultrafiltration. *ACS Sustainable Chemistry & Engineering* **2018,** *6* (7), 9056-9064.
56. Haist, M.; Link, J.; Nicia, D.; Leinitz, S.; Baumert, C.; von Bronk, T.; Cotardo, D.; Eslami Pirharati, M.; Fataei, S.; Garrecht, H., Interlaboratory study on rheological properties of cement pastes and reference substances: comparability of measurements performed with different rheometers and measurement geometries. *Materials and Structures* **2020,** *53*, 1-26.

Chapter 5

Phospholipase D Immobilization on Lignin Nanoparticles for Enzymatic Transformation of Phospholipids

Letizia A. M. Rossato,[*,a] Mohammad Morsali,[b,c] Eleonora Ruffini,[a] Pietro Bertuzzi,[a] Stefano Serra,[d] Paola D'Arrigo[a,d] and Mika Sipponen[*,b,c]

[a] Department of Chemistry, Materials and Chemical Engineering "Giulio Natta", Politecnico di Milano, p.zza L. da Vinci 32, 20133 Milano, Italy.

[b] Department of Materials and Environmental Chemistry (MMK), Faculty of Science Stockholm University, Svante Arrhenius väg 16C, SE-106 91 Stockholm, Sweden.

[c] Department of Materials and Environmental Chemistry, Wallenberg Wood Science Center, Stockholm University, SE-10691 Stockholm, Sweden.

[d] Istituto di Scienze e Tecnologie Chimiche "Giulio Natta", Consiglio Nazionale delle Ricerche (SCITEC-CNR), Via Luigi Mancinelli 7, 20131 Milano, Italy.

Submitted to *Chemsuschem* **2023**

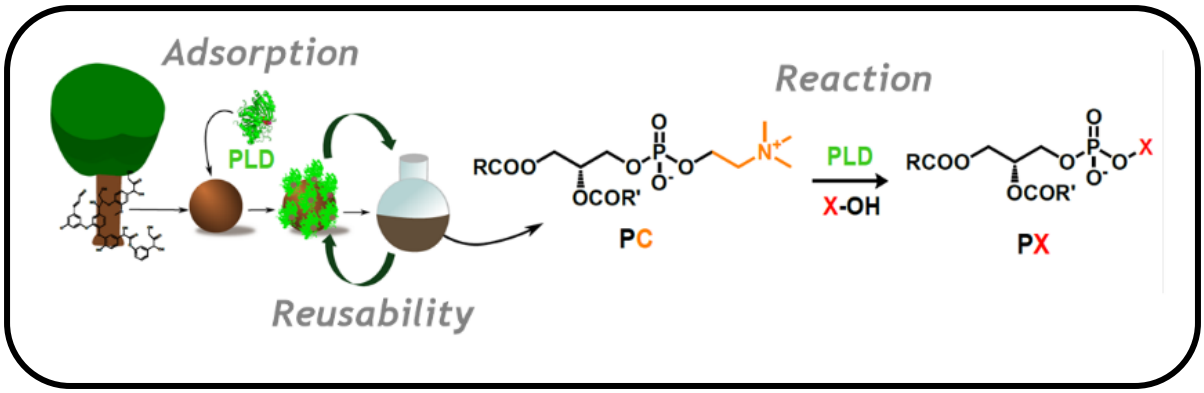

Abstract

Lignin nanoparticles (LNPs) are promising components for various materials, given their controllable particle size and spherical shape. However, their origin from supramolecular aggregation has limited the applicability of LNPs as recoverable templates for immobilization of enzymes. In this study, we show that stabilized LNPs are highly promising for the immobilization of phospholipase D (PLD), the enzyme involved in the biocatalytic production of high-value polar head-modified phospholipids of commercial interest, phosphatidylglycerol, phosphatidylserine and phosphatidyl-ethanolamine. Starting from hydroxymethylated lignin, LNPs were prepared and successively hydrothermally treated to obtain c-HLNPs with high resistance to organic solvents and a wide range of pH values, covering the conditions for enzymatic reactions and enzyme recovery. The immobilization of PLD on c-HLNPs (PLD-c-HLNPs) was achieved through direct adsorption. We then successfully exploited this new enzymatic preparation in the preparation of pure polar head-modified phospholipids with high yields (60-90%). Furthermore, the high PLD-c-HLNPs stability allows its recycling for a number of reactions with appreciable maintenance of its catalytic activity. Thus, PLD-c-HLNPs can be regarded as a new, chemically stable, recyclable and user-friendly biocatalyst, based on a biobased inexpensive scaffold, to be employed in sustainable chemical processes for synthesis of value-added phospholipids.

1. Introduction

Phospholipids, in addition to being the main components of all biological membranes, are the subject of many areas of biomedical research due to their involvement in critical cellular functions, such as cellular regeneration and differentiation, as well as to their ability to promote the biological activity of various membrane-linked proteins and receptors.[1-6] Phospholipids have been successfully employed as therapeutic agents, drug-delivery systems, and diagnostic markers for certain diseases.[7] Furthermore, their role in some neurological pathologies such as stress-related disorders, schizophrenia, dementia and Parkinson's disease has been established as well as the beneficial effects of their use in the diet to prevent a range of diseases including inflammation, cancer, and coronary heart issues.[8-9] Phospholipids are also industrially exploited as natural emulsifiers, surfactants, nutraceuticals, food stabilizers and detergents.[10] Additionally, in the last three years following the onset of the Covid-19 pandemic, phospholipids have been integrated into the design of modern vaccines as liposomal encapsulation systems.[11-12] Moreover, these residues have also been inserted in biocompatible polymers for medical use.[13]
From a structural point of view, natural phospholipids present a glycerol backbone, esterified at *sn-1* and *sn-2* positions with saturated and unsaturated long chain fatty acids, which constitute the lipophilic moieties, and in *sn-3* with a phosphate diester as the polar head group (see Scheme 1 for abundant natural compounds).

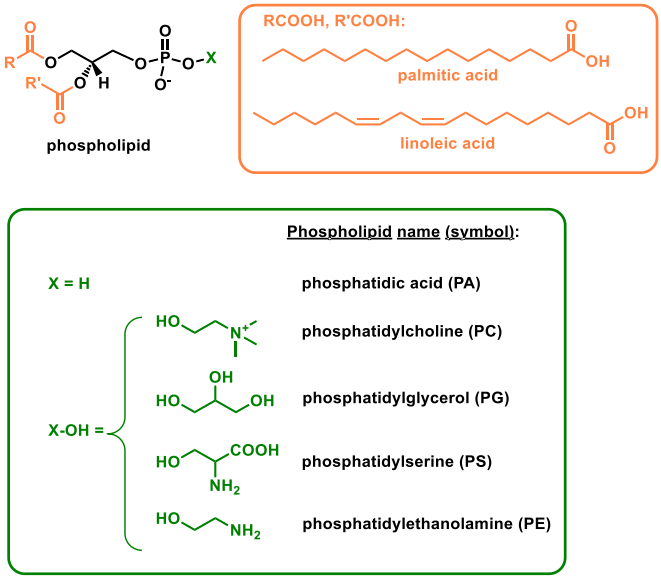

Scheme 1: Structure of the main natural phospholipids. The acyl chains in orange are the most abundant in phospholipids extracted from soybeans.

The possibility to prepare different polar head modified phospholipids constitutes a central point in the research on phospholipids because their biological activity is strictly dependent on the chemical identity of the polar head and the acyl chains, and their commercial values are highly related to the source and the purity of the products. However, the preparation of these products is challenging. In fact, even if phosphatidylcholine (PC), which is the most abundant natural phospholipid, is easily extracted from natural sources, the recovery of the other less abundant derivatives is not feasible on a large production scale: it would in fact be extremely expensive, requiring multiple steps of solvent partitioning and chromatography. Obviously, total chemical synthesis from appropriate homochiral precursors could be exploited but it requires multistep and expensive reagents and the use of complex sequences of protection and deprotection steps in order to introduce selectively the desired functional groups.[14-16] For that reason, new strategies for the production of these high value compounds are highly investigated.[17-19] In this mainframe, biocatalytic production starting from natural compounds is a suitable alternative especially when final products are required for food and pharmaceutical sectors with strict safety standards. In particular, PC can be enzymatically modified in its polar head moiety into high value phospholipids by means of phospholipase D (PLD, EC 3.1.4.4).[20] This enzyme, in addition to its natural capacity to hydrolyze PC into phosphatidic acid (PA), catalyzes, under definite conditions, the transphosphatidylation reaction of PC in the presence of an alcohol (X-OH), leading to a polar head-modified phospholipid reported as PX in Scheme 2.[21-23]

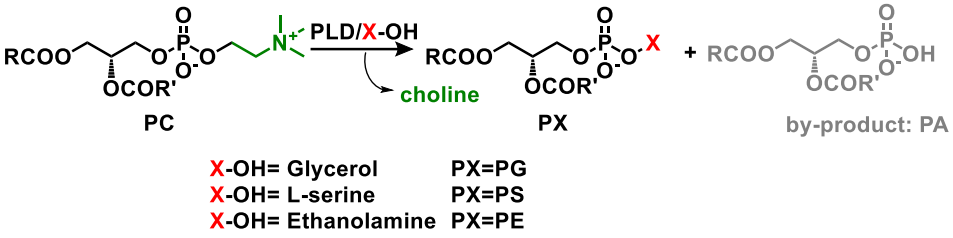

Scheme 2: PLD-catalyzed transformation of PC in polar head modified phospholipids (PXs).

The reaction parameters could be set in order to reduce the entity of the PA formation which constitutes the parasitic reaction in the preparation of PXs. Some improvements of this strategy were recently reported using novel eco-friendly solvents such as ionic liquids (ILs),[24] deep eutectic solvents (DES),[22] and bio-based solvents.[25-27] PLD is very expensive and not commercially available on large scale as only few chemical companies produce this enzyme limiting its application to an internal use. For those reasons, the development of enzymatic synthesis strategies is highly suitable, particularly when the products are intended for biomedical investigations. In this mainframe, our research has focused on immobilization of PLD, aiming to find new sustainable methods to prepare polar head-modified phospholipids, with the final objective of reducing the operational costs by optimizing the process, recycling the enzyme, and enhancing its activity and stability over time.

In the recent years, bio-based enzyme immobilization scaffolds have been highly required to make the industry more sustainable.[28] For that reason, among the components of renewable biomass, a great research interest has grown on lignin, which is an amorphous aromatic polymer constituting the natural glue responsible for structural integrity of plants.[29] Lignin is obtained as a by-product of the pulp and paper industry in which around 70 million tons of lignin are extracted from wood every year based on the FAO data on pulp production. Recently, lignin has become the subject of a wide range of increasingly active research,[30-33] and particularly spherical lignin nanoparticles (LNPs)[34-35] with controllable size, desired shape, high and surface area have broadened the window of applications for lignin.[36-39] LNPs can be prepared using several methods such as pH shifting precipitation,[40-42] mechanical treatment,[43] sonication[40, 44] and solvent exchange.[45-46] The solvent exchange method allows preparation of LNPs of controllable size by dissolving lignin in an organic solvent followed by decreasing the organic solvent concentration, commonly by either adding water, which initiates aggregation of lignin in a way that results in a colloidally stable dispersion. LNPs have been studied for a plethora of different materials chemistry applications, including drug carriers,[47] UV protectants,[48] and hosts for enzyme immobilization,[49] replacing often hazardous nanomaterials.[50-52] Our interest in using LNPs for immobilization of PLD was inspired by some recent publications with redox enzymes.[49, 53-56] For example, Capecchi *et al.* described LNPs for the immobilization of tyrosinase for the synthesis of catechol derivatives,[49] and glucose oxidase and peroxidase immobilization to obtain biosensors for the detection of glucose.[55] In literature, PLD has been immobilized on different supports, such as resins,[57] magnetic nanoparticles,[58] and porous materials,[59] LNPs appear novel in this domain. We decided to use this kind of scaffold because preparing LNPs is simple, cost-effective and allow the preparation of stable material starting from a waste which usually is disposed of, creating a high-value products starting from discards.

However, one of the obstacles limiting widespread use of LNPs in enzyme immobilization has been their instability (aggregation or dissolution) in aqueous and organic solvents. Maintaining the spherical shape and colloidal stability of LNPs is essential not only for the success of the biocatalytic reaction, but also for the extraction processes utilized in the separation of products and the catalyst for subsequent reuse.
In this work, we present the successful immobilization of PLD on stabilized LNPs obtained from hydroxymethylated lignin by direct adsorption without use of any crosslinkers. The immobilized PLD was studied with particular attention paid to enzyme recycling in the biotransformation of PC in three natural high-value polar head-modified phospholipids (as illustrated in Scheme 2): phosphatidylglycerol (PG), phosphatidylserine (PS) and phosphatidylethanolamine (PE). These phospholipids were selected for their commercial value due to their peculiar properties. The first product, PG, present in mammalian membranes in a small percentage (1–2% of the total phospholipids),[60] is highly prevalent in mammalian lungs and its concentration in amniotic fluid is used to evaluate the fetal lung maturity and assess the risk of respiratory distress syndrome in new-borns. Therefore, new surfactants preparations based on PG derivatives for therapeutic treatments of this disease are highly requested. The second compound, PS, localized especially in the brain, presents many nutritional and medical functions being involved in many neurological processes.[61-62] The assumption of PS has been linked to positive benefits in terms of mind and memory enhancement: in particular it reduces age-related decline in mental function, it prevents Alzheimer's and dementia, it is considered a stress reducer and a mood enhancer to cure depression, and it improves athletic performance. Finally the third product PE is interesting owing to its association with Alzheimer, Parkinson and non-alcoholic liver diseases, as well as with the virulence of certain pathogenic organisms.[63-64] Moreover, PE could provide beneficial effects to human health because it presents good antioxidant activity against free radicals and has a significant influence on the heart to prevent cell damage.[65]
The present results indicate that stabilized LNPs effectively adsorb PLD and allow efficient biocatalytic transformation of natural phosphatidylcholine into the aforementioned target products. Overall, HLNPs are a safe and biodegradable material readily prepared from lignin, which is an inexpensive commodity. Thus, PLD-c-HLNPs can be regarded as a new, chemically stable, recyclable and user-friendly biocatalyst to be employed in sustainable chemical processes for phospholipids preparation.

2. Results and Discussion

2.1. Lignin Hydroxymethylation

Our work started with the preparation of stabilized lignin nanoparticles (LNPs) for enzyme immobilization. A commercially available and previously fully characterized wheat straw/Sarkanda grass lignin (Protobind 1000)[66] was used as the starting raw material for the preparation of stabilized cured HLNPs (c-HLNPs) as depicted in Figure 1.

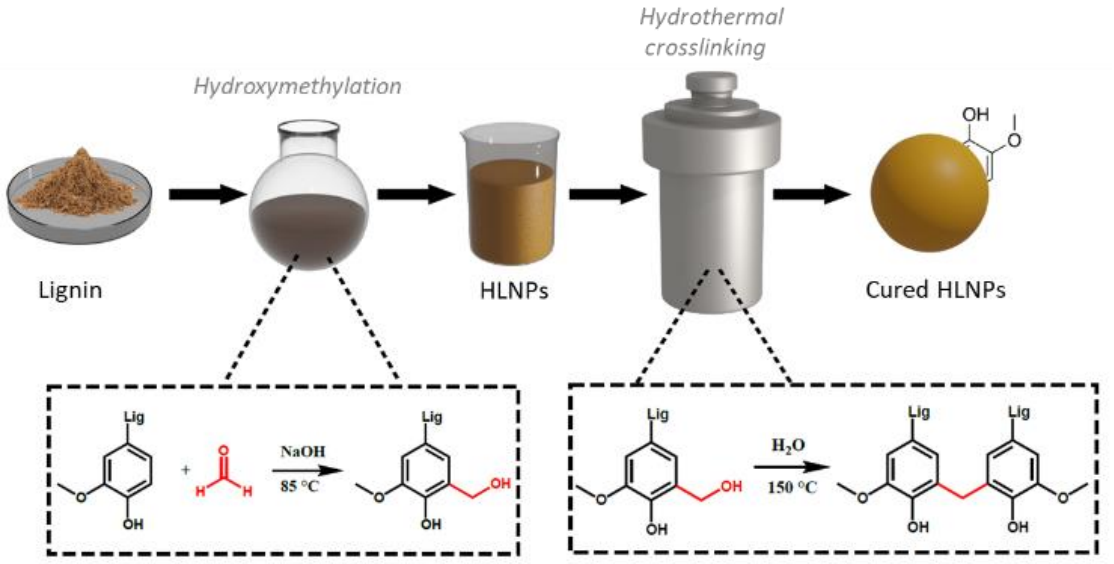

Figure 1: Illustration of the process for the preparation of stabilized c-HLNPs.

In the first step, formaldehyde reacted with lignin at the position 5 of the aromatic ring in an alkaline medium, but some side reaction such as Tollens and Cannizzaro reactions and condensation could take place (reported in Figure S1). For these reasons, several parameters had to be considered: lignin structure, time and temperature. First, it is known that the hydroxymethylation reaction is strongly dependent on the lignin skeleton, in particular on its monolignols composition. In fact, because of its heterogeneous and complex structure, lignin has a low reactivity, and the active site is not available in all aromatic rings.[67-68] Also, the hydroxymethylation is strongly dependent on the temperature and time of reaction, since undesired condensation reactions could take place at higher temperature and longer time. In our study, the successful hydroxymethylation of lignin was confirmed by FTIR and ^{31}P NMR analyses. FTIR spectra showed a broad band absorption in the region of 3400-3200 cm^{-1} which was related to the stretching vibrations of the aliphatic and phenolic O-H groups but the increase in the hydroxyl content was compatible with the increase of the absorbance at 3350 cm^{-1} in hydroxymethylated lignin (HL) spectrum (Figure 2a). The increase also of the signals in the region of 3050-2800 cm^{-1} associated with the C-H bonding stretching in the methyl and methylene groups was also diagnostic. Moreover, the lignin modification was notable by the decrease of the signal at 1112 cm^{-1} corresponding to the presence of guaiacyl-syringyl units, the change at 1452 cm^{-1} typical of C-H deformations of asymmetric methyl and methylene, and the appearance of a shoulder at 1290 cm^{-1} corresponding to the increase in guaiacyl units.[69-70] The hydroxymethylation was also confirmed by the ^{31}P NMR results (all spectra reported in Figure S2), as shown in Figure 2b by the increase in the aliphatic hydroxyl content of the hydroxymethylated lignin, and the increase/decrease in the G units with substituted and vacant 5-positions, respectively.

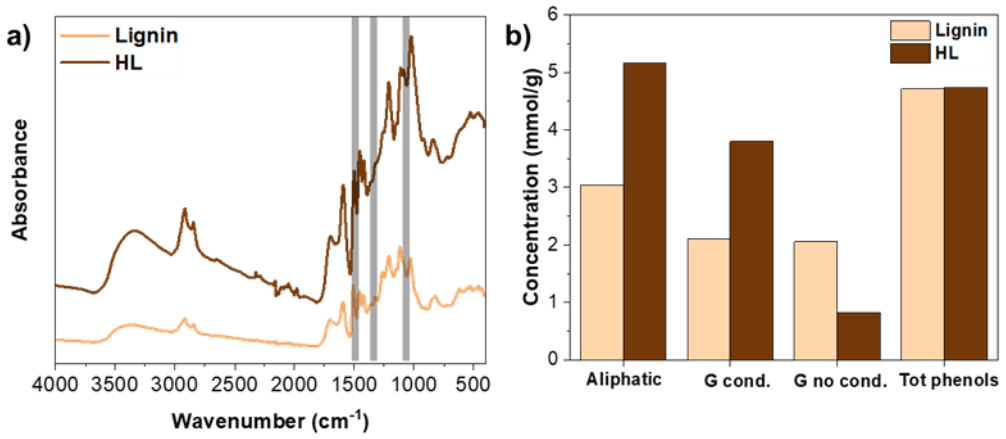

Figure 2: Chemical characterization of LNPs and HLNPs. (a) FTIR spectra of lignin (in light brown) and hydroxymethylated lignin (HL, in brown). (b) Results of quantitative hydroxyl analysis by ^{31}P NMR spectroscopy of lignin (in light brown) and hydroxymethylated lignin (HL, in brown); cond= condensed.

2.2. Preparation of HLNPs from Hydroxymethylated Lignin

After dissolution of hydroxymethylated lignin in a mixture of acetone/water 3/1, HLNPs were prepared by precipitation with the addition of deionized water. After filtration to remove possible aggregates, the recovered HLNPs displayed smaller particle size compared to the regular LNPs (Figure 3a). This observation is consistent with the previous literature based only on Kraft lignin.[71-72] In particular, the size of the LNPs from this kind of lignin is known to decrease with the increasing aliphatic hydroxyl content, and it is also confirmed for LNPs from Protobind lignin, which is a lignin with different chemical and physical properties respect to Kraft.

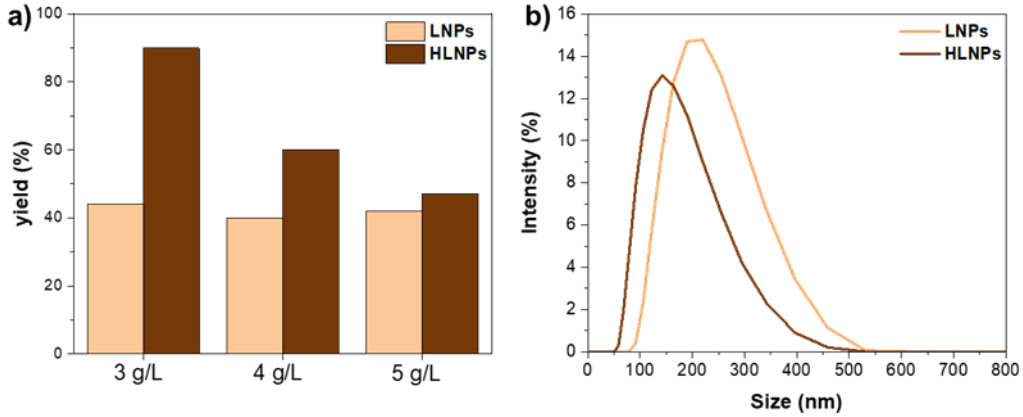

Figure 3: (a) Yields of nanoparticles formation at different lignin concentrations (3, 4 and 5 g/L) for the preparation of LNPs (in light brown) and HLNPs (in brown). (b) Particle size distribution (DLS) of LNPs (in light brown) and HLNPs (in brown) at 3 g/L.

To increase resistance of HLNPs to organic solvents and to a wide range of pH values we carried out a curing step to stabilize the HLNPs via intraparticle curing (see Figure 1). So, the resistance of HLNPs and their cured counterparts (c-HLNPs) to withstand a shift from pH 5 to pH 10 (selected range further investigated in PLD activity assays) was tested with DLS analysis, by monitoring their dimensions and polydispersity (PDI) during a 24 h time period after the addition of an aqueous pH 10 buffer. As reported in Figure 4a, c-

HLNPs showed a high stability over time in a pH range from 5 to 10, with stable size and PDI. In contrast, uncured HLNPs were rapidly disrupted at pH 10, leading to an irregular size distribution and a high PDI (Figure 4b). This was also visible in the images included in the two graphs: c-HLNPs at basic pH could be recovered by precipitation, while the uncured ones immediately disaggregated probably due to their quite total dissolution. Moreover, in addition to alkaline stability, c-HLNPs appeared stable in organic solvents, such as ethanol, acetone, hexane and toluene. This is a crucial factor for their application in biocatalysis, in particular in phospholipids enzymatic transformations since the reactions took place in a biphasic environment (organic solvent-buffer solution). The morphology of the c-HLNPs recovered after incubation at basic pH for 24 h was also analyzed by SEM, showing spherical and intact colloidal particles (see Figure 4c).

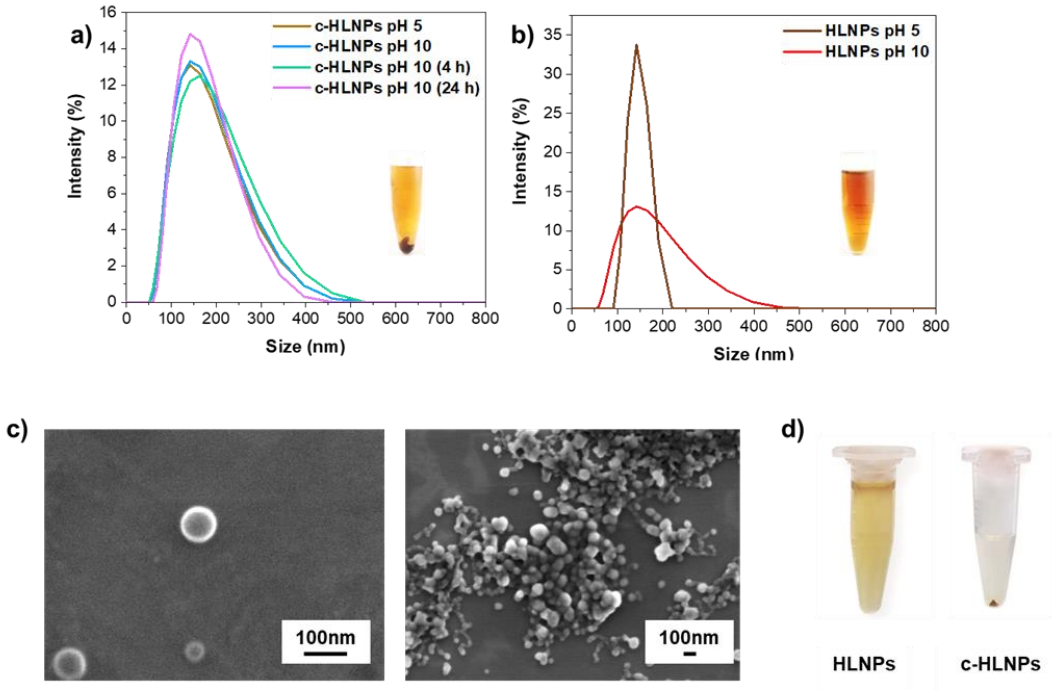

Figure 4: Stability analysis of HLNPs and c-HLNPs. (a) Kinetic of stability for c-HLNPs at pH 10 over 24h in comparison of the HLNPs at pH 5 (the picture inside the graph shows the appearance of c-HLNPs at pH 10 after centrifugation). (b) DLS analysis of HLNPs (not cured) at pH 5 and at pH 10 (the picture inside the graph shows the appearance of HLNPs at pH 10 after centrifugation). (c) SEM image of c-HLNPs at pH 10 (the scale bar in the picture down legend corresponds to 100 nm). (d) Photographs of HLNPs and c-HLNPs suspended in acetone after centrifugation.

2.3. Phospholipase D Immobilization

2.3.1. Phospholipase D Activity

The PLD activity was measured from the fermentation broth (PLD_B), the dialyzed broth (PLD_D) and the freeze-dried preparation (PLD_{DL}) and the results are reported in Table 1. The enzyme obtained post-dialysis (PLD_D) showed a higher activity than the broth itself, due to the performed enzyme precipitation (0.3 vs 0.14 U/mL). However, if we compare the immobilized enzymes, PLD_D-c-HLNPs showed an activity almost equal to the PLD_B-c-HLNPs, probably because a plateau in enzyme immobilization capacity on the c-HLNPs was reached. A confirmation of the occurred immobilization was also given by

the measurement of the activity of the supernatants sampled after the enzyme had been immobilized on c-HLNPs. In fact, the PLD_B activity of the supernatant was 0.08 U/mL and 0.04 U/mL for PLD_D-c-HLNPs, i.e., only 25% and 13% of the corresponding total activities assayed in the supernatant and pellet fractions. It should be pointed out that the supernatants could contain smaller lignin nanoparticles which could be responsible of residual enzymatic activity into these fractions. Furthermore, the immobilized lyophilized PLD (PLD_{DL}-c-HLNPs) showed an activity of 0.43 U/mL, much higher than the immobilized PLD_B/PLDD, thanks to the enzyme concentration step. For PLD_{DL}-c-HLNPs the low residual activity of the recovered supernatant after immobilization (0.04 U/mL) was consistent with the results obtained for PLD_B and PLD_D immobilization, and attested that PLD tended to adsorb on c-HLNPs.

Table 1: Comparison of the PLD activity in free enzyme preparations and in their immobilized forms on c-HLNPs (fermentation broth (PLD_B), immobilized fermentation broth (PLD_B-c-HLNPs), broth post dialysis (PLD_D) and immobilized broth post dialysis (PLD_D-c-HLNPs), lyophilized PLD (PLD_{DL}) and immobilized lyophilized PLD (PLD_{DL}-c-HLNPs).

Free enzyme			**Immobilized enzyme on c-HLNPs (PLD_X-c-HLNPs)**			
Composition	**Acronym**	**Activity**	**Acronym**	**Activity**	**Supernatant activity**	**Retained activity**
Fermentation broth	PLD_B	0.14 U/mL	PLD_B-c-HLNPs	0.26 U/mL	0.08 U/mL	75%
Dialyzed broth	PLD_D	0.30 U/mL	PLD_D-c-HLNPs	0.23 U/mL	0.04 U/mL	87%
Lyophilized enzyme	PLD_{DL}	0.026 U/mg	PLD_{DL}-c-HLNPs	0.43 U/mL	0.04 U/mL	91%

The increase in PLD activity after immobilization has to refer to PLD conformation once it is adsorbed on LNPs surface. In fact, as reported in literature, the enzyme, once its immobilized, loses its flexibility and its 3D structure becomes rigid in the hyperactivated form.[73] The immobilization was also confirmed by the FTIR analysis (Figure 5a), since the spectrum for free PLD_{DL} (reported in light green) and PLD_{DL}-c-HLNPs (dark green) both showed several diagnostic peaks. In particular, there are four main characteristic signals: (i) CONH peptide linkage at 1650 cm^{-1}; (ii) the presence of COC groups at 1100 cm^{-1}; (iii) NH bending signal for amine I in the area between 1650 and 1580 cm^{-1}; (iv) CN stretching typical for aliphatic amine between 1250 and 1020 cm^{-1}. Moreover, the DLS size distribution showed that the immobilization increased the particle diameter compared to the original HLNPs (c-HLNPs: 120 nm; PLD_{DL}-c-HLNPs: 200 nm).

2.3.2. Concentration Effect

The effect of the enzyme concentration was tested to determine the best condition in which almost all the enzyme could be immobilized without losing activity. We tested several different enzyme concentrations in lignin particle dispersions: 9%, 12%, 17%, 20% and 23% v/v (PLD/HLNPs suspension). The results showed that, when the 17% v/v of PLD (equivalent to 48 µg PLD_{DL}/g c-HLNPs and to 1.18% PLD_{DL}/lignin w/w) was immobilized, a plateau was reached and the addition of more enzyme provoked a decrease in the recovered activity (Figure 5b). Most likely, after the level of 17% v/v, all the surfaces of c-HLNPs were covered, and the enzyme started to form multilayers, covering the active site of the enzyme underneath, and causing a decrease in the activity. By

increasing the concentration of PLD, also the activity of the supernatant decreased proving that the enzyme was almost completely immobilized (Figure 5b).

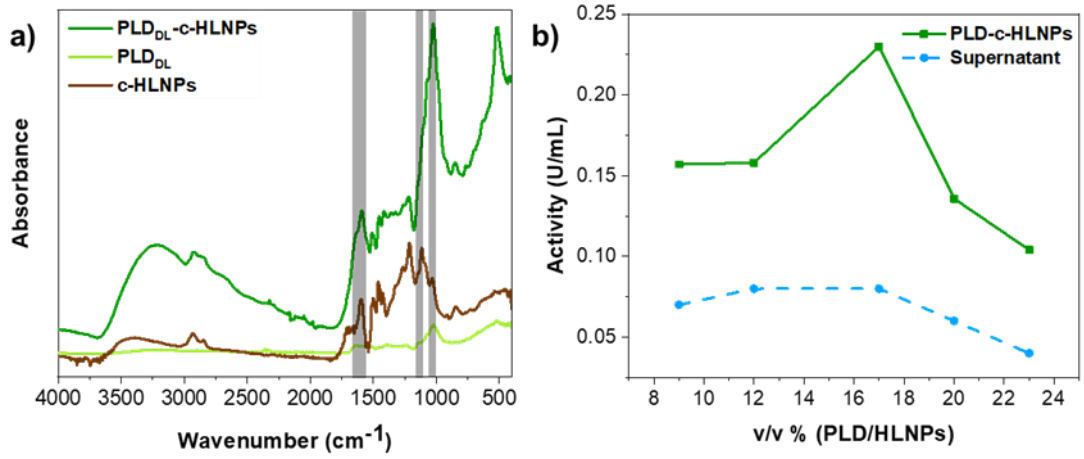

Figure 5: (a) FTIR spectra of PLD_{DL} (in light green), c-HLNPs (in brown) and PLD_{DL}-c-HLNPs (in dark green); (b) Activity (U/mL) of PLD-c-HLNPs (in dark green) and supernatant (in blue) obtained after enzyme immobilization.

2.3.3. Temperature and pH Effect

Temperature and pH were tested to select the best parameters for the biocatalytic transformations. The temperature dependence of the enzymatic activity on PC was assayed in the 10-70 °C range at pH 8. As reported in Figure 6a, PLD-c-HLNPs showed the highest activity at 40 °C. Though the temperature optimum was similar to that of the free PLD, the immobilized enzyme was markedly more active, with almost two-fold activity in comparison to the value obtained for the free enzyme. Concerning the influence of pH on enzymatic activity, PLD-c-HLNPs tested in the 2-13 pH range appeared to be more active at pH 4 whereas the free enzyme was more active at pH 6 (Figure 6b). Also, in this case, the PLD-c-HLNPs were markedly more active than the free enzyme across the pH range. The increase in PLD activity after immobilization even when it is submitted to not-optimal conditions of temperature and pH are due to the fact that the enzyme conformation, once it is immobilized, remains stable, lose the flexibility, overcome its fragile nature, and even tolerate extreme reaction environments such as extreme pH and temperatures.

These results are particularly interesting since the transphosphatidylation reactions reported in this paper are performed at 40 °C and at pH 5.6 (phosphatidylglycerol and phosphatidylethanolamine) and 4.5 (phosphatidylserine). As shown by Figure 6, PLD-c-HLNPs activity is particularly higher at these conditions, and even higher than the free enzyme, making phosphatidylcholine transphosphatidylation particularly advantageous.

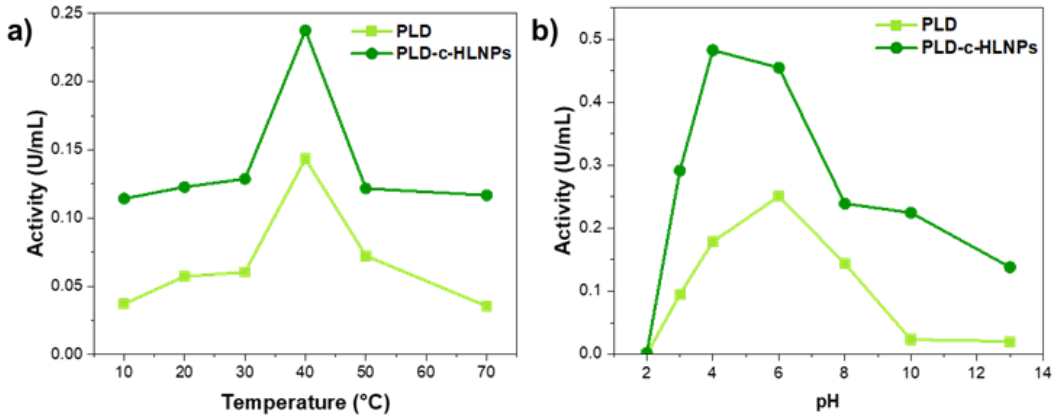

Figure 6: (a) Activity (U/mL) of PLD and PLD-c-HLNPs in a range of temperatures between 10 to 70 °C; (b) Activity (U/mL) of PLD and PLD-c-HLNPs in a pH range from 2 to 13 at 40 °C.

2.4. Enzymatic Synthesis of Polar Head-Modified Phospholipids

Our ultimate objective in the present work, as discussed in the Introduction, was to study the possibility to exploit the immobilized PLD on c-HLNPs in the enzymatic transformation of natural PC investigating a new protocol for the production of three important polar head-modified phospholipids (PXs), namely phosphatidylglycerol (PG), phosphatidylserine (PS) and phosphatidylethanolamine (PE). In these compounds the choline residue of PC is substituted by a glycerol, a L-serine and an ethanolamine moiety respectively (see Scheme 1). For that purpose, purified PC from soya beans was used as substrate. Because of its natural source, the major acyl chain pattern of PC resulted in a mixture of palmitic (C16:0) and linoleic (C18:2) acid chains as previously reported (see Figure S3).[22] PC and the corresponding alcohols (glycerol, L-serine and ethanolamine) were converted into PXs by PLD_{DL}-c-HLNPs in a biphasic system at 40 °C. At the end of each synthetic cycle, after centrifugation of the reaction mixtures, the final products PXs were easily recovered with high yields that in the case of PG and PS exceeded 90%, while for PE it reached 60% (Figure 7). The final products were analyzed by ESI/MS in order to check their high purity and the complete transformation of the starting substrate PC.

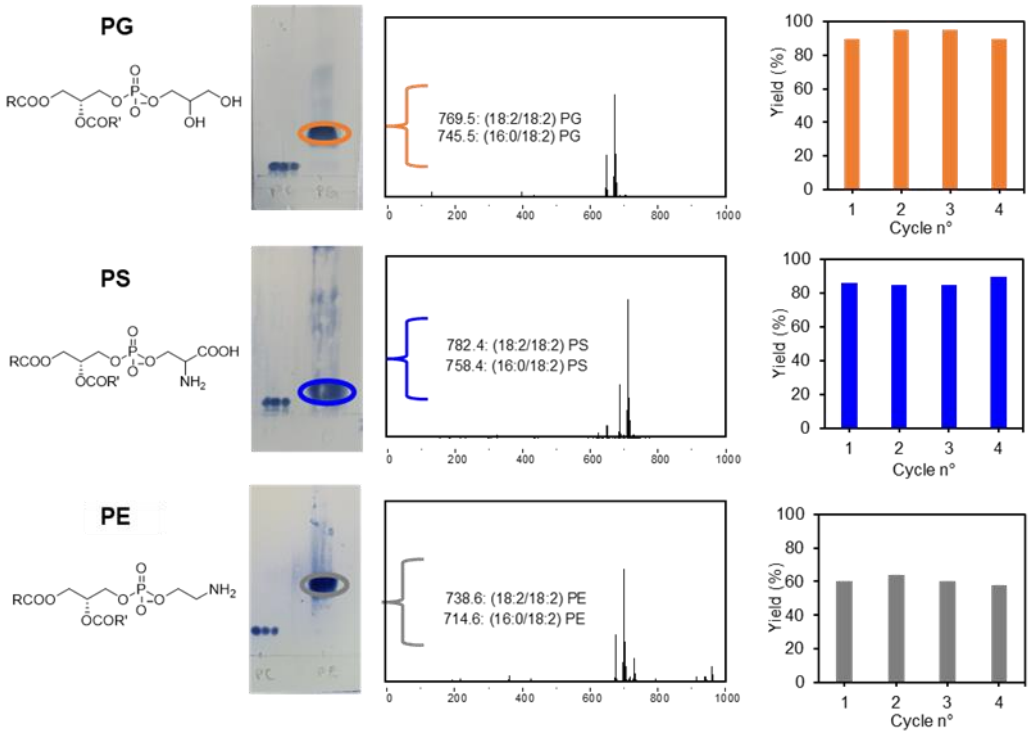

Figure 7: Structure, characterization (TLC and ESI/MS spectra) and yield of production (over 4 cycles) of phosphatidylglycerol (PG), phosphatidylserine (PS) and phosphatidylethanolamine (PE).

The spectra of all the products obtained after four recycling steps are reported in Figure 8 (with PC spectrum for comparison). The supported enzyme preparations were, inside each PX preparation, successfully completely recycled with high activity retention over four synthetic cycles (complete ESI/MS spectra are reported in Figures S4, S5, S6 for PG, PS and PE respectively). It is important to underline that this method of enzyme immobilization allowed, compared to the previously cited literature, to recover the desired products in high yields (consistently with our previous works),[74] constantly over the cycles, and that the enzyme activity remained quite unchanged without losing efficiency. Moreover, the immobilized enzyme showed a higher activity respect to the free one, allowing to reduce the reaction times. These factors make the system suitable for the immobilization and recyclability of the enzyme, paving the way for further investigations for different biocatalytic processes.

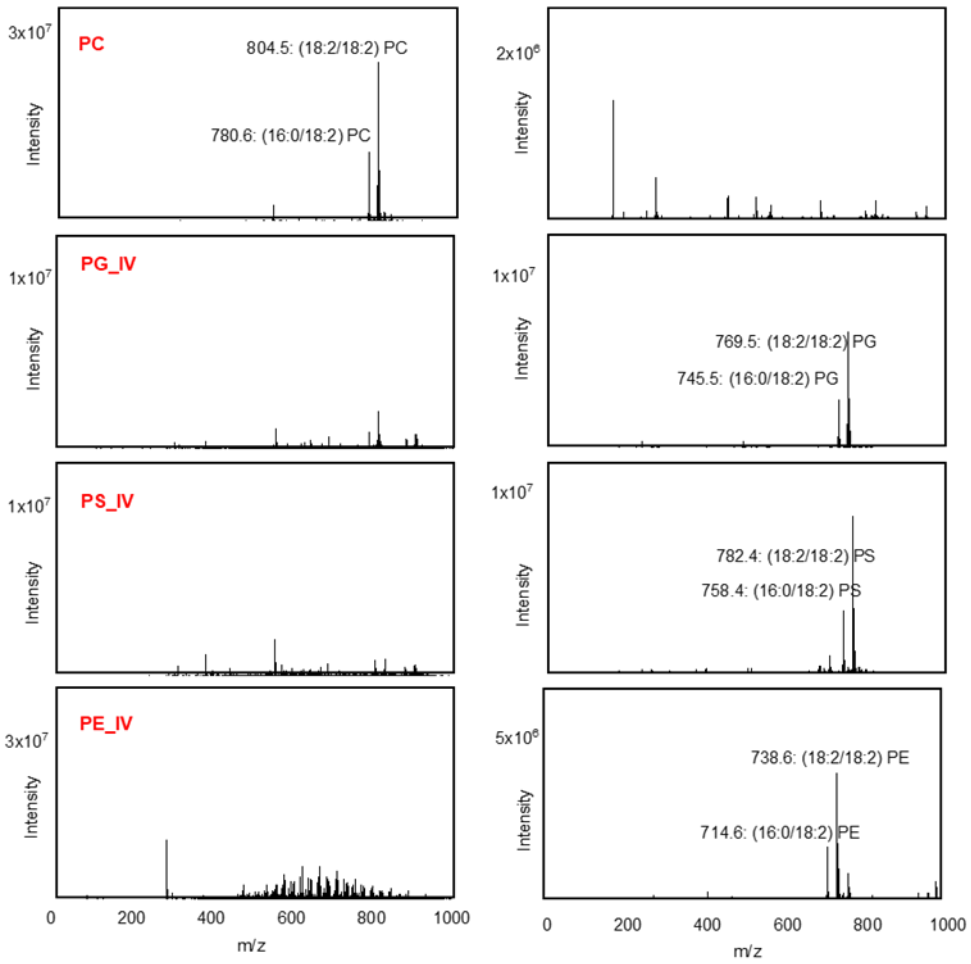

Figure 8: ESI/MS of starting PC and of final PG, PS and PE products obtained with PLD-HLNPs in the fourth step (indicated as PX_IV) of recycling. On the left side the positive ions spectra are reported, on the right side the negative ones.

2.5. Comparison of PLD Immobilization on c-HLNPss and Other Supports

In literature, PLD has been immobilized on different supports, such as magnetic nanoparticles and porous materials. In particular, Li *et al.*[75] immobilized PLD on silicon dioxide nanoparticles using solvent precipitation and glutaraldehyde as cross-linker; Han *et al.*[59] reported the PLD immobilization on silica-coated magnetic nanoparticles only by direct adsorption; finally Li *et al.*[76] synthetized PS by PLD immobilized on an inorganic hierarchical porous material prepared via a template-free approach. All these aforementioned methods resulted in an increased enzyme activity, enhancing its stability over a wide range of temperatures and pH and allowed recycling of the enzyme. In comparison to these works, our technique allows to immobilize PLD on a low-cost, renewable scaffold without the addition of cross-linker, while still increasing the enzyme performance. In fact, the enzyme recovery rate after immobilization was high (>75%), and PLD increased its activity of almost two times at the optimal pH and temperature. These are positive results when compared to the literature. In fact, in Li *et al.* work, thanks to the immobilization on silicon dioxide nanoparticles, PLD activity increased of 1.15 times; while in Han *et al.* one, PLD activity remained constant at the reaction conditions (40 °C, pH 6.2), and the enzyme recovery late was less than 60%. In addition, in Li et

Han works, it is notable a shifting of optimal temperature and pH which no longer correspond to the conditions at which the transphosphatidylation reactions are performed. Instead, in this study PLD preserved its optimal reaction conditions, without shifting of temperature, allowing to perform the transphosphatidylation reactions at 40 °C, as previously reported in literature.[74]

2.6. Green Metric Parameters

This study perfectly reflects the Green Chemistry principles firstly introduced by P.T. Anastas and J.C. Warner in 1998.[77] In this scenario, we calculated some of these parameters to prove the greenness of this technique. In particular, E- factor (g of waste/g product), Atom Economy (Mw product/Mw reagents), productivity (g product/g enzyme/h) and PMI (kg of raw material/kg of products) have been evaluated for all the three products, and they are reported here below. In general, these results show that the reported method produces a low amount of waste and the reaction efficiency is good.

Table 2: Measurements of E-Factor (=mass wastes/mass product) for phosphatidylglycerol (PG), phosphatidylserine (PS) and phosphatidylethanolamine (PE).

Waste	**Quantity**
Glycerol	2.62 g
Serine	2.52 g
Ethanolamine	0.074 g
Phospholipase D	0.03 g
Toluene	3.46 g
Products	
Phosphatidylglycerol	0.038 g
Phosphatidylserine	0.032 g
Phosphatidylethanolamine	0.030 g
E-Factor PG	93.9
E-Factor PS	110.92
E-Factor PE	116.37

Table 3: Measurements of Atom Economy (=Mw product/Mw reagents) for phosphatidylglycerol (PG), phosphatidylserine (PS) and phosphatidylethanolamine (PE).

Reagents	**Mw (g/mol)**
Phosphatidylcholine	776
Choline	104.17
Glycerol	92.10
Serine	105.09
Ethanolamine	61.08
Products	
Phosphatidylglycerol	762.9
Phosphatidylserine	775.91
Phosphatidylethanolamine	731.9
Atom Economy PG	88%
Atom Economy PS	88%
Atom Economy PE	87%

Table 4: Measurements of productivity (=g product/g enzyme/h) for phosphatidylglycerol (PG), phosphatidylserine (PS) and phosphatidylethanolamine (PE).

Products	Quantity
Phosphatidylglycerol	0.038 g
Phosphatidylserine	0.032 g
Phosphatidylethanolamine	0.030 g
Enzyme	
Phospholipase D	0.030 g
Time	24 h x 4 = 96 h
Productivity PG	0.013
Productivity PS	0.011
Productivity PE	0.010

Table 5: Measurements of PMI (=g raw materials/g product) for phosphatidylglycerol (PG), phosphatidylserine (PS) and phosphatidylethanolamine (PE).

Raw materials	Quantity
Phosphatidylcholine	0.04 g
Glycerol	2.62 g
Serine	2.52 g
Ethanolamine	0.074 g
Toluene	3.46 g
Water	5.00 g
Phospholipase D	0.03 g
Products	
Phosphatidylglycerol	0.038 g
Phosphatidylserine	0.032 g
Phosphatidylethanolamine	0.030 g
PMI PG	0.80
PMI PS	0.94
PMI PE	1.01

3. Conclusion

In this work, we performed the immobilization of an expensive enzyme on a sustainable scaffold which has been exploited in the production of high value polar head-modified phospholipids. In particular biobased stabilized nanoparticles were obtained by the precipitation of an hydroxymethylated technical lignin followed by a successive hydrothermal curing step. These c-HLNPs appeared to be stable in organic solvents and at different pH values and were exploited for the immobilization of the expensive enzyme PLD by a facile adsorption process, without the use of covalent crosslinking reactions. The PLD-c-HLNPs system was exploited for the production of phospholipids of high commercial interest such as phosphatidylglycerol, phosphatidylserine, and phosphatidylethanolamine showing even higher catalytic efficiency than free PLD. The method allowed the efficient recycling of PLD and high reaction yields (60-90%), without losing its activity for four cycles. The present work thus constitutes a new sustainable approach for the biocatalytic preparation of polar head-modified phospholipids exploiting lignin nanoparticles as a valuable biobased and inexpensive tool for PLD immobilization, paving the way to the exploitation of this procedure in other biocatalytic processes, in particular when expensive enzymes are required.

4. Experimental section

All chemicals, solvents and enzymes (choline oxidase and peroxidase) were purchased from Merck (Merck Life Science S.r.l., Milan, Italy) and used as received without further purification. Phosphatidylcholine (PC) was supplied from Lucas Meyer (Epikuron 200, soy lecithin) and used after purification by precipitation in cold acetone (10 g of Epikuron 200 dissolved in 15 mL of hexane, added to 300 mL of cold acetone). ^{1}H NMR and ^{31}P NMR spectra were recorded on a 400 MHz Bruker Avance spectrometer (Milano, Italy). Acquisition and data treatment were performed with Bruker TopSpin 3.2 software. Chemical shifts were reported in δ units (ppm), all spectra were recorded in $CDCl_3/CD_3OD$. Deuterated solvents were purchased from Eurisotop (Saint-Aubin, France). Protobind 1000 (a mixed wheat straw/sarkanda grass lignin from soda pulping of non-woody biomass) was purchased from Tanovis (Alpnach, Switzerland) and will be indicated as lignin.

4.1. PLD Preparation

4.1.1. Microrganism Fermentation

PLD from *Streptomyces* was obtained from the fermentation broth of *Streptomyces netropsis* (DSM 40093) as reported in our previous works (see Figure 3).[74] The medium for strain growth and maintenance was composed of glucose 4 g/L; yeast extract 5 g/L; malt extract 10 g/L whereas the medium for PLD preparation contained glucose 5 g/L, yeast extract 5 g/L, malt extract 10 g/L, peptone from soybean 3 g/L, peptone from casein 1 g/L, $MgSO_4$ 0.2 g/L, NaCl 0.2 g/L. The fermentation was performed aerobically, setting a minimum air flow of 2 L/min (0.5 v/v/min), in a sterilized fermenter vessel of a 5 L bioreactor (Biostat A BB-8822000, Sartorius Stedim, Göttingen, Germany) containing 4 L of medium. Temperature, stirring speed, and pH were set to 30 °C, 250 rpm and 7.0, respectively. pH value was controlled by addition of sterilized aqueous solutions (10% w/w in water) of either acetic acid or ammonia. After 48 h, the fermentation broth was filtered through a celite pad, and the clear liquid was stored at 4 °C in dark bottles.

4.1.2. Precipitation and Dialysis

To 1 L of the filtered broth, 430 g of ammonium sulfate were added over 1 h at 4 °C under stirring. After its dissolution, the broth was left precipitating overnight at 4 °C. After 24 h, the pellet was recovered by centrifugation at 8000 rpm for 15 min at 4 °C. The solid was then dissolved in a small amount of supernatant broth and dialyzed with a seamless cellulose tube (D0655 Sigma-Aldrich, Milano, Italy) against 10 mM sodium acetate buffer at pH 5. The dialyzed broth (100 mL), which had an activity of 0.30 U/mL, was finally lyophilized (0.026 U/mg, see Figure S1 for the scheme of PLD preparation).

4.2. Thin Layer Chromatography (TLC)

TLC plates Silica gel 60 SIL G-25 UV254 glass 250 μm (Macherey Nagel) were used for analytical TLC. The eluent was constituted by $CHCl_3/CH_3OH/CH_3COCH_3/CH_3COOH/H_2O$: 50/10/20/10/5 (ratios reported in volume). Detection was performed by staining with cerium molybdate reagent and 0.2% ethanolic ninhydrin solution (TLC reported in Figure S8).

4.3. Electrospray Ionization Mass Spectrometry (ESI/MS)

Mass spectra were recorded on an ESI/MS Bruker Esquire 3000 PLUS (ESI Ion Trap LC/MSn System, Bruker, Milano, Italy), by direct infusion of a dichloromethane solution of compounds with an infusion rate of 4 μL/min. Samples were analyzed using both positive and negative ionization modes to allow the detection of all relevant compounds.

4.4. Preparation of Hydroxymethylated Lignin

Hydroxymethylated lignin (HL) was prepared using an existing method as reported in Morsali *et al*..[71] Briefly, in a round bottom glass, 8.75 mL of deionized water and 11.25 mL of aqueous sodium hydroxide (1 M, 11.25 mmol) were added to 5 g of dry lignin to dissolve lignin at pH 10.5 in room temperature. Then 5 mL of formaldehyde solution (37% formaldehyde, 66 mmol) was added dropwise to the lignin solution and temperature was increased to 85 °C. The reaction was allowed to take place for 4 h. Subsequently, deionized water was used to quench the reaction and the pH was adjusted to 3 with addition of 0.1 M hydrochloric acid drop by drop. The product was centrifuged and washed 3 times with deionized water to remove extra acid and formed salts. The purified products were freeze-dried to collect dry HL.

4.5. Preparation of Nanoparticles from Hydroxymethylated Lignin (HLNPs)

HL (430 mg) was dissolved in acetone/water mixture 3/1 (9.37 g/3.12 g) and let stirring 2 h. Then the sample was filtered to remove the impurities, and the LNPs were produced by quickly pouring deionized water (37 mL) to the lignin solution while stirring. Subsequently acetone was removed by evaporation, and the final aqueous dispersion of HLNPs was obtained by filtration to remove possible aggregates. HLNPs (yield 80%) were diluted to the final concentration of 5 g/L on a total volume of 40 mL. The colloidal dispersion of HLNPs (5 g/L) was hydrothermally cured in a Teflon-sealed reactor at 150 °C overnight to give cured HLNPs (reported as c-HLNPs).

4.6. Dynamic Light Scattering (DLS)

The particle size and zeta potential of HLNPs and PLD-HLNPs were measured using a Zetasizer Nano ZS90 instrument (Malvern Instruments Ltd., UK). Zeta potential was determined using a dip cell probe. Measurements were carried out with three replicates of the particle diameter (Z-average, intensity mean) and zeta potential, and the mean values were used for the study.

4.7. Fourier Transform Infrared Spectroscopy (FTIR)

FTIR data were collected using a Varian 610-IR FTIR spectrometer. The IR absorbance of samples was measured using an attenuated total reflection–Fourier transform infrared spectrophotometer (ATR-FTIR) in the 450-4000 cm^{-1} wavenumber range.

4.8. Scanning Electron Microscopy (SEM)

SEM imaging was conducted using a JEOL JSM-7401F (JEOL Ltd., Japan) using a secondary electron detector. Samples for imaging were diluted 50 times using deionized water and drop-casted on a silicon wafer.

4.9. ^{31}P Nuclear Magnetic Resonance Spectroscopy (^{31}P NMR)

Quantitative analysis of hydroxyl groups of lignin and HL was conducted using ^{31}P NMR spectroscopy following the known procedure.[78] Briefly, the samples (30 mg) were phosphitylated with 2-chloro-4,4,5,5-tetramethyl-1,3,2-dioxaphospholane (0.9 mmol) in the presence of N-hydroxy-5-norbornene-2,3-dicarboxylic acid imine (0.010 mmol) as an internal standard and chromium(III) acetylacetonate as a relaxation agent. The ^{31}P NMR experiments (256 scans, 10 s relaxation delay) were performed with 90° pulse angle and inverse gated proton decoupling (reported in Figure S2).

For phospholipids analysis, 50 mg of sample were dissolved by vigorous stirring with 5 mg of triphenyl phosphate in 0.6 mL of a $CDCl_3$/CH_3OH 2/1 solution mixed with 0.4 mL of a CsEDTA solution (prepared by titration of 0.2 M EDTA in D_2O with $CsCO_3$ until pH 7.6, then diluted 1:4 (v/v) with methanol). After complete solubilization, water (0.2 mL) was added and the solution was stirred again. The solution was transferred into an NMR tube and left to rest in order to achieve the correct separation of the two liquid phases. The ^{31}P uncoupled experiments were performed with the following parameters: D1: 10 s, SW: 40 ppm, O1: -10 ppm, FID size: 32768, ns: 32, T: 320 K.

4.10. Enzyme Immobilization

4.10.1. Fermentation Broth Immobilization (PLD_B-c-HLNPs)

The fermentation broth (PLD_B) was added dropwise to 5 mL of c-HLNPs (5 g/L) suspension under stirring at different concentrations. The mixture was let stirring for 2 h and then centrifuged 3 times at 8000 rpm for 10 min each. The collected supernatant was centrifuged once at 10000 rpm for 15 min to recover the smallest nanoparticles which were then added to the first precipitate and were labelled as PLD_B-c-HLNPs.

4.10.2. Dialysed Broth Immobilization (PLD_D-c-HLNPs)

The concentrated fermentation broth (PLD_D), coming from the dialysis process, was added dropwise to 5 mL of c-HLNPs (5 g/L) suspension under stirring at different concentration. The mixture was stirred for 2 h and then centrifuged 3 times at 8000 rpm x 10 min. The collected supernatant was centrifuged once more at 10000 rpm x 15 min to recover the smallest nanoparticles which were then added to the first precipitate and were labelled as PLD_D-c-HLNPs.

4.10.3. Lyophilized Broth Immobilization (PLD_{DL}-c-HLNPs).

Lyophilized PLD (PLD_{DL}) was immobilized on c-HLNPs by dissolving the enzyme powder at different concentrations in deionized water. Then 1 mL of the enzyme solution was added dropwise to 5 mL of c-HLNPs (5 g/L) suspension under stirring. The mixture was stirred for 2 h and then centrifuged 3 times at 8000 rpm x 10 min. The collected supernatant was centrifuged once at 10000 rpm x 15 min to recover the smallest nanoparticles which were then added to the previous precipitate and were labelled as PLD_{DL}-c-HLNPs.

4.11. PLD Activity Determination

The activity was measured following a standard procedure.[79] Briefly 50 mg of PC were dissolved in 2 mL of Triton-X 10% v/v and 2 mL of buffer TRIS 0.1 M pH 8 (indicated

as buffer T in the present section). 3 mg/mL of 4-aminoantipyrine and 2 mg/mL of phenol were dissolved in buffer T and then mixed together and diluted with buffer T until a final volume of 14.6 mL was reached (Solution A). Choline oxidase was dissolved in buffer T at final concentration of 50 U/mL, while peroxidase at final concentration of 100 U/mL. A solution of $CaCl_2$ 0.1 M in buffer T was also prepared. For each measurement 134 µL of PC were mixed to 34 µL of $CaCl_2$ solution and 10 µL of enzyme. The sample was left stirring 10 min at 40 °C. Then 700 µL of Solution A, 67 µL of peroxidase and 67 µL of choline oxidase were added. If the enzyme was immobilized on the nanoparticles, the suspension was centrifuged before UV analysis. The analyses were performed at λ of 550 nm for 20 min with a UV-Vis Double Beam Spectrophotometer V-730 Jasco (Jasco Europe, Cremella, Italy). The enzymatic activity was calculated with the expression here below:

$$U/mL = [(\Delta Abs/min + Vf) / (\varepsilon \times Ve)] \times D$$

where Vf = cuvette total volume (mL); ε = 6 (M-1cm-1); Ve = enzyme volume (mL); D = dilution factor.

For each experiment, when immobilized PLD and the free enzyme are compared, they have been used in the same amount.

4.12. Concentration-Activity Relationship for PLD-c-HLNPs

The PLD-c-HLNPs system activity was measured by immobilizing different concentrations of enzyme on the c-HLNPs, ranging from 9% to 23% v/v% (PLD/c-HLNPs). The activities of the supernatants were also tested. However, it is important to precise that these last values could be overestimated by the presence of the smallest c-HLNPs which may remain suspended in the supernatants despite the centrifugation steps.

4.13. Temperature-Activity Relationship for PLD-c-HLNPs

The temperature dependence of PLD-c-HLNPs activity was investigated towards PC performing the incubation of the reaction mixture thermostated at temperatures ranging from 10 to 70 °C. Then, after the centrifugation for enzyme recovery, the sample was analysed with the activity test described above.

4.14. pH-Activity Relationship for PLD-c-HLNPs

The pH dependence of the PLD-c-HLNPs activity towards PC was determined by incubating the reaction mixture using the appropriate 0.1 M buffer for 10 min at 40 °C in the 2-13 range adjusted to the appropriate pH with HCl or NaOH. Then, after the centrifugation for enzyme recovery, the sample was analysed with the activity test described above.

4.15. Enzymatic Preparation of Phosphatidylglycerol (PG)

30 mg of lyophilized PLD (0.026 U/mg) were dissolved in 1 mL of 0.1 M sodium acetate buffer pH 5.6 and 0.1 M of calcium chloride, and added dropwise to 5 mL of c-HLNPs (5 g/L). After 2 h, 8 M glycerol was added and the solution brought to pH 5.6 by addition of acetic acid. The solution was added to PC (10 mg) preliminary dissolved in 1 mL of toluene. The reaction was left under stirring at 40 °C for 24 h. Then the two phases were

separated by centrifugation at 8000 rpm 2 min, and the aqueous phase was extracted twice with toluene (2 x 5 mL). The organic phases were collected, dried with sodium sulfate and the solvent was evaporated under reduced pressure. The PLD-c-HLNPs system was collected and recycled for 4 cycles, adding for each of them fresh PC. No addition of glycerol was required. The 3rd and the 4th cycles were left under stirring at 40 °C for 30 h and 48 h respectively to obtain the major conversion of the substrate into PG. For each cycle, the product was recovered in a mass yield of 85-90%. ^{1}H NMR (spectrum reported in Figure S9): 0.75-0.85 (m, 6H, CH_3), 1.15-1.36 (m, 30 H, CH_2 acyl chains), 1.48-1.60 (m, 4H, $\underline{CH_2}$-CH_2-COO), 1.92-2.04 (m, 5 H, $\underline{CH_2}$-CH=CH), 2.18-2.29 (m, 4H, $\underline{CH_2}$-COO), 2.67-2.77 (m, 3H, CH=CH-$\underline{CH_2}$-CH=CH), 3.50-3.66 (m, 2H, CHOH-$\underline{CH_2}$OH), 3.74-4.00 (m, 5H, O$\underline{CH_2}$-CH-$\underline{CH_2}$-OPO_3 and $\underline{CH}$OH-CH_2OH), 4.05-4.15 (m, 1H, OPO_3-$\underline{CH_2}$), 4.28-4.38 (m, 1H, OPO_3-$\underline{CH_2}$), 5.10-5.21(m, 1H, OCH_2-$\underline{CH}$-CH_2-OPO_3), 5.23-5.38 (m, 6H, CH=CH). ESI/MS negative ion spectrum (reported in Figure S4): m/z 16:0/18:2-PG $[745.5]^-$, 18:2/18:2-PG $[769.5]^-$. ^{31}P NMR δ: 0.51 ppm.

4.16. Enzymatic Preparation of Phosphatidylserine (PS)

30 mg of lyophilized PLD (0.026 U/mg) were dissolved in 1 mL of 0.1 M sodium acetate buffer pH 4.5 and 0.1 M of calcium chloride, and added dropwise to 5 mL of c-HLNPs (5 g/L). After 2 h, 3 M L-serine was added and the solution brought to pH 4.5 by addition of acetic acid. The solution was added to PC (10 mg) preliminary dissolved in 1 mL of toluene. The reaction was left at 40 °C under stirring for 24 h. Then the two phases were separated by centrifugation at 8000 rpm for 2 min, and the aqueous phase was extracted with toluene (2 x 5 mL). The organic phases were collected, dried with sodium sulfate and the solvent was evaporated under reduced pressure. The PLD-c-HLNPs system was collected and recycled for 4 cycles, by addition every time of a fresh solution of PC. No further addition of L-serine was required. The 3rd and the 4th cycles were left under stirring at 40 °C for 30 h and 48 h respectively to obtain the major conversion of the substrate into PS. For each cycle, the final product was recovered in a mass yield of 85%. ^{1}H NMR (spectrum reported in Figure S10): 0.75-0.86 (m, 6H, CH_3), 1.17-1.37 (m, 28 H, CH_2 acyl chains), 1.49-1.63 (m, 4H, $\underline{CH_2}$-CH_2-COO), 1.89-2.04 (m, 6 H, $\underline{CH_2}$-CH=CH), 2.18-2.28 (m, 4H, $\underline{CH_2}$-COO), 2.63-2.77 (m, 3H, CH=CH-$\underline{CH_2}$-CH=CH), 3.14-3.19 (CH_3-N-CH_2 residual PC), 3.51-3.62 (m, 1H, CH_2-$\underline{CH}$-NH_2), 3.77-3.97 (m, 4H, $\underline{OCH_2}$-CH-$\underline{CH_2}$-OPO_3), 4.05-4.14 (m, 1H, OPO_3-$\underline{CH_2}$), 4.30-4.40 (m, 1H, OPO_3-$\underline{CH_2}$),5.12-5.22 (m, 1H, OCH_2-CHO-$\underline{CH_2}$-OPO_3), 5.23-5.40 (m, 6H, CH=CH). ESI/MS negative ion spectrum (reported in Figure S5): m/z 16:0/18:2-PS $[758.4]^-$, 18:2/18:2-PS $[782.4]^-$. ^{31}P NMR δ: -0.05 ppm.

4.17. Enzymatic Preparation of Phosphatidylethanolamine (PE)

30 mg of lyophilized PLD (0.026 U/mg) were dissolved in 1 mL of 0.1 M sodium acetate buffer pH 5.6 and 0.1 M of calcium chloride, and added dropwise to 5 mL of c-HLNPs (5 g/L). After 2 h, 2 M ethanolamine was added and the solution brought to pH 5.6 by addition of acetic acid. The solution was added to PC (10 mg) preliminary dissolved in 1 mL of toluene. The reaction was left under stirring at 40 °C for 24 h. Then the two phases were separated by centrifugation at 8000 rpm 2 min, and the aqueous phase was extracted with toluene (2 x 5 mL). The organic phases were collected, dried with sodium sulfate and the solvent was evaporated under reduced pressure. The PLD-c-HLNPs system was collected and recycled for 4 cycles, adding for each of them fresh PC. No addition of

ethanolamine was required. The 3rd and the 4th cycles were left under stirring at 40 °C for 30 h and 48 h respectively to obtain the major conversion of the substrate into PE. For each cycle, the product was recovered in a mass yield of 50-60%. ^{1}H NMR (spectrum reported in Figure S11): 0.79-0.90 (m, 6H, CH_3), 1.15-1.37 (m, 30 H, CH_2 acyl chains), 1.49-1.63 (m, 4H, $\underline{CH_2}$-CH_2-COO), 1.97-2.06 (m, 5 H, $\underline{CH_2}$-CH=CH), 2.20-2.34 (m, 4H, $\underline{CH_2}$-COO), 2.68-2.82 (m, 2H, CH=CH-$\underline{CH_2}$-CH=CH), 3.70-4.09 (m, 6H, $\underline{OCH_2}$-CH-$\underline{CH_2}$-OPO_3 and O-CH_2-$\underline{CH_2}$- NH_2), 4.09-4.17 (m, 1H, OPO_3-$\underline{CH_2}$), 4.30-4.40 (m, 1H, OPO_3-$\underline{CH_2}$), 5.15-5.24 (m, 1H, OCH_2-$\underline{CH}$-CH_2-OPO_3), 5.24-5.41 (m, 5H, CH=CH). ESI/MS spectra (reported in Figure S6): m/z 16:0/18:2-PE $[716.6]^+$, 18:2/18:2-PE $[740.7]^+$, 16:0/18:2- PE $[714.6]^-$, 18:2/18:2-PE $[738.6]^-$. ^{31}P NMR δ: 0.02 ppm.

Supporting Information

Figure S1: Reaction of lignin hydroxymethylation and its side reactions; Figure S2: ^{31}P NMR of lignin and HL; Figure S3: ESI/MS of PC; Figure S4-S6: ESI/MS of the four recycling steps in PG, PS and PE synthesis; Figure S7: Scheme of preparation of PLD_B, PLD_D and PLD_{DL}; Figure S8: TLC of the main products; Figure S9-S11: ^{1}H NMR of PG, PS and PE.

References

1. Drescher, S.; van Hoogevest, P., The phospholipid research center: Current research in phospholipids and their use in drug delivery. *Pharmaceutics* **2020,** *12* (12), 1235.
2. Wang, B.; Tontonoz, P., Phospholipid remodeling in physiology and disease. *Annual review of physiology* **2019,** *81*, 165-188.
3. Falconi, M.; Ciccone, S.; D'Arrigo, P.; Viani, F.; Sorge, R.; Novelli, G.; Patrizi, P.; Desideri, A.; Biocca, S., Design of a novel LOX-1 receptor antagonist mimicking the natural substrate. *Biochemical and Biophysical Research Communications* **2013,** *438* (2), 340-345.
4. Ventura, R.; Martínez-Ruiz, I.; Hernández-Alvarez, M. I., Phospholipid Membrane Transport and Associated Diseases. *Biomedicines* **2022,** *10* (5), 1201.
5. Ahmmed, M. K.; Ahmmed, F.; Tian, H. S.; Carne, A.; Bekhit, A. E., Marine omega-3 (n-3) phospholipids: A comprehensive review of their properties, sources, bioavailability, and relation to brain health. *Compr Rev Food Sci Food Saf* **2020,** *19* (1), 64-123.
6. Baldassarre, F.; Allegretti, C.; Tessaro, D.; Carata, E.; Citti, C.; Vergaro, V.; Nobile, C.; Cannazza, G.; D'Arrigo, P.; Mele, A., Biocatalytic synthesis of phospholipids and their application as coating agents for CaCO3 nano–crystals: characterization and intracellular localization analysis. *ChemistrySelect* **2016,** *1* (20), 6507-6514.
7. D'Arrigo, P.; Scotti, M., Lysophospholipids: synthesis and biological aspects. *Current Organic Chemistry* **2013,** *17* (8), 812-830.
8. Küllenberg, D.; Taylor, L. A.; Schneider, M.; Massing, U., Health effects of dietary phospholipids. *Lipids in health and disease* **2012,** *11*, 1-16.
9. Wang, C. C.; Du, L.; Shi, H. H.; Ding, L.; Yanagita, T.; Xue, C. H.; Wang, Y. M.; Zhang, T. T., Dietary EPA-Enriched Phospholipids Alleviate Chronic Stress and LPS-Induced Depression-and Anxiety-Like Behavior by Regulating Immunity and Neuroinflammation. *Molecular nutrition & food research* **2021,** *65* (17), 2100009.
10. Hayes, D. G.; Smith, G. A., Biobased surfactants: overview and industrial state of the art. *Biobased surfactants* **2019**, 3-38.
11. Liu, W.; Liu, K.; Du, H.; Zheng, T.; Zhang, N.; Xu, T.; Pang, B.; Zhang, X.; Si, C.; Zhang, K., Cellulose Nanopaper: Fabrication, Functionalization, and Applications. *Nanomicro Lett* **2022,** *14* (1), 104.
12. Aldosari, B. N.; Alfagih, I. M.; Almurshedi, A. S., Lipid nanoparticles as delivery systems for RNA-based vaccines. *Pharmaceutics* **2021,** *13* (2), 206.
13. D'Arrigo, P.; Giordano, C.; Macchi, P.; Malpezzi, L.; Pedrocchi-Fantoni, G.; Servi, S., Synthesis, platelet adhesion and cytotoxicity studies of new glycerophosphoryl-containing polyurethanes. *The International Journal of Artificial Organs* **2007,** *30* (2), 133-143.

14. Massing, U.; Eibl, H., New optically pure dimethylacetals of glyceraldehydes and their application for lipid and phospholipid synthesis. *Chemistry and physics of lipids* **1995,** *76* (2), 211-224.
15. Fasoli, E.; Arnone, A.; Caligiuri, A.; D'Arrigo, P.; de Ferra, L.; Servi, S., Tin-mediated synthesis of lyso-phospholipids. *Organic & Biomolecular Chemistry* **2006,** *4* (15), 2974-2978.
16. D'Arrigo, P.; Fasoli, E.; Pedrocchi-Fantoni, G.; Rossi, C.; Saraceno, C.; Tessaro, D.; Servi, S., A practical selective synthesis of mixed short/long chains glycerophosphocholines. *Chemistry and physics of lipids* **2007,** *147* (2), 113-118.
17. D'Arrigo, P.; de Ferra, L.; Pedrocchi-Fantoni, G.; Scarcelli, D.; Servi, S.; Strini, A., Enzyme-mediated synthesis of two diastereoisomeric forms of phosphatidylglycerol and of diphosphatidylglycerol (cardiolipin). *Journal of the Chemical Society, Perkin Transactions 1* **1996,** (21), 2657-2660.
18. Juneja, L. R.; Hibi, N.; Inagaki, N.; Yamane, T.; Shimizu, S., Comparative study on conversion of phosphatidylcholine to phosphatidylglycerol by cabbage phospholipase D in micelle and emulsion systems. *Enzyme and Microbial Technology* **1987,** *9* (6), 350-354.
19. Struzik, Z. J.; Biyani, S.; Grotzer, T.; Storch, J.; Thompson, D. H., Synthesis of Phosphatidyl Glycerol Containing Unsymmetric Acyl Chains Using H-Phosphonate Methodology. *Molecules* **2022,** *27* (7), 2199.
20. D'Arrigo, P.; Servi, S., Using phospholipases for phospholipid modification. *Trends in Biotechnology* **1997,** *15* (3), 90-96.
21. Allegretti, C.; Denuccio, F.; Rossato, L.; D'Arrigo, P., Polar head modified phospholipids by phospholipase D-catalyzed transformations of natural phosphatidylcholine for targeted applications: an overview. *Catalysts* **2020,** *10* (9), 997.
22. Allegretti, C.; Gatti, F. G.; Marzorati, S.; Rossato, L. A. M.; Serra, S.; Strini, A.; D'Arrigo, P., Reactive Deep Eutectic Solvents (RDESs): A new tool for phospholipase D-catalyzed preparation of phospholipids. *Catalysts* **2021,** *11* (6), 655.
23. Carrea, G.; D'Arrigo, P.; Secundo, F.; Servi, S., Purification and applications of a phospholipase D from a new strain of Streptomyces. *Biotechnology letters* **1997,** *19*, 1083-1085.
24. D'Arrigo, P.; Cerioli, L.; Chiappe, C.; Panzeri, W.; Tessaro, D.; Mele, A., Improvements in the enzymatic synthesis of phosphatidylserine employing ionic liquids. *Journal of Molecular Catalysis B: Enzymatic* **2012,** *84*, 132-135.
25. Duan, Z.-Q.; Hu, F., Highly efficient synthesis of phosphatidylserine in the eco-friendly solvent γ-valerolactone. *Green Chemistry* **2012,** *14* (6), 1581-1583.
26. Qin, W.; Wu, C.; Song, W.; Chen, X.; Liu, J.; Luo, Q.; Liu, L., A novel high-yield process of phospholipase D-mediated phosphatidylserine production with cyclopentyl methyl ether. *Process Biochemistry* **2018,** *66*, 146-149.
27. Bi, Y.-H.; Duan, Z.-Q.; Du, W.-Y.; Wang, Z.-Y., Improved synthesis of phosphatidylserine using bio-based solvents, limonene and p-cymene. *Biotechnology letters* **2015,** *37*, 115-119.
28. Bié, J.; Sepodes, B.; Fernandes, P. C.; Ribeiro, M. H., Enzyme immobilization and co-immobilization: Main framework, advances and some applications. *Processes* **2022,** *10* (3), 494.
29. Lewis, N. G.; Yamamoto, E., Lignin: occurrence, biogenesis and biodegradation. *Annual review of plant biology* **1990,** *41* (1), 455-496.
30. Bajwa, D.; Pourhashem, G.; Ullah, A. H.; Bajwa, S., A concise review of current lignin production, applications, products and their environmental impact. *Industrial Crops and Products* **2019,** *139*, 111526.
31. Bertella, S.; Luterbacher, J. S., Lignin functionalization for the production of novel materials. *Trends in Chemistry* **2020,** *2* (5), 440-453.
32. Ekielski, A.; Mishra, P. K., Lignin for bioeconomy: The present and future role of technical lignin. *International journal of molecular sciences* **2020,** *22* (1), 63.
33. Korányi, T. I.; Fridrich, B.; Pineda, A.; Barta, K., Development of 'Lignin-First'approaches for the valorization of lignocellulosic biomass. *Molecules* **2020,** *25* (12), 2815.
34. Yadav, V. K.; Gupta, N.; Kumar, P.; Dashti, M. G.; Tirth, V.; Khan, S. H.; Yadav, K. K.; Islam, S.; Choudhary, N.; Algahtani, A., Recent advances in synthesis and degradation of lignin and lignin nanoparticles and their emerging applications in nanotechnology. *Materials* **2022,** *15* (3), 953.
35. Moreno, A.; Liu, J.; Morsali, M.; Sipponen, M. H., Chemical modification and functionalization of lignin nanoparticles. In *Micro and Nanolignin in Aqueous Dispersions and Polymers*, Elsevier: 2022; pp 385-431.
36. Ma, M.; Dai, L.; Xu, J.; Liu, Z.; Ni, Y., A simple and effective approach to fabricate lignin nanoparticles with tunable sizes based on lignin fractionation. *Green Chemistry* **2020,** *22* (6), 2011-2017.
37. Iravani, S.; Varma, R. S., Greener synthesis of lignin nanoparticles and their applications. *Green Chemistry* **2020,** *22* (3), 612-636.

38. Zhao, W.; Simmons, B.; Singh, S.; Ragauskas, A.; Cheng, G., From lignin association to nano-/micro-particle preparation: extracting higher value of lignin. *Green Chemistry* **2016,** *18* (21), 5693-5700.
39. Pang, T.; Wang, G.; Sun, H.; Wang, L.; Liu, Q.; Sui, W.; Parvez, A. M.; Si, C., Lignin fractionation for reduced heterogeneity in self-assembly nanosizing: Toward targeted preparation of uniform lignin nanoparticles with small size. *ACS Sustainable Chemistry & Engineering* **2020,** *8* (24), 9174-9183.
40. Agustin, M. B.; Penttila, P. A.; Lahtinen, M.; Mikkonen, K. S., Rapid and direct preparation of lignin nanoparticles from alkaline pulping liquor by mild ultrasonication. *ACS Sustainable Chemistry & Engineering* **2019,** *7* (24), 19925-19934.
41. Petrie, F. A.; Gorham, J. M.; Busch, R. T.; Leontsev, S. O.; Ureña-Benavides, E. E.; Vasquez, E. S., Facile fabrication and characterization of kraft lignin@ Fe3O4 nanocomposites using pH driven precipitation: Effects on increasing lignin content. *International journal of biological macromolecules* **2021,** *181*, 313-321.
42. Pylypchuk, I.; Sipponen, M. H., Organic solvent-free production of colloidally stable spherical lignin nanoparticles at high mass concentrations. *Green Chemistry* **2022,** *24* (22), 8705-8715.
43. Beisl, S.; Adamcyk, J.; Friedl, A., Direct precipitation of lignin nanoparticles from wheat straw organosolv liquors using a static mixer. *Molecules* **2020,** *25* (6), 1388.
44. Camargos, C. H.; Rezende, C. A., Antisolvent versus ultrasonication: Bottom-up and top-down approaches to produce lignin nanoparticles (LNPs) with tailored properties. *International Journal of Biological Macromolecules* **2021,** *193*, 647-660.
45. Tribot, A.; Amer, G.; Alio, M. A.; de Baynast, H.; Delattre, C.; Pons, A.; Mathias, J.-D.; Callois, J.-M.; Vial, C.; Michaud, P., Wood-lignin: Supply, extraction processes and use as bio-based material. *European Polymer Journal* **2019,** *112*, 228-240.
46. Lievonen, M.; Valle-Delgado, J. J.; Mattinen, M.-L.; Hult, E.-L.; Lintinen, K.; Kostiainen, M. A.; Paananen, A.; Szilvay, G. R.; Setälä, H.; Österberg, M., A simple process for lignin nanoparticle preparation. *Green Chemistry* **2016,** *18* (5), 1416-1422.
47. Henn, A.; Mattinen, M.-L., Chemo-enzymatically prepared lignin nanoparticles for value-added applications. *World Journal of Microbiology and Biotechnology* **2019,** *35*, 1-9.
48. Schneider, W. D. H.; Dillon, A. J. P.; Camassola, M., Lignin nanoparticles enter the scene: A promising versatile green tool for multiple applications. *Biotechnology Advances* **2021,** *47*, 107685.
49. Capecchi, E.; Piccinino, D.; Delfino, I.; Bollella, P.; Antiochia, R.; Saladino, R., Functionalized Tyrosinase-Lignin Nanoparticles as Sustainable Catalysts for the Oxidation of Phenols. *Nanomaterials (Basel)* **2018,** *8* (6).
50. Zhang, Z.; Terrasson, V.; Guénin, E., Lignin nanoparticles and their nanocomposites. *Nanomaterials* **2021,** *11* (5), 1336.
51. Cavalcante, F. T.; Cavalcante, A. L.; de Sousa, I. G.; Neto, F. S.; dos Santos, J. C., Current status and future perspectives of supports and protocols for enzyme immobilization. *Catalysts* **2021,** *11* (10), 1222.
52. Bilal, M.; Asgher, M.; Cheng, H.; Yan, Y.; Iqbal, H. M., Multi-point enzyme immobilization, surface chemistry, and novel platforms: a paradigm shift in biocatalyst design. *Critical reviews in biotechnology* **2019,** *39* (2), 202-219.
53. Muthuvelu, K. S.; Rajarathinam, R.; Selvaraj, R. N.; Rajendren, V. B., A novel method for improving laccase activity by immobilization onto copper ferrite nanoparticles for lignin degradation. *International journal of biological macromolecules* **2020,** *152*, 1098-1107.
54. Piccinino, D.; Capecchi, E.; Botta, L.; Bollella, P.; Antiochia, R.; Crucianelli, M.; Saladino, R., Layer by layer supported laccase on lignin nanoparticles catalyzes the selective oxidation of alcohols to aldehydes. *Catalysis Science & Technology* **2019,** *9* (15), 4125-4134.
55. Capecchi, E.; Piccinino, D.; Tomaino, E.; Bizzarri, B. M.; Polli, F.; Antiochia, R.; Mazzei, F.; Saladino, R., Lignin nanoparticles are renewable and functional platforms for the concanavalin a oriented immobilization of glucose oxidase–peroxidase in cascade bio-sensing. *RSC Advances* **2020,** *10* (48), 29031-29042.
56. Moreno, A.; Sipponen, M. H., Biocatalytic nanoparticles for the stabilization of degassed single electron transfer-living radical pickering emulsion polymerizations. *Nature Communications* **2020,** *11* (1), 5599.
57. Mao, S.; Zhang, Z.; Ma, X.; Tian, H.; Lu, F.; Liu, Y., Efficient secretion expression of phospholipase D in Bacillus subtilis and its application in synthesis of phosphatidylserine by enzyme immobilization. *International Journal of Biological Macromolecules* **2021,** *169*, 282-289.
58. Han, Q.; Zhang, H.; Sun, J.; Liu, Z.; Huang, W.-c.; Xue, C.; Mao, X., Immobilization of phospholipase D on silica-coated magnetic nanoparticles for the synthesis of functional phosphatidylserine. *Catalysts* **2019,** *9* (4), 361.

59. Zhang, Y.; Zhu, L.; Wu, G.; Wang, X.; Jin, Q.; Qi, X.; Zhang, H., Design of amino-functionalized hollow mesoporous silica cube for enzyme immobilization and its application in synthesis of phosphatidylserine. *Colloids and Surfaces B: Biointerfaces* **2021,** *202*, 111668.
60. Furse, S., Is phosphatidylglycerol essential for terrestrial life? *J Chem Biol* **2017,** *10* (1), 1-9.
61. Kim, H. Y.; Huang, B. X.; Spector, A. A., Phosphatidylserine in the brain: metabolism and function. *Prog Lipid Res* **2014,** *56*, 1-18.
62. Glade, M. J.; Smith, K., Phosphatidylserine and the human brain. *Nutrition* **2015,** *31* (6), 781-786.
63. Calzada, E.; Onguka, O.; Claypool, S. M., Phosphatidylethanolamine Metabolism in Health and Disease. *International review of cell and molecular biology* **2016,** *321*, 29-88.
64. Patel, D.; Witt, S. N., Ethanolamine and Phosphatidylethanolamine: Partners in Health and Disease. *Oxid Med Cell Longev* **2017,** *2017*, 4829180.
65. Cui, L.; McClements, D. J.; Decker, E. A., Impact of phosphatidylethanolamine on the antioxidant activity of α-tocopherol and trolox in bulk oil. *Journal of Agricultural and Food Chemistry* **2015,** *63* (12), 3288-3294.
66. Allegretti, C.; Fontanay, S.; Rischka, K.; Strini, A.; Troquet, J.; Turri, S.; Griffini, G.; D'Arrigo, P., Two-step fractionation of a model technical lignin by combined organic solvent extraction and membrane ultrafiltration. *ACS omega* **2019,** *4* (3), 4615-4626.
67. Paananen, H.; Alvila, L.; Pakkanen, T. T., Hydroxymethylation of softwood kraft lignin and phenol with paraformaldehyde. *Sustainable Chemistry and Pharmacy* **2021,** *20*, 100376.
68. Gilca, I. A.; Ghitescu, R. E.; Puitel, A. C.; Popa, V. I., Preparation of lignin nanoparticles by chemical modification. *Iranian Polymer Journal* **2014,** *23*, 355-363.
69. Malutan, T.; Nicu, R.; Popa, V. I., Contribution to the study of hydroxymetylation reaction of alkali lignin. *BioResources* **2008,** *3* (1), 13-20.
70. Faix, O., Classification of lignins from different botanical origins by FT-IR spectroscopy. **1991**.
71. Morsali, M.; Moreno, A.; Loukovitou, A.; Pylypchuk, I.; Sipponen, M. H., Stabilized Lignin Nanoparticles for Versatile Hybrid and Functional Nanomaterials. *Biomacromolecules* **2022,** *23* (11), 4597-4606.
72. Pylypchuk, I. V.; Riazanova, A.; Lindström, M. E.; Sevastyanova, O., Structural and molecular-weight-dependency in the formation of lignin nanoparticles from fractionated soft-and hardwood lignins. *Green Chemistry* **2021,** *23* (8), 3061-3072.
73. Zhao, X.; Guo, M.; Li, X.; Liu, B.; Li, B.; Wang, J., Immobilization of Bio-imprinted Phospholipase D and Its Catalytic Behavior for Transphosphatidylation in the Biphasic System. *Applied Biochemistry and Biotechnology* **2023**, 1-13.
74. Allegretti, C.; Bono, A.; D'Arrigo, P.; Gatti, F. G.; Marzorati, S.; Rossato, L. A.; Serra, S.; Strini, A.; Tessaro, D., Exploitation of Soybean Oil Acid Degumming Waste: Biocatalytic Synthesis of High Value Phospholipids. *ChemistrySelect* **2021,** *6* (34), 9157-9163.
75. Li, B.; Wang, J.; Zhang, X.; Zhao, B., An enzyme net coating the surface of nanoparticles: a simple and efficient method for the immobilization of phospholipase D. *Industrial & Engineering Chemistry Research* **2016,** *55* (40), 10555-10565.
76. Liu, Q.; Yuan, T.; Fu, Q.-j.; Bai, Y.-y.; Peng, F.; Yao, C.-l., Choline chloride-lactic acid deep eutectic solvent for delignification and nanocellulose production of moso bamboo. *Cellulose* **2019,** *26*, 9447-9462.
77. Anastas, P. T.; Warner, J. C., Principles of green chemistry. *Green chemistry: Theory and practice* **1998,** *29*, 14821-42.
78. Moreno, A.; Morsali, M.; Sipponen, M. H., Catalyst-free synthesis of lignin vitrimers with tunable mechanical properties: Circular polymers and recoverable adhesives. *ACS Applied Materials & Interfaces* **2021,** *13* (48), 57952-57961.
79. Imamura, S.; Horiuti, Y., Enzymatic determination of phospholipase D activity with choline oxidase. *The Journal of Biochemistry* **1978,** *83* (3), 677-680.

Conclusion

In this work, the exploitation of different types of DESs has been investigated for the valorization of waste biomasses into high added value compounds, in accordance with the Green Chemistry and Circular Economy principles.

In fact, we presented a deep study about DESs nature and exploitation, showing their versatility as new green solvents. Initially, we exploited the measurement of ^{1}H NMR relaxation time to assess how HBA/HBD ratio and water content could influence the eutecticity of the DES mixture. The presented new methodology compares well in terms of simplicity and machine time with other analytical methods, such as differential scanning calorimetry (DSC).

Furthermore, we demonstrated how, by preparing various combinations of HBA and HBD, DESs can be used for several applications, from biocatalysis to biomass fractionation. For what concern biocatalysis, we presented an innovative approach for the biocatalytic preparation of polar head-modified PLs. In fact, DESs were here used both as solvent and as reactant, enabling the enzymatic preparation of high-value phospholipids of commercial interest easily recovered by precipitation, avoiding the use of organic solvent both in the reaction medium and in the extraction steps.

Regarding biomass fractionation, we set-up a new multistep process for the efficient fractionation of two waste agrifood biomasses, BSG and RH, which allowed the recovery of their main fractions. We have focused particularly on lignin fractions, which were deeply analyzed, tested as precursors of superplasticizers and exploited as starting material for nanoparticles preparation. Thus, we performed the immobilization of an expensive enzyme on a commercial lignin-based scaffold which has been employed in the production of high value polar head-modified PLs.

In the next future, different items will be faced. Firstly, we plan to use our recovered lignins from waste biomasses for the preparation of nanoparticles for PLD immobilization. These new immobilized catalysts will be tested for PLs biotransformation also in DESs media. Moreover, the possibility to immobilize other classes of enzymes on these biobased scaffolds will be tested. Finally, the exploitation of the recovered sugars–enriched fractions derived from the biomass fractionation will be investigated, aiming for a comprehensive valorization of the entire biomass material.

APPENDIX: Executive Summary

The present Executive Summary is part of the final PhD Report presented to the Faculty Board of the PhD programme on 11/09/2023 together with a summary of the work of the third year, the CV and a list of publications.

1. Abstract

This PhD thesis has focused on the study and the exploitation of deep eutectic solvents (DESs), which represent a promising class of new solvents in the context of sustainable processes development. DESs were here deeply studied in their formulation and, thanks to their versatility and specific properties, exploited for two main different applications, biocatalysis and biomass fractionation. In this mainframe we investigated a new method to understand the optimal eutectic composition and the influence of water on DESs properties. In details, ^{1}H NMR relaxation time measurements were exploited to determine the eutectic point of different DESs and the correlation between eutecticity and the amount of water. The first DESs application has been their utilization in the biocatalytic synthesis of polar head modified phospholipids. In particular alcohol-based DESs were exploited both as solvents and as reactants to perform the enzymatic transphosphatidylation of phosphatidylcholine, which constitutes the most abundant natural phospholipid, for the preparation of high value phospholipids. The second application has been the set-up of a multistep DES-mediated process to fractionate two abundant regional agrifood wastes, brewers' spent grain and rice husk, in order to recover and exploit their main fractions, with a particular attention focused on lignin. The recovered lignin fractions have been deeply characterized, and a preliminary evaluation of their potentiality as precursors of cement water reducers gave encouraging results. Finally, lignins were also exploited as starting material for nanoparticles preparation with the final aim of building a sustainable scaffold for enzyme immobilization that could be employed in phospholipids biotransformations.

2. State of the art

2.1. DESs. Deep eutectic solvents (DESs) are described as a binary or ternary mixture between a hydrogen bond donor (HBD) and a hydrogen bond acceptor (HBA) which form a [HBD···HBA] supramolecule. The term "deep eutectic solvent" was first reported by Abbott in 2003,[1] to describe a liquid eutectic mixture with a lower melting temperature than its components, a property derived from the charge delocalization caused by the formation of ion-dipole interactions and hydrogen bonds. The preparation of DESs is straightforward, as it only requires mixing the main components (solid and liquid, or solid and solid) at high temperatures (50-100 °C) for a few hours, until a clear and homogeneous mixture is obtained. DESs are particularly attractive not only for the many possible components combinations and their easy preparation, but also due to their peculiar physicochemical properties, such as low volatility, non-flammability low vapour pressure, chemical and thermal stability, and low toxicity.[2] Despite DESs are studied in many different fields, scientific community is still highly debating about what can be considered a DES and what just a simple mixture of compounds, which are the main parameters to consider in defining a DES, and how the presence of water influences DES formation.

2.2. Phospholipids. One of the biomasses investigated in this research work was the edible residue from the vegetable oil industry, which is particularly rich in phospholipids (PLs),

the main components of natural membranes. From a structural point of view, PLs are amphiphilic compounds that present a glycerol backbone, esterified at *sn-1* and *sn-2* positions with saturated and unsaturated long chain fatty acids, which constitute the lipophilic moieties, and in *sn-3* with a phosphate diester as the polar head group. The composition of acyl chains and polar head group varies depending on the source of PLs and is crucial for their physical and biological properties (see Figure 1).

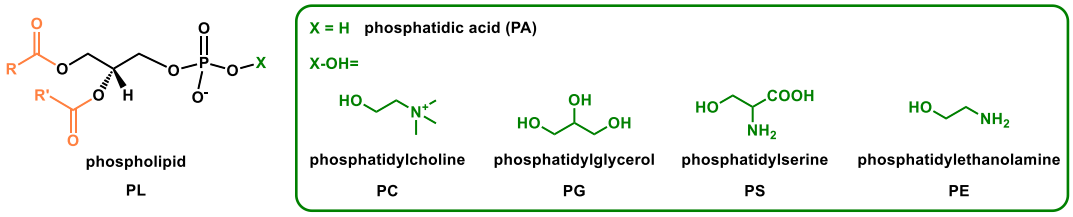

Figure 1: Structure and nomenclature of the main natural phospholipids (RCOOH and R'COOH: long chain fatty acids).

PLs are highly investigated in the biomedical field since they are involved in many cellular processes, and they are also used as nutraceuticals, emulsifiers[3] and food stabilizers. All these applications lead to a strong demand for even new PLs preparation methodologies, and the possibility to prepare different polar head-modified PLs from phosphatidylcholine (PC), which is the most abundant natural PL, constitutes a central point in the research on PLs. Consequently, there is a constant need for novel green strategies to produce these valuable compounds. One such strategy is the use of phospholipase D (PLD, EC 3.1.4.4)[4] which performs the enzymatic transformation of PC in the presence of an alcohol (X-OH), to produce a polar head-modified PL.

2.3. Lignocellulose waste biomasses. Brewer's spent grain (BSG) and rice husk (RH) biomasses are two lignocellulosic materials mainly composed of polysaccharides (cellulose (40-60%) and hemicellulose (20-40%)) and lignin (10-24%) linked together to form a recalcitrant structure, and their percentages vary according to their origin.

BSG is the most abundant by–product of the brewing industry, accounting for 85% w/w of the total solid residues generated,[5] and consists of 15-25% proteins, 50-70% fibers (hemicellulose, cellulose, and lignin), 5-10% fats, and 2-5% ashes. Most frequently, BSG, which is highly degradable, is immediately delivered to neighbouring farms as cattle feed or as a fertilizer in agriculture, but problems arise when breweries are located in heavily urbanized areas or in remote non-agricultural areas. In these cases, BSG cannot be rapidly delivered and has to be disposed of, constituting a waste of resource and a significant cost for the brewery. For these reasons it is necessary to promote the recovery and the treatment of BSG for the obtainment of high added-value products. In fact, its full fractionation could provide precursors for the synthesis of high-value compounds, allowing the maximum exploitation of the whole material. RH is the external hull covering the brown rice grain, and it is the second most abundant by–product in the rice production line, generated during the paddy rice dehusking process. Rice is the second most consumed cereal crop globally, and the annual production of paddy rice is around 755 million tons, 20% of which is treated with parboiling process (a hydrothermal process carried out on the rice grain, which then undergoes the dehusking process) and is called parboiled rice.[6] RH composition depends on many factors, but it is mainly composed by cellulose (29-42%), hemicellulose (14-29%), lignin (13-24%). However, RH differs from other lignocellulosic biomass by its inherently high silica and ash content (10-15%), which makes it suitable for the

production of building materials, as well as for the production of bio–based adsorbents for pollutants removal from wastewater.

3. Aim and Objectives

The final aim of this research work was to explore the use of DESs for treating and valorizing biomasses that are particularly abundant in our region and typically disposed of as wastes. This work fits into the green chemistry and circular economy concepts, which comprehend respectively the utilization of less hazardous solvents and renewable feedstocks, and the creation of a market for secondary raw materials, that can be fed back into the economy as new high value-added compounds. In particular, we chose to focus on the study of DESs, which have gained significant attention within the scientific community thanks to their interesting properties and the natural origin of their main components. Specifically, the present research work has been focused on three main topics:

1- Preparation of DESs and investigation, through NMR experiments, of their nature with a particular focus on the effect of HBD molar ratio and the water influence on DESs structure.

2- Exploitation of DESs in the biocatalytic conversion of a natural phosphatidylcholine into two polar head-modified phospholipids, using phospholipase D as enzyme. In this work these solvents were considered reactive DESs (RDESs) because they were not only the reaction solvents, but also the donors of the alcoholic moiety reacting with the substrate, allowing the preparation of high value-added compounds recovered easily only by filtration, avoiding the use of hazardous organic solvents.

3- Lignocellulosic waste biomass DES-mediated fractionation. Different fractions were recovered (cellulose, hemicellulose and lignin) and in particular lignin was deeply analyzed and tested as water reducers for concrete preparations and as starting material for nanoparticles preparation to be used as bio-based scaffolds for further enzyme immobilization.

4. Programme and Methodology

4.1. DES preparation

DESs were prepared by mixing a HBA (choline chloride, trimethylglycine betaine which from now on will be mentioned as betaine) with a HBD (ethylene glycol, triethylene glycol, 1,3-propandiol, glycerol, L-lactic acid) at different molar ratios, heating under magnetic stirring until a homogeneous and clear liquid phase was obtained. The synthesized DESs were analyzed by ^{1}H NMR.

4.2. ^{1}H NMR spin-lattice relaxation time (T_1)

DESs composed by mixtures of betaine and ethylene glycol, triethylene glycol and 1,3-propandiol were submitted to NMR analysis on an Avance 400 Bruker instrument at 75 °C or at 29 °C, using an automation routine (IconNMR software). ^{1}H-NMR T_1 relaxation times were measured using the Bruker library inversion recovery pulse program (Topspin software, version 2.5). D_2O was used as external lock in coaxial tube (5 mm), and the chemical shift calibration was done on the HDO residual signal. Acquisition and processing parameters: number of scans= 1; relaxation delay d1= 20 s; dummy scans ds= 2; variable delay list (s): 0.1,0.2, 0.3, 0.5, 0.7, 1.0, 1.4, 1.8, 2.3, 2.8, 3.4, 4.1, 5.0, 7.0, 9.0, 12.0, 16.0, 20.0; line broadening lb= 2 Hz. T_1 fittings were obtained using Dynamic Center software, version 2.7.4.

4.3. Enzymatic synthesis of polar head-modified phospholipids

PC was firstly dissolved in RDES (HBA: choline chloride/betaine-HBD: glycerol/ethylene glycol; HBA/HBD in molar ratio 1:2), then buffer 0.1 M of sodium acetate pH 5.6, 0.1 M of calcium chloride, and lyophilized PLD were added to the solution. The mixture was left stirring at 45 °C for 40 h. The product (phosphatidylglycerol or phosphatidylethyleneglycol) precipitated in the reaction mixture and was isolated by filtration, then purified from residual RDES and analyzed by ESI/MS and NMR.

4.4. Lignocellulosic biomasses DES-mediated fractionation

4.4.1. Pretreatments and fractionation

BSG was provided by the Brewery "Orso Verde" from Busto Arsizio (VA, Italy) and, as received, it was brought to dryness in a ventilated oven, ground, suspended in deionized water and heated in an autoclave (121 °C, 15 min). After filtration, the soluble fraction was successfully employed in the preparation of valuable growing media for different microbial fermentations, while the solid residue was dried, leading to BSG_T (treated BSG).

Raw and parboiled RHs, provided by "Riso Scotti" S.p.A., were suspended in distilled water and heated in autoclave. The solid residues, designated respectively as r- and pRH_T (treated RH), were recovered by filtration, while phenyl-propanoid acids were extracted from the aqueous solution.

DES choline chloride/L–lactic acid 1/5 was prepared and biomass was suspended in DES (1/10 w/v) in a round–bottom flask under magnetic stirring at 130 °C for 24 h. After cooling, ethanol was added to precipitate and recover a final cellulose-enriched fraction, and the filtrate was concentrated under vacuum to eliminate the solvent. Water was then added and the suspension was stirred at 4 °C, for 24 h. The obtained precipitate was centrifuged, filtered, and washed three times for 1 h with a solution of water/ethanol 9/1. After centrifugation, filtration, and solvent evaporation, a final solid lignin-enriched fraction was recovered.

4.4.2. Lignins characterization

Lignins extracted from BSG and RHs were characterized by assessing their solubility in different organic solvents, molar mass (GPC), composition (FT-IR), chemical structure (^{31}P NMR, Folin-Ciocalteu assay, bicinchoninic test), thermal behavior (DSC, TGA), and potentiality as precursors of cement water reducers.

4.5. Lignin nanoparticles and enzyme immobilization for phospholipids biotransformation

4.5.1. LNPs preparation and enzyme immobilization

Hydroxymethylated lignin (HL) was prepared by the reaction of lignin and formaldehyde at basic pH for 4 h. Subsequently, HL was used for the preparation of nanoparticles (HLNPs) by its dissolution in acetone/water mixture 3/1, and then by addition of deionized water under stirring to the mixture. Acetone was then removed by evaporation. The obtained colloidal dispersion of HLNPs was hydrothermally cured in a Teflon-sealed reactor at 150 °C overnight to give cured HLNPs (c-HLNPs). All the LNPs were analyzed by Dynamic Light Scattering (DLS) and Scanning Electronic Microscopy (SEM). Successively the enzyme PLD was immobilized by direct adsorption on c-HLNPs and the system (PLD-c-HLNPs) was collected by centrifugation. Its activity was tested and compared to the free enzyme.

4.5.2. Preparation of phosphatidylglycerol, phosphatidylserine and phosphatidylethanolamine

PC was preliminary dissolved in toluene, then the immobilized enzyme, suspended in sodium acetate buffer, was added together with the opportune reagent (glycerol/L-serine /ethanolamine) at the desired pH. The reaction was left under stirring at 40 °C for 24 h. After twice extraction with toluene, the organic phases were collected and evaporated under reduced pressure. PLD-c-HLNPs were collected and recycled for 4 cycles. The final products were analyzed by ^{1}H NMR, ^{31}P NMR and ESI/MS.

5. Results and Discussion

5.1. ^{1}H NMR spin-lattice relaxation time (T_1) studies

DESs based on betaine and ethylene glycol (D1), triethylene glycol (D2) and 1,3-propandiol (D3) were prepared and the correlation between OH T_1 and the diol molar fraction (X) was tested starting from the betaine/ethylene glycol mixtures. The diagram T_1 *versus* X_{D1} exhibited a minimum in correspondence of the molar composition betaine/ethylene glycol = 1:3. Besides, in the *supra* eutectic region, the relaxation time increased linearly as the X_{D1} increased, while, on the other hand, in the *infra* eutectic region of the diagram, the relaxation time became longer as X_{D1} decreased. Finally, the 1:3 eutectic stoichiometry found by OH T_1 measurements was confirmed by differential scanning calorimetry (DSC) analysis, and a eutectic temperature (T_e) of -100 °C was determined. The relaxation time measurements of the betaine/ethylene glycol mixtures were repeated on samples containing three and then six equivalents of water with respect to the HBA. As reported in Figure 2, by adding H_2O the T_1 value at the eutectic point became longer, and the slopes of both regions of the diagram decreased remarkably.

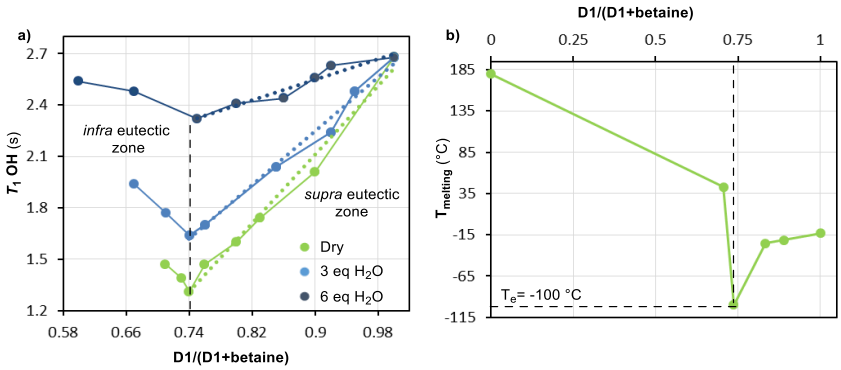

Figure 2: a) Plot of OH T_1 (measured with external lock) *vs* X_{D1} at 75 °C for the betaine/ethylene glycol system. Green solid line: mixtures without addition of water; light blue solid line: addition of 3 eq. of H_2O with respect to betaine; blue-navy solid line: addition of 6 eq. of H_2O with respect to betaine. The dashed lines correspond to the linear regression fitting.
b) DSC analysis: plot of melting point T (°C) *vs* X_{D1}, without addition of water.

These observations suggested that the addition of water reduced the viscosity, while the eutecticity of the system was partially conserved; however, higher concentrations of water promoted the complete dissociation of the eutectic supramolecule in the individual hydrated components. Lastly, we repeated the T_1 measurements for the betaine/triethylene glycol and betaine/1,3-propandiol mixture, and analogously to that observed for the betaine/ethylene glycol system, the OH mobility of each diol decreased linearly to a minimum value in the correspondence of the eutectic point. With this work, we aimed to propose to the scientific community a new tool for the study of optimal DESs composition which we demonstrated to be

comparable in term of time request and simplicity with other standard analytical methods, such as DSC.

5.2. RDES preparation and exploitation for phospholipids transformations

Four different RDESs consisting of mixtures of HBA (choline chloride or betaine)/HBD (glycerol or ethylene glycol) in a 1:2 molar ratio have been prepared with the final aim of transforming natural PC in polar head-modified PLs phosphatidylglycerol (PG) and phosphatidylethyleneglycol (P-EG) (see Figure 3). These PLs were usually prepared from PC in presence of the opportune alcohol by a PLD-mediated process in an organic solvent/buffer biphasic system. In this work, a new protocol was investigated to substitute the organic solvent with a DES/aqueous phase (ratio 1:1 v/v). Moreover, we decided to set the composition of the DES in order to exploit the HBD component as the X-OH necessary for the PC transphosphatidylation. In detail, PC was fully solubilized in the suitable so-called "reactive DES (RDES)" and then a buffer solution containing PLD was added. After 40 h at 45 °C, the products precipitated in the reaction mixture and were recovered by simple filtration and analyzed. Remarkably, the extraction of the residual reaction mixture demonstrated that most of the products were effectively in the precipitate and just a minor amount (≈5%) remained dissolved in the RDES/buffer medium.

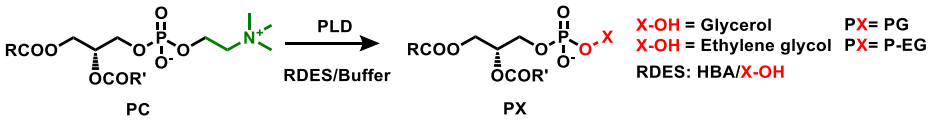

Figure 3: Scheme of the reaction of transphosphatidylation.

For what concerned the preparation of both products, they were obtained by the complete transformation of PC only when RDES betaine/HBD was used, since the presence of choline chloride as HBA probably prevented the reaction to be completely shifted versus products because of its opposite mass effect.

5.3. Lignocellulose DES-mediated fractionation

The lignocellulosic biomasses studied in this section were BSG, raw RH (rRH) and parboiled RH (pRH). They were submitted to a two-step integrated process reported in Figure 4.

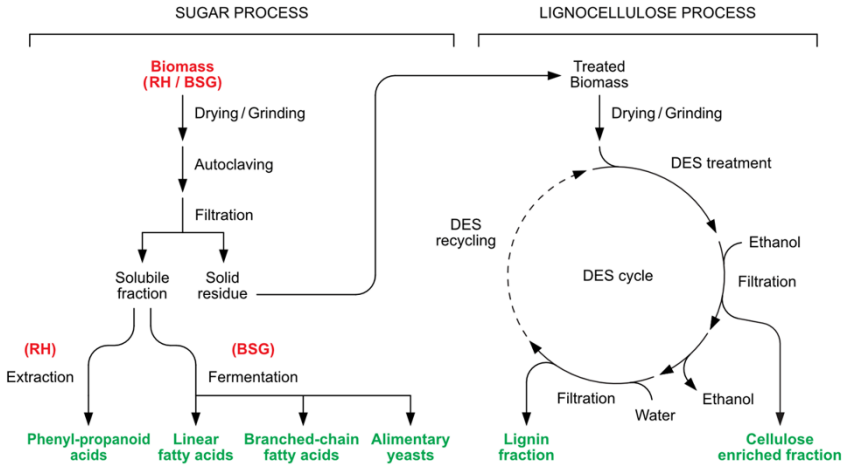

Figure 4: Integrated process for BSG/RHs fractionation.

In detail, the process was based on an initial biomass pretreatment in hot water in autoclave that led to the formation of a soluble fraction and of an insoluble one. For BSG, the soluble fraction (accounting for 25% of the initial biomass) consisted in sugars subsequently used for the preparation of growing media for microbial fermentation, instead in RHs cases we recovered, by extraction, phenyl-propanoid acids (2-3%). For all biomasses, after filtration, the insoluble fraction was successively submitted to the so-called lignocellulose process. The biomass was dissolved in DES for 24 h at 140 °C. Ethanol was then added to selectively precipitate the cellulose-enriched fraction. Successively, ethanol was evaporated and lignin precipitated by addition of water. The final DES was then recycled. In the present work, the focus has been set in particular on the recovered lignin fractions (almost 15-20% of the initial biomass). They were deeply analyzed and compared to an industrial technical lignin (Protobind). The main data are reported in Table 1 here below.

Lignin	M_w (g/mol)	M_n (g/mol)	PDI (M_w/M_n)	VAE (mmol/g)	-OH aliphatic (mmol/g)	-OH aromatic (mmol/g)	-COOH (mmol/g)	Reducing sugars/Biomass (w/w)
BSG_T-Lignin	670	1630	2.43	1.2	1.78	3.21	3.99	3.3%
rRH_T-Lignin	1360	5195	3.82	1.3	2.48	7.10	1.02	9.2%
pRH_T-Lignin	1310	3860	2.95	1.7	3.08	7.49	1.36	14%
Protobind	830	2800	3.37	3.1	3.00	4.67	1.42	13%

Table 1: Summary of characterization results for BSG, RHs compared to Protobind lignin. (M_w (weight average molecular weight), M_n (number average molecular weight) and PDI (polydispersity) were measured by GPC. VAE= vanillin equivalents measured through Folin-Ciocalteu assay. Content of -OH aliphatic/aromatic and -COOH measured by ^{31}P NMR. The reducing sugars were measured by Bicinchoninic assay).

According to these results, all these lignins were tested for their water reduction capacity in concrete formulations, in collaboration with Dr. Alberto Strini (ITC-CNR, San Giuliano Milanese, Italy). In particular, BSG- and RHs-Lignins showed a comparable water reduction capability, equivalent to that of Protobind (see Figure 5), and these results suggested that lignins extracted through DES–mediated fractionation could be suitable as starting materials to develop new sustainable water reducers for production of concrete, paving the way for further investigations.

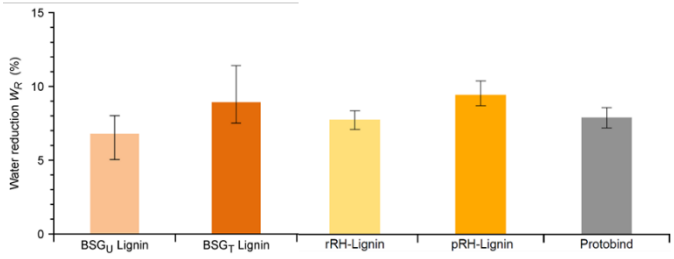

Figure 5: Measured water reduction capability for cement pastes containing 0.2% wt. of lignin.

5.4. Lignin nanoparticles and enzyme immobilization for phospholipids biotransformation

Our studies on lignin recovery from waste biomasses led us recently to exploit this material for nanoparticles (NPs) preparation. Initially, we started the set-up of the NPs synthesis protocol using the technical lignin Protobind thanks to its quite low cost and large availability in our laboratory. The process for the preparation of stabilized LNPs is reported in Figure 6.

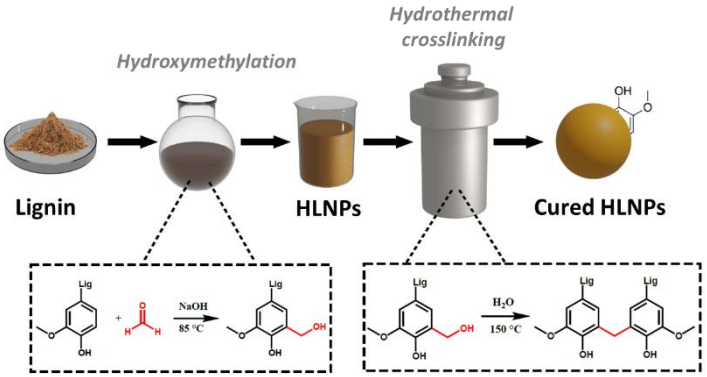

Figure 6: Illustration of the process for the preparation of stabilized c-HLNPs.

So, firstly, lignin was hydroxymethylated (HL), and this was confirmed by FT-IR and ^{31}P NMR analyses, that showed an increase in the hydroxyl content. Subsequently HL was employed to prepare hydroxymethylated nanoparticles (HLNPs), which displayed smaller particle size compared to the regular LNPs, since the size of the LNPs is known to decrease with the increasing aliphatic hydroxyl content. Then, to increase resistance of HLNPs to organic solvents and to a wide range of pH values, we carried out a curing step to stabilize the HLNPs via intraparticle curing, leading to cured HLNPs (c-HLNPs).

After c-HLNPs were completely analyzed, due to our interest in PLs synthesis, we decided to exploit LNPs as a scaffold for PLD immobilization, since PLD is a very expensive enzyme which is not commercially available on large scale as only few chemical companies produce this enzyme, limiting its application to an internal use. PLD was immobilized on c-HLNPs by direct adsorption without the necessity of any crosslinker. A demonstration of the occurred immobilization was given by the measurement of the almost absent activity of the supernatants samples after the enzyme had been immobilized. It was also confirmed by the FT-IR analysis, and by the size distribution, since the immobilization increased the particles diameter compared to the original HLNPs. Many parameters of the immobilized enzyme were tested, such as concentration, temperature and pH effect, in order to determine the best conditions in which almost all the enzyme could be immobilized without losing activity. The immobilized PLD was studied with particular attention paid to enzyme recycling in the biotransformation of PC in three natural high value polar head-modified PLs (PXs): phosphatidylglycerol (PG), phosphatidylserine (PS) and phosphatidylethanolamine (PE) (see Figure 1 for structures). These PLs were selected for their commercial value due to their peculiar properties. PC and the corresponding alcohols (glycerol, L-serine and ethanolamine respectively) were converted into PXs by PLD-c-HLNPs in a biphasic system toluene/buffer at 40 °C. At the end of each synthetic cycle, the final products PXs were easily recovered with high yields (for PG and PS $\geq$ 90%, for PE $\sim$ 60%). The supported enzyme preparations were successfully completely recycled with high activity retention over four synthetic cycles. Finally, PLD-c-HLNPs can be regarded as a new, chemically stable, recyclable and user-friendly biocatalyst to be employed in sustainable chemical processes for phospholipids preparation.

6. Conclusions and research impact

In this work, a deep study about DESs nature and exploitation was presented, showing the versatility of these new green solvents. Firstly, we proposed a smart new tool to assess how HBA/HBD ratio and water content could influence the eutecticity of the DES mixture exploiting the measurement of ^{1}H NMR relaxation time. This methodology compared well in terms of simplicity and time request with other analytical methods.

Also, we reported how, preparing different combinations of HBA and HBD, it is possible to use DESs for several applications, from biocatalysis to biomass fractionation. For what concern biocatalysis, DESs were used both as solvent and as reactant, allowing the enzymatic preparation of high-value phospholipids of commercial interest easily recovered by precipitation, avoiding the use of organic solvent both in the reaction medium and in the extraction steps. Regarding biomass fractionation, we set-up a new multistep process for the efficient fractionation of two waste agrifood biomasses, BSG and RH, which allowed the recovery of their main fractions. We have focused particularly on lignin fractions, which were deeply analyzed, tested as precursors of superplasticizers and exploited as starting material for nanoparticles preparation. Thus, we performed the immobilization of an expensive enzyme on a commercial lignin-based scaffold which has been exploited in the production of high value polar head-modified PLs.

In the next future, different items will be faced. Firstly our recovered lignins from waste biomasses will be employed for the preparation of nanoparticles to be exploited for PLD immobilization. These new immobilized catalysts will be tested for PLs biotransformation also in DESs media. Moreover, the possibility to immobilize other categories of enzymes on these biobased scaffolds will be tested. Finally, the exploitation of the recovered sugars–enriched fractions derived from the biomass fractionation will be investigated, aiming to a complete a valorization of the whole biomasses material.

References

1. Abbott, A. P.; Capper, G.; Davies, D. L.; Rasheed, R. K.; Tambyrajah, V., Novel solvent properties of choline chloride/urea mixtures. *Chemical Communications* **2003,** (1), 70-71.

2. El Achkar, T.; Greige-Gerges, H.; Fourmentin, S., Basics and properties of deep eutectic solvents: a review. *Environmental Chemistry Letters* **2021,** *19* (4), 3397-3408.

3. Ozturk, B.; McClements, D. J., Progress in natural emulsifiers for utilization in food emulsions. *Current Opinion in Food Science* **2016,** *7*, 1-6.

4. Carrea, G.; D'Arrigo, P.; Secundo, F.; Servi, S., Purification and applications of a phospholipase D from a new strain of Streptomyces. *Biotechnology Letters* **1997,** *19* (11), 1083-1085.

5. Steiner, J.; Procopio, S.; Becker, T., Brewer's spent grain: source of value-added polysaccharides for the food industry in reference to the health claims. *European Food Research and Technology* **2015,** *241* (3), 303-315.

6. Balbinoti, T. C. V.; Nicolin, D. J.; de Matos Jorge, L. M.; Jorge, R. M. M., Parboiled Rice and Parboiling Process. *Food Engineering Reviews* **2018,** *10* (3), 165-185.